Upregulation of nicotinic acetylcholine receptors in hippocampal neurones and SH-SY5Y cells: a study into the cellular mechanisms underlying upregulation and the functional properties of nAChR

Ridley, Diana L.

Award date:
2000

Awarding institution:
University of Bath

Upregulation of nicotinic acetylcholine receptors in hippocampal neurones and SH-SY5Y cells: a study into the cellular mechanisms underlying upregulation and the functional properties of nAChR.

Submitted by Diana L. Ridley
for the degree of Ph. D. of the University of Bath, 2000.

ProQuest LLC
789 East Eisenhower Parkway
P.O. Box 1346
Ann Arbor, MI 48106-1346

In memory of Guy Harper
(30th March 2000):

Breath of Time.

Tick tock goes the clock,
As I ponder where I'm going
Every second of time.

To get from here to there,
From being this to becoming that,
To be adorned with respect
In this life of ours.

Striving to the highest objects,
To live the life we dream,
Till we draw the last breath,
And move on to the next life.

Guy Benson Harper.

Summary.

Nicotine, the psychoactive component of tobacco smoke, binds to neuronal nicotinic acetylcholine receptors (nAChR) through which it mediates pharmacological effects. The present study demonstrates that [^{125}I]-α-bungarotoxin ([^{125}I]-α-bgt) binding sites are upregulated in primary hippocampal neurones and SH-SY5Y cells after chronic treatment with nicotine, 3, 4-dimethylaminocinnamylidene anabaseine (DMAC) and KCl. KCl-evoked upregulation is prevented in the presence of the calcium channel blocker, verapamil or the specific Ca^{2+}-calmodulin-dependent protein kinase II (CaM-kinase II) inhibitor 1-[*N*,*O*-bis-(5-isoquinolinesulfonyl)-*N*-methyl-L-tyrosyl]-4-phenylpiperazine, (KN-62). Upregulation elicited by nicotinic agonists is unaffected by these drugs. These data suggest that upregulation evoked by nicotinic agonists and KCl depolarisation is mediated by different cellular mechanisms. [^{3}H]-Epibatidine binding to SH-SY5Y cells identified that nicotine and DMAC upregulated α3-containing (α3*) nAChR. Mechanisms governing upregulation of α3* nAChR, investigated by co-application of verapamil or KN-62 or 3-[1-[3(amidinothio)propyl-1H-indol-3-(1-methyl-1H-indol-3-yl)maleimide methane sulfonate (RO 31-8220) with either nicotine or DMAC, did not prevent upregulation of [^{3}H]-epibatidine binding. In contrast to its action on [^{125}I]-α-bgt binding, KCl did not upregulate α3* nAChR in SH-SY5Y cells.

An investigation into the quantitation of α3 and α7 subunit RNA after chronic nicotine, DMAC or KCl treatment to SH-SY5Y cells shows that these treatments differentially effect subunit expression. Nicotinic agonist treatment does not alter the total RNA expression for either α3 or α7 subunits, whereas KCl is without effect on the expression of α3 subunit RNA but dramatically increases the expression of the α7 transcript. A preliminary confocal analysis identifies that chronic nicotinic agonist treatment upregulates intracellular α3 and α7 nAChR subunits in SH-SY5Y cells. Together these findings support the concept that nicotinic agonists and KCl depolarisation modulate nAChR binding sites by different cellular mechanisms and that KCl increases the expression of α7 subunit RNA by a mechanism involving transcription.

Functional assays using fura-2 loaded SH-SY5Y cells were used to construct concentration-response curves for nicotine and KCl showing increases in intracellular calcium ($[Ca^{2+}]_i$) in a Ca^{2+}-dependent manner. The nicotine-evoked increase in $[Ca^{2+}]_i$ is mediated in part by L-type Ca^{2+} channels, α3* and α7* nAChR. The data reveal that chronic drug treated SH-SY5Y cells with drug regimes that produce upregulation of nAChR, produce a variety of changes in the functioning of upregulated nAChR present on the surface of SH-SY5Y cells.

Continued study of neuronal nAChR will help to elucidate physiological functional roles for these receptors. The demonstration that both α3* and α7* nAChR are upregulated after different drug treatments may provide an insight for relevant roles for nicotine and KCl depolarisation in neuronal development, in terms of neurite retraction and neurite outgrowth and also in the therapeutic application of nicotinic agonists not only in tobacco use but in smoking cessation strategies and in neuroprotection in the treatment of Alzheimer's and Parkinson's disease.

Acknowledgements.

First of all I would like to thank Dr Susan Wonnacott for giving me the opportunity to join her lab in December 1996 and for all the help, support and guidance that she has given me both work related and on a personal level. Thanks also to members of labs 0.44 and 0.47, past and present, who have made the past three and a half years go by so quickly. In particular thanks goes to Dr Adrian Rogers (Jolly) who has been around since I began my PhD to show me a thing or two including initial techniques, Dr Lev Soliakov for his quiet and understanding ways, Dr Ian Jones for all his help with the confocal protocol and Dr Donald Dunbar and Catherine Critten for their advice and help with molecular procedures performed at Organon and Bath respectively. Thanks also to Clare Wells who was a project student under my supervision and helped with the generation of the PKC data. Thanks also to the MRC and Organon Laboratories for funding of my PhD. In particular a big thanks goes to Adrian, Lucy and Amie for support and many laughs whilst writing up and keeping me sane by supplying me with beer, vodka, and a steady stream of amusement with 'nylon coats and white shoes!'

Thanks also to my mum, dad and sister Julie for their support and encouragement throughout my PhD and who will (hopefully) once again see me through another graduation ceremony, I promise there will be no more and I will soon have a 'proper' job!!! Finally to Karen and Kerry for their valued friendship that I have been blessed with over the years and in particular the past few months.

Publications:

Ridley D. L., Rogers A. and Wonnacott S. (2000). Differential effects of chronic nicotinic drug and KCl depolarisation treatment on nicotinic binding sites in primary hippocampal cultures and the SH-SY5Y human neuroblastoma cell line. (*Submitted to Br. J. Pharmacol.*).

Ridley D. L. and Wonnacott S. (2000). Effects of acute and chronic drug treatments on nicotinic receptor-mediated functional responses in the SH-SY5Y human neuroblastoma cell line. (*Submitted to Br. J. Pharmacol.*).

Communications:

Ridley D. L. and Wonnacott S. (1998). Modulation of alpha 7-containing nicotinic receptor expression in SH-SY5Y cells and primary hippocampal neurones. *Br. J. Pharmacol.*, **125**: no. SS, p. P78.

Ridley D. L. and Wonnacott S. (1998). Modulation of α7- and α3-containing nicotinic receptor expression in SH-SY5Y cells and primary hippocampal neurones. *Soc. Neurosci.*, **24**: p831, no. 331.5.

Ridley D. L. and Wonnacott S. (1999). Effects of acute and chronic drug treatments on nAChR-mediated increases in intracellular calcium in SH-SY5Y cells. *Neuronal Nicotinic Receptors*, Venice, Italy Oct 1999.

List of Contents:

List of illustrations:

List of figures.

List of tables.

Abbreviations.

ACh	Acetylcholine
AD	Alzheimer's disease
AMPA	α-Amino-3-hydroxy-5-methyl-4-isoxazole propionic acid
ANOVA	Analysis of variance
α3*	α3-Containing
α7*	α7-Containing
α-bgt	α-Bungarotoxin
α-CTX	α-Conotoxin
B_{max}	Maximal concentration of binding sites
bp	Base pairs
BSA	Bovine serum albumen
$[Ca^{2+}]_i$	Concentration of intracellular calcium
CaM	Calmodulin
CaM-Kinase II	Calcium-calmodulin-dependent protein kinase
cDNA	Complementary deoxyribose nucleic acid
CLSM	Confocal laser scanning microscope
CNS	Central nervous system
CSPD®	Disodium 3-(4-methoxyspiro {1,2-dioxetane-3,2'-(5'-chloro) tricyclo [3.3.1.1^{3,7}] decan}-4-yl) phenyl phosphate
2-D	Two-dimensional
3-D	Three-dimensional
DA	Dopamine
DEPC	Diethyl pyrocarbonate
DFP	diisopropyl fluorophosphate
DHβE	Dihydro-β-erythroidine
DIC	Differential interference contrast
DIG	Digoxigenin
DMAB	3-(4)-dimethylaminobenzylidine anabaseine
DMAC	3, 4-dimethylaminocinnamylidene anabaseine
DMEM	Dulbecco's modified Eagle medium

DMPP	1, 1-dimethyl-4-phenylpiperazinium
DMSO	Dimethylsulfoxide
DNA	Deoxyribose nucleic acid
d-TC	d-Tubocurarine
DTNB	5, 5'-dithiobis-(2-nitrobenzoic acid)
DTT	Dithiothreitol
E18	Embryonic day 18
EC_{50}	Concentration producing a half-maximal response
EDTA	Ethane diamino-N,N'-tetraacetic acid
EGTA	Ethyleneglycol-bis-(β-aminoethylether)-N,N,N',N'-tetraacetic acid
EM	Electron microscope (or microscopy)
FCS	Fetal calf serum
FITC	Fluorescein isothiocyanate
Fura-2	1-[2-(5-carboxyoxazol-2-yl)-6-aminobenzofuran-5-oxy]-2(2'-amino-5'methylphenoxy)ethane N, N, N', N'-tetraacetic acid
GABA	γ-Aminobutyric acid
GFAP	Glial fibrillary acidic protein
GLR-1	AMPA-type glutamate receptor
GTP	Guanine triphosphate
GTS-21 (DMXB)	2, 4-dimethoxybenzilidene
HEK-cells	Human embryonic kidney cells
HEPES	(N-(2-hydroxyethyl)piperazine-N'-2-ethane) sulphonic acid
5-HT	5-hydroxytryptamine, serotonin
IC_{50}	Ligand concentration which reduces radioligand binding or functional response to half-maximum
IP_3	Inositol triphosphate
i.p.	Intraperitoneal
IU	International unit
i.v.	Intravenous
K_D	Equilibrium dissociation constant
kDa	Kilodaltons
K_i	Equilibrium binding inhibition affinity constant

KN-04	*N*-[1-[*N*-methyl-*p*-(5-isoquinolinesulfonyl)-benzyl]-2-(4-phenylpiperazine) ethyl]-5-isoquinoline sulfonamide
KN-62	1-[*N*,*O*-bis-(5-isoquinolinesulfonyl)-*N*-methyl-L-tyrosyl]-4-phenylpiperazine
λ	Wavelength
LB	Luria-Bertani
LGIC	Ligand gated ion channel
LTP	Long term potentiation
M(1-4)	Membrane spanning regions (1-4)
mAb	Monoclonal antibody
mAChR	Muscarinic acetylcholine receptor
MBTA	4-[*N*-maleimido] benzyltrimethyl-ammonium iodide
MESA	2-[*N*-morpholino]ethanesulphonic acid
MLA	Methyllycaconitine
MPTP	*N*-[4-maleimido] phenyltrimethyl-ammonium iodide
MOPS	3-[*N*-morpholino]propanesulfonic acid
M_r	Relative molecular mass
mRNA	Messenger ribose nucleic acid
nAChR	Nicotinic acetylcholine receptor(s)
n-bgt (κ-bgt)	Neuronal bungarotoxin
NE	Norepinephrine
NEAA	Non-essential amino-acids
NGF	Nerve growth factor
n_H	Hill number
NMDA	N-methyl-D-aspartic acid
6-OHDA	6-hydroxydopamine
O.D	Optical density
P2	Pellet from medium speed centrifugation
PBS	Phosphate buffered saline
PC12 cells	Pheochromocytoma cells
PCR	Polymerase chain reaction
PEI	Polyethyleneimine

PKA	Protein kinase A
PKC	Protein kinase C
PLC	Phospholipase C
PLL	Poly-L-lysine
PMSF	Phenylmethylsulphonyl fluoride
PTFE	Polytetrafluoroethylene
QNB	Quinnuclidinyl benzilate
R_{max}	The fluorescence of Ca^{2+}-saturated dye
R_{min}	The fluorescence signal quenching of the dye
RNA	Ribose nucleic acid
RO 31-8220	3-[1-[3(amidinothio)propyl-1H-indol-3-(1-methyl-1H-indol-3-yl)maleimide methane sulfonate
RT-PCR	Reverse transcriptase – polymerase chain reaction
S1 and S2	Supernatant fraction from low speed centrifugation
s.c.	Subcutaneous
SCG	Superior cervical ganglion
SDS-PAGE	Sodium dodecyl sulphate polyacrylamide gel electrophoresis
S.E.M.	Standard error of the mean
SN	Substantia nigra
TAE	Tris-acetate
d-TC	d-Tubocurarine
TDF	p-(trimethylammonium)benzenediazonium fluoroborate
TID	Trifluoromethyl-iodophenyldiazarine
Tm	Melting point temperature
TPMP	Triphenylmethylphosphonium
Tris	Tris(hydroxymethyl)amino-methane
TTX	Tetrodotoxin
UV	Ultraviolet
VOCC	Voltage operated calcium channel
VTA	Ventral tegmental area

1.1. Nicotine:

Nicotine was first isolated in a pure form from the tobacco plant, *nicotiana tabacum* by two students Wilhelm Heinrich Posselt and Ludwig Reimann in 1828 (see Ashton and Stepney, 1982). It then took a further 110 years to elucidate that this alkaloid, nicotine, when biochemically isolated and extracted from the hundreds of other different chemicals present within tobacco, was the pharmacologically active agent (Johnston, 1942). Nicotine is a weak base composed of carbon, hydrogen and nitrogen (empirical formula $C_{10}H_{14}N_2$) which assemble together to form a dibasic, tertiary amine incorporating a weakly basic pyridine and strongly basic pyrrolidine ring in its structure (Barlow and Hamilton, 1962; Benowitz, 1996). Once nicotine is within the body, it is in the form of its free base. Nicotine in this form is readily absorbed and extensively distributed throughout the body. The structure of nicotine and the nicotinium ion (free base) are shown in Figure 1.1.

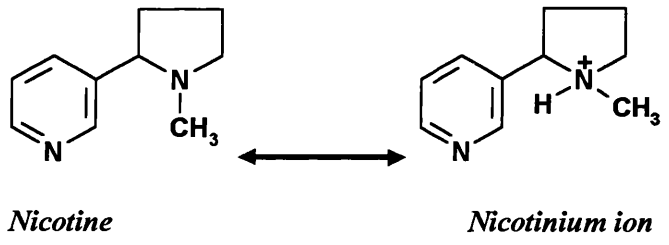

Nicotine *Nicotinium ion*

Figure 1.1 ***The structures of nicotine and the nicotinium ion.***

1.2. An introduction to the *Torpedo* nAChR:

At physiological pH nicotine is predominantly in its ionised state in the form of the univalent nicotinium ion (Benowitz and Jacob, 1998). This is the active form of nicotine and in this state the alkaloid is capable of acting at neuromuscular junctions, at

autonomic ganglia and on many neurones in the central nervous system (CNS) via ligand-gated ion channel (LGIC) cholinoceptors. In order to provide a thorough and comprehensive study on the biochemical and pharmacological properties of nicotine and to characterise the LGIC where it binds, large quantities of this LGIC are essential and necessary in a highly purified form.

Initial characterisation of the nAChR, as reviewed by Changeux (1981), used nAChR obtained from the electric organs of the electric eel (*Electrophorus*) and the electric ray (*Torpedo californica*). Within the electric organs from these fish, large quantities of highly enriched nicotinic synapses derived from embryonic muscle-type cells can be found and purified for biochemical analysis. Muscle nAChR are considered as the 'prototype' of all other members of the LGIC superfamily. Molecular, immunological and electrophysiological studies have greatly expanded the knowledge and biochemical insight into functional nAChR present in vast abundance as a rich homogeneous source on postsynaptic membranes of the electric organs of *Torpedo* (hundreds of mg nAChR per kg of fresh *Torpedo* electric organ). α-Bgt, a 8 kDa polypeptide from the venom isolated from the East Asian banded krait, *Bungarus multicinctus* (Loring and Zigmond, 1988), with high affinity for nAChR at the neuromuscular synapse present in *Torpedo*, has facilitated the initial purification and characterisation of this nAChR.

After initial isolation and affinity purification, the muscle receptor protein was found to be a large, transmembrane, oligomeric glycoprotein complex with an apparent molecular mass in the region of 290 kDa. Due to the receptor being a membrane bound glycoprotein multimer complex, it has been difficult to use conventional techniques of crystallisation and X-ray diffraction to determine and solve the quaternary structure of nAChR. This has led to the three-dimensional (3-D) receptor structure image being analysed by using the electron microscope (EM) to view isolated postsynaptic

membrane-bound molecules that are readily converted to form helical, tubular vesicles and when rapidly frozen retain much structural information of the receptor complex. Kubalek *et al* (1987) were able to locate the binding sites and determine the arrangement of the subunits around the channel pore of the nAChR using electron image analysis of tubular crystals of receptors grown from postsynaptic membranes of *Torpedo marmorata* electric organ preserving its structure within its native environment. Unwin (1993a, 1995) has since used electron image reconstruction of two-dimensionally-ordered arrays of the *Torpedo* receptor in electric postsynaptic tissue membrane fragments that were embedded in amorphous ice to determine the 3-D structure of the *Torpedo* ray nAChR. Images obtained have been at a higher resolution of 9Å in both the resting closed channel configuration and also in the activated open channel formation after acetylcholine- (ACh) induced changes (Unwin, 1993a, 1995). More recently the receptor complex has been resolved to a resolution of 4.6 Å in the closed conformation which has also aided the identification of prominent structural features of these receptors and build upon the picture that is already forming on the functional architecture of these receptors (Miyazawa, 1999) (Figure 1.2).

The use of molecular weight estimates has helped to identify the number of subunits present within nAChR. It is now agreed that these LGIC receptor complexes are assembled from five transmembrane spanning polypeptide subunits with high sequence homology and are arranged in a pentameric ring fashion (Cartaud *et al.*, 1973: Cooper *et al.*, 1991; Decker *et al.*, 1995). The subunits are arrayed to form a barrel-like structure that is toroidal in shape with a pseudosymmetric 5-fold axis, delineating a central, cation conducting pore through the membrane (Karlin, 1993; Unwin, 1993a). Sodium dodecyl sulphate polyacrylamide gel electrophoresis (SDS-PAGE), analysis have shown

that vertebrate skeletal neuromuscular and electric organ nAChR consists of four subunits.

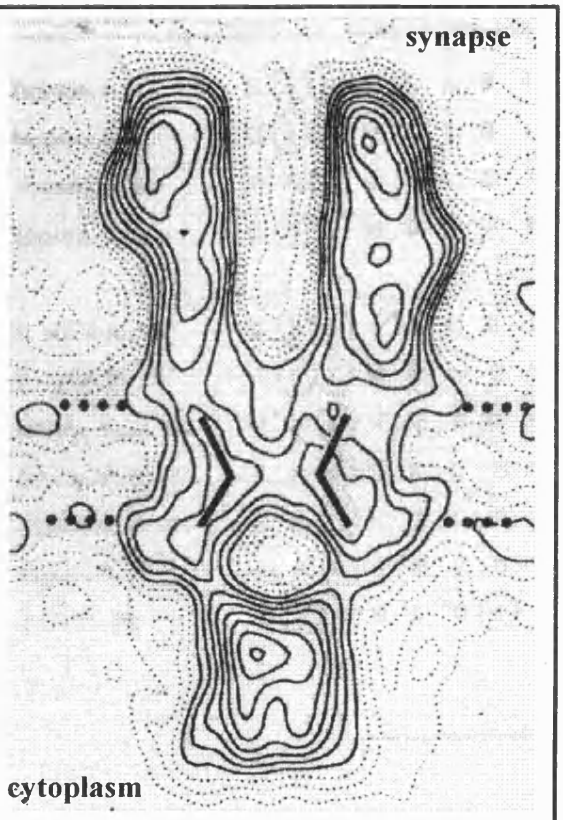

Figure 1.2 The Torpedo nAChR in axial section through the ion channel at 9Å resolution by electron microscopy *(taken from Unwin, 1993a).*

The subunits are designated as α (often termed as α1; 40 kDa), β (50 kDa), γ (60 kDa) and δ (66 kDa) (Schmidt and Raftery, 1973; Claudio *et al.*, 1983), with the stoichiometry of α_2, β, γ, δ (Raftery *et al.*, 1980; Clarke, 1992; as reviewed by, Stroud *et al.*, 1990). Analysis has shown that the clockwise arrangement of this five subunit assembly, around the receptor complex, when viewed from the synaptic cleft could be

α, β, α, γ and δ or α, γ, α, β and δ or α, γ, α, δ, and β within the lipid bilayer (Kubalek *et al.*, 1987; Pedersen and Cohen, 1990; as reviewed by Arias, 2000).

Comparisons of the amino acid sequences of cloned nAChR subunit cDNA show that the subunits of this gene family display similar structural compositions and homology in vertebrate, invertebrate species and also within the peripheral nervous system. This strongly suggests that the subunits are evolutionarily related proteins that have evolved by the process of gene duplication from a single common genetic ancestor (Noda *et al.*, 1983a, b). Partial or complete cDNA sequences have revealed that each of the nAChR subunits (and members of their super gene family) share similar characteristic regions and certain motifs within their tertiary structure. Sequence alignment analysis of the α subunit (Noda *et al.*, 1982) shows that the β and δ subunits share 19% (Noda *et al.*, 1983a), and the γ subunit share 54% homology (Noda *et al.*, 1983b). Some of the shared motifs include the following (Stroud *et al.*, 1990; as reviewed by Arias, 2000 and Paterson and Norberg, 2000) (Figure 1.3);

1). the nAChR subunits have a large, extracellular hydrophilic amino-terminal domain of approximately 200 conserved amino acids which aids in the formation of the cholinergic agonist binding site,

2). a 15-residue cysteine loop, and *N*-glycosylation sites are contained within the amino-terminal domain (Ortells and Lunt, 1995),

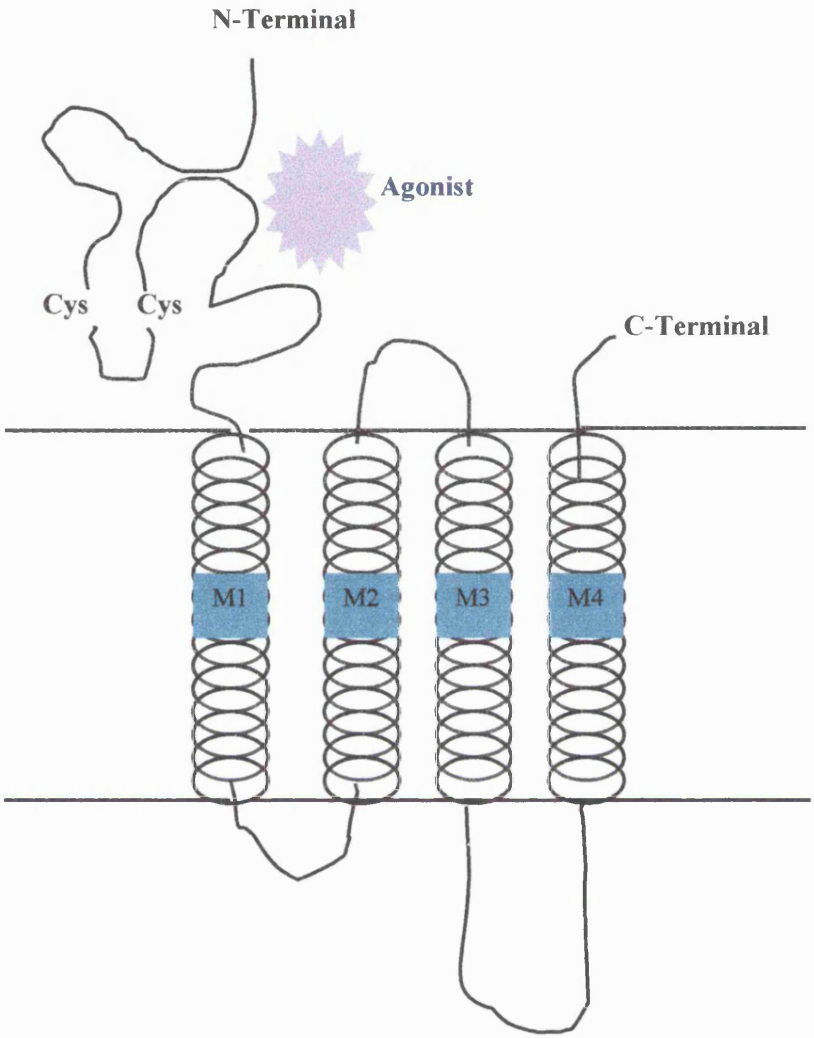

Figure 1.3 Proposed transmembrane topology of nAChR superfamily subunits. *Each subunit contains a large extracellular N-terminus (location of the agonist binding sites), followed by four highly hydrophobic transmembrane regions (M1 to M4) which have strong sequence homology. The M2-domain is thought to be exposed to the lumen of the pore throughout the length of the receptor and therefore contributes to the lining of the receptor ion-channel pore. There is also a long intracellular M3-M4 loop with a small extracellular C-terminal domain contained within nAChR subunits.*

3). a transmembrane spanning domain which is comprised of four short hydrophobic membrane spanning regions. These segments, designated as M1-M4 contain a stretch of 27, 20, 20 and 19 uncharged amino acid residues respectively (Claudio *et al.*, 1983; Noda *et al.*, 1983b); the domains M1-M3 are connected by short intra- and extra-cellular loops. The α-helical M2 transmembrane segment contributes to the formation of the lining of the receptor ion channel complex and also aids in the gating of ion flow through the channel due to conserved residues contained in this domain (Akabas *et al.*, 1994; Ortells and Lunt, 1995; Unwin, 1995),

4). a large, variable, hydrophilic intracellular, cytoplasmic loop located between M3 and M4 (about 100-200 amino acids in length) containing consensus serine/threonine and tyrosine phosphorylation sites,

5). a short, extracellular C-terminus of 20 amino acids that is highly variable and hydrophilic.

The nAChR can be reconstituted into lipid bilayers; the resulting receptor can be identified by the binding of specific ligands and is capable of desensitising. The ion channel pore permits the flux of monovalent and divalent cations and non-electrolytes and is capable of discriminating against anions (Dani and Eisenman, 1987; as reviewed in Galzi *et al.*, 1991). This property of the receptor channel having a high conductance for cations may be explained in part to the negatively charged amino acids located in the channel vestibule which would serve to repel anions and therefore attract and contribute to the concentration of positively charged ions (Dani and Eisenman, 1987; Stroud *et al.*, 1990). The pore is a narrow-membrane spanning water-filled portion of the receptor

complex approximately 30 Å in length (Toyoshima and Unwin, 1988), the lining of which is made up of the five α-helical M2 segments from each of the polypeptide chains (Herz *et al.*, 1989). Within the middle of each of the pore lining M2 domains, there is a leucine residue that is highly conserved across most subunits (Filatov and White, 1995; Labarca *et al.*, 1995). The role of this conserved amino-acid, is thought to be involved in the setting of the mean opening time of the receptor channel once activated by ligand binding (Filatov and White, 1995). The M2 segments come together in close proximity near the middle of the membrane to produce the gate of the receptor in the absence of ACh or binding ligand (Unwin, 1993a, b) (Figure 1.4).

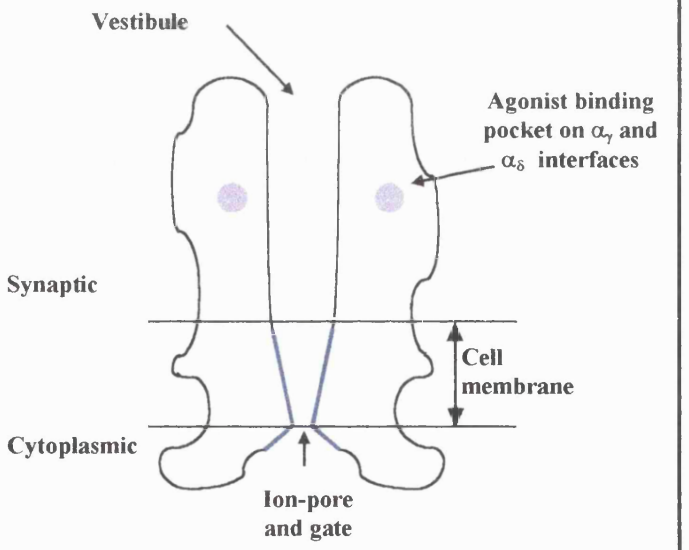

Figure 1.4 Diagram of an axial section through the structure of the nAChR possible locations for agonist binding are shown. *The receptor traverses the membrane with the majority of the receptor complex on the synaptic side of the cell membrane. Shown are the two putative agonist binding sites at the α_γ and α_δ subunit interfaces. Each receptor is a heteromer composed of α, β, γ and δ subunits.*

nAChR ion channels are activated after the binding of agonist molecules to regions located on the two α subunits at α-γ and α-δ interfaces and mediates the opening of the ion permeation pathway of the LGIC gate. The two molecules of, for example, ACh bind in a non-cooperative fashion to the α subunits resulting in the opening of the nAChR channel. Both of the α subunits contained in muscle and *Torpedo* nAChR have identical amino acid sequences (Changeux, 1990), but differ in their affinities for agonists and competitive antagonists. Differences between the two non-equivalent α subunits arise due to contributions from the neighbouring γ and δ subunits which are in contact with the α subunits leading to the formation of ligand binding sites at the α-γ and α-δ interfaces (Stroud *et al.*, 1990; Sine *et al.*, 1995). nAChR contain a readily reducible disulphide bond, following reduction, the conserved ACh binding sites on α-γ and α-δ subunit interfaces in native nAChR are susceptible to, and uniquely identified by, affinity labelling with electrophilic reagents containing quaternary ammonium moieties, for example, the inhibitory affinity label 4-[*N*-maleimido] benzyltrimethyl-ammonium iodide (MBTA), *N*-[4-maleimido] phenyltrimethyl-ammonium iodide (MPTA) and p-(trimethylammonium) benzenediazonium fluoroborate (TDF) (Kao *et al.*, 1984). These affinity labelling agents covalently react with two bridged cysteines positions 192 and 193 associated near the ACh or ligand binding site in the *N*-terminal extracellular portion of the receptor and are therefore incorporated solely to the α subunits (Kao *et al.*, 1984; Ortells and Lunt, 1995). The South American arrow tip poison, d-tubocurarine (d-TC) is a potent competitive neuromuscular nicotinic antagonist that binds non-equivalently with markedly different affinities to the two ACh agonist binding sites in nAChR present in *Torpedo* (Pedersen and Cohen, 1990; Chiara and Cohen, 1997). This natural aromatic alkaloid ligand, when irradiated with 254 nm UV light, is covalently photoincorporated in a concentration dependent and

pharmacologically specific, agonist inhibitable fashion into the α, γ and δ nAChR subunits in *Torpedo* (Pedersen and Cohen, 1990; Chiara and Cohen, 1997). This further demonstrates, and is consistent with previous reports, that the neighbouring γ and δ subunits contribute direct effects to the high- and low-affinity d-TC binding sites in addition to the α subunit (Pedersen and Cohen, 1990; Sine and Claudio, 1991). The binding of agonist molecules to the nAChR activates the receptor, by triggering distinct localised changes at the binding sites (Figure 1.5). These disturbances produce rapid, transient allosteric changes of the cation channel (Léna and Changeux, 1993; Unwin, 1995).

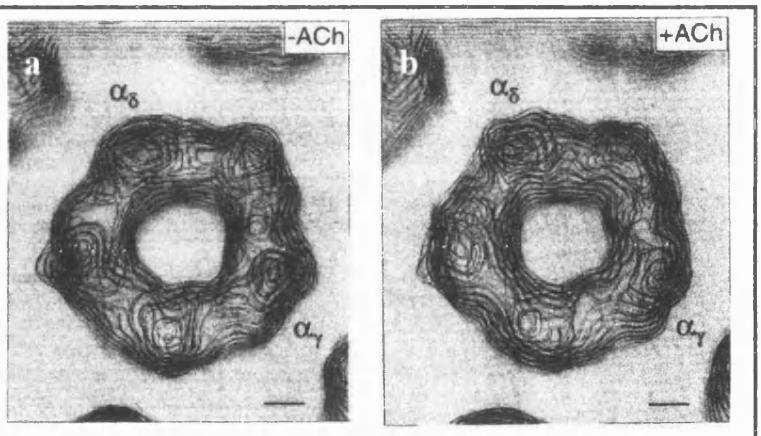

Figure 1.5: Views from the synaptic cleft of the mouth of a Torpedo nAChR embedded in the membrane (a) before and (b) after activation by ACh. *Images determined by electron microscopy, scale bars, 10 Å (taken from Unwin, 1995).*

Small clockwise rotations of the α subunits can be considered as a trigger for channel opening after ACh binds to extracellular surface sites located on the membrane. This signal is transmitted to the channel gate within the nAChR, on the cytoplasmic surface of the membrane, producing a global conformational twist resulting in the opening of the nAChR ion channel. The cations Na^+, K^+ and Ca^{2+} flux through the channel

vestibule along their electrochemical concentration gradients (Galzi and Changeaux, 1995; Akabas *et al.*, 1994). This depolarisation leads to an increase in the concentration of intracellular calcium ($[Ca^{2+}]_i$) and mediates other calcium dependent intracellular processes. The activation of the nAChR is terminated and the gate of the channel closes after ACh is unbound from the receptor and removed from the synaptic cleft by diffusion or hydrolysed by acetylcholinesterase. On longer or continual exposure to ACh, the nAChR proceeds from the closed resting state, to a transient open state and then to a transient desensitised state before reaching a stable inactivated desensitised state (Karlin, 1991; see Marks, 1998 for review). During this phenomenon of desensitisation, ACh is bound tighter to the nAChR than in the resting state and the ion channel is closed (Figure 1.6), this state will last until ACh is removed and the initial resting state of the receptor complex is resumed.

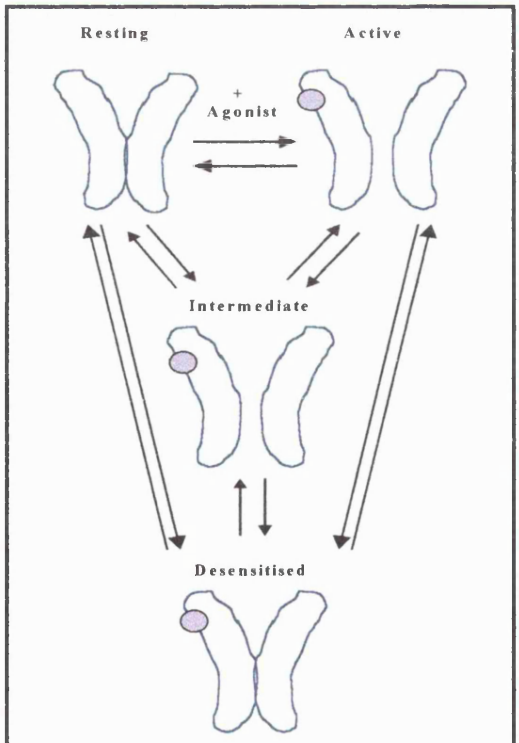

Figure 1.6 Different states of allosteric modulation of nAChR function. *Adapted from Galzi and Changeux (1995).*

1.3. Cloning of neuronal nAChR subunits:

After the discovery, characterisation, isolation and cloning of the amino acid sequences of the subunits comprising the nAChR from *Torpedo* electroplax, the search for nAChR in both the mammalian peripheral and central nervous system followed. nAChR located at the neuromuscular junction have the subunit composition of $(\alpha 1)_2\beta 1\delta\gamma$ or $(\alpha 1)_2\beta 1\delta\varepsilon$ (Karlin, 1991; Ortells and Lunt, 1995). The γ subunit is expressed in embryonic muscle and during muscle development the homologous ε subunit replaces the γ-subunit and is expressed in adult muscle with the α, β and δ subunits to form functional receptor complexes (Takai *et al.*, 1985; Mishina *et al.*, 1986). Differences identified between fetal and adult muscle nAChR channel gating properties and conductance are a result of the contribution of either the γ or ε subunits respectively (Mishina *et al.*, 1986). These mammalian muscle nAChR are analogous to the muscle-type *Torpedo spp.* receptors due to similarities in their *N*-terminus sequences and the four types of subunits they are composed from (Devillers-Thiéry *et al.*, 1979, Raftery *et al.*, 1980). This discovery led to the identification (De Blas and Mahler, 1978), purification and characterisation (Whiting and Lindstrom, 1988) of a family of genes coding for homologous subunits expressed in neurones that also bind ACh.

The *Torpedo* muscle-type nAChR is the best-characterised neurotransmitter-gated ion-channel involved in fast synaptic transmission. Diversity within the nAChR family results from the expression of genes that code for one or more of the nAChR subunit subtypes which, when combined together, form a plethora of functional receptors. These excitatory nAChR, although diverse, share a homologous conserved primary subunit structure (see Figure 1.3). Each nAChR subunit gene is a member of the same gene family and also to the larger supergene family of LGIC. This supergene family includes

the excitatory LGIC sensitive to the neurotransmitter serotonin (5-HT which binds to the 5-HT_3 receptor; Marciq *et al.*, 1991) and the inhibitory ligand-gated receptors for glycine (Grenningloh *et al.*, 1987a, b; Langosch *et al.*, 1988; Betz, 1990) and γ-aminobutyric acid A ($GABA_A$; Wisden and Seeburg, 1992) which are selective for anions (Barnard, 1992; Deneris *et al.*, 1991; Lindstrom *et al.*, 1990; Sargent, 1993; Ortells and Lunt, 1995; as reviewed by Changeux and Edelstein, 1998).

Amino acid alignments of the receptor subunit sequences contained within this gene family identify that there is a high degree of sequence conservation between the subunits present in nAChR, 5-HT_3 and $GABA_A$ receptors. The close functional similarity of this gene family of receptors may be reflected in them all sharing a common protein architectural structure. This includes similar distributions of the highly hydrophobic sequence segments (designated M1-M4), also interpreted as membrane-spanning domains (as reviewed by Popot and Changeux, 1984; and Arias, 2000) and the possession of two conserved cysteine residues (128 and 142, *Torpedo californica* α subunit numbering) separated by 13 other residues to form the analogous cys-loop (reviewed in Ortells and Lunt, 1995).

The principal excitatory receptors in the CNS are glutamate gated ion channels (Nakaniski, 1992; Cully *et al.*, 1994), these receptors are not included in the same gene family of receptors as nAChR. Glutamate receptors, although permitting the flux of cations, have a different membrane topology for their subunits and hence a different 3-D structure. They are composed of three membrane spanning segments (M1, M3 and M4) and a membrane embedded loop that is thought to be the M2 domain (Figure 1.7) (Bennett and Dingeldine, 1995).

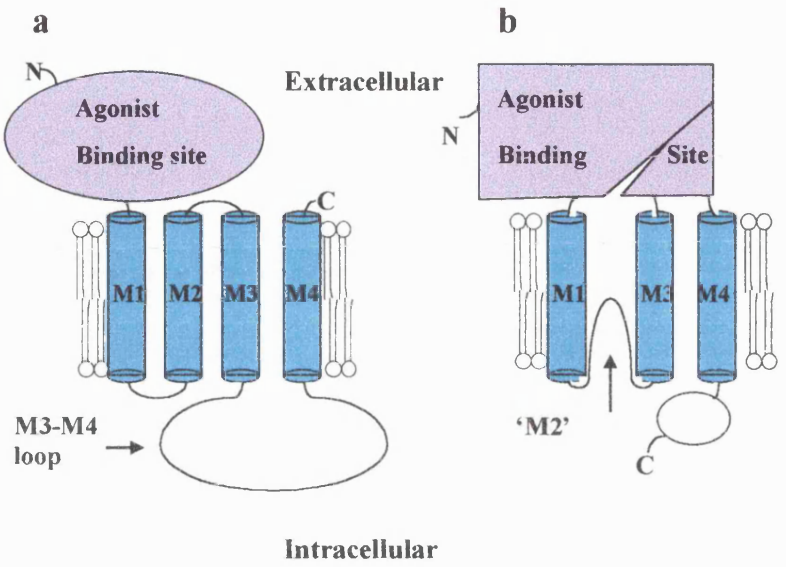

Figure 1.7. The membrane topologies of (a) cys-loop receptors and (b) glutamate receptors. *(a) Proposed transmembrane topology of nAChR subunits, showing an external N-terminus containing the agonist binding sites, four transmembrane segments (M1-M4), a long intracellular M3-M4 loop and a small extracellular C-terminus. (b) Proposed transmembrane topology of the glutamatergic subfamily of subunits which have a more extensive N-terminal extracellular region, that combines with the extracellular M3-M4 loop forming the glutamate-binding site. This leads to an intracellular C-terminus. The 'M2' hydrophobic sequence is a re-entrant loop that is situated within the membrane leaflet.*

The structural transmembrane topology of muscle receptor subunits (Figure 1.3) and the high degree of amino acid sequence identity between neuronal-type nAChR subunits (Figure 1.7a) suggests that this transmembrane topology is present in all nAChR subunits and other receptors contained in this supergene family (Stroud *et al.*, 1990; Karlin, 1991). It is now widely accepted that the main psychopharmacological effects associated with tobacco usage and therefore 'nicotine addiction', are mediated via interactions with one or more of these nAChR located on neuronal membranes

(Wonnacott, 1987, 1990). Since the first cloning of a neuronal nAChR subunit gene in 1986, molecular cloning has identified many of the putative neuronal nAChR subunit isoforms within the CNS by means of probes based on previous oligonucleotide sequences for muscle receptor subunits (not expressed in neurones), which express considerable sequence homology to neuronal nAChR.

Classically, several lines of evidence including immunoaffinity purification using monoclonal antibodies (mAbs) and the development of cDNA probes (Whiting and Lindstrom, 1988; Whiting *et al.*, 1991a, b) established that neuronal nAChR can be broadly divided into two main subtypes of subunits which is in contrast to the four types found in muscle-type receptors (Karlin, 1991) (see sections 1.5.1). Pioneering affinity labelling studies identified that any receptor subunit cDNA containing homologues of the vicinal cysteine residues homologous to positions 192 and 193 of muscle α subunits are characteristic of and were termed as α subunits (Karlin and Akabas, 1995). Homologous neuronal subunits designated as β subunits lack the cysteine pair and distinguishes them from α subunits (Karlin and Akabas, 1995). This neuronal family of receptor subunits is assumed to assemble in a pentameric fashion similar to the membrane topology of *Torpedo spp.* receptors and those receptors at the neuromuscular junction (Anand *et al.*, 1991). The subunits are therefore arranged in a narrow waisted barrel style formation, perpendicular to the membrane, and delineating a central water-filled pathway that permits the flux of specific cations namely Na^+, Ca^+ and K^+, to and from the ion-channel.

The neuronal subunit cDNAs that have been cloned, sequenced and expressed to date in the vertebrate CNS are the eight α subunits α2-α9 (containing the two conserved cysteine residues in the *N*-terminus domain; for review see Ortells and Lunt, 1995), and

the three β subunits, β2-β4 which lack the pair of cysteines (as reviewed by Sargent, 1993; McGehee and Role, 1995). Therefore neuronal nAChR consist of several subtypes with various functional characteristics, compared to only two muscle-type nAChR consisting of either fetal (α1β1γδ) or adult (α1β1εδ) nAChR.

Molecular and immunological techniques indicate that these subunits are capable of assembling to produce a diverse spectrum of receptor ion-channel complexes *in vitro* (Whiting *et al.*, 1987; Sargent, 1993; Decker *et al.*, 1995; McGehee and Role, 1995; Wang *et al.*, 1996; Fenster *et al.*, 1997). Diversity in nAChR lies partially with the nAChR genes that code the various nAChR subunits and differences in receptor composition and therefore stoichiometry. The association of differential combinations of α and β subunits reflects the vast number of putative functional neuronal receptor oligomers that could potentially be expressed within the CNS. Different receptor stoichiometries produce nAChR that display different pharmacological, physiological and biochemical profiles in relation to agonist binding, antagonist affinities (Galzi and Changeaux, 1995; Luetje and Patrick, 1991), ion permeability, conductance kinetics and the degree to which the receptors desensitise (Cachelin and Jaggi, 1991).

1.4. Characterisation of neuronal nicotinic binding sites:

The ability of nicotine to mediate central psychopharmacological effects is now widely accepted as a result of this alkaloid binding to receptors located on neuronal membranes. Progress in this field has allowed for the identification and localisation of populations of subtype specific nAChR in neuronal membranes to be detected by the binding of specific radiolabelled ligands. Radioligands have made it possible to identify and distinguish between the main pharmacological classes of putative native neuronal

nAChR present within the mammalian nervous system. Classically neuronal nAChR can be subdivided into at least two broad categories. They comprise of 1). the predominant high affinity nicotine sites that bind nicotine, ACh and cytisine with high affinity and bind the neurotoxin α-bgt with low affinity and 2). those nAChR that are sensitive to α-bgt, α-conotoxin IMI (α-CTX-IMI; see section 1.7.2.1) and low nanomolar concentrations of methyllycaconitine (MLA; see section 1.7.1) with low affinity for the nicotinic agonists nicotine, ACh, epibatidine and cytisine (Clarke *et al.*, 1985; Marks *et al.*, 1986; Pabreza *et al.*, 1990; Marks *et al.*, 1998; Whiteaker *et al.*, 1999, 2000; Perry *et al.*, 1995, 2000).

1.4.1. High affinity [^{3}H]-nicotinic agonist binding sites:

nAChR, as their name suggests, all bind nicotine but with different affinities. nAChR that have high affinity for [^{3}H]-nicotine bind this tritiated radioligand with a K_D measurable in the nanomolar region or lower (Wonnacott, 1987). Initial binding experiments designed to elucidate [^{3}H]-nicotine binding to subfractions of mouse brain were performed in the mid-seventies (Schleiffer and Eldefrawi, 1974). Romano and Goldstein (1980) later demonstrated that there was a saturable, high affinity site and a multitude of low affinity binding sites detected in rat brain membranes using racemic (±)-[^{3}H]-nicotine. These sites were hypothesised to correspond to the high affinity nAChR and α-bgt-sensitive sites respectively. In these binding studies tritiated nicotinic agonists are used to label and distinguish the appropriate high affinity nicotinic binding sites as the classical nicotinic antagonists, for example hexamethonium, mecamlyamine and α-bgt (with dihydro-β-ethroidine (DHβE) being the exception) have lower affinity and are poor, ineffective competitive inhibitors of high affinity nicotine and ACh

binding sites (Romano and Goldstein, 1980; Schwartz *et al.*, 1982; Marks and Collins, 1982). The naturally occurring (-)-enantiomer of nicotine binds to brain nicotinic sites 70 times more potently than the (+)-isoform, showing the strong stereospecific nature of nicotine binding (Romano and Goldstein, 1980; Wonnacott, 1987). This led to the production of enantiomerically pure (-)-[^{3}H]-nicotine, which is now commercially available as a tool for pharmacological characterisation studies.

In vitro binding techniques have characterised nAChR binding sites in the mammalian CNS that saturably bind [^{3}H]-nicotine with high affinity (Lippiello *et al.*, 1987). The ganglionic agonist (-)-cytisine, an alkaloid found in the seed of *Laburnum anagyroides* (Pabreza *et al.*, 1990), ACh (Schwartz *et al.*, 1982), *N*-methylcarbamylcholine (Anderson and Arneric, 1994) and epibatidine (Houghtling *et al.*, 1995; Perry *et al.*, 1995), are other nicotinic agonists, which when tritiated, detect high affinity neuronal nAChR binding site populations with similar regional distributions (Schwartz *et al.*, 1982; Schwartz and Kellar, 1985; Martino-Barrows and Kellar, 1987; Pabreza *et al.*, 1990; Houghtling *et al.*, 1995). The population of binding sites identified and densely labelled by the snake toxin, α-bgt have a distinct distribution within the brain and display different pharmacological properties compared to the binding sites labelled by classical nicotinic agonists (Clarke *et al.*, 1985, 1992; Marks and Collins, 1982; Marks *et al.*, 1986).

Marks *et al.* (1986) compared the binding of radiolabelled acetylcholine, nicotine and α-bgt to rat and mouse brain. This study found that the [^{3}H]-nicotine and [^{3}H]-ACh bind with high affinity in a saturable and reversible manner to receptor sites located on neuronal membranes. These tritiated agonists compete for high affinity neuronal nAChR binding sites, have low non-specific binding and similar apparent affinities for the receptor and the maximum number of sites identified by these tritiated agonists are

similar. All of these merits make them useful tools for further biochemical analyses on nAChR (Marks *et al.*, 1986). The two binding sites for nicotinic agonists on a nAChR respond identically when challenged with the following treatments; nicotinic agents, thermal denaturation and dithiothreitol (DTT) treatment and reversal of this effect with 5, 5'-dithiobis-(2-nitrobenzoic acid) (DTNB).

These data are consistent with the hypothesis that proposes a specific class of cholinoceptor is labelled by [^{3}H]-nicotinic agonists in both mouse and rat brain. There does appear to be interspecies differences in the regional distribution of these two radiolabelled binding sites and is supported by extensive autoradiographical analysis performed using various rat and mouse brain regions. These analyses reveal the widespread distribution of high affinity nAChR throughout the nervous system labelled with [^{3}H]-acetylcholine and have a similar if not identical distribution and pharmacological profile of neuroanatomical binding to populations of nAChR recognition sites labelled by [^{3}H]-nicotine (Clarke *et al.*, 1985; Marks *et al.*, 1986).

The identity of the receptor complex binding site that exhibits high affinity for [^{3}H]-nicotinic agonists was revealed by immunoprecipitation analysis performed with avian and mammalian brain. Initial immunoprecipitation attempts used the monoclonal antibody (mAb) mAb 35, raised against receptors from *Electrophorus* electric organ, to immunopurify a high affinity [^{3}H]-nicotine binding site from chick brain (Whiting and Lindstrom, 1986). Analysis revealed the nAChR as an integral membrane glycoprotein comprised of two subunit populations, identified as two bands of 49 and 59 kDa apparent mass on a SDS-Page gel. The smaller polypeptide subunit also binds antisera to α subunits and mAb 210, clearly suggesting that this subunit is homologous to the α subunit found in muscle nAChR.

A second antibody, mAb 270, capable of precipitating all high affinity nicotinic binding sites from extracts of rat brain was used to purify and further characterise the neuronal nAChR found in chick brain. mAb 270 is made to receptors immunoaffinity purified from chick brain using mAb 35 which has low affinity for receptors in rat brain but high affinity for receptors in chick brain (Whiting and Lindstrom, 1987a). This chicken brain derived mAb 270 cross-reacts with rat brain and identifies the presence of two subunits 51 kDa (homologous to the subunit found as a 49 kDa band from chick brain) and 79 kDa (homologous to the 75 kDa subunit identified by mAb 286 found in chicken brain (Whiting and Lindstrom, 1987a)). Further analysis identifies that there are at least two populations of nAChR contained within chick brain that bind [^{3}H]-nicotine with high affinity; those containing the 49 and 59 kDa subunits and those containing 49 and 75 kDa subunits (Whiting and Lindstrom, 1987a).

Immunopurification using mAb 270 identifies the α4 and β2 subunits as the principal high affinity neuronal [^{3}H]-nicotine binding sites in rat brain. Flores *et al.* (1992) generated antisera against α4 and β2 subunits, these specifically immunoprecipitate receptors labelled by [^{3}H]-cytisine. Few radiolabelled receptors were left in the solubilised rat brain supernatant, further emphasising that greater than 90% of high affinity nicotinic cholinergic recognition sites are α4β2 nAChR. Other antisera generated against α2, α3, α5, β3 and β4 subunits did not decrease the amount of precipitable α4 or β2 subunits (Flores *et al.*, 1992).

As mentioned above, [^{3}H]-epibatidine (also see section 1.6.3) has been used to explore and characterise the diversity of nAChR binding sites in rat and human brain due to its ability to interact with various nAChR subtypes with high affinity (Houghtling *et al.*, 1995; Perry *et al.*, 1995). Epibatidine displays its highest affinity at the α4β2

nAChR with an affinity value (K_D) of 43 pM in rat brain by competition against [^{3}H]-cytisine (Sullivan *et al.*, 1994). In human post-mortem brain tissue the presence of two high affinity nAChR were identified in the cortex, with K_D values of 0.3 and 28.4 pM. The first is thought to represent the α4β2 nAChR while the second site was thought to be representative of an α3-containing (α3*; Lukas *et al.*, 1999) nAChR (Houghtling *et al.*, 1995). The use of [^{3}H]-epibatidine for autoradiography revealed a binding pattern similar to [^{3}H]-cytisine but with greater intensity in the optic nerve, optic chiasm and optic tract. [^{3}H]-epibatidine is therefore labelling an additional nAChR binding site, thought to contain the α3 nAChR subunit (Perry and Kellar, 1995). Zoli *et al.* (1998) performed autoradiography with [^{3}H]-epibatidine in mouse brain and identified that this tritiated nicotinic agonist produced a greater density of binding when compared with [^{3}H]-nicotine, [^{3}H]-cytisine, [^{3}H]-ACh and [^{3}H]-methylcarbamylcholine in a variety of brain regions including the medial habenula and interpenducular nucleus. The concentrations of tritiated radioligands used in this study are such that they are not expected to interact with α3* nAChR except for [^{3}H]-epibatidine, which further confirms it reliably labels α3* nAChR with high affinity (Zoli *et al.*, 1998).

A recent study by Wang *et al.* (1996) showed that [^{3}H]-epibatidine binds to two α3* nAChR sites in the SH-SY5Y cell line with K_D values of 0.15 and 7.4 nM, representing the α3β2 and α3β4 nAChR respectively. Sullivan *et al.* (1994) demonstrated that epibatidine has lower affinity at α-bgt-sensitive nAChR with an affinity of 230 nM in rat brain by competition binding studies performed against [^{125}I]-α-bgt. Epibatidine has shown little or no affinity for other receptors including opioid, 5-HT$_3$, AMPA, kainate, NMDA and GABA$_A$ (Bonhaus *et al.*, 1995). [^{3}H]-epibatidine is therefore a radioligand

that can be used in the present study to reliably identify numbers of α3* nAChR binding sites in SH-SY5Y cells.

1.4.2. High affinity [^{125}I]-α-bgt binding sites:

The α-neurotoxin α-bgt is a toxin isolated from *Bungarus multicinctus* venom, initially used in the characterisation of the prototypical *Torpedo* and neuromuscular type nAChR and has also been utilised, when iodinated, to study the binding sites labelled in brain sections and also in cell culture. α-Bgt binds competitively and with high affinity to neuronal membranes (De Blas and Mahler, 1978; Clarke *et al.*, 1985). As mentioned in the section above, α-bgt is poor at displacing [^{3}H]-nicotine from high affinity nAChR binding sites, as it possesses low affinity for these sites. In comparison to the substantial number of studies performed to map [^{3}H]-nicotinic agonist binding sites, essentially no radioligand binding studies with [^{125}I]-α-bgt have been performed in human post-mortem brain, probably due to post-mortem deterioration. Autoradiographical analysis in mouse (Marks and Collins, 1982; Marks *et al.*, 1986), rat (Clarke *et al.*, 1985) and in human brain (Rubboli *et al.*, 1994; Spurden *et al.*, 1997) show neuronal labelling with [^{125}I]-α-bgt. These binding sites reveal a single high affinity site with a different and distinct distribution to that of [^{3}H]-nicotinic agonist. This signifies that these radiolabelled ligands are not tagging the same populations of neuronal receptors (Clarke *et al.*, 1985). The α-bgt-sensitive receptor can be found densely populating the hippocampal formation and other neuronal populations of rat brain (Séguéla *et al.*, 1993). The nAChR proteins that bind [^{125}I]-α-bgt with high affinity also selectively bind [^{3}H]-MLA (Ward *et al.*, 1990; Davies *et al.*, 1999) and displays strikingly similar distributions as detected by autoradiography (Whiteaker *et al.*, 1999). MLA is a

norditerpenoid alkaloid isolated from the seeds from the *Delphinium* plant that has selective competitive antagonistic actions at α7* nAChR (Ward *et al.*, 1990; Davies *et al.*, 1999) (see section 1.7.1).

The development and availability of mAbs against and different cDNA probes for nAChR subunits has aided in the affinity purification of nAChR and enhanced the ability to locate α-bgt binding proteins within neuronal tissue. The α-bgt binding protein was isolated from chick brain using a mAb raised against the muscle nAChR of chicken (Conti-Tronconi *et al.*, 1985). Purification using α-bgt affinity columns produced bands with apparent molecular masses between 45 and 70 kDa upon SDS-Page analysis. A 54-55 kDa band was alkylated by MBTA and the acetylcholine analogue, bromoacetylcholine, are two cholinergic affinity labels shown to abolish α-bgt binding, indicative that the α-bgt binding protein contains a pair of cysteines like those also located on the α subunits of muscle-type nAChR (Kemp *et al.*, 1985; Kao and Karlin, 1986; see section 1.2 and Figure 1.3).

Initial chick brain cDNA clones (based on α-bgt binding peptide sequences purified from chick brain) were used to discover two nicotinic α subunits that encode α-bgt-sensitive binding proteins in chick brain (Schoepfer *et al.*, 1990). These α-bgt binding subunits were originally designated as α1 and α2 (Schoepfer *et al.*, 1990) are now referred to as α7 and α8 subunits respectively (Britto *et al.*, 1992). These α-bgt binding proteins have had subunit specific mAbs raised bacterially and identify that there are at least two different populations of such α-bgt binding proteins in embryonic day 18 (E18) chick brains. Evidence has revealed that embryonic chick sympathetic neurones express at least three subtypes of native α7* nAChR (Yu and Role, 1998a, b). The predominant subunit in E18 chick brain was the α7* receptor (approximately 75%) and

the minor α-bgt-sensitive receptor population consisted of both α7 and α8 subunits (approximately 15%) (Schoepfer *et al.*, 1990; Keyser *et al.*, 1993). The stoichiometry of these α7α8* nAChR complexes has yet to be elucidated. In addition to these two receptor subtypes, there appeared to be a major receptor complex expressed in chick retina as a homooligomer composed of only α8 subunits. The α8 subunit thus far appears to be uniquely expressed in avians. Based on electrophysiological responses and sensitivity to agonists and antagonists, the α5 subunit has been shown as a candidate subunit expressed with α7 subunits to form heteromeric receptors in chick sympathetic ganglia (Yu and Role, 1998b).

Couturier *et al.* (1990) cloned and sequenced cDNA and genomic clones encoding the α7 nAChR subunit around the same time as Schoepfer *et al.* (1990). The injection into *Xenopus* oocytes of either α7- (Couturier *et al.*, 1990) or α8-cRNAs, allow for the assembly of homomeric complexes (Gerzanich *et al.*, 1994). These subunits efficiently assemble as robust homomeric ACh-gated cation channels that are capable of producing functional nAChR with electrophysiological responses and properties similar to those of certain native α-bgt-sensitive nAChR (Peng *et al.*, 1994a). The responses shown by the α-bgt-sensitive homomeric α7* and α8* receptors when expressed in oocytes are characterised by their high permeability to Ca^{2+}, which triggers the activation of a Ca^{2+}-dependent chloride current, rapid desensitisation, exhibit strong inward rectification (Couturier *et al.*, 1990; Bertrand *et al.*, 1992; Amar *et al.*, 1993; Séguéla *et al.*, 1993; Gerzanich *et al.*, 1994; Castro and Albuquerque, 1995). These studies conclude that native α7 nAChR are homomeric because of the remarkable similarities in kinetic profiles and pharmacological properties of reconstituted homomeric α7 subunits as nAChR when compared to nAChR found in native neuronal tissue preparations (Anand

et al., 1993a). Chen and Patrick (1997) provided further evidence using affinity-purified polyclonal antibodies in Western blot analyses of immunoisolated α-bgt binding proteins purified from rat brain. The data produced was in agreement with the previous hypothesis that the functional α7* nAChR (57 kDa band) is homomeric in nature as this study found no evidence that the α7 subunit was associated with other subunits in the α-bgt sensitive nAChR (Chen and Patrick, 1997).

Another subunit, α9, has been identified, isolated and functionally characterised from the nAChR gene family that binds α-bgt with high affinity (Elgoyhen, *et al.*, 1994). The cloned α9 subunit can be localised in vertebrate cochlear hair cells and assembles as a homomeric receptor after α9-cDNA injection into *Xenopus* oocytes (Elgoyhen, *et al.*, 1994); there was no evidence of expression of the α9 gene in rat brain after in situ hybridisation on rat brain sections (Elgoyhen, *et al.*, 1994). Section 1.5.1 will discuss in more detail the functional expression of these homomeric and heteromeric nAChR complexes.

The snake venom from the protected species of the Taiwanese banded krait *Bungarus multicinctus* contains a mixture of α-toxins, one being α-bgt and another minor component called neuronal-bgt (n-bgt; κ-bgt) (Loring and Zigmond, 1988). When iodinated, this minor component [^{125}I]-neuronal-bgt ([^{125}I]-n-bgt) showed initial promise as it recognised and labelled two sites with high affinity, and has also been shown to antagonise cholinergic transmission in the chick ciliary ganglion (Chiappinelli, 1983). Extensive blockade of α3β2 and partial blockade of α4β2 neuronal receptors was achieved with 10 nM and 1 μM n-bgt respectively (Luetje *et al.*, 1990). Problems arise with availability of the protected *B. multicinctus* species and in the purification process of n-bgt from the venom. There are high concentrations of other contaminating α-toxins

that must be removed to obtain pure n-bgt. This has restricted the usefulness of this ligand for a pharmacological tool in laboratory practice.

1.5. Heterologous expression using *Xenopus* oocytes as a functional expression system:

A profusion of cDNAs for neuronal nAChR subunit subtypes have been identified by molecular cloning techniques (α2-α9, β2-β4; Boulter *et al.*, 1987; Deneris *et al.*, 1989; Nef *et al.*, 1988; Boulter *et al.*, 1990; Couturier *et al.*, 1990) (as mentioned in section 1.3). The use of heterologous expression systems led to the confirmation that nAChR subunit genes encode nAChR subunits by their ability to form functional channels that are responsive to ACh or nicotine (Boulter, 1987; Ballivet *et al.*, 1988). By injecting the synthetic RNAs encoding different α or β neuronal nAChR subunits from rat, chick or human into oocytes of the clawed toad *Xenopus laevis*, provides a transient model of expression to study the electrophysiology and pharmacology of nAChR subtypes (Boulter *et al.*, 1987; Cooper *et al.*, 1991; Luetje and Patrick, 1991; Gerzanich *et al.*, 1994; Peng *et al.*, 1994a). By way of pentameric co-assembly (Anand *et al.*, 1991), the injected subunit RNAs combine to create viable robust *in vitro* heteromeric or homomeric receptor combinations with various stoichiometries, herein lies the diversity of nAChR subtypes (Luetje and Patrick, 1991). nAChR complexes will have different channel properties depending on the particular α and β subunits expressed and contained within their pentameric structure.

Further analysis can distinguish if there are differences between the pharmacological properties of receptors expressed endogenously in their native environment *in vivo* and those of receptor complexes expressed either in *Xenopus* oocytes or in transfected cell

lines *in vitro*. These expression systems are useful to aid in the pharmacological determination of individual nAChR with known stoichiometries and consequently deducing nAChR subtypes that assemble *in vivo*. Different subunit combinations form a plethora of functional receptors in the brain with significant pharmacological diversity from receptor to receptor (Luetje *et al.*, 1990).

1.5.1. Neuronal nAChR subunits expressed *in vitro* as functional receptors:

1.5.1.1. Heteromeric nAChR expression:

Xenopus oocytes were found to express functional nAChR channels after co-injection of pairwise combinations of either β2 or β4 subunit mRNAs with α2, α3 or α4 receptor subunit mRNAs (Deneris *et al.*, 1991; Sargent, 1993; McGhee and Role, 1995). Boulter *et al.* (1987) demonstrated that functional neuronal receptors could be reconstituted from as few as one or two types of subunit gene product, described as homomeric and heteromeric nAChR respectively. Boulter *et al.* (1987) concluded that heterodiomeric receptors in their study were derived from combinations of a specific α RNA (either α3 or α4) and the other from β2 RNA. When expressed on its own, the β2 transcript produced no response to ACh. The presence of either α3 or α4 subunit RNA was necessary for the formation of a fully functional nAChR, as identified by testing for depolarisation in response to perfused ACh (Boulter *et al.*, 1987). This is also true for the α3 transcript when expressed alone, no response is observed and requires the presence of the synthetic RNA corresponding to the β2 subunit to produce a functional cationic channel. Similar ACh induced currents, that were reversibly blocked by hexamethonium and showed little sensitivity to or were resistant to functional blockade

by α-bgt, were recorded from oocytes co-injected with full-length cDNAs for α4 and a "structural" β subunit of avian brain nAChR (Boulter *et al.*, 1987; Ballivet *et al.*, 1988).

Most of the neuronal α and β subunit transcripts (α2-α4 and β2 and β4 respectively) when expressed individually in oocytes are not capable of forming functional nicotinic ionophores, indicating that they exist as heteromeric complexes. One study established a cholinergic response in a third of all oocytes injected and expressed with the α4 subunit alone (Boulter *et al.*, 1987). Homomeric nAChR constituted from α4 clones assemble as unstable, weakly functional LGIC capable of producing a small depolarisation and opening of the ion-channel only in the presence of high concentrations of ACh (Boulter *et al.*, 1987).

The sensitivity of the six putative functional neuronal nAChR assembling after co-injecting synthetic RNA encoding one of two different β subunits (β2 or β4) and one of three different α subunits (α2, α3 or α4) expressed in *Xenopus* oocytes were investigated with respect to their rank order of potency for nicotinic agonists, ACh, nicotine, cytisine and 1, 1-dimethyl-4-phenylpiperazinium (DMPP) (Luetje and Patrick, 1991). These observations indicate that heteromeric nAChR assemble from α and β subunits with both subunits contributing to the pharmacological and functional profile of the nAChR LGIC (Luetje and Patrick, 1991). The β subunit has a profound affect on the rate at which agonist binds to receptors to evoke opening and also in agonist and antagonist dissociation rates from nAChR (Papke and Heinemann, 1991; Papke *et al.*, 1993; Luetje *et al.*, 1993; Harvey and Luetje, 1996; Harvey *et al.*, 1996). The resulting nAChR complexes display unique patterns of sensitivity to basic pharmacological agents and display distinct physiological properties. nAChR composed of α2, α3 or α4 with β2 were generally less sensitive to cytisine than the corresponding β4* receptors.

This led to the conclusion that the β subunit contributes, most noticeable, to the sensitivity of the receptor to cytisine the most potent of the nicotinic agonists studied. Cytisine acts as a partial agonist at receptors assembling with the β2 subunit, while being a full agonist and therefore more sensitive at β4* nAChR (Luetje and Patrick, 1991).

The α subunits are also important in the determination of the rank order of potency in either β2* or β4* nAChR complexes (Luetje and Patrick, 1991). Oocytes injected with either chick neuronal α3 or α4 cDNA expression vectors constituted with a β2 subunit cDNA displayed functional receptors readily distinguished by their sensitivity and desensitisation to ACh (Gross *et al.*, 1991). As the β2 subunit was conserved in both subunit subtypes, it denotes the α subunits as responsible for the observed functional differences. α3 Subunit cDNA expressed a nAChR in oocytes with a lower agonist sensitivity and a stronger desensitisation profile than α4/β2 receptors (Gross *et al.*, 1991). Sensitivity depends on the affinity of agonist binding to a receptor and the efficiency of the agonist once bound to mediate channel opening of a receptor and is a measure of the dose of agonist required to evoke the desired effect. Desensitisation is defined as when a receptor loses the ability to evoke a response as a consequence of a prolonged stimulus. As well as the α subunit playing a role in desensitisation in chick neuronal nAChR, there is also evidence for the importance of the "structural" β subunit being important in the time course of desensitisation in both *Torpedo* and neuronal rat α3* nAChR (Unwin *et al.*, 1988; Cachelin and Jaggi, 1991 respectively). The latter study discovered that in α3β2 nAChR desensitisation occurred faster and was more extensive than that observed with α3β4 nAChR and complements previous results from other groups.

Native receptors have been suggested to be composed of more than two subunit subtypes, due to the difference in pharmacological and physiological properties of expressed receptors in heterologous expression systems with only two subunit types (Sivilotti *et al.*, 1997). This has been extrapolated from immunoprecipitation studies that show neurones can express more than two subunit subtypes (Conroy and Berg, 1995). Oocytes can indeed form functional heterotrimeric nAChR from three nAChR subunits. Expression of cDNA coding for (α3, β2 and β4) rat subunits and (α3, α5, and β4) and (α5, α4 and β2) subunits of chick have been demonstrated to form functional heterotrimeric nAChR (Colquhoun and Patrick, 1997, Vernallis *et al.*, 1993; Ramirez-Latorre *et al.*, 1996; Conroy and Berg, 1995). The α3β2β4 nAChR possessed mixed characteristics of the α3β2 and α3β4 nAChR when expressed in oocytes. The heterotrimeric α3β2β4 nAChR was therefore activated by cytisine and blocked by n-bgt (Colquhoun and Patrick, 1997). The functional response evoked by cytisine and the n-bgt inhibition of the α3β2β4 nAChR is donated by the α3β4 and α3β2 subunits pairs respectively.

The α5 subunit did not form functional receptors when expressed as a homopentameric complex or when co-injected with any one subtype of β subunit alone (Boulter *et al.*, 1990; Ramirez-Latorre *et al.*, 1996), nor did they assemble as pairs with α3 subunits (Wang *et al.*, 1996). Functional nAChR assembled on the cell surface of oocytes when either the human α3 and β2 or α3 and β4 subunit RNAs were co-injected with the α5 receptor subunit RNA into *Xenopus* oocytes (Wang *et al.*, 1996). The α5 subunit also forms functional receptors when co-expressed with α3 and β4 subunit cDNAs in the human BOSC-23 cell line (Fucile *et al.*, 1997). The presence of the α5 subunit incorporated into a heterotrimeric receptor appears to increase the rate of

desensitisation of the nAChR, produce a receptor with a greater probability of opening and a greater chance of being activated by nicotinic agonists (Ramirez-Latorre *et al.*, 1996; Wang *et al.*, 1996).

The α6 nAChR subunit was termed as an "orphan" receptor subunit until recently, as it had not been shown to form a functional LGIC. cDNA encoding the chick α6 subunit forms a heteromeric functional nicotinic LGIC in oocytes when expressed with β4 subunit cDNA (Gerzanich *et al.*, 1997). The rat β3 nicotinic subunit does not participate in the formation of functional nAChR activated by nicotine or ACh when co-injected in the form of mRNA with wild-type α2, α3, α4 or α7 genes into oocytes (Deneris *et al.*, 1989; McGehee and Role, 1995; Palma *et al.*, 1999). A reason may be that although the β3 subunit is nicotinic and may be able to assemble with cloned nAChR subunits, they are perhaps just not able to form functional nicotinic channels with these nAChR subunits that have been identified to date. Failure of the β3 subunit to form functional channels with other wild-type nAChR subunits in *Xenopus* oocytes may be simply that the gene products do not assemble correctly together in this expression system or they may require a specific post-translational modification process not made by the oocytes in order for them to function. Forsayeth and Kobrin (1997) transfected COS cells with cDNAs for α4, β2, β3 and β4 subunits which coassembled to form a functional LGIC. By omitting a single subunit cDNA from the transfection it was possible to establish the role of each subunit in the α4β2β3β4 receptor subtype. The β3 subunit appears to function as a structural component that links the α4β2 heterodimer to the more stable α4β4 receptor subtype. It has also been demonstrated that the β3 subunit gene can form functional channels in oocytes with a mutant α7 nAChR subunit (^{L247T}α7) (Palma *et al.*, 1999). The β3 subunit, when inserted with a reporter mutation (V273T) to produce

$^{V273T}\beta3$, can also be expressed in oocytes with α3 and β4 subunits to form functional channels; the mutation converts the hydrophobic residue in the middle of the transmembrane domain M2 into a hydrophilic residue and would be expected to increase the channels sensitivity to agonists (Groot-Kormelink *et al.*, 1998).

To demonstrate the reliability and accuracy of *Xenopus* oocytes as a heterologous expression system, the expression of a known subunit composition of mouse muscle nAChR in oocytes displayed similar single-channel currents that were characteristic of those reported for the same receptors expressed in BC3H-1 cells (Luetje and Patrick 1991). This study therefore suggests that oocytes are capable of accurately expressing LGIC with similar properties to those expressed in their native environment. The ultimate goal of using heterologous expressions systems is to elucidate the function and stoichiometry of nAChR found *in vivo* in their native environment which to date is still poorly understood.

1.5.1.2. Homomeric nAChR expression:

Reports involving heterologous *in vitro* expression studies revealed that most of the α and β subunits co-assemble to form functional nAChR channels. The mRNA for α7-α9 nAChR subunits can efficiently be expressed to give subunits that assemble in *Xenopus* oocytes, resulting in the formation of robust fully functional homomeric cation LGIC (Couturier *et al.*, 1990; Séguéla *et al.*, 1993; Gerzanich *et al.*, 1994; Elgoyhen *et al.*, 1994; Chen and Patrick 1997). These homomeric channels are activated by ACh and channel responses are potently blocked in the presence of nanomolar concentrations of α-bgt (IC_{50} = 0.7 nM).

As members of a family of LGIC, the nAChR family has an apparently simple functional repertoire: they bind a specific ligand, open the channel pore, conduct specific ions across the membrane and can result in receptor desensitisation. The entry of positively charged cations through nAChR leads to depolarisation and is a classical example of how these receptors can influence the biology of the cell. Homomeric receptors share the characteristics of desensitising rapidly and have a high permeability to Ca^{2+} when compared to heteromeric pairwise combinations of neuronal α and β subunits. Homomeric α7 subunits expressed in oocytes have a Ca^{2+}: Na^{2+} permeability ratio close to 20 compared to receptors composed of various α/β stoichiometries which have a ratio of 1:1.5 (McGehee and Role, 1995; Role and Berg, 1996). The recognition that these homomeric nAChR have a high Ca^{2+} permeability has opened the possibility that they are capable of directly mediating several Ca^{2+}-dependant intracellular processes and demonstrate a relevant role for nAChR in Ca^{2+} signalling (Séguéla *et al.*, 1993; Chan and Quik, 1993; Pugh and Berg, 1994; Role and Berg, 1996; Pugh and Margiotta, 2000).

The pharmacological characteristics of homomeric α7 subunits expressed in oocytes (Anand *et al.*, 1993a; Peng et al., 1994a; Castro and Albuquerque, 1995; Alkondon *et al.*, 1998) or in cells stably transfected with human or rat nAChR subunit α7 cDNA (Gopalakrishnan *et al.*, 1995; Quik *et al.*, 1996) show an excellent correlation to and are similar to native α-bgt-sensitive nAChR (as reviewed by McGehee and Role, 1995). When ligand binding studies are compared there was found to be a 50 fold discrepancy with regard to the binding affinity of cytisine for this receptor, which brought about debate on whether the native α7 receptor is homomeric in nature (Anand *et al.*, 1993a). Co-injections of a mixture of any of the muscle subunits α, β, γ, or the neuronal α3, α5, β2, β3 and β4 nAChR subunits with the α7 subunit gene, do not modify the sensitivity

or physiological characteristics of the α7 subunit when expressed alone. This indicates that in oocytes at least, α7 subunits do not combine with other known neuronal nAChR subunits and therefore assemble as homomers (Couturier *et al.*, 1990; Séguéla *et al.*, 1993; McGehee and Role, 1995). As mentioned in section 1.4.2, there are cases where the α7 subunit is thought to form receptors *in situ* by combining with the α8 subunit to create functional receptor channels containing both the α7 and α8 subunits in chicken brain (Keyser *et al.*, 1993).

In the avian and mammalian CNS, the α7 homomeric nAChR is the predominant α-bgt-sensitive binding site (Anand *et al.*, 1991b). Homomeric α8 nAChR are predominantly expressed in chick retina and when reconstituted in oocytes share many of the functional channel properties and elicit time course responses that are indistinguishable from homomeric α7 channels (Couturier *et al.*, 1990; Séguéla *et al.*, 1993; Gerzanich *et al.*, 1994). α8 Homomers exhibit lower affinity for α-bgt but higher affinity for other nicotinic agonists (Gotti *et al.*, 1994; Gerzanich *et al.*, 1994). The affinities and efficacies of ligands for chick α7 and α8 homomers expressed in oocytes have also been shown to reflect the ligand-binding characteristics of natively expressed α7 and α8 nAChR (Gerzanich *et al.*, 1994).

Homomeric α9 nAChR have distinctive pharmacology and electrophysiological properties when compared to α7 and α8 homo-oligomers (Elgoyhen *et al.*, 1994). These receptors have a mix of nicotinic and muscarinic properties, in that the nicotinic agonists ACh, DMPP, and the muscarinic agonist oxotremonine activate the receptor. α9 nAChR are also functionally blocked in the presence of moderate concentrations of α-bgt and n-bgt (100 nM), nicotine, muscarine, d-TC and atropine. These pharmacological characteristics of the homomeric α9 nAChR expressed in oocytes,

reveals remarkably similar properties to the cholinergic receptor present at the synapse between cochlear efferent neuronal terminals and hair cells in the chick and guinea pig cochlea. It remains to be elucidated whether this homomeric α9 receptor is representative of the native α9 receptors obtained from rat cochlear hair cells (Elgoyhen *et al.*, 1994).

The production of functional nAChR channels after artificially expressing neuronal nAChR subunits in non-neuronal cell systems has helped to demonstrate that different subunit combinations display similar pharmacological properties to those receptors found *in situ*. Stable transfection of subunit cDNAs into neuronal/non-neuronal cell lines provide a means of expression to characterise pharmacological, physiological and biochemical properties of the various combinations of both homomeric and heteromeric receptors in a cellular environment, for example, α7, α4β2, α3β2* and α3β4* nAChR. Comparisons then can be drawn from the responses evoked by receptors stably transfected *in vitro* and compared to responses elicited by native neuronal receptors expressed *in vivo* (Gopalakrishnan *et al.*, 1996; Quik *et al.*, 1996). It still remains to be elucidated whether many of the artificial nAChR subtype combinations generated *in vitro* are representative of, and occur within their natural neuronal membrane environment *in vivo*. It is becoming apparent that the stoichiometry of neuronal nAChR is more complex than was first thought and therefore the diversity of nAChR may have been underestimated. The expression of multiple nAChR subtypes within the same neuron may be explained by the diverse functional and regulatory features associated with individual receptors providing them with their unique pharmacological profiles for ion permeability, channel opening duration, agonist and antagonist affinities and various physiological functions *in vivo*.

1.6. Introduction to some nicotinic agonists of interest to this thesis:

1.6.1. Anabaseine:

Anabaseine, 2-(3-pyridyl)-3,4,5,6-tetrahydropyridine, is a pyridine nicotinoid alkaloid neurotoxin found in some marine worms, nemertines e.g. the hoplonemertine *Paranemertes peregrina*, and isolated from venom glands of some terrestrial insects, ants (Wheeler *et al.*, 1981; for review, see Kem, 1985). These naturally occurring toxins are thought to have offensive and defensive functional roles, perhaps against predators or to capture prey after prolonged topical administration. The chemical structure of anabaseine (Figure 1.8) resembles nicotine and anabasine, the homolgue of nornicotine, which are two of the major naturally occurring alkaloids found in the tobacco plant (see Holladay *et al.*, 1998).

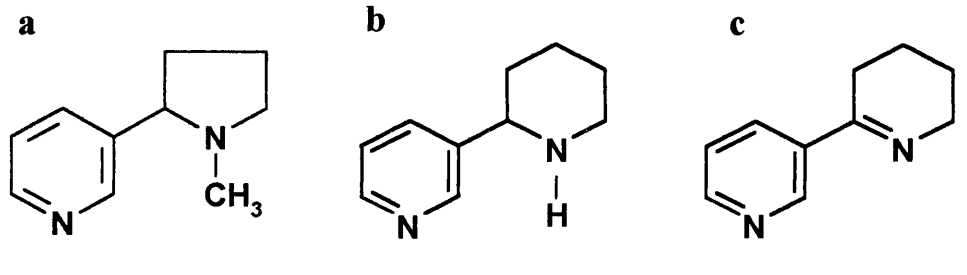

Figure 1.8. The structure of (a) nicotine, (b) anabasine and (c) anabaseine.

Anabaseine is pharmacologically appealing and has been useful as a molecular model for nicotinic drug design, due to its potency as an agonist at both peripheral and central nicotinic receptors (Kem *et al.*, 1971, Meyer *et al.*, 1994). This compound was found to have pharmacological activity at all of the nicotinic subtypes tested in muscle and neuronal preparations in a variety of systems investigated, including *Xenopus*

oocytes, cultured cells, and contractility assays using muscle strips (Kem *et al.*, 1997). Anabaseine was selective for activity at nAChR and this compound did not possess activity at rat brain muscarinic receptors, except at high concentrations > 100 μM (Kem *et al.*, 1997). Anabaseine has also been demonstrated to cause upregulation of central nicotinic binding sites (Collins *et al.*, 1990).

Anabaseine exhibits a twenty-fold weaker affinity than nicotine at high affinity nicotine binding sites in rat brain and in contrast is highly efficacious at stimulating α7-homomeric channels in oocytes displaying high affinity for neuronal α-bgt binding sites in the high nanomolar range (De Fiebre *et al.*, 1995; Kem *et al.*, 1997). In terms of affinity, the rank order of potency of anabaseine was compared to the tobacco alkaloid compounds at rat brain membrane α-bgt binding sites was anabaseine > anabasine > nicotine (Kem *et al.*, 1997). At the α4β2 nAChR subtype the apparent affinities and efficacies of anabaseine and anabasine were less than observed with nicotine, showing their weak partial agonist activity (Kem *et al.*, 1997). When these compounds were tested on different autonomic nAChR differences in potency resulted. This may be attributed to the expression of different nAChR subtypes.

Several novel anabaseine-derived compounds have been synthesised after reactions with aldehydes to produce 3-substituted derivatives (Zoltewicz *et al.*, 1993). Some of these derivatives are thought to possess cytoprotective and also memory-enhancing properties (see section 1.6.2.1). It has been proposed that these actions of novel anabaseine derivatives may arise due to their interaction with brain nAChR and have been subject to pharmacological evaluation. This was the impetus for Meyer *et al.* (1994) to test the ability of anabaseine derived compounds to displace the binding of [^{3}H]-cytisine from rat brain membranes, [^{125}I]-α-bgt binding from neuronal nicotinic

binding sites, and to alter the function of α4β2 and α7* nAChR expressed in *Xenopus* oocytes (De Fiebre *et al.*, 1995). Results suggest that these anabaseine 3-substituted derivatives do not diminish peripheral nervous system nAChR activity and α4β2 activity and thus these compounds may be candidates as partial α7 agonists and antagonists at α3β4 and other nAChR (De Fiebre *et al.*, 1995). Advances in this field will be advantageous, to identify compounds with selective activities at specific nAChR subtypes. In view of the narrow therapeutic window for nicotine and its undesirable peripheral actions (tachycardia, increased blood pressure, nausea and abdominal pain), these anabaseine-related compounds may be of physiological value and have clinical potential as candidate neurological tools, employed as therapies for the possible treatment of neurological disorders and dementia (Shimohama, 1996).

1.6.2. Novel Anabaseine derivatives:

1.6.2.1. 3-(2, 4)-dimethoxybenzylidene anabaseine (GTS-21; DMXB):

An anabaseine derivative, 2, 4-dimethoxybenzilidene, (GTS-21; DMXB, Figure 1.9) has been evaluated for its neuroprotective properties as a therapeutic drug for the treatment of Alzheimer's disease (AD) (Kem *et al.*, 1996; Meyer *et al.*, 1997). GTS-21 has been characterised with respect to activity at nAChR subtypes and has been shown to displace high affinity [^{125}I]-α-bgt and [^{3}H]-acetylcholine binding (Hunter *et al.*, 1994). [^{3}H]-cytisine binding was displaced by GTS-21 in both rat brain preparations and in the K177 cell line (Meyer *et al.*, 1994; Briggs *et al.*, 1997). Studies using *Xenopus* oocyte preparations indicate that GTS-21 possesses partial agonist activity at human and rat α7* homomers and not at the human or rat α4β2 nAChR subtype (or other combinations including, α2β2, α3β2, α2β4,α3β4 and α4β4) expressed in oocytes,

indicating its apparent specificity as a novel α7-selective agonist (Hunter *et al.*, 1994; De Fiebre *et al.*, 1995; Meyer *et al.*, 1997).

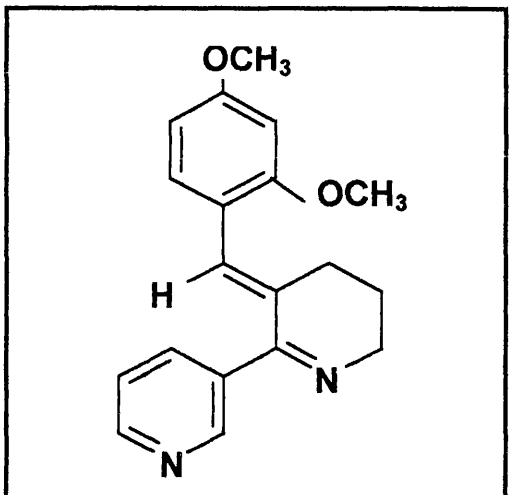

Figure 1.9. The structure of DMXB.

In vivo microdialysis analysis of cortical extracellular ACh, dopamine (DA), norepinephrine (NE) and 5-HT levels has been investigated after the administration of either anabaseine or GTS-21 (Summers *et al.*, 1997). Anabaseine was found to increase cortical levels of ACh and NE above baseline controls (in a mecamylamine sensitive manner) without having significant effects on DA or 5-HT. Contrasting results were obtained with GTS-21 in that it increased NE and DA without affecting ACh and 5-HT levels. Mecamylamine applied before the administration of GTS-21 led to an increase in ACh and 5-HT levels, with a slight decrease in the release of cortical NE and DA when compared to GTS-21 applied alone (Summers *et al.*, 1997). nAChR present may normally have a tonic inhibitory effect on ACh release. If this effect is blocked by mecamylamine, this could be a possible explanation of the increase in ACh evoked by GTS-21 after a pre-administration of mecamylamine, thus permitting the stimulatory

effect of GTS-21 at α7 receptors to be revealed. Further *in vivo* analysis will be essential to characterise the effects of GTS-21 and the other anabaseine derivatives. GTS-21 can also release [^{3}H]-DA from rat striatal slices that can be blocked by the nicotinic antagonist DHβE (Briggs *et al.*, 1997).

This compound has been used in animal models of cognition, has potential learning and memory-enhancing actions as it was found to facilitate the induction of LTP in rat hippocampus (Hunter *et al.*, 1994; Briggs *et al.*, 1997; Meyer *et al.*, 1997). When GTS-21 was administered to mice it appeared not to have adverse effects and displayed low toxicity in comparison to nicotine. A dose of 185 μg/mol/kg administered i.p. to mice was lethal. GTS-21 also has neuroprotective actions against β-amyloid neurotoxicity, and protects against neocortical neuronal cell loss induced by lesions of the nucleus basalis magnocellularis in rats (Meyer *et al.*, 1994; Arendash *et al.*, 1995; Shimohama, 1996, 1998; Nanri *et al.*, 1997). This compound may therefore be a putative therapy capable of treating dementia and is currently undergoing clinical trials. This identifies other neuronal nAChR subtypes other than α4β2 as targets for putative therapy for dementia and a new class of agent as a target for drug discovery in the treatment of these neurological disorders.

1.6.2.2. 3-[(4-Dimethylamino) cinnamylidene] anabaseine maleate (DMAC).

Another synthetic analogue of anabaseine is DMAC (see Figure 1.10 for structure). DMAC has been reported to displace high affinity [^{3}H]-cytisine binding from rat brain membranes (Meyer *et al.*, 1994); its relative potency for displacement of 1 nM [^{3}H]-cytisine binding, compared to the parent compound and other novel anabaseine derivatives, is: anabaseine > 3-(4)-dimethylaminobenzylidine anabaseine (DMAB) =

DMXB >anabasine > DMAC (Meyer *et al.*, 1994; De Fiebre *et al.*, 1995). This demonstrates that DMAC is the least potent at displacing [^{3}H]-cytisine from rat brain membranes, therefore exhibiting low binding potency for the α4β2 nAChR subtype.

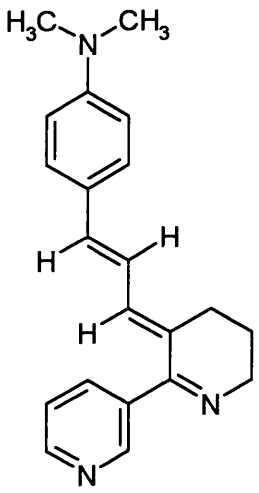

Figure 1.10. The structure of DMAC.

When DMAC was examined for potency at the α7* nAChR it was found to be more potent than nicotine, ACh, anabaseine and the other 3-substituted anabaseine derivatives at displacing [^{125}I]-α-bgt sensitive binding from rat brain membranes (De Fiebre *et al.*, 1995). The relative K_i values for DMAC at displacing [^{125}I]-α-bgt, when compared to the parent compound and other novel substituted derivatives, is: anabaseine < DMXB < DMAB < DMAC. Hunter *et al.* (1994) also demonstrated that DMAC was a α7-selective agonist and the most potent compound compared to anabaseine and its series of novel derivatives at activating the α7 subtype. All of the anabaseine derivatives displayed significant agonist activity at the α7 nAChR, unlike agonist activity at the α4β2 subtype, with DMAC being the most potent at displacing [^{125}I]-α-bgt binding and activating α7* nAChR (De Fiebre *et al.*, 1995). The response evoked by DMAC was

assessed at other nAChR subtypes in oocytes expressing either α4β2, α4β4, α2β2, α3β2 or α1β1γδ cRNA. This DMAC evoked response was compared to the response elicited by ACh. Maximal responses were obtained with DMAC using concentrations ranging from 1-500 μM and these responses were approximately 1% of the ACh control response (De Fiebre *et al.*, 1995) showing little agonist activity at other nAChR subtypes.

In summary, previous data indicate that the 3-substituted anabaseine derivatives characterised to date selectively activate α7 nAChR over α4β2 subtypes, indicating some degree of selectivity. DMAC, when compared with anabaseine and other novel anabaseine-derived compounds, is the most potent at displacing [^{125}I]-α-bgt binding from its putative α7 receptor binding site and is least potent when displacing [^{3}H]-cytisine binding from the putative α4β2 nicotinic receptor subtype found in rat brain membranes. The selectivity of these anabaseine-derived compounds for α7* nAChR will be useful to elucidate the physiological function and decipher putative roles for neuronal α7 nAChR in normal CNS functioning and in human CNS pathologies, for example AD and their putative roles as cytoprotective and memory enhancing agents.

DMAC was synthesised by Organon (Newhouse) for analyses documented in this thesis (Chapter 2 and 3). Initial experiments were conducted to draw comparisons the potency of DMAC at different nAChR binding sites by using [^{3}H]-nicotine, [^{3}H]-epibatidine, [^{125}I]-α-bgt and [^{3}H]-MLA in competitive binding assays initially using rat brain membranes with DMAC (see section 2.7.2.1). This compound will also be examined with nicotine and KCl with respect to chronic drug treatment and investigating its ability to produce upregulation of α3* and α7* nAChR in primary hippocampal and also SH-SY5Y cell cultures (Chapter 2 and 3).

1.6.3. Epibatidine:

Epibatidine is a potent nicotinic ligand that was first isolated from skin extracts of an Ecuadorian poison frog *Epipedobates tricolor* (Figure 1.11), by Daly and co-workers who also elucidated its structure (Spande *et al.*, 1992), shown below in Figure 1.12.

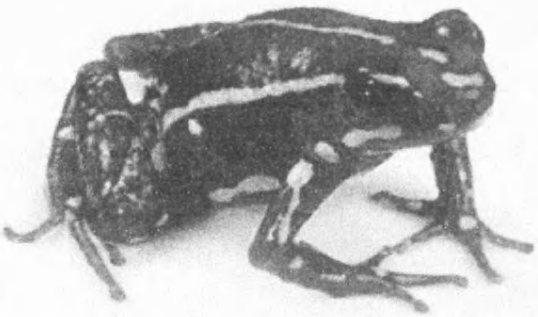

Figure 1.11. Epipedobates tricolor.

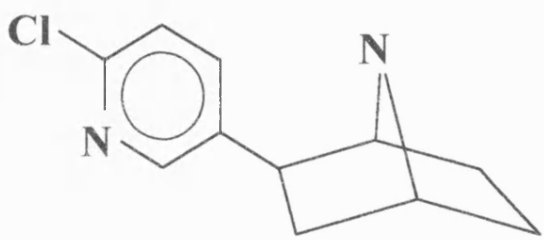

Figure 1.12. The structure of (+)-epibatidine, the natural enantiomer.

After the structure of epibatidine was established, epibatidine was readily synthesised. Both enantiomers are pharmacologically equipotent in most cases and display high affinity for nAChR sites in whole rat brain studies (Badio and Daly, 1994; Damaj *et al.*, 1994; Bonhaus *et al.*, 1995; Badio *et al.*, 1995). A K_i value of between 20-60 pM for epibatidine at α4β2 receptors was found in rat brain by competition against [^{3}H]-nicotine and [^{3}H]-cytisine demonstrating that this is the highest affinity ligand known at these receptors (Badio and Daly, 1994; Damaj *et al.*, 1994; Sullivan *et al.*, 1994).

This azabicycloheptane alkaloid displays potent analgesic-like effects *in vivo* that are not reversed by naloxone, an opiate receptor antagonist (Spande *et al.*, 1992; Damaj *et al.*, 1994). These effects were blocked by the neuronal nAChR channel blocker mecamylamine, which crosses the blood brain barrier, and DHβE, but not blocked by

hexamethonium, a compound that does not cross the blood brain barrier (Qian *et al.*, 1993; Badio and Daly, 1994; Damaj *et al.*, 1994; Rupniak *et al.*, 1994; Badio *et al.*, 1995; Bonhaus *et al.*, 1995). These findings identify epibatidine as an analgesic agent that acts highly selectively and potently via a neuronal nicotinic mechanism (Qian *et al.*, 1993; Rupniak *et al.*, 1994). Epibatidine exerts other effects consistent with potent actions at nAChR. When injected into mice there is a mecamylamine-sensitive reduction in body temperature and a decrease in the observed locomotor activity at doses more potent than nicotine in evoking similar behavioural responses (Damaj *et al.*, 1994; Sullivan *et al.*, 1994). Epibatidine when administered in high doses also displays toxic effects of laboured respiration, reduced activity and convulsions resembling those toxic effects produced by nicotine.

Epibatidine has in fact got high affinity for both neuronal and neuromuscular nAChR with little or no significant affinity for other (non-nicotinic) receptors. This was shown by the lack of effect of epibatidine (10 μM) when used in a range of radioligand-binding assays for opioid, muscarinic, adrenergic, DA, 5-HT, AMPA, kainate, NMDA and $GABA_A$ receptors (Qian *et al.*, 1993; Badio and Daly, 1994; Rupniak *et al.*, 1994; Bonhaus *et al.*, 1995). This potent ligand therefore has been used to pharmacologically explore the diversity of nAChR subtypes. Epibatidine is available as a tritiated ligand which can be used reliably to label a variety of nAChR complexes with extraordinarily high affinity, which is in contrast to other nicotinic ligands and in particular [^{3}H]-nicotine which only reliably labels the α4β2 site and displays a large proportion of non-specific *in vivo* binding (London *et al.*, 1995) (see section 1.4.1). Both enantiomers of epibatidine displace the binding of [^{3}H]-nicotine to rat brain membranes (Damaj *et al.*, 1994; Rupniak *et al.*, 1994). Both of the enantiomers of epibatidine behaved as full agonists when examined in *Xenopus* oocytes using a variety of species neuronal nAChR

subtypes including chicken (α3β2, α3β4, α4β2, α7 and α8) and human (α3β2, α3β4 and α7) (Gerzanich *et al.*, 1995).

[^{3}H]-epibatidine can be used in radiolabelled binding assays to detect α3* nAChR with high affinity (Perry and Kellar, 1995; Lukas *et al.*, 1999). Hence the utility of this tritiated agonist to label α3* nAChR endogenously expressed in the human neuroblastoma SH-SY5Y cells or ganglionic-type nAChR present in rat pheochromocytoma PC12 cells used in this thesis. [^{3}H]-Epibatidine saturably binds at an α3* nAChR expressed in PC12 cells with a K_D of 83 pM and to two sites, α3β2 and α3β4 nAChR in SH-SY5Y with K_D values of 0.15 and 7.4 nM respectively (Wang *et al.*, 1996). In rat forebrain homogenates, where a heterogeneous population of nAChR are expressed, [^{3}H]-epibatidine was found to saturably bind to two distinct sites with low non-specific binding. [^{3}H]-epibatidine bound with K_D values of 15 pM and 360 pM putatively representing the α4β2 and α3* nAChR binding sites respectively (Houghtling *et al.*, 1995). Each site was found to represent 50% of [^{3}H]-epibatidine binding as each site appeared to be present in equal densities within the rat forebrain homogenates. Autoradiographical analysis comparing the binding of [^{3}H]-epibatidine to that found with [^{3}H]-nicotine and [^{3}H]-cytisine identifies differential maps for these radioligands in rat and mouse brain slices (Perry and Kellar, 1995; Marks *et al.*, 1998; Zoli *et al.*, 1998).

Zoli et al. (1998) combined data relating to the pharmacological properties of nAChR, their location and functional responses evoked from defined brain regions and compared responses in wild-type mice and those lacking the β2 subunit. In mice lacking the β2 subunit four distinct subtypes of nAChR were identified after autoradiography and patch-clamp recordings in thin murine brain slices (Zoli *et al.*, 1998). Type 1

nAChR are α-bgt-sensitive and the pattern of [^{125}I]-α-bgt binding obtained from autoradiography did not change significantly in β2 mutant mice, but was abolished in α7 mutant mice (Orr-Utreger *et al.*, 1997) identifying the presence of α7 and not β2 subunits. Type 2 nAChR represent the vast majority of high affinity [^{3}H]-epibatidine binding sites in mouse brain and contain the β2 subunit as high affinity [^{3}H]-nicotine binding was abolished in β2 mutant mice. α-Bgt did not bind to these receptors, in contrast all nicotinic agonists bound to these nAChR with high affinity and are therefore thought to be α4β2 nAChR. Type 3 nAChR bind [^{3}H]-epibatidine with high affinity, their persistence in β2 mutant mice strongly suggests they lack the β2 subunit and are probably composed of α3β4 subunits. Type 4 nAChR bind both [^{3}H]-epibatidine and [^{3}H]-cytisine with high affinity, this binding is maintained in β2 mutant mice indicating that these nAChR do not contain the β2 subunit. The putative composition of these receptors could either be α2 and/or α4 with β2 subunits or α3 and/or α4 with β4 subunits. The binding differences observed with [^{3}H]-epibatidine therefore reflect nAChR heterogeneity and the ability of [^{3}H]-epibatidine to label more than one nAChR subtype with high affinity, revealing an α3* component.

Epibatidine has lower affinity for the displacement of [^{125}I]-α-bgt from the neuronal α7 α-bgt-sensitive nAChR subtype present in rat brain (K_i = 230 nM) but is more potent when competing for the receptor present in *Torpedo* electroplax (K_i = 2.7 nM) (Sullivan *et al.*, 1994). [^{3}H]-Epibatidine opens new avenues to characterise and deduce pharmacological properties of nAChR due to its exceptionally high affinity for these receptor sites in brain, periphery, ganglia and in cell lines. The high potency of epibatidine provides a structural basis to model new compounds as selective probes with high affinity for specific nAChR subtypes within the brain and to help in the study

of central nicotinic cholinergic systems. Such compounds may be useful in clinical trials as safe and efficacious non-opioid analgesic therapies that would overcome unwanted side effects of narcotic analgestics, which include respiratory depression, emesis, sedation and dependence, or as potential tools in the treatment of pathological conditions involving central neuronal nAChR function.

1.7. Some nicotinic antagonists of interest to this thesis:

1.7.1. Methyllycaconitine (MLA):

MLA is a tertiary norditerpenoid alkaloid isolated from the seeds of *Delphinium brownii*, and found to have a markedly greater affinity for the [^{125}I]-α-bgt binding site (MacAllan *et al.*, 1988; Ward *et al.*, 1990) in brain compared to the muscle type nAChR (Ward *et al.*, 1990), with approximate K_i values of 1 nM and 1 μM respectively. The reversible concentration-dependent inhibition by MLA was also observed on ACh and anatoxin-a evoked currents in cultured fetal rat hippocampal neurones (Alkondon *et al.*, 1992). The action of MLA was specific to nAChR, no blockade of the responses to NMDA, quisqualate, kainate or GABA receptor agonists were observed in neurones (Alkondon *et al.*, 1992).

MLA is a potentially useful probe to dissect nAChR subtypes and to characterise the pharmacological and physiological functions of α7* α-bgt-sensitive nAChR from their α-bgt-insensitive counterparts in the mammalian nervous system. MLA is a small, reversible, potent, competitive antagonist compared to the large, pseudo-irreversible nature of the snake neurotoxin α-bgt. In the tritiated form, [^{3}H]-MLA is a relatively novel radioligand that binds to a single class of binding site in rat brain membrane preparations (Davies *et al.*, 1999). Autoradiographic analysis with [^{3}H]-MLA in mouse

brain sections reveals binding that closely parallels that obtained with [^{125}I]-α-bgt (Whiteaker *et al.*, 1999). [^{3}H]-MLA may therefore help to quantitate and unveil characteristics of the neuronal α-bgt sensitive nAChR binding site as it displays rapid association and dissociation kinetics (Davies *et al.*, 1999).

1.7.2. α-Conotoxins:

α-Conotoxins (α-CTX) are members of a family of small, paralytic peptides characterised from the venom produced from the carnivorous *Conus* vermivorous, piscivorous or mollusc hunting marine snails (for reviews, see Gray *et al.*, 1988; Olivera *et al.*, 1990; Arias, 2000; McIntosh *et al.*, 2000). The venom contains a complex mixture of disulfide-rich peptides, each of which is capable of targeting specific macromolecular receptors (Olivera *et al.*, 1984, review, 1990). One large class of these hypervariable toxins is the α-CTX that target muscle or neuronal subtypes of nAChR. In contrast to snake α-neurotoxins (60-80 amino acids), the α-conotoxins are about 12-25 amino acids in length. They are the smallest of the major paralytic conotoxins and are the smallest peptidergic selective, competitive antagonists that show promise in targeting and characterising both native and heterologously expressed subtype specific nAChR and are capable of inhibiting neuromuscular transmission (Myers *et al.*, 1991; Johnson *et al.*, 1995). Three different fish-hunting *Conus* species, *Conus geographus*, *Conus striatus*, and *Conus magus* produce venom containing α-CTX peptides that inhibit muscle-nAChR located at the vertebrate neuromuscular junction e.g. α-CTX-MI and α-CTX-GI with IC_{50} values of 12 and 20 nM respectively (Myers *et al.*, 1991; Johnson *et al.*, 1995; McIntosh *et al.*, 1999; Arias, 2000).

Due to their size being between that of smaller nicotinic ligands and the larger α-neurotoxin snake venom polypeptides (α-bgt, α-cobratoxin), the α-conotoxins are useful novel chemical probes for receptors and ion-channels, in particular nAChR. The small size of the α-conotoxins enables them to be synthesised by chemical techniques in biologically active forms. To date there are approximately 500 different species of *Conus* predatory gastropods, each having its own set of venom, many containing α-CTXs that can be purified and sequenced (Olivera *et al.*, 1990). These disulfide-rich peptides all have high structural homology in their conserved cysteine sequence motifs, which provides a means to identify specific target receptors, but are hypervariable in their intercysteine disulfide bonding patterning. The consensus sequence *X*CC(H/N)PACG*XX*(Y/F)*X*C is shared by most of the α-CTXs purified from piscivorous-hunting cone snails (not α-CTX-MII; Cartier *et al.*, 1996) (Hopkins *et al.*, 1995) (see Table 1.1).

Table 1.1. ***Peptide sequences of some of the α-contoxins.*** *The fish-hunting Conus species from which each toxin was isolated is indicated (reviewed by Arias, 2000).*

Conotoxin	Sequence	Source	Reference
α-GI	ECCNPACGRHYSC-NH_2	*C. geographus*	Gray *et al.* (1984, 1988)
α-GIA	ECCNPACGRHYSCGK-NH_2	*C. geographus*	Gray *et al.* (1981)
α-GII	ECCHPACGKHFSC-NH_2	*C. geographus*	Gray *et al.* (1988)
α-SI	ICCNPACGKNFDC-NH_2	*C. striatus*	Zafaralla *et al.* (1988)
α-MI	GRCCHPACGKNYSC-NH_2	*C. magnus*	McIntosh *et al.* (1982)
α-MII	GCCSNPVCHLEHSNLC-NH_2	*C. magus*	Cartier *et al.* (1996)

α-CTXs purified from the non-fish hunting Conus have sequences that retain a cysteine residue framework $X_nCCX_nCX_nCX_n$ (Hopkins *et al.*, 1995). Differences in the primary structure of these peptides probably accounts for the specificity attributed to each toxin for nAChR subtypes.

1.7.2.1. α-Conotoxin-IMI:

α-Conotoxin-ImI (α-CTX-ImI) is a 12 amino acid peptide neurotoxin, GCCSDPRCAWRC-NH_2, isolated from the vermivorous marine snail *C. imperialis* (McIntosh *et al.*, 1994; Johnson *et al.*, 1995). This α-neurotoxin has been found to selectively target specific subtypes of nAChR when expressed in *Xenopus* oocytes. α-CTX-ImI selectively blocks α7-homomeric nAChR with an apparent affinity (IC_{50}) of 0.2 μM and α9 homomers with 8-fold less potency (IC_{50} = 1.8 μM) (Johnson *et al.*, 1995). α-CTX-ImI had negligible effects on mammalian neuromuscular transmission and other combinations of neuronal nAChR subunits α2β2, α3β2, α4β2, α2β4, α3β4, α4β4 (Johnson *et al.*, 1995; Pereira *et al.*, 1996). Patch-clamp analysis applied to hippocampal neurones in culture was also used to study the effect of α-CTX-ImI on native α-bgt–sensitive neuronal nAChR (Pereira *et al.*, 1996). If hippocampal neurones were pre-exposed for 5 min with α-CTX-ImI, there was a competitive, reversible concentration-dependent decrease in the peak amplitude of native α7* α-bgt-sensitive currents (Pereira *et al.*, 1996). The action of α-CTX-ImI was specific for α-bgt-sensitive nAChR, as this compound had no effect on GABA, glycine, NMDA, kainate or quisqualate-gated currents.

1.7.2.2. α-Conotoxin-MII:

A relatively novel 16 amino acid peptide has been sequenced from the venom of the marine snail *Conus magus* (Cartier *et al.*, 1996). This α-CTX is thought to selectively target α3β2* nAChR subtypes with subnanomolar affinity (IC_{50} = 0.5 nM) expressed in *Xenopus* oocytes (Cartier *et al.*, 1996). α-CTX-MII selectively blocks the slowly decaying current in avian ciliary ganglion (Ullian *et al.*, 1997) and blocks approximately 93% of the ACh-induced response in α3β2-expressing oocytes (McIntosh *et al.*, 2000). The peptide sequence of α-CTX-MII is shown in Table 1.1. Its sequence identifies both structural and functional differences from the previously isolated, cloned and sequenced α-neurotoxins. Most of the previously identified α-CTXs target muscle-type receptors, subsequently the identification of α-CTX-ImI (Pereira *et al.*, 1996) and α-CTX-AUIB (Luo *et al.*, 1998) were selectively found to target α7 and α3β4 nAChR respectively. α-CTX-MII has been demonstrated to act as a competitive antagonist that targets α3β2* nAChR (Cartier *et al.*, 1996; Ullian *et al.*, 1997; McIntosh *et al.*, 2000), partially blocks nicotine–stimulated DA release (Kulak *et al.*, 1997; Kaiser *et al.*, 1998) and when iodinated as [^{125}I]-α-CTX-MII, identifies a novel population of nAChR in mouse brain (Whiteaker *et al.*, 2000).

The α-CTXs represent a group of potent and selective ligands capable of discriminating functional responses evoked by various nAChR subtypes and provide support for the vast diversity of nAChR targeted toxins present in the *Conus* species'. Further analysis of these peptide neurotoxins may help to locate amino acid residues that determine specific nAChR selectivity. The ability of these conotoxins to be synthesised means that they are free from any potential venom contaminants and can be

chemically modified to covalently incorporate radioactive or fluorescent moieties used to identify structure-function relationships and in imaging analysis studies.

1.8. Nicotine and the tobacco smoking habit in man:

A major stimulus of research into nAChR has been the desire to understand the molecular and cellular basis of nicotine dependence. The chronic use of tobacco in man leads to tolerance, physical and psychological dependence along with the subjective euphoric effects (Johnston, 1942; Perkins *et al.*, 1993). Tolerance develops rapidly to the initial aversive effects of nicotine to the human body including the feelings of nausea and vomiting, mediated in part by the peripheral nervous system. It is now widely accepted that nicotine causes predominantly psychological dependence in habitual smokers (Balfour, 1990). This results in a combination of objective and subjective states, euphoria, cognitive enhancement, changed adaptation to stress, which together support the maintenance of drug seeking behaviour (Stolerman and Jarvis, 1995). After inhaling tobacco smoke nicotine is readily absorbed via the buccal cavity, nasopharengeal tract and the lungs before entering the arterial circulation for distribution around the body (Benowitz, 1996). Chronic smokers tend to maintain an elevated plasma nicotinic level which is further increased after each tobacco smoke inhalation, persisting over the course of a day. The resultant accumulation of nicotine causes the development of neuroadaptation as the tobacco smoker's day progresses (Ashton and Stepney, 1982; Benowitz, 1991).

The absorption of inhaled nicotine from a bolus of tobacco smoke is extremely rapid with the onset of central effects within 10 seconds of inhalation (Russell, 1991; Benowitz, 1996). This rapid delivery is an effective rewarding process as reinforcement

is almost immediate and plays an essential role in reward learning mechanisms and maintaining the addiction of cigarette smoking. The rapid delivery of nicotine from inhaled tobacco smoke allows the smoker to carefully adjust their smoking pattern and to titrate their plasma nicotine levels accordingly, hence alleviating their mood (Benowitz, 1991). It is advantageous to analyse the pharmacological profile of nicotine after inhalation and the rate at which nicotine is absorbed into the body when trying to achieve a successful therapeutic smoking cessation treatment (Sutherland *et al.*, 1992). The pharmacological profile of dosing with nicotine gums or patches produce a gradual dosing of nicotine which does not mimic the efficient and rapid dosing via the pulmonary route observed with inhalation of tobacco smoke (Rose *et al*, 1985; Russell, 1991). Smoking cessation aids with a slower entry time of nicotine to the brain have a longer delay elapsing before the desired subjective effects are produced (for review see, Leischow and Cook, 1998). Consequently, the positive reinforcing effects of nicotine within the CNS will be weaker compared to those perceived after smoking a cigarette (Benowitz, 1991). This different pharmacological profile of the drug response may alter the degree of desensitisation of the nAChR and will in turn reflect the degree of reinforcement experienced. To ensure that rapid reinforcement develops it is important that the association between drug-taking behaviour and its pharmacological consequences occurs rapidly without a substantial delay.

The craving for the rewarding properties of an addictive drug and the avoidance of the unpleasant symptoms on drug withdrawal are both likely to contribute to the maintenance of drug-taking behaviour (Balfour, 1991; Wilner and Jones, 1996). Nicotine is considered to act both as a positive and as a negative reinforcer (Stolerman and Jarvis, 1995). The concept of positive reinforcement correlates with the pleasurable experiences associated with smoking. If a person smokes to escape the 'psychological

discomfort' related to withdrawal and thus relieve anxiety, depression, psychosis and the unpleasant consequences whenever they are deprived from nicotine, under these circumstances nicotine acts as a negative reinforcer (Di Chiara, 1992). This demonstrates the importance of the aversive withdrawal phenomena in situations concerning the maintenance of the tobacco smoking habit and perhaps in the initiation of smoking after cessation. Negative reinforcement contributes to the tobacco smoking habit but by no means is the principal driving force to continue nicotine abuse (West and Schneider, 1987; Wilner and Jones, 1996). Dependence on nicotine can be considered as when abstinent smokers relapse due to the craving for nicotine and to obtain the rewarding, euphoric effects of the drug.

Each inhaled puff of cigarette smoke contains nicotine in suspension on tiny droplets of tar and will evoke a series of intermittent boli of the alkaloid. Individual characteristic styles of smoking have developed and has split the smoking population into either 'peak seekers' or 'trough maintainers' (Russell, 1990) depending on their daily cigarette consumption. The former can also be termed indulgent smokers as they smoke in a fashion as to create peak plasma nicotine levels after a cigarette. In contrast, trough maintainers are perhaps smoking on a more frequent basis and are considered as heavy smokers, who will regulate their smoking consumption to establish a relatively constant body nicotine level which remains higher than a baseline level. Habitual smokers will dose themselves with enough nicotine to produce the desired effects that are most rewarding on both their brain and behaviour. The actual intake of nicotine can be considered as lying within a rewarding window, avoiding nicotine toxicity from over smoking and withdrawal from under smoking (Rose *et* al., 1993).

1.9. Beneficial roles for nicotine and nAChR subtypes involved:

It has been shown that nicotine, when in a pure state, free from tobacco carcinogens including carbon monoxide, polycyclic aromatic hydrocarbons and tar (Benowitz, 1991; Jarvik, 1991), is able to alleviate the symptoms of withdrawal from tobacco smoking and may prove to be a therapeutically active and a valuable pharmaceutical agent for treating other conditions (see Decker and Arneric, 1998). Different nAChR subtypes have been implicated in cognitive processes, including short-term memory and vigilance and in pathological conditions. nAChR subtypes have also been implicated with exerting changes within the CNS on various neurotransmitter systems (Balfour, 1982, 1989, 1994; Soliakov and Wonnacott, 1996; Kaiser *et al.*, 1998). These principally include the catecholaminergic, serotonergic and cholinergic neural pathways. Tobacco smokers therefore benefit from nicotine in the smoke, as it helps to alleviate some of the symptoms of such pathological disorders eg. schizophrenia and Alzheimer disease deficits. The identification of the specific subtypes of nAChR involved in particular medical conditions, using nAChR subtype specific ligands, offers the prospect that these receptors can be targeted with selective drugs to evoke beneficial effects or alleviate symptoms of a particular condition. The continued development of selective nAChR ligands will help to elucidate and unravel the physiological roles of nAChR in both normal neuronal functioning and in diseased conditions.

1.9.1. Neuronal development and neuroprotective-related actions:

The role of nAChR in the CNS, other than their involvement in the mediation of synaptic transmission, is well documented and recognised. It has been suggested that a possible role for transmission via nAChR is the determination of the fate of specific

neuronal populations. The α7* nAChR is highly permeable to Ca^{2+} and may regulate target cell function via Ca^{2+}-dependent processes, such as second messenger systems (Vijayaraghavan *et al.*, 1992) and the induction of immediate-early gene expression. α-Bgt-sensitive receptors have also been implicated in development and synapse formation (Mandelzys *et al.*, 1994), neuronal development and in the context of neuroprotection after toxic insults to cells (Semba *et al.*, 1996; Miñana *et al.*, 1998). It has been demonstrated that activation of α7* nAChR promotes survival of spinal cord motoneurones (Messi *et al.*, 1997) and nicotine, by activation of α7* nAChR, prevents NMDA and glutamate neurotoxicity in primary cultures of cerebellar neurones (Miñana *et al.*, 1998) and is neuroprotective against excitotoxic insults applied to striatal, cortical, and hippocampal neurons (Marin *et al.*, 1994; Semba *et al.*, 1996; Kihara *et al.*, 1997).

1.9.2. Alzheimer's Disease and memory-related actions:

The ageing process of the human brain is associated with reductions in various nAChR subtypes; in the case of Alzheimer's and Parkinson's disease (AD and PD respectively) these changes are selective (see Gotti *et al.*, 1997 for an overview). AD is a progressive neurodegenerative disorder affecting individuals over the age of 65 years. Intracellular neurofibrillary tangles and senile plaques in combination with extensive cellular atrophy and cell loss are all distinct neuropathological features of this disease displayed in AD brains on post-mortem examination (see Selkoe, 1999 for review). The cholinergic innervation to the cerebral cortex and hippocampus is degenerated in AD brains, and results in the progressive deterioration of higher cognitive function and the loss of memory. This has led to studies characterising the changes in choline

acetyltransferase levels and nAChR density in AD brains. The level of cortical acetyltransferase and [^{3}H]-nicotine binding sites are significantly decreased in AD patient (Perry *et al.*, 1982, 1995; Aubert *et al.*, 1992; Sihver *et al.*, 1999). The reduction in nicotinic binding sites has also been confirmed in the temporal cortex, frontal cortex, substantia nigra and the hippocampus using ^{11}C-nicotine in *in vivo* PET studies (Nordberg *et al.*, 1995). It has been demonstrated that in the cortex there is a selective loss of α4 subunits detected by subunit immunoreactivity and a reduction in [^{3}H]-nicotine and [^{3}H]-epibatidine binding. The α3 and α7 nAChR subunits were not affected likewise the binding of [^{125}I]-α-bgt was unaltered in AD brain compared to control (Perry *et al.*, 2000). These findings indicate that AD is associated with a loss of nicotinic binding sites that incorporate the α4 nAChR subunit.

The α7-selective agonists DMXB (see section 1.6.2.1) and DMAC (see section 1.6.2.2) enhance performance in several spatial and non-spatial memory-related paradigms in rats (Meyer *et al.*, 1994, 1997; Bjugstad *et al.*, 1996) and may be of therapeutic value to treat age-associated memory impairment and AD. An injection of ibotenic acid, an excitotoxin, into the nucleus basalis magnocellularis significantly decreases the number of neuronal cells in the cerebral cortex, providing an animal model similar to AD (Nanri *et al.*, 1997). The protective action of DMXB was observed after treatment to lesioned rats when compared to control untreated animals (Nanri *et al.*, 1997), due to the α7 selective nature of DMXB, it can be speculated that α7* nAChR may be implicated in memory-related behaviours and play a role in this cytoprotctive action and neuronal survival. In this thesis, the related drug DMAC will be examined for its ability to displace a variety of nicotinic ligands and evoke upregulation of nAChR.

1.9.3. Parkinson's disease:

PD is characterised by muscle rigidity, tremor and bradykinesia, postural deficits, impaired gait and dementia in a minority of patients (for review see, Dunnett and Björklund, 1999). The main pathological features of this neurological disease are the detection of Lewy bodies, hyaline inclusions in the cytoplasm of neurones and the substantial loss of forebrain dopaminergic neurones predominantly from the substantia nigra. There are reports of a negative correlation between the development of PD and smoking (Morens *et al.*, 1996) and that changes in the symptomatology were observed after PD patients were treated with nicotine gum and patches (Fagerström *et al.*, 1994). Nicotinic agonists may therefore have therapeutic potential to compensate and alleviate the cognitive deficits associated with AD and PD patients and help to slow the progression of neurodegeneration (Decker and Arneric, 1998).

1.9.4. Schizophrenia:

The incidence of tobacco smoking amongst the population who suffer from mental illness is higher than the general population. A high incidence of smoking (50%-84%) has also been found in schizophrenic patients (Hughes *et al.*, 1986). Schizophrenia is characterised by symptoms of delusions, hallucinations (auditory), disorganised thinking and speech and a deficit in their auditory processing (for review see, Leonard *et al.*, 1998). Nicotine normalises the processing of this sensory deficit in schizophrenic patients and on post-mortem examination, schizophrenic brain contains aberrant expression and regulation of nAChR (Leonard *et al.*, 1998, 2000). In this disorder the intake of nicotine proves beneficial and indeed neuroprotective. nAChR are therefore implicated in the sensory deficit in schizophrenics and this has been mapped to a

chromosomal region that contains the α7 nAChR subunit gene (Freedman *et al.*, 1997), revealing another importance of this nAChR subtype in normal neuronal functioning. Much research still needs to be completed in this field to elucidate the functional implications of nicotine and nAChR subtypes in neuropsychiatric and neurological disorders, in relation to long term exposure without creating long term side effects or dependence on the drug.

1.10. Neuronal receptor changes relating to tolerance:

Chronic drug exposure leads to the development of adaptive changes within neural networks leading to the production of tolerance to the acute peripheral effects of nicotine and also to drug dependency (Marks *et al.*, 1983, 1985; Schwartz and Kellar, 1985). This is the case with the psychoactive drug nicotine, which is sufficient to create an addictive state after chronic nicotine exposure in rodents or in dependent tobacco smokers (Marks *et al.*, 1983; as reviewed by Balfour, 1991). The adaptations produced within the CNS after long term exposure to nicotine correspond to changes in the number of neuronal nAChR where nicotine exerts its effects within the brain. In neurophysiological terms this adaptation is also known as receptor desensitisation (see Marks, 1998). Conventionally, chronic stimulation of receptors by repeated agonist treatment is expected to lead to down-regulation of neurotransmitter receptors (for review, see Creese and Sibley, 1980). The action of chronic nicotine is now well documented in that it exerts a paradoxical increase, or upregulation, of the high affinity tritiated agonist and α-bgt-sensitive binding site densities within the CNS, attributed to a protracted functional blockade of these nAChR complexes (as reviewed by Wonnacott, 1990).

1.10.1. Chronic nicotine treatment upregulates high affinity [^{3}H]-agonist and [^{125}I]-α-bgt binding sites:

The ability of chronic nicotine treatment to produce upregulation and elicit adaptation of neuronal tissue must be due to the prolonged nicotine enriched environment. Binding assays have shown that chronic exposure to nicotine differentially affects [^{3}H]-nicotine, [^{3}H]-cytisine, [^{125}I]-α-bgt and [^{3}H]-quinuclidinyl benzilate ([^{3}H]-QNB) binding in different brain regions after similar chronic drug treatment regimes (Marks *et al.*, 1983, 1985; Schwartz and Kellar, 1983, 1985; Pauly *et al.*, 1991; Sanderson *et al.*, 1993). Chronic nicotine increases the density of the high affinity [^{3}H]-nicotine and [^{125}I]-α-bgt-sensitive nAChR binding sites with no change in binding of [^{3}H]-QNB binding (Marks *et al.*, 1983, 1985). [^{3}H]-QNB identifies muscarinic binding sites within the brain and this study reveals that the upregulatory action of nicotine is specific to nAChR.

Marks *et al.* (1983) investigated the effects of constantly infusing nicotine at different rates (0.2, 1.0, 5.0 mg/kg/h) into female mice for a period of 8-10 days. Nicotine binding was assessed in several brain regions with [^{3}H]-nicotine. Results confirmed a significant dose-dependent increase in nAChR binding sites in the following 5 brain regions: the cortex, midbrain, hindbrain, hypothalamus and the hippocampus. Upregulation was evoked with doses of nicotine lower than those required to elicit changes in the number of [^{125}I]-α-bgt binding sites. Populations of neuronal nAChR identified by α-bgt binding were also significantly increased in both the midbrain and hippocampal regions after chronic infusion with a high dose of nicotine (5 mg/kg/h). This is consistent with the ability of nicotine to bind to [^{3}H]-nicotinic agonist sites with greater affinity than to [^{125}I]-α-bgt binding sites.

Quantitative autoradiographic analysis of mouse brains, previously subjected to chronic infusions of nicotine ranging from 0.25-2.0 mg/kg/h for 10 days, revealed that [^{3}H]-nicotine binding sites were increased in a dose-dependent manner within most of the brain regions studied, compared to saline infused control animals (Pauly *et al.*, 1991). [^{125}I]-α-Bgt binding observed in cryostat sections was increased after chronic nicotine treatment but in a less robust fashion compared to those sites labelled with [^{3}H]-nicotine. Muscarinic binding sites were not affected by chronic nicotine treatment. These data support and compliment the previously reported homogenate binding assays used to measure the magnitude of upregulation of receptor ligand binding in dissected brain regions. This study provides more detailed maps of the regional specificity and distribution of upregulated nAChR binding sites in mouse brain (Pauly *et al.*, 1991). Upregulation of putative nAChR binding sites by the administration of chronic nicotine to experimental animals is now a well-documented phenomenon (as reviewed by Wonnacott, 1990).

These results are also supported by the increase observed in [^{3}H]-ACh binding sites in the cerebral cortex of rats administered with chronic nicotine for 10 days with no significant effect on [^{3}H]-QNB sites (Schwartz and Kellar, 1983). Schwartz and Kellar (1983) measured the effect of chronic administration of diisopropyl fluorophosphate (DFP), a cholinesterase inhibitor capable of increasing the concentration of ACh at synapses by retarding its hydrolysis and thereby prolonging cholinergic receptor stimulation. DFP produces an opposite effect compared to that of nicotine. Chronic DFP treatment decreases [^{3}H]-ACh binding by 20-38%, which is proposed to be an adaptative response to the increased synaptic levels of ACh (Schwartz and Kellar, 1983, 1985). This down-regulation of brain nicotinic cholinergic sites labelled with [^{3}H]-ACh is similar to the decrease in both nicotinic and muscarinic binding sites observed after

chronic administration of another acetylcholinesterase inhibitor, disulfoton (2 mg/kg/day for 10 days) to rats (Costa and Murphy, 1983).

Schatchard analysis of the changes in radioligand binding in all of these studies demonstrates an increase in the number, and therefore density, of receptor binding sites B_{max} with no change in the apparent affinity (K_D) of nicotine binding for its receptors (Marks *et al.*, 1983, 1985; Schwartz and Kellar, 1983; Rowell and Wonnacott, 1990; Sanderson *et al.*, 1993; Bhat *et al.*, 1994; Yates *et al.*, 1995). This change in B_{max} is also extrapolated to the decrease in [^{3}H]-ACh binding sites observed after chronic DFP treatment to rats, which was due to a decrease in the apparent density of these tritiated agonist binding sites in the various regions analysed (Schwartz and Kellar, 1985).

Marks *et al.* (1985) performed a range of experiments investigating the time course relating to the onset and loss of tolerance to nicotine in mice when chronically administered a continuous i.v. infusion of nicotine. The results reported that maximum tolerance was observed after 4 days of chronic drug infusion with a parallel increase in the number of [^{3}H]-nicotine and [^{125}I]-α-bgt binding sites and no change in the muscarinic sites labelled with [^{3}H]-QNB in any of the brain regions examined at any time point during the study. More prolonged treatments did not evoke more extensive changes, this implies that at a given dose nicotine will increase the number of nAChR binding sites until a steady state is achieved. Brain nicotinic binding sites returned to control binding values after 4 and 8 days after withdrawal of nicotine treatment (relating to α-bgt and nicotine binding sites respectively) indicating that nicotine-induced increases in nAChR binding sites are reversible in mice (Marks *et al.*, 1985) and also in rats (Schwartz and Kellar, 1985). This can be related to the number of nAChR binding sites in former smokers which are not significantly different from numbers documented for non-smokers (Breese *et al.*, 1997).

The time course for the development of increases in B_{max} evoked by chronic i.v. nicotine infusion reported by Marks *et al.* (1985) is similar to the observed time course of increases in [^{3}H]-ACh binding after repeated injections of nicotinic agonists. Either nicotine or the nicotinic agonist cytisine administered to rats for 5-21 days, or a one week treatment with the nicotinic agonist (+)-anatoxin-a, administered via osmotic minipumps, elicited similar time courses for the development of upregulation of functional [^{3}H]-nicotine binding sites (Schwartz and Kellar, 1985; Rowell and Wonnacott, 1990, respectively). Similarly nicotine administered to rats (4 mg/kg/day) via minipumps increased [^{3}H]-nicotine binding sites by 59% and 48% in the cortex and the hippocampus respectively in a time-dependent manner (Sanderson *et al.*, 1993). Schwartz and Kellar (1985) showed an increase of 20% in [^{3}H]-ACh binding sites after 5 days of chronic nicotine treatment, with the maximum increase of 28-30% being found in the cortex, thalamus, striatum and hypothalamus after 10 days. Upregulation was not evoked with cotinine the major metabolite of nicotine. When animals were sacrificed after 7 days following the 10 day chronic nicotine treatment, nAChR binding site numbers had returned to values comparable to those in control untreated conditions which is also consistent with the observations noted by Marks *et al.* 1985. To investigate whether the upregulation of nAChR binding sites could be mediated by mere occupancy of the receptor, centrally active nicotinic antagonists were administered to rats. Neither mecamylamine nor DHβE significantly altered [^{3}H]-ACh binding following 10-14 days of their administration to rats, signifying that occupancy and activation of the [^{3}H]-agonist recognition site is a requirement for upregulation (Marks *et al.*, 1985). Collectively these studies demonstrate that nAChR are differentially upregulated by chronic treatment with nAChR agonists and antagonists when analysing and comparing data generated *ex vivo* from rodent brain.

Not all chronic nicotine treatment regimes have resulted in an increase in nicotinic binding sites (Benwell and Balfour, 1984; Pauly *et al.*, 1992). This can be explained if considerably lower doses of nicotine are administered less frequently, for example a s.c. injection of 0.4 mg/kg/day nicotine on a once daily basis (Benwell and Balfour, 1984). Under these conditions [^{3}H]-nicotine binding sites in nicotine-treated rats were found not to be significantly different from those in drug-naïve animals, even after 39 days of chronic drug treatment (Benwell and Balfour, 1984). However, in another study low doses of nicotine treatment ranging from 0.1-0.4 mg/kg did produce an increase of between 18-26% in cortical nAChR (Ksir *et al.*, 1985). Concentration and injection schedules of nicotine previously used in rat protocols to evoke upregulation of nAChR, may not elicit upregulation of [^{3}H]-nicotine or [^{125}I]-α-bgt sites after daily nicotine injections administered to mice (Pauly *et al.*, 1992). This could be due to species differences between rats and mice, and can be explained in terms of the half-life of nicotine being shorter and perhaps receptor turnover occurring more rapidly in the neuronal tissue of mice.

The majority of results produced from animal studies using rodents, different drug regimes and also different routes of chronic drug administration, show that nicotinic agonist treatment produces upregulation of high affinity neuronal [^{3}H]-agonist binding sites correlating with the predominant α4β2 receptor subtype (Flores *et al.*, 1992). The effect of cigarette smoking on alterations of the binding site densities of high affinity nAChR within brain tissue taken from prolonged cigarette smokers was compared to the brain tissue of age-matched non-smoking controls at post-mortem examination (Benwell *et al.*, 1988; Breese *et al.*, 1997; Perry *et al.*, 1999). Studies using human post-mortem tissue produced evidence of an increase in the density of nAChR in both the hippocampal formation and the hippocampal neocortex along with significant increases

in the gyrus rectus and the median raphé nuclei of the midbrain (Benwell *et al.*, 1988). This phenomenon of upregulation of nAChR exhibited in human brains of smokers has been demonstrated to be due to an increase in receptor density measured by high affinity nicotinic binding rather than a change in the apparent affinity of the receptor for nicotine.

It therefore seems likely that upregulation of neuronal nAChR in various brain regions in human smokers' can be attributed to chronic exposure of nicotine present in tobacco smoke (Benwell *et al.*, 1988; Breese *et al.*, 1997). This relationship between upregulation of nAChR following cigarette smoking being similar to those effects observed *in vitro* is strengthened by the results of a study involving rats exposed to mainstream cigarette smoke 1 h/day for 5 days over a period of 13 weeks (Yates *et al.*, 1995). Smoke-exposed rats had significant increases in [^{3}H]-nicotine binding to sites within the cortex, striatum and cerebellum when compared to sham-exposed control animals. This reinforces the proposal that nicotine contained in tobacco smoke evokes upregulation of nAChR *in vivo* and probably by a mechanism similar to that underlying chronic exposure to cigarette smoke in animals (Yates *et al.*, 1995). Breese *et al.* (1997) also reported that individuals who had ceased to smoke two months before their death had nAChR levels the same or below that of control non-smoker autopsy brain tissue. This reveals that in humans the nicotine-induced upregulation of neuronal nAChR is reversible after smoking cessation (Breese *et al.*, 1997) as is observed in rats after chronic nicotine administration (Marks *et al.*, 1985).

As demonstrated *ex vivo*, the chronic administration of nicotine to animals produces upregulation of both [^{3}H]-agonist and also the [^{125}I]-α-bgt binding sites identifying α4β2* and α7* nAChR respectively. Similar changes in [^{3}H]-agonist binding sites binding and nicotinic receptor density following chronic nicotinic drug treatment have

been reproduced in primary cultures of fetal rat cortical neurones (Bencherif *et al.*, 1995), clonal cell lines expressing endogenous nAChR (Peng *et al.*, 1997; Warpman *et al.*, 1998) and in cells transfected with specific nAChR subtypes *in vitro* (Peng *et al.*, 1994a, b; Bencherif *et al.*, 1995; Gopalakrishnan *et al.*, 1996; Warpman *et al.*, 1998; Whiteaker *et al.*, 1998). The mouse fibroblast M10 and the human embryonic kidney, HEK 293 cell lines have been stably transfected with α4 and β2 nAChR subunits under the control of a dexamethasone-inducible promoter (Peng *et al.*, 1994b; Bencherif *et al.*, 1995; Gopalikrishnan et al., 1995; Whiteaker *et al.*, 1998). Peng *et al.* (1994b) found that mecamylamine upregulated nAChR in M10 cells thus showing that upegulation does not require ion flow through the channel. Gopalakrishnan *et al.* (1997) reported that d-TC, DHβE and MLA all upregulated [^{3}H]-cytisine binding sites in HEK 293 cells. The M10 and HEK 293 cell lines do not contain endogenous nAChR subunit gene promoter elements, yet are still capable of producing an analogous upregulation in nAChR densities with no change in affinity of [^{3}H]-agonist for its sites (Peng *et al.*, 1994b; Bencherif *et al.*, 1995; Gopalakrishnan *et al.*, 1997; Whiteaker *et al.*, 1998). This suggests that upregulation is not an adaptive response dependent on neuronal factors unique to neurones where these receptor subtypes are normally endogenously expressed, but must be the result of an intrinsic attribute of the receptor complex itself (Peng *et al.*, 1994b; Bencherif *et al.*, 1995; Zhang *et al.*, 1995; Rothhut *et al.*, 1996).

This phenomenon of upregulation of [^{125}I]-α-bgt binding sites is also displayed and preserved after chronic nicotine treatment to primary cultures of rat hippocampal neurones (Barrantes *et al.*, 1995a), human SH-SY5Y neuroblastoma cells (Peng *et al.*, 1997) and human embryonic kidney cells (HEK) stably transfected with α7 subunits (Molinari *et al.*, 1998). Concentration-dependent increases were observed in [^{125}I]-α-bgt binding sites in HEK 293 cells stably transfected with the α7 neuronal nAChR subunit,

after long-term treatment with (±)-epibatidine, GTS-21, DMPP and MLA (Molinari *et al.*, 1998). Upregulation is evoked after exposure to activator or antagonist ligands and indicates that the mere occupancy of the receptor binding site may be adequate to prompt receptor upregulation.

De Koninck and Cooper (1995) observed that upregulation of α7* nAChR could be elicited by KCl depolarisation in sympathetic neurones. KCl depolarisation provoked a corresponding increase in the level of α7 mRNA when compared to control. This upregulation was proposed to be a result of Ca^{2+} influx through L-type Ca^{2+} channels and also through a CaM-kinase II pathway (see sections 2.1.4, 2.7 and 3.18.1). KCl is thought to be physiologically important in neurite outgrowth during development and also neural sprouting after injury (Pugh and Berg, 1994; Solem *et al.*, 1995; Soler *et al.*, 1998; Egea *et al.*, 1999; also see Chapter 5).

In addition to α7* nAChR-evoked upregulation, Peng *et al.* (1997) reported upregulation of α3* nAChR, using [^{3}H]-epibatidine binding to the SH-SY5Y cell line and in transfected tsA201 cells (a derivative of the HEK 293 cell line) after chronic nicotine treatment (1 mM for 4 days, Peng *et al.*, 1997; Wang *et al.*, 1998). Wang *et al.* (1998) have shown that chronic nicotine treatment stimulates upregulation of the α3β2 but not the α3β4 nAChR complexes in SH-SY5Y cells.

1.10.2. Mechanisms underlying upregulation of the high affinity [^{3}H]-agonist and [^{125}I]-α-bgt binding sites:

The underlying cellular mechanism of nAChR upregulation still remains to be fully elucidated despite all of these investigations undertaken to date. Collectively, the previously mentioned studies in section 1.10.1 generate data suggesting that

upregulation of α4β2, α3* and α7* nAChR evoked by chronic treatment with nicotinic ligands is independent of increased transcription levels or stabilisation of the subunit mRNA (Marks *et al.*, 1992; Flores *et al.*, 1992; Peng *et al.*, 1994b, 1997; Bencherif *et al.*, 1995; Rothhut *et al.*, 1996). Although upregulation was demonstrated, there was little effect on the intensity of signal for the nicotinic subunit mRNAs encoding either α2, α3, α4, α5 or the β2 nAChR subunits of mice chronically treated with nicotine, compared to saline treated controls (Marks *et al*, 1992). The failure of chronic nicotine treatment to elevate corresponding subunit mRNA levels encoding the upregulated nAChR subunit subtypes strongly implicates that upregulation is not a result of increased protein synthesis but mediated via a post-transcriptional mechanism (Marks *et al.*, 1992; Flores *et al.*, 1992; Peng *et al.*, 1994b, 1997; Bencherif *et al.*, 1995; Rothhut *et al.*, 1996; Warpman *et al.*, 1998). The precise mechanism is controversial and putative mechanisms proposed to account for nAChR upregulation include the following (see section 3.18);

1). a decrease in the rate of receptor turnover due to nicotine evoked metabolic stabilisation either by a decrease in the rate of degradation of the receptor complex (Peng *et al.*, 1994b; Wang *et al.*, 1998), or an increase in the rate of assembly and enhanced recruitment of pre-existing receptor complexes present in a finite reserve pool (Bencherif *et al.*, 1995; Wang *et al.*, 1998),

2). altered rates of translation (Gopalakrisnan *et al.*, 1997),

3). enhanced subunit maturation, transport or assembly, leading to an improved ability of the receptors to form receptor complexes (Rothhut *et al.*, 1996).

An obvious question is, are these upregulated receptor complexes functional? Functional properties of receptors can be measured using either [^{3}H]-neurotansmitter

release, $^{86}Rb^{+}$ efflux assays (Marks *et al.*, 1993a) or Ca^{2+}-evoked responses in oocytes or using fluorescently labelled cells in suspension. Chronic exposure of mice to nicotine (0.25-4.0 mg/kg/h) for 10 days resulted in a dose-dependent increase in [^{3}H]-nicotine binding. This was accompanied by a decrease in the tolerance of mice to nicotine-induced decreases in body temperature and locomotor activity. Biochemically in functional assays, chronic nicotine decreased the maximal effect of nicotine. A 20% decrease in nicotine-induced [^{3}H]-DA release from the striatum and a 50% decrease in $^{86}Rb^{+}$ efflux per nicotine binding site was observed for nicotine-evoked efflux in synaptosomes from chronically treated mice (Marks *et al.*, 1993b). A decrease in $^{86}Rb^{+}$ efflux also indicated the loss of nAChR function from PC12 cells and the TE671/RD human clonal cell line (Lukas, 1991). Lapchack *et al.* (1989) noted that a schedule of chronic nicotine administered to rats for 10 days, known to yield maximal increases in nAChR density (B_{max}), was accompanied by a decrease in nicotine-induced acetylcholine release from brain tissue. An analogous result, consistent with functional data from native brain analyses, was obtained from HEK 293 cells expressing α4β2* nAChR, a consistent decline in the maximal ACh-evoked ion flux was displayed after cells were chronically treated with nicotine (>1 mM) (Gopalakrishnan *et al.*, 1997). When the relative functional response for control cells is compared to chronic drug-treated cells there is an observed reduction of 75% (Peng *et al.*, 1994b) and 65% (Gopalakrishnan *et al.*, 1996, 1997) in the functional response per unit binding site when upregulation of α4β2 nAChR numbers are at a maximum.

These results illustrate an uncoupling of receptor density and their functional status in different species and cell lines in relation to either an attenuation of hormone, neurotransmitter release, or behavioural tolerance (Lapchack *et al.*, 1989; Gopalakrishnan *et al.*, 1997). This down-regulation of receptor function after chronic

nicotine exposure could either be explained as a consequence of a treatment that evokes an increase in receptor density or as the cause that evokes receptor upregulation (Lapchack *et al.*, 1989; Hulihan-Giblin *et al.*, 1990; Marks *et al.*, 1993b). Hsu *et al.* (1996) investigated the effects of prolonged exposure to varying concentrations of nicotine, comparing the responsiveness of both the α3β2 and the α4β2 nAChR when co-injected and expressed in oocytes. Results indicated that both receptor combinations elicited a diminished responsiveness to an acute challenge of nicotine after prior chronic exposure to nicotine. α3β2 nAChR recovered quicker than the α4β2 subtype after removal of nicotine. This proposed decrease in responsiveness can be attributed to a receptor-inactivated state, which may explain the paradoxical increase in nAChR density after chronic nicotine exposure to compensate for these sub-maximally functioning upregulated receptors.

Together these data support the hypothesis that chronic nicotine administration evokes behavioural tolerance to the physiological effects mediated by nicotine and is a consequence of down-regulation of function that leads to upregulation of neuronal nAChR in most brain regions. This is perhaps an adaptive process as a result of accumulation of chronically desensitised receptors and recovery of receptor function *in vivo* may require several days (Schwartz and Kellar, 1983; Lapchack *et al.*, 1989; Marks *et al.*, 1993a, b; Fenster *et al.*, 1999). Studies performed on the functionality of receptors obtained from chronically treated animals or dissected neuronal tissue will usually have had a rigorous wash procedure in the protocol which will lead to the removal of the nicotine enriched environment. This should return the upregulated receptors to a state in which they are no longer in a functionally "inactive" desensitised conformation due to removal of residual nicotine. The presence of residual nicotine therefore does not seem to be a plausible explanation for the decrease in receptor

function in the study by Marks *et al.* (1993b). The cellular mechanisms relating to functional down-regulation of nAChR function are unknown, likewise it remains to be elucidated whether this loss of nAChR function is a uniform decrease in the function of each nAChR subtype, or the presence of functionally active populations of nAChR and a pool of inactive nAChR.

1.11. Aims of this thesis:

The work described in this thesis aims to explore the upregulation of nAChR after chronic exposure to nicotinic agonists and KCl depolarisation and has been the impetus for investigating the cellular mechanisms underlying the process of nAChR upregulation. The study focuses on nAChR in primary hippocampal neurones and in the SH-SY5Y human neuroblastoma cell line.

The areas of focus for this thesis are summarised below:

1). To establish drug treatments that reliably lead to the phenomenon of receptor upregulation of α3* and α7* nAChR. [^{125}I]-α-bgt is a high affinity antagonist used for the detection of α7* nAChR in intact E18 primary hippocampal cultures *in situ* and in SH-SY5Y cells. The α7* nAChR is predominantly expressed in the hippocampus and has been proposed to be involved in neuronal development, neuronal plasticity and also in neuroprotection and is therefore of interest to the present study. [^{3}H]-epibatidine is used to detect changes in the level of expression of α3* nAChR in intact SH-SY5Y cells after chronic drug treatments. These data

can then be compared to changes in the level of expression of α7* nAChR in SH-SY5Y cells after [^{125}I]-α-bgt binding.

2). To compare the cellular mechanisms underlying the process of nAChR upregulation evoked by nicotinic agonists and KCl. Both nicotine and KCl have been reported to be involved in neurite retraction and neuronal survival which may be mediated via activation of α7* nAChR. It is of interest to determine whether these drug treatments differentially upregulate α3* and α7* nAChR and if a common or different cellular mechanism is involved. The effects of KCl and nicotinic agonist treatment on the level of expression of α3 and α7 nAChR subunit RNA after chronic drug treatment to SH-SY5Y cells will also be investigated to determine if transcription is involved as a possible mechanism resulting in nAChR upregulation.

3). Chronic drug treatments that have been shown to upregulate nAChR in the SH-SY5Y cell line will be applied to examine the functional status of upregulated nAChR in response to acute challenges with either nicotine or KCl. Fluorescence changes in fura-2 loaded SH-SY5Y cells will be used to determine nAChR-evoked changes in $[Ca^{2+}]_i$ responses to acute challenges with either nicotine or KCl. These experiments will provide an insight into the functional properties of responses to both acute and chronic application of nicotinic agonists and KCl depolarisation.

Chapter 2. Upregulation of nAChR in Primary Hippocampal Neurones after Chronic Drug Treatment.

2.1 Introduction.

Previous studies have shown that human brain tissue contains nAChR that are defined by [^{3}H]-nicotine binding. It has been observed that the density of these high affinity [^{3}H]-nicotine binding sites is increased in brain tissue taken from prolonged tobacco smokers examined post-mortem, compared with age-matched non-smoking controls (Benwell *et al.*, 1988; Breese *et al.*, 1997; Perry *et al.*, 1999). Upregulation of nAChR has been attributed to chronic exposure of the alkaloid nicotine present in tobacco smoke. This is due to comparable changes observed in nAChR density from specific regions of rodent brain tissue after chronic nicotine treatment *in vivo* (for review, see Wonnacott, 1990; Flores *et al.*, 1992; Rowell and Li, 1997). High affinity binding of [^{3}H]-nicotine (and [^{3}H]-cytisine) has been correlated with nAChR comprised of α4 and β2 subunits (Whiting *et al.*, 1987; Flores *et al.*, 1992). More recently, upregulation of this nAChR subtype has been demonstrated *in vitro*, after chronic exposure to nicotine, in stably transfected cell lines (Peng *et al.*, 1994b, Gopalakrishnan *et al.*, 1996) and also in the human neuroblastoma SH-SY5Y cell line (Peng *et al.*, 1997). M10 cells transfected with chick α4 and β2 subunits and HEK 293 cells transfected with human α4 and β2 subunits, treated with nicotine for a few days results in a dramatic increase in the number of α4β2 nAChR measured by the binding of [^{3}H]-nicotine (Peng *et al.*, 1994b; Bencherif *et al.*, 1995; Zhang *et al.*, 1995), [^{3}H]-cytisine (Gopalakrishnan *et al.*, 1996) or [^{3}H]-epibatidine (Whiteaker *et al.*, 1998).

Other subtypes of nAChR are also upregulated by chronic nicotine treatment. [^{125}I]-α-bgt labels a nicotinic site correlated with α7* nAChR in rat brain (Séguéla *et al.*, 1993; Barrantes *et al.*, 1995a). Chronic nicotine regimes *in vivo* upregulate [^{125}I]-α-bgt binding sites in some brain regions (as reviewed by Wonnacott, 1990; Collins *et al.*,

1990), although this response is less robust than that observed with high affinity [^{3}H]-nicotine binding sites and requires higher nicotine doses (Pauly *et al.*, 1991; Peng *et al.*, 1997). More recently hippocampal (Barrantes *et al.*, 1995a) and cortical (Bencherif *et al.*, 1995) cultures have both been used as model *in vitro* systems for the study of chronic nicotine treatment. [^{125}I]-α-Bgt bound to hippocampal cultures with a B_{max} of 128 fmoles/mg protein and a K_D of 0.6 nM. Barrantes *et al.* (1995a) showed that one day of nicotine (10 μM) treatment produced a minimum upregulation of putative α7* nAChR in rat hippocampal cultures. However, significant upregulation was not detected until either 4 or 7 days of chronic exposure to nicotine, detected by an increase in the number of cell surface [^{125}I]-α-bgt binding sites. Upregulation of cell surface [^{125}I]-α-bgt binding sites has also been reproduced in cell lines transfected with the rat α7 subunit (Quik *et al.*, 1996; Molinari *et al.*, 1998). This Chapter describes experiments using primary cultures of hippocampal neurones that have previously been dissected from the brains of E18 rat fetuses. At this stage of gestation the generation of pyramidal cells is essentially complete. One pregnant rat will yield 7 x 10^6 neurones from approximately 15 E18 hippocampi and these can be plated into 24 well plates to provide a high density hippocampal neuronal culture with only 5% glial cells if grown in serum-free medium (Banker and Waxman, 1988).

2.1.1 Dissociated cell cultures:

When tissue is dissected and prepared directly from an animal to form suspensions of individual cells for plating into sterile flasks or culture dishes, these cultures are referred to as primary cultures. Neurones in dissociated cultures have the advantage of providing an accessible means of studying living cells following transplantation into culture plates

and also the ability to investigate receptor complexes and cellular processes occurring in intact cells within their native environment. Primary neurones grown in culture maintain their individual identities. After a few days in culture medium, primary dissociated neuronal cell tissue cultures lay down an extensive dense neural network composed of axons and dendritic arbours after neuronal maturation. Morphological and physiological properties of the neurones *ex vivo* closely correspond to the characteristics of the cell populations found *in vivo* in their original tissue location (Banker and Waxman, 1988). This resemblance is probably attributable to the neurones being of a postmitotic nature and are hence committed in the process of their cellular differentiation.

Accomplishing optimum growth conditions for primary cells in culture can often be a laborious procedure to ensure that cultures are viable, permit maturation and are growing reproducibly over time. Once these criteria have been met, it is possible to perform biochemical analysis and to detect and pharmacologically characterise specific populations of cells and the receptors that they express, for example by the binding of specific radiolabelled ligands. Such embryonic neuronal cultures although amenable to study, have the disadvantage of not being capable of dividing once plated in culture. This limits the quantity of material obtainable for these cultures and therefore limits the number of experiments capable of being performed. In contrast, cell lines grown in culture will divide, can be passaged and further subcultured into sterile flasks to generate many cells for biochemical analysis, although these cells may express receptor complexes differing in composition to those found natively in primary cultures.

2.1.2 The hippocampus:

When using primary neuronal cultures the heterogeneity of cell types contained within the tissue of choice may complicate biochemical analysis if specific cell populations are to be targeted and analysed. Therefore, for successful primary neuronal cultures the choice of tissue is of main importance. There are a few regions within the CNS that contain a single principal cell type. These include the cerebellar cortex and the hippocampus, which predominantly contain granule cells and pyramidal cells, respectively, within their structures (Banker and Goslin, 1991).

The hippocampal formation is composed of two layers of interconnected neurones. The first layer consists of three neighbouring cortical areas termed as CA fields (cornu Ammonis or Ammons' horn) also known as the hippocampus proper, comprised of the subicular complex and entorhinal cortex which is continuous with the neocortex (see Figure 2.1).

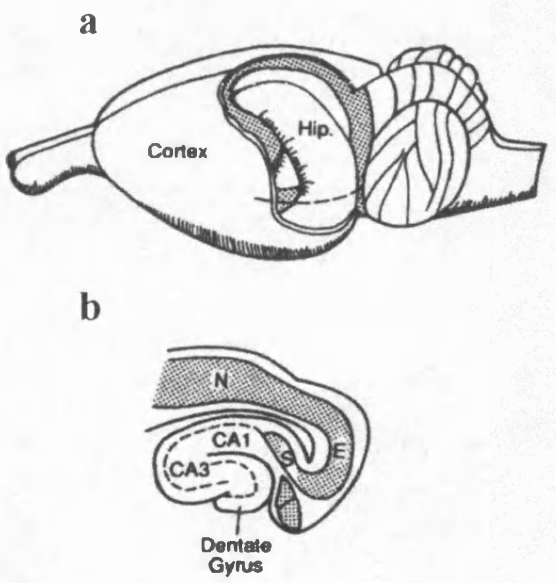

Figure 2.1. Schematic representation of the rat hippocampal formation. *(a) Schematic diagram of the rat brain showing the location of the hippocampal formation (Hip). (b) Schematic representation of a horizontal section through the hippocampal formation and the overlying neocortex (N). The dashed lines and shaded portions represent layers of neuronal bodies. The CA1 and CA3 areas of the hippocampus, the entorhinal cortex (E) and the subiculum (S) are shown.*

The CA fields are comprised of pyramidal neurones with their cell bodies packed into narrow layers, tucked under the edge of the neocortex. The axons from these neocortical pyramidal neurones project to the entorhinal cortex (as shown in Figure 2.1) and through to the subiculum and into the dentate gyrus by a fan of axons known as the perforant pathway (Figure 2.2). The second layer of the hippocampal formation is the dentate gyrus, which contains tightly packed granule cells.

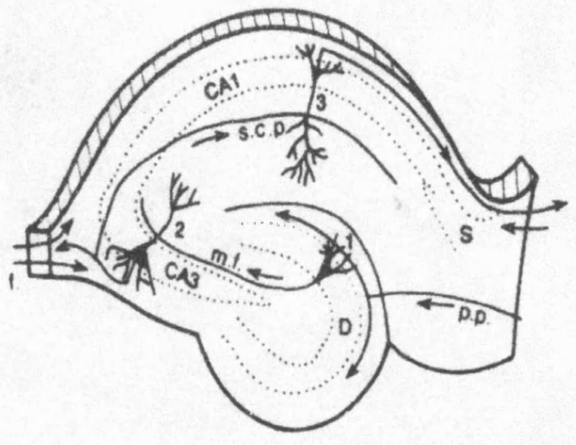

Figure 2.2. Schematic diagram of the trisynaptic circuit in a hippocampal slice. *The dashed lines depict the outlines of tightly packed layers of cell bodies. The areas lying outside the dashed lines contain axons, dendrites and numerous synaptic contacts. Additional axons project to the hippocampus through the fimbria (f), or through the subicular complex (S) and entorhinal cortex. (s.c.p. is the Schaffer collateral pathway; p.p. is the perforant pathway and D is the dentate gyrus).*

A major part of the hippocampal network is the trisynaptic circuit which is preserved when thin coronal slices of the hippocampus are sectioned (Figs 2.1b and 2.2). Axons from the perforant pathway synapse onto dentate granule cells, the axons of these cells

(also known as mossy fibres) project to synapse on dendrites of pyramidal cells in the CA3 field within the hippocampus proper. The CA3 area contains pyramidal cells with highly branched axons that either leave the hippocampus or loop around to form synapses in the CA1 field with dendrites of pyramidal cells in this area, also known as the Schaffer collateral pathway. CA1 neurones project axons to dendrites of neurones contained in the subicular complex which in turn project axons to the entorhinal cortex, thus completing the circuit.

Within the brain the hippocampus is a structure involved in learning, memory and cognitive processes (for reviews, see Squire and Zola-Morgan, 1988; Eichenbaum *et al.*, 1996; Bear, 1996). The neurodegenerative condition of Alzheimer's disease (AD) is characterised behaviourally by a progressive impairment in memory and cognitive function, and neuropathologically by the appearance of neuritic plaques and neurofibrillary tangles, implicating a cholinergic dysfunction (for review, see Selkoe, 1999; see section 1.9.2). Within the cerebral cortex and the hippocampi of AD patients there is a reduction of the neurotransmitter ACh, choline acetyltransferase and high affinity choline uptake and a substantial (> 70%) and selective degeneration of the cholinergic pathways that innervate these target regions (Whitehouse *et al.*, 1982). These patients also have reduced numbers of neurones in the nucleus basalis of Meynert and decreased numbers of nAChR (Aubert *et al.*, 1992). The ability of nicotine to enhance cognition in some animal models, in humans and also its neuroprotective properties, suggests a possible role for nAChR agonists as potential treatments to reverse the effects of these deficits in some neurological disorders and dementia (see Holladay *et al.*, 1995; James and Norberg, 1995). These cholinomimetic drugs may be able to restore some of the proposed physiological functions of nAChR contained within the circuitry of the hippocampal formation.

The development of subtype specific ligands has enabled the neuroanatomical distribution and pharmacological characterisation of nAChR to be recognised. Ospina *et al.* (1998) performed quantitative autoradiography to compare the binding of α7-type nAChR, detected by [^{125}I]-α-bgt, in fetal and adult rat hippocampus. Results showed that throughout the fetal CA1 field, high levels of [^{125}I]-α-bgt were observed with a significant reduction of [^{125}I]-α-bgt binding density in adult hippocampus (Ospina *et al.*, 1998). Séguéla *et al.* (1993) used the technique of *in situ* hybridisation to localise the α7-transcript, high levels were expressed in the hippocampus, hypothalamus, the amygdala and the cerebral cortex. Alkondon and Albuquerque (1991) initially characterised the nAChR in E17-18 rat hippocampal neurones by whole-cell patch clamp analysis. Results demonstrated that 83% of the fetal hippocampal neurones tested exhibited the presence of a functional nAChR subtype that displayed inward rectification with currents reversibly blocked by micromolar concentrations of d-TC and DHβE and irreversibly blocked by nanomolar concentrations of n-bgt, α-bgt and α-cobratoxin (Alkondon and Albuquerque, 1991, 1993). These data are consistent with an α7* nAChR (Amar *et al.*, 1993).

The hippocampus is of interest for this project as it is a source of a relatively homogeneous population of neurones containing a high preponderance of α7* nAChR. The hippocampus is composed primarily of pyramidal neurones that account for approximately 85-90% of the total neuronal population (reviewed by Goslin and Banker, 1991). This cell type is also the principal primary hippocampal neurone grown in culture in serum free medium. Pyramidal neurones have a characteristic, well-defined shape with a single axon and projections of several highly branched dendrites (typically shorter basilar dendrites branching from a long apical dendrite). These dendrites make direct contact and extensive synaptic connections with one another in culture wells

through the continual process of development and neuronal maturation. Therefore fetal (E18) hippocampal material is a good candidate tissue to study the effect of chronic drug treatment on the numbers of α7* nAChR binding sites *in vitro*, and to try to elucidate the underlying cellular mechanisms of upregulation. The detection, disruption or exploitation of these underlying physiological processes may be beneficial in the treatment of neurological disorders including cognitive dysfunction, perhaps clarifying the role of specific nAChR subtypes in different brain regions.

2.1.3. Cultures of hippocampal neurones:

When using primary hippocampal cultures, the hippocampi are typically obtained from E18 fetuses (Goslin and Banker, 1991; Barrantes *et al.*, 1995a). At this stage of gestation, the generation of pyramidal neurones is essentially complete and a relatively low percentage of glial cells is present. The hippocampi at this stage are also easily dissociated into small pieces and fragmented by passage though a Pasteur pipette: this prevents reaggregation of the neuronal tissue and the formation of clumps. The cells can then be plated onto polyethyleneimmine (PEI) (see Goslin and Banker, 1991; Barrantes *et al.*, 1995a) to enhance cell adhesion and simply left to attach to the lower surface of these culture well plates. In these protocols, the embryonic neuronal cells are plated and initially grown in a serum rich medium containing fetal calf serum (FCS) to aid in the process of cell attachment. Glial cell growth is minimised by maintaining the neurones in a serum-free medium, as serum-containing media will allow for the rapid proliferation and survival of endogenous glial cells (see Goslin and Banker, 1991). The discovery in 1979, that neuroblastoma cells could be grown and proliferate rapidly in the absence of serum in a synthetic supplemented medium with insulin, transferrin,

progesterone, selenium and putrescine was an important advance in cell culture (Bottenstein and Sato, 1979). Supplemented medium is used in the cell culture of primary hippocampal cultures described in this Chapter (see section 2.4.1) to support the growth and maintain the survival of these neurones. After a few days, the hippocampal neurones begin to extend processes from their cell bodies and form contacts synapsing with one another. Immunocytochemical markers are widely available to stain and therefore visualise the morphology and development of axons, neurite outgrowth of dendrites or the presence of glial cells in neuronal cultures.

As with all *ex vivo* neuronal studies, caution has to be taken when interpreting results. The primary hippocampal cultures will resemble their native tissue *in vivo* however, due to the dissection there will be a less complex neural network due to loss of extrinsic afferents innervating this region and target cells due to removal of the hippocampi from their native environment. In all, the results obtained indicate that primary neuronal rat cultures are a useful system to study a snapshot of α7* nAChR during development (Barrantes *et al.*, 1995a; Samuel *et al.*, 1997; Dávila-García *et al.*, 1999).

2.1.4. Physiological significance of α7* nAChR and KCl treatment:

The expression, upregulation and roles of neuronal nAChR *in vivo* are complex, and are still poorly understood. Primary hippocampal neurones grown in culture provide a system that is considerably less complex than whole animal studies *in vivo*, making neuronal cultures more amenable to experimental manipulation and facilitating the interpretation of experimental results. For this reason, the experimental work performed in this Chapter was carried out using *in vitro* primary rat hippocampal cultures as a

system to model, probe and elucidate the mechanisms underlying the cellular processes of upregulation of [^{125}I]-α-bgt binding sites representative of α7* nAChR. The extrasynaptic location of α-bgt binding sites in embryonic and mature chick ciliary neurones and synaptic location in the hippocampus raises questions about the functional physiological relevance of α7* nAChR complexes (Horch and Sargent, 1995).

The α7 nAChR mRNA and [^{125}I]-α-bgt binding peaks in the developing rat somatosensory cortex (S1), a region of the neocortex, approximately 1 week postnatal before declining to adult levels (Broide *et al.*, 1996). The transient increased expression of α7 mRNA and its corresponding increase in binding-site density expression during the early postnatal period, identify a possible role for α-bgt-sensitive nAChR in critical stages of synaptogenesis during the course of CNS development (Fiedler *et al.*, 1987; for review, see Role and Berg, 1996). Earlier studies have also demonstrated that the α7 nAChR subunit protein is developmentally regulated at the transcriptional level (Couturier *et al.*, 1990) and that activation of this receptor induces the elevation of intracellular free Ca^{2+} ($[Ca^{2+}]_i$) in neurones by influx through the receptor cation channel pore (Vijayaraghavan *et al.*, 1992; Séguéla *et al.*, 1993; Zhang *et al.*, 1994). The marked permeability to Ca^{2+} ions and the resulting increase in $[Ca^{2+}]_i$ mediated by activation of α7* nAChR, suggests a possible role for these receptors in influencing or triggering a variety of intracellular Ca^{2+}-dependent cytoplasmic events in specific cholinoceptive neuronal populations to modulate target cell function. This provides the possibility of interesting functional roles of the α7-gene product in early neuronal development. These roles include neuronal survival and the termination of axonal neurite outgrowth during development and also an involvement in neural sprouting after

injury due to sufficient Ca^{2+} entry into the neurite after activation of α-bgt binding sites (Pugh and Berg, 1994; Messi *et al.*, 1997; Pugh and Margiotta, 2000).

Previously KCl has been shown to produce an increase in α-bgt binding sites in cultured ciliary ganglion neurones in culture (Smith *et al.*, 1983). A range of concentrations of KCl (2-50 mM; 3 days) have been used to determine whether changing the K^+ concentration could influence the number of α-bgt binding sites located on chromaffin cells grown in culture (Geertsen *et al.*, 1988). Geertsen *et al.* (1988) demonstrated that KCl upregulated α-bgt binding sites in chromaffin cells in a concentration-dependent manner with a maximum effect at 20 mM KCl. De Koninck and Cooper (1995) observed that upregulation of surface α7* nAChR in cultured neonatal rat sympathetic neurones was evoked by chronic KCl depolarisation (40 mM; 1-2 days). Upregulation of α-bgt-sensitive nAChR was accompanied by a corresponding increase in the level of α7 mRNA, compared to control cultures. This KCl-evoked upregulation was proposed to result from Ca^{2+} influx through L-type Ca^{2+} channels and activation of a Ca^{2+}-CaM-kinase II pathway. In the present study, the effect of chronic treatment with nicotinic ligands and KCl depolarisation on [^{125}I]-α-bgt binding sites in E18 primary rat hippocampal cultures were compared. The binding data described in this Chapter reveal that nicotine and KCl upregulate α7* nAChR via distinct mechanisms.

2.2. Aims:

The aim of this Chapter is to examine the effect of KCl on upregulation of [^{125}I]-α-bgt binding sites in primary rat hippocampal neurones and to evaluate if the same mechanisms operate, as reported by De Koninck and Cooper (1995). The effect of

chronic treatment with the nicotinic agonists, nicotine and DMAC will also be investigated on [^{125}I]-α-bgt-sensitive nAChR sites. The cellular mechanisms underlying KCl- and nicotine-evoked upregulation will be compared.

2.3. Materials and methods.

2.3.1. Drugs and reagents:

Tissue culture media, serum and plasticware were from Gibco BRL (Paisley, Renfrewshire, Scotland). Media supplements, biochemicals, (-)-nicotine, (±)-verapamil hydrochloride and α-bgt were purchased from Sigma Co. (Poole, Dorset, U.K.). KN-62 was purchased from Calbiochem-Novabiochem Corporation; KN-04 from AMS Biotechnology. DMAC, was provided by Organon Laboratories Ltd., Newhouse, Lanarkshire. GFAP (NCL-GFAP-GA5) was from Novocastra Laboratories Ltd. (Newcastle upon Tyne, U.K.), the secondary anti-mouse IgG fluorescein linked whole antibody from sheep was purchased from Life Sciences, Amersham. Optiphase Safe scintillant was purchased from Fisons Chemicals, Loughborough, U.K. All other chemicals used were of analytical grade and obtained from standard commercial sources.

[^{3}H]-MLA (specific radioactivity, 25 Ci/mmol) was from Tocris Cookson Ltd. (Bristol, U.K.). [^{3}H]-epibatidine (specific radioactivity, 33.8 Ci/mmol) was obtained from Dupont-NEN Ltd., (Boston, MA). (-)-*N*-methyl-[^{3}H]-nicotine (specific radioactivity 75 Ci/mmol) and [^{125}I]-NaI were obtained from Amersham International (Aylesbury, U.K.). The α-bgt was iodinated by the chloramine-T method to a specific

activity of approximately 700 Ci/mmol and stored in 10 mM phosphate, pH 7.5 at 4°C for up to 4 weeks (see section 2.6.1 and 2.6.2).

2.3.2. Preparation of rat brain P2 membranes:

Crude rat brain membranes were prepared as previously described (MacAllan *et al.*, 1988). In brief, fresh brain tissue (minus cerebellum) from adult male Sprague-Dawley rats were homogenised (10% weight/volume (w/v)) in ice-cold 0.32 M sucrose containing 1 mM EDTA, 0.1 mM phenylmethylsulfonyl fluoride (PMSF), 0.01 % (w/v) sodium azide, pH 7.4), before centrifugation (1,000 x g, 4°C, 10 min). The supernatant fraction (S1) was decanted and retained on ice. The pellet (P1) was resuspended in ice-cold 0.32 M sucrose (5 ml/g original wet weight) and re-centrifuged. The supernatant was combined with S1 and centrifuged at 12,000 x g (4°C, 30 min). The pellet (P2) was resuspended (2.5 ml/g original wet weight) in ice cold phosphate buffer (50 mM potassium phosphate buffer containing 1 mM EDTA, 0.1 mM PMSF, 0.01% (w/v) sodium azide, pH 7.4), and washed twice by centrifugation (12,000 x g, 4°C, 30 min). The washed pellet was resuspended in phosphate buffer (2.5 ml/g original wet weight) and restored in 5 ml aliquots at -20°C. The protein content was determined using the method of Markwell *et al.* (1978), using bovine serum albumen (BSA) as the standard.

2.3.3. Competition binding assays with DMAC:

The nicotinic agonist DMAC, was assessed for its ability to displace the binding of a number of nicotinic radioligands by means of competition binding assays. Competition binding assays were performed against [^{125}I]-α-bgt (1 nM) and [^{3}H]-MLA (1 nM) or

against [^{3}H]-epibatidine (200 pM) and [^{3}H]-nicotine (10 nM) binding to rat brain P2 membranes to identify the potency of DMAC against α7* or α4β2* nAChR respectively, as described by (Davies *et al.*, 1999). In brief, for [^{125}I]-α-bgt binding, P2 membranes were diluted in assay buffer (phosphate buffer supplemented with 0.1 % (w/v) BSA, 1 mg/ml (Davies *et al.*, 1999). Membranes were incubated with [^{125}I]-α-bgt (final concentration of 1 nM) and a range of dilutions of the competing drug, DMAC or unlabelled α-bgt at 37°C for 3 h. Following incubation, samples were diluted with 0.5 ml of ice cold phosphate buffered saline (PBS; 20 mM Na_2HPO_4, 5 mM KH_2PO_4, 150 mM NaCl, pH 7.4) at 4°C. Membranes were pelleted at 12,000 x g (2 min) in a microcentrifuge and resuspended in 1.25 ml of ice cold PBS before centrifuging (12,000 x g for 2 min). The supernatant was removed and the radioactivity contained in the pellets was determined using a Packard Cobra II gamma-counter to detect bound [^{125}I]-α-bgt.

Competition binding assays were also performed with [^{3}H]-MLA, [^{3}H]-epibatidine and [^{3}H]-epibatidine as follows: P2 membranes were diluted in assay buffer (Krebs Ringer-Tris Hepes buffer composed of 118 mM NaCl, 4.8 mM KCl, 2.5 mM $CaCl_2$, 20 mM Hepes, 200 mM Tris, 0.1 mM PMSF, 0.01% sodium azide, pH 7.4) to give the desired protein content (typically 0.5 mg protein for [^{3}H]-MLA competition binding assays and 1-2 mg protein/ml for the [^{3}H]-epibatidine and [^{3}H]-nicotine binding assays, all in final assay volumes of 250 µl) supplemented with 0.1% (w/v) BSA. P2 membranes were incubated with [^{3}H]-MLA (final concentration 1 nM) and a suitable range of dilutions of the competing drug, DMAC. Assay tubes were incubated at 37°C for 2 h. Non-specific binding was detected in the presence of 10 µl of cold MLA (final concentration 1 µM) and in the absence of DMAC. P2 membranes were also incubated

with either [^{3}H]-epibatidine or [^{3}H]-nicotine (final concentration 200 pM and 10 nM respectively) and a suitable range of dilutions of DMAC. Assay tubes were incubated at room temperature for 2.5 h or 3o min at room temperature followed by 1 h at 4°C. Non-specific binding was detected in the presence of 10 µl of cold nicotine (final concentration 1 mM) and in the absence of DMAC. Incubations were terminated by dilution with 4 ml of ice cold PBS at 4°C and rapid filtration through Whatman GFA/E glass filters (Gelman Sciences), pre-soaked in 0.3% (v/v) PEI for 3 h to reduce non-specific binding, using a Brandel Cell Harvester. Filters were washed twice with 4 ml of ice cold PBS at 4°C and bound radioactivity determined by liquid scintillation spectrometry in a Packard Tri-Carb liquid scintillation counter 1600 spectrometer (counting efficiency 45%)

2.3.3.1. Determination of IC_{50} and K_D:

The data from the competition binding assays were calculated as percentages of total radioligand binding minus non-specific binding in the absence of competing cold ligand. The IC_{50} values were calculated by fitting plots to the Hill equation, using the non-linear least squares curve fitting facility of Sigma Plot version 2.0 for Windows:

$$\% \text{ Bound} = 100\% / 1 + ([\text{Ligand}]/IC_{50})^{nH}$$

where n_H is the Hill number, [Ligand] is the concentration of the competing ligand, and IC_{50} is the concentration of ligand that displaces 50% of specific radioligand binding. The affinity constant (K_i) values were derived from IC_{50} values for DMAC against each of the radiolabelled nicotinic ligands according to the method of Cheng and Prusoff (1973):

$$K_i = IC_{50} / (1 + [Ligand]/K_D)$$

Where [Ligand] is the concentration of the labelled radioligand, and K_D is the equilibrium displacement binding constant. Displacement binding K_D values of 10.2 pM and 10 nM for [^{3}H]-epibatidine and [^{3}H]-nicotine respectively and 1 nM for [^{125}I]-α-bgt and [^{3}H]-MLA were assumed (Whiteaker *et al.*, 1998; Davies *et al.*, 1999; Sharples *et al.*, 2000).

2.4. Cell culture: E18 primary rat hippocampal cultures:

2.4.1. Dissociation and maintenance of hippocampal neurones:

High density hippocampal neuronal cultures were prepared from E18 rat fetuses by microdissection as previously described (Goslin and Banker 1991; Barrantes *et al.*, 1995a). In summary, rats were killed by cervical dislocation and the entire uterus containing the fetuses was removed; each fetus was separated one at a time by cutting the umbilical cord. The fetuses were decapitated, and the cerebral hemispheres were separated from the diencephalon and brainstem using fine spring mounted scissors and style forceps under 20 x magnification. The thalamus and meninges were removed in one piece. At this stage, the hippocampi are visible on the posterior half of the hemisphere and were then dissected by cutting the boundaries between the hippocampus and the adjoining cortex (see Figure 2.3).

The dissected hippocampi were placed into a 35 mm Petri dish containing Dulbecco's modified Eagle medium (DMEM), cut into pieces and transferred into a 12 ml test tube to enable further cell dissociation. The tissue pieces were washed twice with 10 ml of phosphate buffered saline (PBS; 150 mM NaCl, 8 mM K_2HPO_4, 2 mM KH_2PO_4, pH 7.4) by centrifugation (500 x g, 5 min).

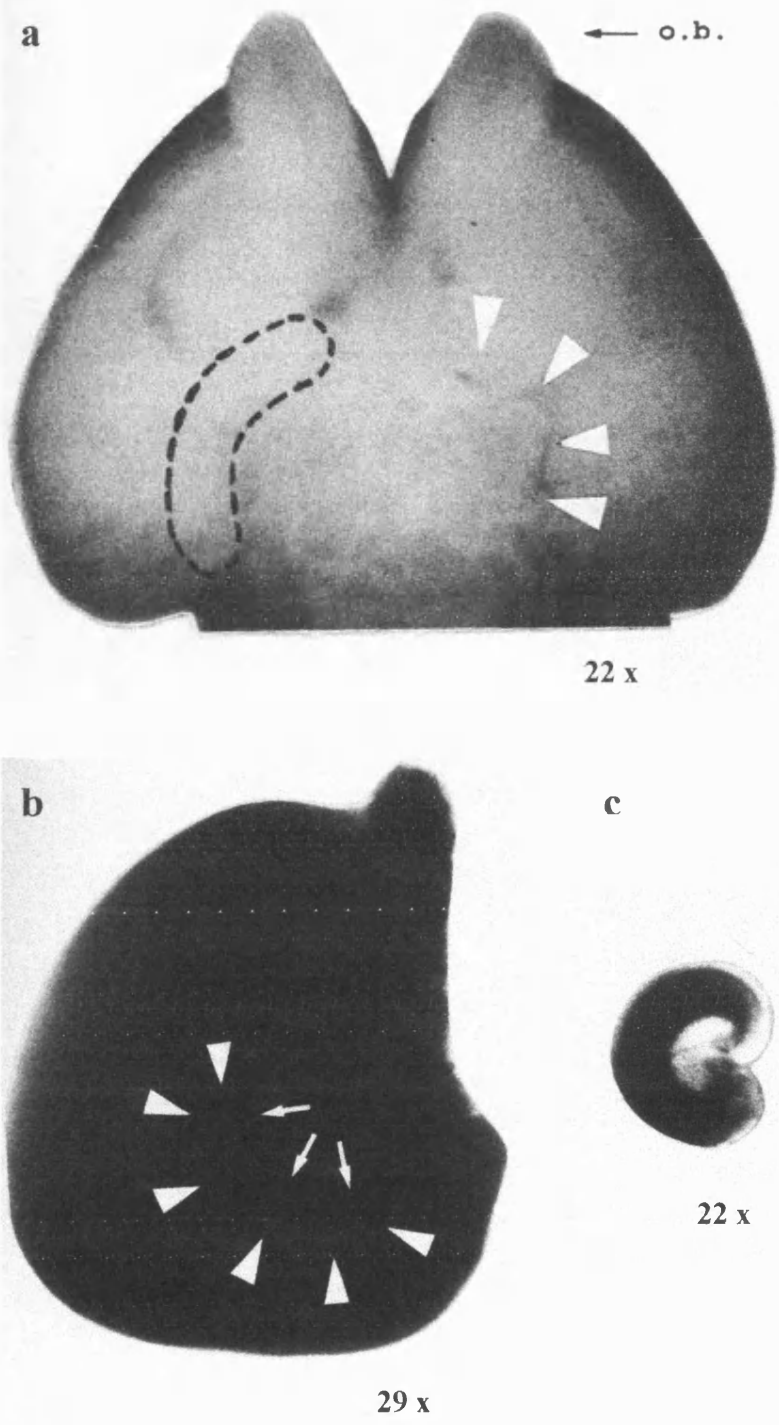

Figure 2.3. Dissection of E18 hippocampi. *(a) Ventral aspect of E18 rat brain (olfactory bulbs are identified as o.b.). The dashed line represents the position of the right hippocampus projected unto the ventral surface of the hemisphere. (b) Shows the left hemisphere when viewed from the midline after removal of the meninges. Arrowheads denote boundary between hippocampus and the adjoining cortex. (c) A hippocampus after dissection. Magnification is indicated.*

The washed hippocampal tissue was incubated at 37° in 2 ml of PBS, in the presence of trypsin (100 µl) and D-glucose 20%. The enzyme reaction was terminated by the addition of 8 ml of serum supplemented chemically defined medium. The tissue suspension was centrifuged and resuspended by triturating the hippocampal tissue with a Pasteur pipette. Once a cloudy suspension was obtained the cells were ready to be plated into a sterile, PEI-coated 24 x 16 mm well Falcon plate at a high plating density (1.5×10^5 cells/cm^2).

Cell density was determined using a haemocytometer. This is a thickened microscope slide ruled with a grid pattern and a counting chamber of 0.1 mm in depth. To count viable cells, the dye trypan blue was used to exclude the proportion of cells that were damaged by the dissociation process. Viable cells have intact membranes and do not incorporate the dye, thus appearing as white cells with bright halos. Damaged cells appear blue in colour as they will take up the dye. The standard protocol used was to take an equal volume of cell suspension to 0.08% trypan blue solution, pipette into the haemocytomoeter chamber and examine the viable to damaged cells by taking the mean value of viable cells counted within 3 different 16 square ruled grids (the mean (n) is equivalent to $n \times 10^4$ cell per ml). A simple calculation allows for the dilution factor so that a final plating concentration of 1.5×10^5 cells/cm^2 is achieved.

Initially cells were plated in serum supplemented (10%, FCS chemically defined DMEM (1 ml for each well; DMEM; (glucose 4.5 g/l): Nutrient Mixture F12 (Ham) (3:1), supplemented with L-glutamine (2 mM), penicillin (50 IU/ml), streptomycin (50 µg/ml), human transferrin (100 µg/ml), putrescine (100 µM), insulin 5 µg/ml), progesterone (20 nM) and sodium selenite (30 nM)) for 2 h, to ensure attachment of neuronal cells. After 2 h the medium was replaced with serum-free chemically defined medium and the neurones were allowed to mature for three days (Barrantes *et al.*,

1995a). This procedure resulted in viable cultures of robust neurones with less than 5% contamination with glial cells (see Figure 2.5b). For long-term survival, cultures were fed every 3-4 days by replacing half of the medium in the wells with fresh chemically defined serum-free medium. Drug dilutions were prepared in 'conditioned' medium and were applied to mature cultures for either 4 or 7 days.

2.4.2. Drug treatment:

Initial experiments used confluent hippocampal neurones cultured in 24 well Falcon plates. Cultures were chronically treated with a number of drugs, alone or in combination, for 7 days. Subsequently a 4 day drug exposure was employed. Nicotine, KCl and (±)-verapamil hydrochloride were made up freshly in 'conditioned' chemically defined medium on day 1 of drug treatment (equates to day 3 in culture). KN-62 and DMAC were made up in dimethylsulfoxide (DMSO) in stock solutions of 10 mM so that the final concentration of DMSO on cultures did not exceed 0.1%. Chronic exposure to this concentration of DMSO had no effect on subsequent ligand binding assays. All drugs were applied to confluent cultures and after 4 or 7 days of drug treatment, a binding assay with [^{125}I]-α-bgt was performed (see section 2.6.3).

2.5. Detection of glial cells in hippocampal cultures by fluorescence cytochemistry:

Seven day old E18 hippocampal cultures were grown in x 6 well plates, in the absence of drugs, were washed x 3 with 1 ml warm PBS before being fixed and permeabilised by the drop-wise addition of 200 µl cold acid ethanol solution (5% acetic

acid in 70% ethanol). After 15 min, the cultures were washed x 3 with 500 µl of PBS. Blocking solution (sheep serum in PBS; 1 ml of 1%) was applied to hippocampal cultures for 1 h at room temperature before applying the glial fibrillary acidic protein (GFAP) (1:400 dilution) monoclonal antibody (mAb). Negative controls for non-specific fluorescence omitted the primary antibody from the procedure and were incubated in the presence of the sheep serum blocking solution thus determining non-specific binding. After 1 h incubation the cultures were washed x 3 with 1 ml of the sheep serum blocking solution before the addition of 250 µl of the secondary anti-mouse IgG fluorescein-linked whole antibody from sheep (1:100) dilution. After 1 h incubation in the dark, the neurones were washed x 3 with 1 ml PBS and mounted with Vectashield (Vector Labs.) before being viewed in a Nikon inverted microscope equipped for epifluorescence.

2.6. Radioligand binding with [^{125}I]-α-bgt on cultured cells *in situ*:

2.6.1. Procedure for iodination of α-bgt to high specific activity:

Sephadex G25 beads (25 g) were allowed to swell and washed in reaction buffer before being poured into a Pharmacia column (0.9 x 12 cm). The column was packed with Sephadex to within 5 cm from the top, and then washed with 30 ml of elution buffer. The iodination was performed in a fume hood with suitable protection and shielding from the radiolabelled compound.

A reaction tube (LP3 tube) was clamped over a magnetic stirrer and the following were added, a magnetic flea to constantly stir the reaction mixture, α-bgt (20 µl, 2.5 nmol), reaction buffer (10 µl; 0.05 M potassium phosphate, pH 7.5) and [^{125}I]-NaI (20 µl, 2 mCi). The reaction was started by the addition of chloramine T (10 µl; 5 mg/ml in

reaction buffer). The reaction was terminated after 1 min by the addition of 0.75 ml sodium metabisulphite (0.16 mg/ml in reaction buffer) and 0.2 ml potassium iodide (10 mg/ml in reaction buffer). The column was drained of any elution buffer that was covering the G25 Sephadex before transferring the reaction mixture by Pasteur pipette to the top of the G25 Sephadex column. The reaction tube was rinsed by the addition of 0.5 ml elution buffer (0.01 M potassium phosphate, pH 7.5 containing 1% BSA) which was then transferred to the column. When the sample had drained into the Sephadex, the column was washed with elution buffer and approximately 20 fractions (1 ml) were collected. From each fraction, 5 µl was counted for radioactivity (Packard Cobra II Auto Ultra γ counter). Characteristic elution profiles are shown in Figure 2.4.

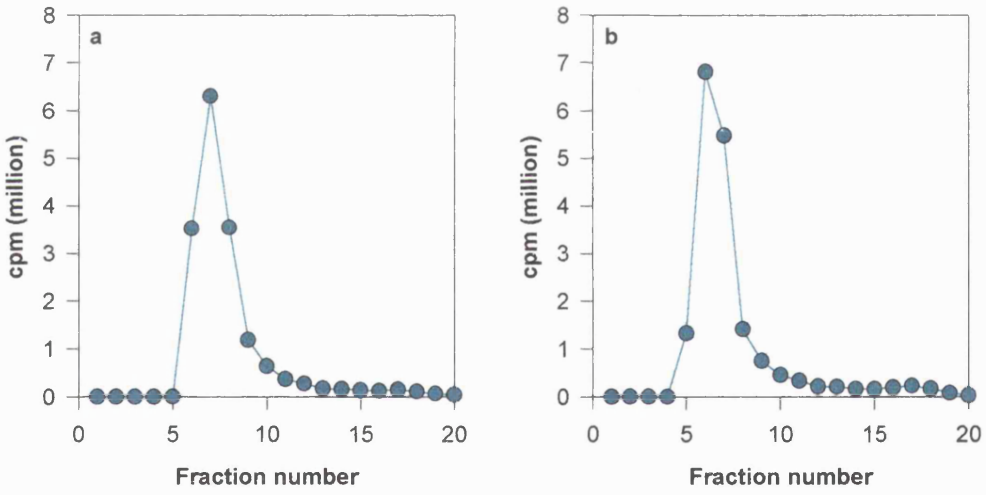

Figure 2.4. ***Typical elution profiles for the iodination of α-bgt.*** *In both traces a and b, there are two radioactive peaks. The first predominant peak (sample 6 or 7) corresponds to [^{125}I]-α-bgt (mono-iodinated or di-iodinated product) and the second, lower peak (samples 16-18) corresponds to the free [^{125}I].*

2.6.2. Calculation of specific activity of [^{125}I]-α-bgt:

Typical values obtained from a successful iodination of α-bgt are: a concentration of > 0.5 pmol α-bgt/ml, 0.4 μCi ^{125}I/ml, > 90% incorporation of ^{125}I into α-bgt and specific activity of 700 Ci/mmol for the resulting [^{125}I]-α-bgt. Typical results obtained for the iodination procedure are shown in Table 2.1.

Table 2.1. Typical values obtained from two separate iodination experiments.

	pmol α-bgt/ml	μCi ^{125}I /ml	% incorporation of ^{125}I into α-bgt	Specific activity of [^{125}I]-α-bgt
Elution profile A	0.54	0.42	95.6	766 Ci/mmol
Elution profile B	0.71	0.5	88.0	700 Ci/mmol

2.6.3. Assay for [^{125}I]-α-bgt binding to hippocampal cultures:

[^{125}I]-α-Bgt binding assays were performed on primary rat hippocampal cultures grown in the presence of drugs for either 4 or 7 days in 24 x 16 mm culture well plates. The binding assays were performed essentially as described by Barrantes *et al.* (1995a). In brief, on the day of assay, cultures were washed four times with warm medium over a 3 h period prior to the assay, to remove all traces of drugs from the cultures that could interfere with specific binding whilst being a long enough period not to have significant changes on receptor numbers due to nAChR turnover (Dr Rogers personal communication). After 3 h, non-specific binding was defined by pre-incubation of cultures (in triplicate) with 2 μM α-bgt (made in chemically defined medium containing 0.01% BSA (200 μl; 1 h; 25°C)). Total binding was defined in parallel cultures with

200 µl of 0.01% BSA containing medium (1 h; 25°C). After this incubation period, [^{125}I]-α-bgt (final concentration 10 nM) was applied to all culture wells and further incubated for 2 h at 25°C. The cultures were subsequently washed three times with 1 ml warm PBS, solubilised in 0.1 M NaOH (200 µl; 16 h at 4°C), counted for radioactivity (Packard Cobra II Auto Ultra γ counter) and then assayed for protein (Markwell *et al.*, 1978). Radioactivity bound was then directly related to protein values.

All raw data (fmol/mg protein) generated in this thesis were analysed statistically using an analysis of variance (ANOVA). Quoted significance values obtained ($p<0.05$) relate to values obtained using the Tukey test which was used as a multiple range test when the ANOVA gave significance of $p<0.05$. The raw data are presented as normalised data throughout the thesis unless otherwise stated, with control conditions being represented as 100% and the S.E.M. being normalised from the S.E.M. obtained for the fmoles of radioligand bound/mg protein.

2.7. Results.

2.7.1. Fluorescence cytochemistry:

The panels shown in Figure 2.5 were obtained from high density E18 primary rat hippocampal cultures that had been growing in culture for 7 days. The top panel (a) shows the normal field of vision when cultures were viewed by ordinary bright phase contrast (tungsten) under a light microscope. The lower panel (b) shows the same field of view immunolabelled with mAb-GFAP to identify glial cells in the hippocampal cultures when viewed under a u.v. filter. Glial cells contribute to approximately 5% of the mature hippocampal neuronal population that has developed an extensive network of neurites (Figure 2.5). Chronic treatment with nicotinic drugs or KCl depolarisation does not alter this proportion of glial cells within hippocampal neuronal populations.

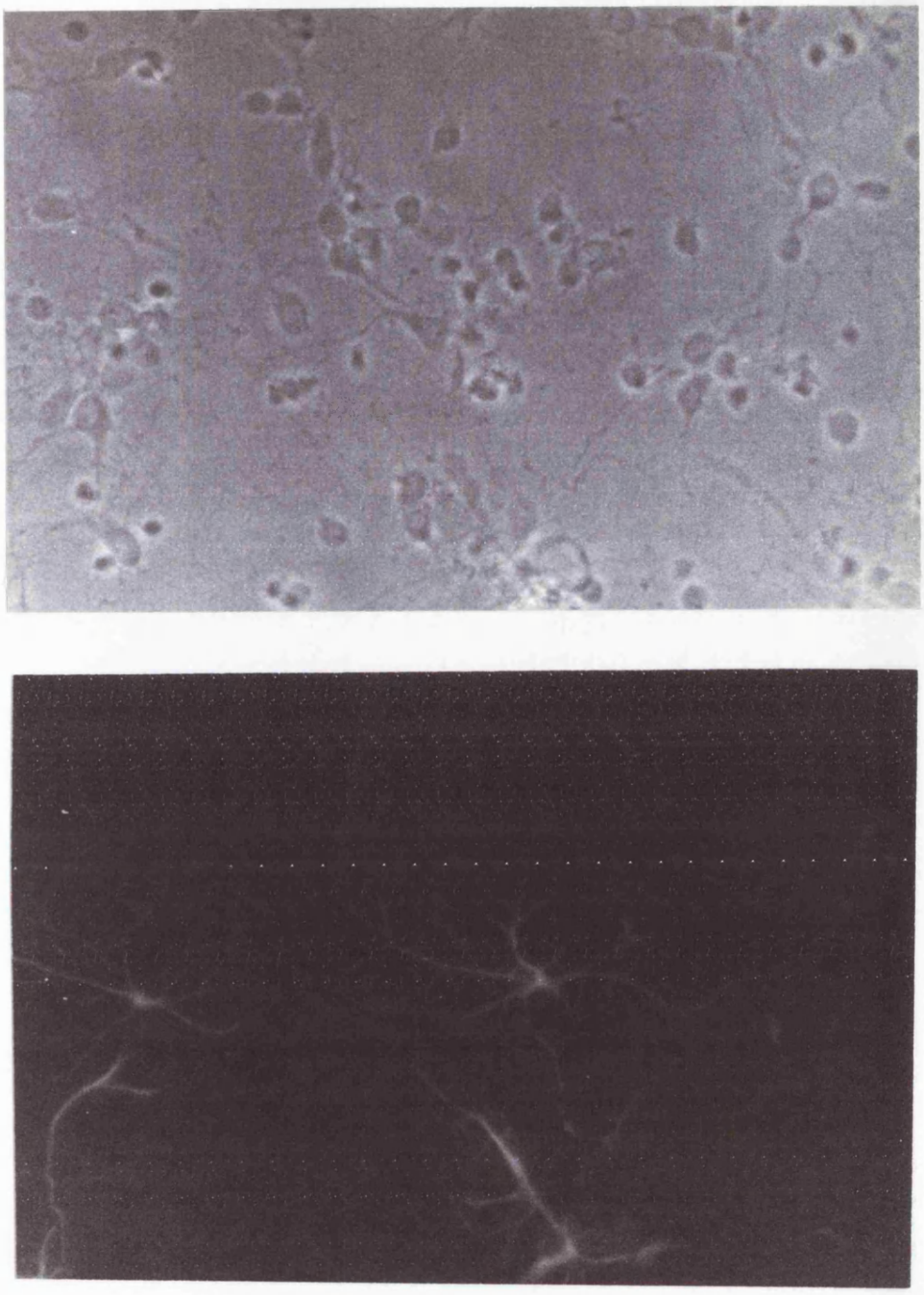

Figure 2.5. mAb-GFAP immunostaining of E18 rat hippocampal neuronal cultures. *Seven day old E18 rat hippocampal cultures were fixed/permeabilised with 5% acetic-acid - 70% ethanol solution. Preparations were blocked with 1% normal sheep serum in PBS to reduce non-specific immunostaining. Cells were incubated with mAb-GFAP to determine total immunostaining. Anti-mouse Ig, fluorescin linked whole antibody was applied to the preparations as a secondary antibody. The fields viewed correspond to the same preparation and the same field of view observed either under (a) ordinary bright phase contrast (tungsten) or (b) u.v. filter using x 20 objective.*

2.7.2. Upregulation of [^{125}I]-α-bgt binding sites in hippocampal cultures:

2.7.2.1 Pharmacological characterisation: effects of nicotinic agonists and KCl:

Upregulation of [^{125}I]-α-bgt binding sites in response to exposure to nicotine has previously been shown to be concentration-dependent when applied to primary hippocampal cultures for 7 days (Barrantes *et al.*, 1995a); 1 μM nicotine had no influence on binding site density, 10 μM nicotine produced an increase of 30 ± 3% (n=27) and high concentrations of nicotine (100 μM) proved toxic to the neurones within 7 days (Rogers and Wonnacott, 1997). It was therefore decided to use nicotine at a dose of 10 μM which was not toxic to the neurones in culture and which would establish detectable levels of upregulation of [^{125}I]-α-bgt binding sites.

In the present study control hippocampal cultures expressed 92 ± 5 fmol of [^{125}I]-α-bgt binding/mg protein. Hippocampal cultures grown in the presence of nicotine for 7 days displayed an increase in the number of surface [^{125}I]-α-bgt binding sites to 28 ± 3% (n=4) above control levels of binding (100%) (Table 2.2). The values obtained for upregulation of [^{125}I]-α-bgt binding sites represent a real increase in numbers of α7* nAChR subtypes, rather than reflecting a change in cell density, as the [^{125}I]-α-bgt binding site density was calculated in terms of protein, determined for each assay well (see methods 2.6.3).

Table 2.2. Upregulation of [^{125}I]-α-bgt binding sites in E18 hippocampal cultures following chronic exposure to nicotine (10 μM) or KCl (20 mM) for either 4 or 7 days. *Control values are expressed as fmoles [^{125}I]-α-bgt bound/mg protein; the upregulation mediated by nicotine and KCl is expressed as a percentage of control. Significantly different from control, *p<0.05, (one way ANOVA).*

	[^{125}I]-α-bgt binding sites		
Drug treatment (days)	**Control (fmol/mg protein)**	**10 μM Nicotine (% control)**	**20 mM KCl (% control)**
4	92 ± 14 (n=14)	125 ± 3% (n=6)*	159 ± 13% (n=12)*
7	92 ± 5 (n=24)	128 ± 3% (n=4)*	157 ± 14% (n=6)*

To determine if general depolarisation had any influence on the numbers of surface [^{125}I]-α-bgt binding sites, cultures were exposed for 7 days to medium in which the KCl concentration was increased from 5 to 20 mM. This produced a 57 ± 14% (n=6) increase in the number of binding sites (Table 2.2).

The effect of shorter drug exposure times was examined by treatment of hippocampal cultures for 4 days with the nicotinic agonists, nicotine and DMAC or KCl depolarisation. Nicotine and KCl produced similar increases in the numbers of [^{125}I]-α-bgt binding sites after 4 days compared to those seen after 7 days (Table 2.2, Figure 2.6). Therefore subsequent experiments used a 4 day drug exposure protocol, which also reduced the risk of contamination to the primary cultures.

DMAC, a novel nicotinic agonist with putative α7-selectivity (see section 1.6.2.2; De Fiebre *et al.*, 1995), evoked a concentration-dependent upregulation of [^{125}I]-α-bgt binding sites when applied to hippocampal cultures for 4 days: 1 μM DMAC did not upregulate numbers of [^{125}I]-α-bgt binding sites compared to control, whereas 10 μM

DMAC increased [^{125}I]-α-bgt binding by 26 ± 1% above control levels (n=3; significantly different from control *p<0.05, one way ANOVA) (Figure 2.6). This is similar to the degree of upregulation produced by 10 μM nicotine compared to untreated control cells, 25 ± 3% (n=6) (Table 2.2).

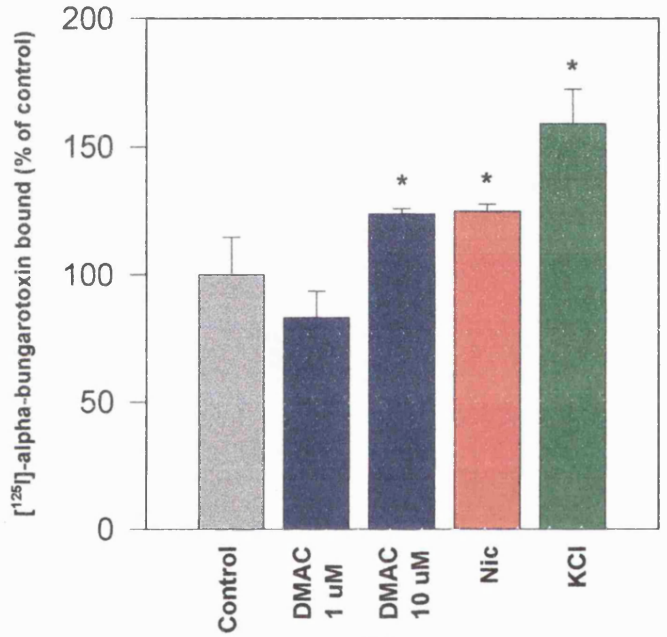

Figure 2.6. Upregulation of [^{125}I]-α-bgt binding sites in hippocampal cultures. *Hippocampal cultures were exposed to chronic drug treatment with either nicotinic agonists DMAC (1 μM, 10 μM), nicotine (nic; 10 μM) or KCl depolarisation (20 mM) for 4 days before the binding assays were performed. Values are the mean ± S.E.M. from at least 3 independent cultures. * Significantly different from control at p<0.05; one way ANOVA.*

The putative reported α7-selectivity of DMAC compared to other nAChR subtypes led to an investigation to examine the ability of DMAC to displace the binding of [^{125}I]-α-bgt, [^{3}H]-MLA, [^{3}H]-nicotine and [^{3}H]-epibatidine from rat brain membranes was assessed in competition binding assays (Figure 2.7; Table 2.3). DMAC was 4-5 fold

more potent at displacing [^{3}H]-epibatidine and [^{3}H]-nicotine binding than at displacing the α7-selective radioligands [^{125}I]-α-bgt and [^{3}H]-MLA.

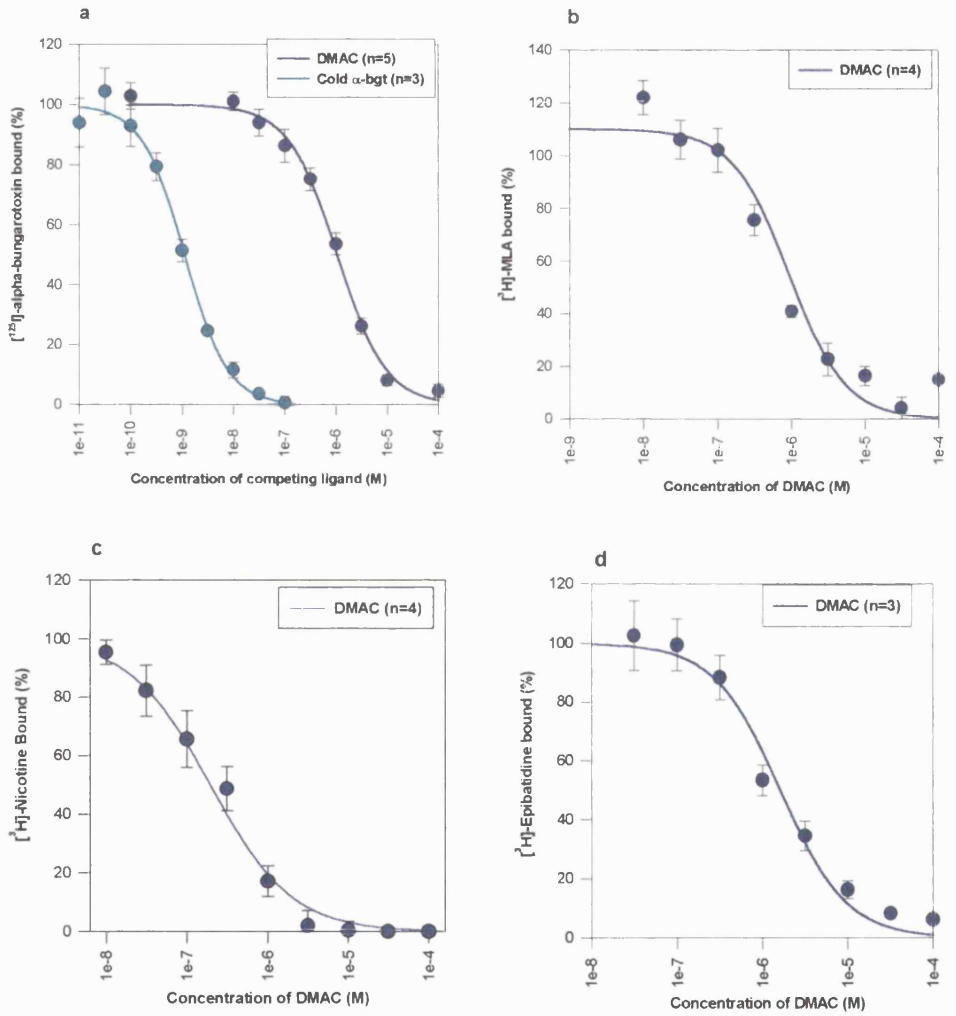

Figure 2.7. Competition binding assays for [^{125}I]-α-bgt, [^{3}H]-MLA, [^{3}H]-nicotine and [^{3}H]-epibatidine performed on rat brain membranes. *A range of concentrations of DMAC or cold α-bgt were used as competing ligands to displace (a) [^{125}I]-α-bgt (10 nM), or DMAC was used to displace (b) [^{3}H]-MLA binding, (c) [^{3}H]-nicotine binding and (d) [^{3}H]-epibatidine binding, from rat brain membranes. Points are the mean of at least 3 independent experiments performed in triplicate ± S.E.M.*

Table 2.3. K_i values obtained for DMAC against the binding of [^{125}I]-α-bgt, [^{3}H]-MLA, [^{3}H]-nicotine and [^{3}H]-epibatidine to rat brain membranes. Each value represents the mean ± S.E.M. of at least three separate binding experiments.

Radioligand	K_i values (nM)
[^{125}I]-α-bgt	426.0 ± 85
[^{3}H]-MLA	392.9 ± 65
[^{3}H]-Nicotine	102.9 ± 6
[^{3}H]-Epibatidine	72.6 ± 6

2.7.2.2. Mechanisms of nicotine- and KCl-evoked upregulation of [^{125}I]-α-bgt binding sites in hippocampal cultures:

To investigate whether the upregulation induced by nicotine (10 μM) and a depolarising concentration of KCl (20 mM) might arise through a common cellular pathway, further experiments were performed in the presence of inhibitors of putative intermediate steps. The effect of verapamil, an L-type Ca^{2+} channel blocker, was examined to determine whether alterations in Ca^{2+} entry into hippocampal cells might play a role in the upregulation of hippocampal [^{125}I]-α-bgt binding sites. Exposure of hippocampal cultures to 5 μM verapamil for 4 days had no significant effect on numbers of binding sites when applied alone but prevented the upregulation elicited by KCl (Figure 2.8a).

To determine whether upregulation involves a CaM-kinase II pathway, cultures were incubated with either 10 μM nicotine or 20 mM KCl in the absence or presence of KN-62, a selective CaM-kinase II inhibitor (Tokumisto *et al.*, 1990). Upregulation elicited by KCl was totally abolished by co-incubation with KN-62, which itself had no effect

on the level of [^{125}I]-α-bgt binding to these cultures (Figure 2.8b). In contrast, nicotine-induced upregulation was not blocked in the presence of 5 μM KN-62; the number of [^{125}I]-α-bgt binding sites remained at 29 ± 9% above control after treatment with KN-62 and nicotine, compared with a 25 ± 3% increase produced by nicotine alone (Figure 2.8c). These results suggest that the process of upregulation of [^{125}I]-α-bgt binding sites in hippocampal neurones evoked by nicotine and by KCl occur through different cellular mechanisms.

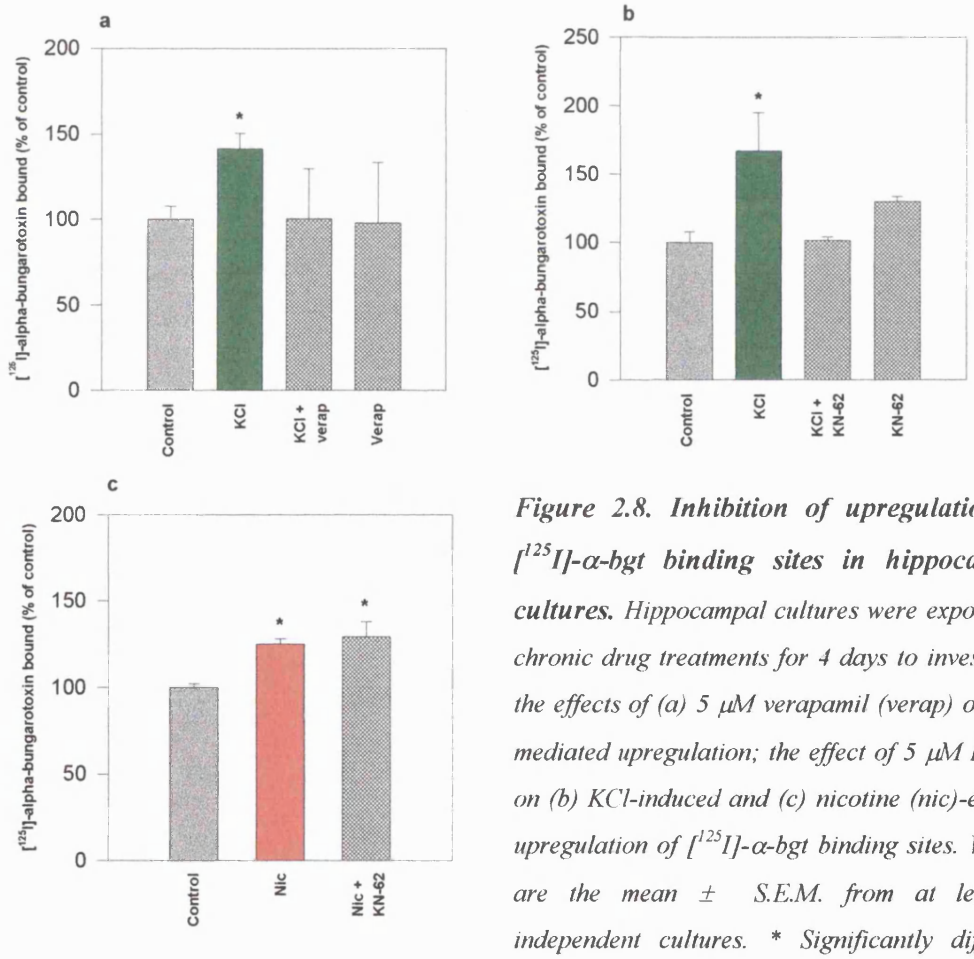

Figure 2.8. Inhibition of upregulation of [^{125}I]-α-bgt binding sites in hippocampal cultures. *Hippocampal cultures were exposed to chronic drug treatments for 4 days to investigate the effects of (a) 5 μM verapamil (verap) on KCl mediated upregulation; the effect of 5 μM KN-62 on (b) KCl-induced and (c) nicotine (nic)-evoked upregulation of [^{125}I]-α-bgt binding sites. Values are the mean ± S.E.M. from at least 3 independent cultures. * Significantly different from control at $p<0.05$; one way ANOVA.*

2.8. Discussion.

This Chapter has demonstrated that chronic exposure to the nicotinic agonists nicotine and DMAC or after KCl depolarisation, evoke an upregulation of the numbers of [^{125}I]-α-bgt binding sites in primary hippocampal neurones. However, the underlying cellular mechanisms of upregulation differ between nicotine- and KCl-evoked upregulation: only the upregulation evoked by the latter chronic treatment is blocked by the CaM-kinase II inhibitor, KN-62.

2.8.1. Upregulation of [^{125}I]-α-bgt binding sites in hippocampal cultures – pharmacological characterisation:

These data confirm that primary hippocampal neurones can be dissociated and grown in high density cultures containing low expression of glial cells and detect reproducible binding of [^{125}I]-α-bgt (Goslin and Banker, 1991; Barrantes *et al.*, 1995a). The data described in this Chapter confirm and extend previous observations that chronic exposure of cell cultures *in vitro*, to nicotine, the prototypical agonist for neuronal nAChR, produces an upregulation of [^{125}I]-α-bgt binding sites after 4 or 7 days of chronic drug treatment (Barrantes *et al.* 1995a; Peng *et al.*, 1997; Molinari *et al.*, 1998). Radiolabelled binding assays with this large polypeptide snake toxin ([^{125}I]-α-bgt) were performed on cells *in situ*, therefore only the surface α7* nAChR population of receptors was labelled. Therefore the upregulation of [^{125}I]-α-bgt binding sites observed in these assays reflects an increase in the number of surface binding sites. Furthermore, the fact that α-bgt binds to all conformations of α7* nAChR makes the increased density of binding sites with an increase receptor number unambiguous.

Previous experiments have demonstrated that primary hippocampal cultures provide an *in vitro* system that can be used to explore the concentration- and time-dependent upregulation of [^{125}I]-α-bgt binding to surface sites after chronic nicotine treatment (Barrantes *et al.*, 1995a). Initial experiments performed in this study indicate that detectable increases of α7* nAChR result after 7 days of chronic drug treatment with nicotine or 20 mM KCl. Previously, upregulation of [^{125}I]-α-bgt binding sites evoked by KCl has been demonstrated not to be mediated by an increase in the ionic strength by changing the osmolarity. This was concluded by increasing NaCl, rather than KCl: increased NaCl did not effect [^{125}I]-α-bgt binding sites in chromaffin cells or in hippocampal cultures (Geertsen *et al.*, 1988; Rogers and Wonnacott, 1997). Previous data indicate that increasing the concentration of KCl (> 30 mM) is toxic to cultures (Rogers and Wonnacott, 1997).

After 4 days, in the presence of either nicotine or KCl, significant upregulation of [^{125}I]-α-bgt binding sites was observed in the same range as that produced after 7 days. This can be related to the work performed by Marks *et al.* (1985) who chronically administered nicotine to mice and investigated the time course relating to the onset and loss of tolerance. Results identified that maximum tolerance was observed after 4 days of continuous nicotine infusion and was paralleled by increases in the number of [^{3}H]-nicotine and [^{125}I]-α-bgt binding sites. Prolonging the nicotine treatment did not significantly evoke more extensive changes. Therefore in subsequent experiments in this study a drug regime of 4 instead of 7 days of chronic treatment was used to reduce the risk of contamination of the primary cultures. The level of upregulation observed by nicotine (approximately 30%) is consistent with previous data for α7* nAChR upregulation (Barrantes *et al.*, 1995a; Quik *et al.*, 1996; Peng *et al.*, 1997). The magnitude of upregulation reported *in vitro* is reminiscent of the magnitude of

upregulation of [^{125}I]-α-bgt binding sites (between 33 and 40%) reported after *in vivo* administration of nicotine (Marks *et al.*, 1985; Conroy and Berg, 1995). However, nicotine-evoked upregulation of α7* nAChR is low compared to the enormous increases in upregulation of α4β2 nAChR in transfected cell lines (e.g. 1500% in HEK 293 cells, Gopalakrishnan *et al.*, 1996). The presence of expression vectors may contribute to this huge response.

The ability of chronic nicotine treatment to upregulate the number of [^{125}I]-α-bgt nAChR binding sites has previously been documented (Barrantes *et al.*, 1995a; Peng *et al.*, 1997; Molinari *et al.*, 1998). These studies demonstrate that upregulation reflects an increase in B_{max} of [^{125}I]-α-bgt binding sites without a change in K_D in cells transfected with α7 cDNA or in cells endogenously expressing the α7 subunit gene (Quik *et al.*, 1996; Peng *et al.*, 1997).

In addition to nicotine, chronic exposure of cultures to the putative α7-selective agonist DMAC yielded increases in [^{125}I]-α-bgt binding sites comparable to those observed after nicotine treatment. DMAC, an anabaseine derivative, was first described by De Fiebre *et al.* (1995). In competition binding assays these authors found DMAC to be 10-fold more potent at displacing [^{125}I]-α-bgt binding than [^{3}H]-nicotine binding from rat brain membranes. The competition binding assays of DMAC described in this Chapter indicate that DMAC is 10 times less potent at α7 binding sites than previously reported (Table 2.3). This might reflect the different salt of the anabaseine derivative. Nevertheless, this compound was only 4-fold less potent at α7 sites (identified by displacing [^{125}I]-α-bgt and [^{3}H]-MLA binding) than at high affinity agonist binding sites (predominantly α4β2 nAChR subtype). At α7* nAChR expressed in *Xenopus* oocytes,

DMAC is a potent agonist, whilst it behaves as a weak partial agonist with little efficacy at other subtypes (De Fiebre *et al.*, 1995).

Rogers and Wonnacott (1997) also showed upregulation of [^{125}I]-α-bgt binding sites in PC12 cells in response to nicotine and also cytisine. Both of these nicotinic agonists are tertiary amines which enables them to cross the cell membrane efficiently. This would not exclude a putative intracellular mechanism underlying the upregulation of nAChR. This could be a mechanism which promotes conformational maturation of the α7 subunits, an increase in the efficiency of assembling α7 subunits as homomeric nAChR (modified from α4β2 in Peng *et al.*, 1994b) or nicotinic agonists could increase α7* nAChR levels by enhancing receptor stabilisation. The quaternary nitrogen containing amine, DMPP acts as a partial agonist with very low efficacy on chick α7* nAChR expressed in *Xenopus* oocytes (Amar *et al.*, 1993), and is capable of evoking comparable concentration-dependent increases of [^{125}I]-α-bgt binding sites in primary hippocampal cultures (Rogers and Wonnacott, 1997) and in HEK-293 cells transfected with human α7 subunits (Molinari *et al.*, 1998). DMPP is membrane impermeant in nature, providing suggestive evidence that upregulation of α7* nAChR is mediated by this agonist acting outside the cell at α7* nAChR present on the surface of the cell membrane, therefore dismissing an intracellular mechanism. A similar conclusion for the upregulation of α7* nAChR in SH-SY5Y cells has been obtained using carbamylcholine (Peng *et al.*, 1997). Peng *et al.* (1997) conclude that the process of nicotine-evoked upregulation is achieved without an increase in transcription of the α7* nAChR subunit gene, due to unaltered levels of α7 subunit mRNA compared to control. This presumes that a post-transcriptional mechanism may underlie the process of upregulation. Such a mechanism could be one already proposed to account for the

upregulation of the high affinity α4β2 nAChR, including a decrease in nAChR turnover (Peng *et al.*, 1994b; Rothhut *et al.*, 1996), increase in the rate of receptor assembly (Wang *et al.*, 1998), or an increase in receptor recruitment from a pre-existing intracellular receptor pool (Bencherif *et al.*, 1995).

The α7 nAChR subunit mRNA is expressed and [^{125}I]-α-bgt binding peaks early during development in the postnatal period of rat in the S1 neuronal region (Broide *et al.*, 1996). The transient increase in expression of α7 mRNA and the corresponding increase in [^{125}I]-α-bgt binding site density expression during the early postnatal period, identify a possible role for α-bgt-sensitive nAChR being important in critical stages of CNS development (Broide *et al.*, 1996; Role and Berg, 1996), may have a role in the termination of axonal neurite outgrowth during development and also an involvement in neural sprouting after injury by high Ca^{2+} influx after α7* nAChR activation (see Chapter 5; Pugh and Berg, 1994). α-Bgt-sensitive nAChR have also been shown to play an important role as modulators of synaptic strength in the CNS (McGhee *et al.*, 1995; Gray *et al.*, 1996), and roles in neuroprotection (see section 1.9.1; Semba *et al.*, 1996; Miñana *et al.*, 1998), and in the pathophysiology of disorders including schizophrenia (see section 1.9.4; Freedman *et al.*, 1997).

The major objective of this Chapter was to compare the mechanisms of nicotine-evoked and depolarisation-induced upregulation of α7* nAChR, based on previous findings reported by De Koninck and Cooper (1995) on KCl-induced changes in α7 nAChR in rat sympathetic neurones. In agreement with De Koninck and Cooper (1995), a modest depolarising concentration of KCl was found to increase the number of [^{125}I]-α-bgt binding sites on the surface of hippocampal neurones, and this upregulation was sensitive to both the L-type voltage-operated calcium channel (VOCC) blocker

verapamil and the CaM-kinase II inhibitor KN-62 (Figure 2.8) Membrane depolarisation is a survival factor for some developing neurones, and physiologically may contribute to synapse formation and strengthening. In rat sympathetic neurones, KCl-induced increases of surface [^{125}I]-α-bgt binding were correlated with increased levels of α7 mRNA gene expression, suggesting a mechanism involving enhanced transcription (De Koninck and Cooper, 1995). The key observation in this Chapter that KN-62 did not prevent the nicotine-induced upregulation of [^{125}I]-α-bgt binding sites in these primary rat hippocampal cultures suggests that nicotine-evoked upregulation occurs by a different mechanism (see discussion Chapter 3).

Primary cultures are potentially very useful in experimental analysis as they provide information on the native receptors obtained *ex vivo* after dissection from a living system, but these cultures introduce a few inconveniences. Studies on primary hippocampal cultures are severely limited by the paucity of material available from dissection and the labour intensive techniques involved in the preparation of cultures to provide sufficient material for these experiments. The inability of primary cultures of neurones to divide encouraged us to seek an alternative system to circumvent this problem, namely the use of cell lines derived from neuronal tumours. Chapter 3 describes initial experiments performed with the rat pheochromocytoma PC12 cell line and then progression on to the SH-SY5Y human neuroblastoma cell line for further studies to investigate the effects of chronic drug treatment and the cellular mechanisms underlying nAChR upregulation.

Chapter 3. Upregulation and localisation of nAChR in SH-SY5Y cells.

3.1. Introduction.

As described in Chapter 2, primary hippocampal cultures were grown and exposed to chronic drug treatments before determining the number of [^{125}I]-α-bgt binding sites. Using primary hippocampal tissue has several drawbacks; first the paucity of hippocampal material which yields low numbers of cells with a limited life span. The labour intensive preparation of hippocampal material and the low tolerance of these neurones to chronic drug treatment regimes, provide criteria and considerable advantages for the search of a suitable cell line over primary neuronal cultures. A cell line used as an alternative model system would help to circumvent these problems, enabling us to extend the investigation of the mechanisms underlying upregulation of nAChR and the level of expression of the α3 and α7 nAChR subunits *in vitro*. Preliminary data was generated using the rat pheochromocytoma PC12 cell line before advancing to the SH-SY5Y cell line.

The relative ease and inexpensive nature of using cell lines compared to using primary cultures is immediate and has helped to expand and compare the cellular mechanisms underlying upregulation already obtained with primary hippocampal cell cultures. Using cell lines is typically a matter of defrosting a vial of cells of low passage number, plating the cells into a sterile flask with chemically defined medium and leaving them to grow to confluency. Once confluent cells can either be subcultured into tissue culture plates or flasks, or frozen to maintain cell stocks. Some additional advantages of robust cell lines are that they consist of a homogeneous population of cells, identical to each other that should produce reliable results within the same culture and also between cultures over a period of time (see Lukas, 1998). This is in contrast to *in vivo* studies that can be expensive with respect to the quantity of animals often needed to overcome individual experimental variation and of course, is subject to

ethical considerations. Despite the many advantages of using cell lines, a disadvantage is that the functioning of cells in culture does not represent the full complexity of an intact, native neural network laid down in the CNS, with the many biochemical and biophysical interactions occurring between different neural regions as observed with *in vivo* techniques. Cell culture techniques have the additional advantage that an exact drug concentration can be applied to cells without the hindrance of the blood brain barrier. Drug treatment can be directly correlated to receptor numbers by the use of specific radiolabelled ligands. As far as binding data is concerned, cell lines have proved to be invaluable as model systems, producing results that closely parallel receptor changes observed *in vivo*.

This Chapter is divided into four main sections:

1). Section 1 investigates the cellular mechanisms underlying upregulation of α3* and α7* nAChR in SH-SY5Y cells.

2). Section 2 introduces molecular biological techniques used to detect and quantitate the level of expression of α3 and α7 subunit RNA after chronic drug treatment to SH-SY5Y cells compared to control.

3). Section 3 is a preliminary investigation into the visualisation of upregulated α3 and α7 nAChR subunits after chronic nicotinic agonist and KCl treatment compared to control untreated SH-SY5Y cells.

4). Section 4 discusses the results obtained in this Chapter.

Sections 1-3 will contain a brief introduction, methods and materials with a results section to follow. A final overall discussion is presented in Section 4 to incorporate and discuss the results obtained from all sections on the SH-SY5Y cell line experimental data.

Section 1: Upregulation of nAChR in SH-SY5Y cells.

3.1.1. The rat pheochromocytoma (PC12) cell line:

PC12 cells are a clonal cell line initially established from a transplantable rat adrenal pheochromocytoma tumour (Greene and Tischler, 1976). This cell line displays phenotypic properties associated with pheochromocytomas and they resemble their neoplastic counterparts, noradrenergic adrenal medulla (chromaffin) cells. PC12 cells are therefore capable of synthesising and storing catecholamines (DA and NE) (Greene and Tischler, 1976; Inoue and Kenimer, 1988) and express α3, α5, α7, β2, β3 and β4 nAChR subunits (Boulter *et al.*, 1990; Rogers *et al.*, 1992; Ishiguro *et al.*, 1997). When growing PC12 cells in culture, one important feature is that upon the addition of nerve growth factor (NGF) the cells will be prevented from further division and hence proliferation (Greene, 1978; Henderson *et al.*, 1994). This differentiation of PC12 cells causes a dramatic change in the cellular phenotype by the development of long branching neuronal processes from the cell bodies, the cells become electrically excitable to ACh (Greene, 1978; see Greene *et al.*, 1991) and there is a change in the expression of nAChR genes encoding α3, α5, α7, β2 and β4 subunits (Rogers *et al.*, 1992; Henderson *et al.*, 1994; Hu *et al.*, 1994). In contrast, NGF deprivation promotes PC12 cell death (Batisatou and Greene, 1991), and this process could be subsequently reversed by the application of nicotine (1-100 μM), revealing neuroprotective effects mediated through nAChR (Yamashita and Nakamura, 1996).

Long-term nicotine treatment has previously been shown to produce a concentration-dependent increase in [^{3}H]-nicotine binding to PC12 cells without altering the levels of α3, α5, α7 or the β4 nAChR subunit genes, but increasing the mRNA level of the β2 nAChR subunit gene (Madhok *et al.*, 1995). The former nAChR subunit mRNAs were

down regulated by treatment with forskolin, indicating the possible involvement of a protein kinase A (PKA) pathway (Ishiguro *et al.*, 1997). Nicotine treatment failed to enhance [^{3}H]-nicotine binding to PC12 cell mutants deficient in PKA, suggesting that this protein kinase may be required for upregulation of nAChR in response to nicotine (Madhok *et al.*, 1994, 1995). Long-term treatment with the nicotinic agonist, carbamoylcholine, produced a decrease in the responsiveness, also termed "functional down-regulation", of wild-type PC12 cells (Robinson and McGee, 1985). In contrast to nicotine, KCl depolarisation (50 mM) for 4 days was found not to have an effect on the subsequent responsiveness of PC12 cells to nicotinic cholinergic stimulation, or regulate neuronal nAChR on PC12 cells (De Lorme and McGee, 1988) or to affect [^{3}H]-epibatidine binding after chronic KCl treatment for 7 days (Rogers and Wonnacott, 1997). PC12 cells were therefore employed as a useful model cell line system, as a starting point to further the data generated from primary hippocampal neuronal cultures.

3.1.2. The SH-SY5Y cell line:

The SH-SY5Y neuroblastoma clonal cell line was initially established through sequential subcloning from the SHSY line and the parental epithelial cell-like subclone of the SK-N-SH human neuroblastoma-derived cell line established from a biopsied, metastatic tumour diagnosed as a peripheral neuroblastoma (Lukas *et al.*, 1993). This cell line, of sympathetic adrenergic ganglion origin, expresses two types of nAChR: 1) ganglionic AChR that are normally post-synaptic and are tentatively composed of the α3, α5, β2 and β4 nAChR subunits, and 2) neuronal α-bgt-sensitive nAChR, which are probably extrasynaptic and contain α7 subunits. The SH-SY5Y cell line offers advantages over primary hippocampal cultures and transfected cell lines due to these

cells endogenously expressing α3, α5, α7, β2 and β4 nAChR subunit subtypes (Lukas *et al.*, 1993). Due to more than one defined receptor subtype being expressed in the SH-SY5Y cell line, these subunits will combine in a variety of homomeric and heteromeric combinations, that can be elucidated by using specific antagonists for specific nAChR subtypes. Thus in addition to expressing native [^{125}I]-α-bgt binding sites representative of putative α7* nAChR, the SH-SY5Y cell line has enabled this study to encompass α3* nAChR. These nAChR are heterogeneous, comprising combinations of α3 with α5, β2 and/or β4 subunits. These α-bgt-insensitive nAChR are labelled with the novel, potent, high affinity nicotinic agonist [^{3}H]-epibatidine. [^{3}H]-Epibatidine is a radiolabelled pharmacological tool introduced in section 1.6.3. It has been demonstrated that approximately half of the α3* nAChR in SH-SY5Y cells also contain the β2 subunit (Wang *et al.*, 1996). Other studies have shown that SH-SY5Y cells resemble human fetal sympathetic neurones grown in primary culture, express noradrenergic biosynthetic enzymes and functional muscarinic and opioid receptors (Adem *et al.*, 1987; Kazmi and Mishra, 1987).

3.1.3. Previous studies performed with SH-SY5Y cells:

Lukas *et al.* (1993) demonstrated an agonist-sensitive cation flux mediated by α3* post-synaptic-type nAChR present in SH-SY5Y cells. Radioligand binding studies with SH-SY5Y cells have identified the expression of a single class of nicotinic [^{125}I]-α-bgt binding site, that binds [^{125}I]-α-bgt with high affinity (K_D = 4 nM) and binds other nicotinic ligands with lower affinity (in the μM range) (Lukas *et al.*, 1993). Previous experiments with this human neuroblastoma cell line have shown that chronic nicotine exposure upregulates both α3* and α7* nAChR subtypes (Peng *et al.*, 1997). Wang *et*

al. (1998) indicated that chronic nicotine or carbamylcholine treatment upregulates α3β2 and α3β2α5 nAChR subtypes, with no effect on β4* nAChR combinations. This demonstrates that upregulation of α3* nAChR depends upon the presence of β2 but not β4 subunits (Wang *et al.*, 1998).

Upregulation of either α3* or α7* nAChR was evoked at concentrations of nicotine greater than those required to elicit upregulation of the α4β2 nAChR expressed in fibroblasts (Peng *et al.*, 1994b, 1997; Warpman *et al.*, 1998). These higher levels of nicotine may not be physiologically relevant to the plasma nicotine concentrations found in smokers. However, the underlying mechanism of nicotine-evoked upregulation of α3* and α7* nAChR has been proposed to be the same as that for α4β2 nAChR, with regard to the lack of increased gene transcription (Peng *et al.*, 1997). This was indicated by the failure of nicotine to increase α3 or α7 subunit mRNA, suggesting that these nAChR subunits are upregulated via a post-transcriptional mechanism (Peng *et al.*, 1997). This section shows that nicotinic agonists, nicotine and DMAC, and KCl depolarisation upregulate α7* nAChR via distinct mechanisms whereas α3* nAChR are not responsive to KCl treatment.

3.2. Aims:

This section aims to compare the effects of chronic drug treatments applied to SH-SY5Y cells in culture, drug treatments that have previously been shown to produce upregulation of [^{125}I]-α-bgt binding sites in rat primary hippocampal cultures after 4 days of treatment (see section 2.7.2). Detection of α3* nAChR expressed in the SH-SY5Y cell line will be investigated in terms of upregulation and the underlying cellular

mechanisms of this phenomenon and will be compared to α7* nAChR evoked upregulation.

3.3. Materials and methods.

3.3.1. Drugs, reagents and cell lines:

Tissue culture media, serum and plasticware were from Gibco BRL (Paisley, Renfrewshire, Scotland). Media supplements, biochemicals, cycloheximide and poly-L-lysine (hydrobromide) were purchased from Sigma Co. (Poole, Dorset, U.K.). *N*-[1-[*N*-methyl-*p*-(5-isoquinolinesulfonyl)-benzyl]-2-(4-phenylpiperazine)ethyl]-5-isoquinoline sulfonamide (KN-04) was from AMS Biotechnology and 3-[1-[3(amidinothio)propyl-1H-indol-3-(1-methyl-1H-indol-3-yl)maleimide methane sulfonate (Ro 31-8220) was purchased from Calbiochem. Cell culture equipment was supplied by Beckton Dickinson (Oxford, U.K.) or Sterilin (Stone, Staffs., U.K.). PC12 and SH-SY5Y cells were from the European Collection of Cell Cultures (ECACC), Porton Down (Salisbury, Wilts., U.K.).

3.3.2. Maintenance of PC12 cells and the SH-SY5Y cell line:

PC12 cells adhere poorly to tissue culture plastic, therefore stock cultures and sub-cultures were routinely maintained in tissue culture vessels to which poly-L-lysine (PLL) (1 mg/ml prepared in 150 mM sodium borate buffer (pH 8.4)), an adhesive coating, had been previously applied for at least 4 h and rinsed with sterile water to remove remaining traces of the PLL. PC12 cells were maintained in RPMI 1640

medium supplemented with horse serum (10%), FCS (5%), penicillin (25 IU/ml) and streptomycin (25 μg/ml).

SH-SY5Y human neuroblastoma stock cultures were routinely maintained in a DMEM:Ham's F12 (1:1) modified medium containing 1% non-essential aminoacids (NEAA) and supplemented with FCS (15%), glutamine (2 mM), penicillin (50 IU/ml) and streptomycin (50 μg/ml).

Cultures of both cell lines were seeded into 75 cm^2 flasks containing 20 ml of supplemented medium and maintained at 37°C in a humid atmosphere containing 5% CO_2/humidified air. Stock cultures were passaged 1:4 weekly at approximately 80% confluency. Optimum proliferation of PC12 cells was obtained by feeding cultures every 3 to 4 days, with approximately 65% of the medium in the culture being exchanged so as to leave a portion of RPMI "conditioned" medium in the culture to facilitate growth. SH-SY5Y cultures were fed twice weekly with modified DMEM: Ham's F12 medium. Cultures for binding assays were subcultured in 24 well plates at a seeding density of 5 x 10^5 cells/ml or 10 x 10^5 cells/ml for PC12 and SH-SY5Y cells respectively (adapted from Vaughan *et al.*, 1993). Once confluent, cultures were treated chronically with drugs.

3.3.3. Drug treatment:

In initial experiments, PC12 cells were incubated with varying concentrations of NGF (0-200 ng/ml) for 7 days. Confluent SH-SY5Y cultures in 24 well plates were chronically treated with a number of drugs, either alone or in combination, for 4 days. All drug solutions were made up as described previously in section 2.4.2. KN-04 and Ro 31-8220 were made up in DMSO stock solutions of 10 mM so that the final

concentration of DMSO on cultures did not exceed 0.1%. Binding assays were performed with [^{3}H]-epibatidine binding after 7 or 4 days (PC12 or SH-SY5Y cells respectively), or with [^{125}I]-α-bgt binding after 4 days of chronic drug treatment to SH-SY5Y cells.

3.3.4. Radioligand binding assays on Cultured Cells *in situ*.

3.3.4.1. [^{3}H]-Epibatidine binding to PC12 cells and SH-SY5Y cultures:

Cultures were washed x 4 with warm medium over 3 h prior to the assay, to remove all traces of drugs from the cultures. After 3 h the cultures were incubated with 1 ml PC12 or SH-SY5Y medium containing [^{3}H]-epibatidine (500 pM; specific activity 33.8 Ci/mmol) for 2 h at 25°C. Non-specific binding was defined in parallel cultures in the presence of 1 mM nicotine. The cultures were subsequently washed x 3 with warm PBS and solubilised in 800 µl 0.1 M NaOH (16 h at 4°C). An aliquot (500 µl) was added to 5 ml Optiphase Safe scintillant (Fisons Chemicals, Loughborough, U.K.) and counted for radioactivity in a Packard Tri-Carb liquid scintillation counter 1600 spectrometer (counting efficiency 45-50%) to give total bound and non specific bound cpm, and a 200 µl aliquot was assayed for protein using the method of Markwell *et al.* (1978). Radioactivity counts and protein assay data were combined to give total and non-specific binding (and hence specific = total binding – non-specific binidng) in terms of fmol [^{3}H]-epibatidine bound/mg protein.

3.3.4.2. [^{125}I]-α-bgt binding to SH-SY5Y cultures:

[^{125}I]-α-Bgt binding assays were performed on intact SH-SY5Y cells as described for hippocampal cultures (see section 2.6.3) to measure surface [^{125}I]-α-bgt binding sites representative of putative α7* nAChR.

3.3.5. Radioligand binding to SH-SY5Y membrane preparations:

3.3.5.1. SH-SY5Y membrane preparation protocol:

Confluent 7 day old SH-SY5Y cells in 175 cm^2 flasks were scraped into 10 ml of ice cold PBS pH 7.5 containing 10 mM EDTA, 1 mM PMSF and centrifuged at 500 x g for 3 min. The pellet was resusupended in 10 ml of PBS per flask of cells and sonicated for 3 x 10 s at an amplitude of 9 microns, resuspensions were kept on ice. The homogenate was centrifuged at 35,000 x g for 30 min and the pellet washed by an identical centrifugation step. Finally, the pellet was resuspended in 1 ml ice cold Tris Ringer (N-(2-hydroxyethyl)piperazine-N'-2-ethane) sulphonic acid (HEPES) buffer (118 mM NaCl, 4.8 mM KCl, 2.5 mM $CaCl_2$, 2 mM $MgSO_4$, 20 mM HEPES, 200 mM Tris, 0.1 mM PMSF and 0.01% sodium azide, pH 7.4) per original flask and stored in 2 ml aliquots at -20°C until required for assay.

3.3.5.2. Optimisation of tissue quantity used in membrane [^{3}H]-MLA binding assays:

Protein assays were performed on the SH-SY5Y cell membrane batches by the method of Bradford (1976), as the Markwell assay is incompatible with a Tris based buffer. SH-SY5Y cell membranes (200, 100, 50, 25, 10 μg) were diluted in a final

volume of 250 µl in Tris-Ringer HEPES buffer containing 1 mg/ml BSA and 20 nM [^{3}H]-MLA. Non-specific binding was determined in the presence of 1 mM nicotine and non-specific/total binding were determined in triplicate. Samples were incubated for 2 h at 37°C. Following this, samples were washed x 3 with ice cold PBS and filtered using a Brandel cell harvester through Gelman GFA/C filters presoaked in 0.3% PEI in PBS, pH 7.4. The filters were transferred into tubes and 5ml Optiphase Safe scintillation cocktail added and the contents mixed before counting for 5 min in a Packard 1600 Tricarb counter (counting efficiency 45-50%). Radioactivity counts and protein assay data were combined to give total and non-specific binding in terms of fmol [^{3}H]-MLA bound/mg protein.

3.3.5.3. [^{3}H]-MLA saturation binding to SH-SY5Y membranes:

For total binding 10 µl of Tris-Ringer HEPES buffer (containing 1 mg/ml BSA) and 10 µl of [^{3}H]-MLA were incubated with 230 µl of SH-SY5Y membranes (final protein concentration of 200 µg per sample tube). Non-specific binding was determined in the presence of 1 mM nicotine. Assays were performed in triplicate with a range of concentrations of [^{3}H]-MLA ranging from 2.5 nM to 20 nM and incubated for 2 h at 37°C to measure total [^{3}H]-MLA binding sites (i.e. surface and intracellular located α7* nAChR). The reaction was terminated, and assay tube contents filtered and counted as described above in section 3.3.5.2.

3.3.5.4. Data analysis:

Data obtained from the [^{3}H]-MLA saturation binding assays were fitted to the hyperbolic curve equation $[B_{max}*[L]]/K_D + [L]$ using Sigma Plot V2.0 for windows

(Jandel Scientific, Corte Madera, CA, USA). K_D and B_{max} were directly calculated from the saturation binding curves. Each saturation binding isotherm was transformed to linearity by using the Scatchard equation in order to characterise the number of binding sites.

3.4. Results.

3.4.1. NGF treatment on PC12 cells:

The high affinity of epibatidine for neuronal nAChR (Sullivan *et al.*, 1994; Houghtling *et al.*, 1995; Gerzanich *et al.*, 1995) suggests that these receptors in PC12 will be labelled by [^{3}H]-epibatidine. Preliminary data described in this section is from binding assays performed on the PC12 cell line *in situ* using 500 pM [^{3}H]-epibatidine. Initial assays using PC12 cells were performed after exposure to varying concentrations of NGF for 7 days before being assayed for [^{3}H]-epibatidine binding. Results produced a profile of increasing specific binding with increased NGF concentration showing that NGF produces a concentration-dependent increase in the number of [^{3}H]-epibatidine binding sites. Results are shown in Figure 3.1.

A concentration of approximately 100 ng/ml NGF produces maximum increases and a steady state binding of [^{3}H]-epibatidine to PC12 cells which is 5-6 fold greater than [^{3}H]-epibatidine binding found in PC12 cells grown in the absence of NGF. However, due to persistent problems experienced with this cell line in this laboratory, for example contamination from source, it was decided to investigate the cellular mechanisms mediating upregulation of nAChR in another cell line, SH-SY5Y cells, and abandon further investigations with the PC12 cell line.

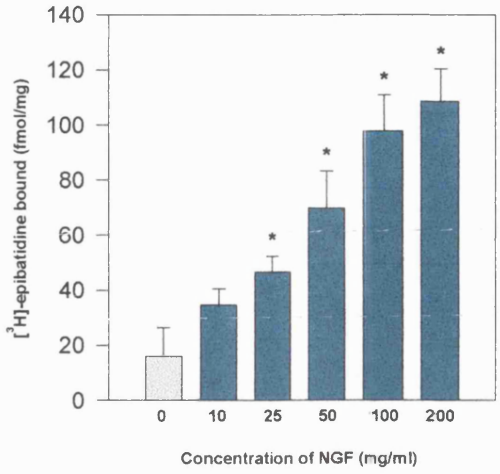

Figure 3.1. [^{3}H]-Epibatidine binding sites after NGF treatment to PC12 cells. *PC12 cell cultures were exposed to various concentrations of NGF ranging from 0-200 ng/ml for 7 days before performing [^{3}H]-epibatidine binding assays. Values are the mean ± S.E.M. from at least 3 independent cultures performed in duplicate. * Significantly different from control at $p<0.05$; one way ANOVA.*

3.4.2. Upregulation of [^{125}I]-α-bgt binding sites in SH-SY5Y cultures:

Initial experiments were performed to examine the upregulation of α-bgt binding sites in SH-SY5Y cell cultures, for comparison with the findings obtained from primary rat hippocampal cultures as described in section 2.7.2. In the absence of drugs, SH-SY5Y cells expressed 25 ± 2 fmol [^{125}I]-α-bgt binding/mg protein (Table 3.1). Nicotine (10 μM), DMAC (10 μM) and KCl (20 mM), applied for 4 days, increased the number of putative [^{125}I]-α-bgt binding sites by 37 ± 5 % (n=13), 20 ± 6% (n=4), and 51 ± 10% (n=9; Table 3.1, Figure 3.2) respectively. These values closely parallel the changes in [^{125}I]-α-bgt binding sites produced in hippocampal cultures (Table 2.2) and represent a

real increase in numbers of α7* nAChR subtypes as the [^{125}I]-α-bgt binding site density was calculated in terms of protein, determined for each assay well (see methods 2.6.3).

Table 3.1. Upregulation of [^{125}I]-α-bgt and [^{3}H]-epibatidine binding sites in SH-SY5Y cultures treated for 4 days with either nicotine (10 μM), DMAC (10 μM), or KCl (20 mM). *Control values of [^{125}I]-α-bgt and [^{3}H]-epibatidine binding sites are expressed as fmoles radioligand bound/mg protein (expressed as 100%) and the upregulation elicited by nicotine, DMAC and KCl are expressed as a percentage of these control conditions. Significantly different from control, *p<0.05, (one way ANOVA).*

	Radioligand	
	[^{125}I]-α-bgt	**[^{3}H]-epibatidine**
Control (fmol radioligand binding/mg protein)	25 ± 2 (n=14)	69 ± 4 (n=43)
Nicotine (10 μM) (% control)	137 ± 5% (n=13)*	136 ± 6% (n=15)*
DMAC (10 μM) (% control)	120 ± 6% (n=4)*	143 ± 8% (n=13)*
KCl (20 mM) (% control)	151 ± 10% (n=9)*	107 ± 5% (n=13)

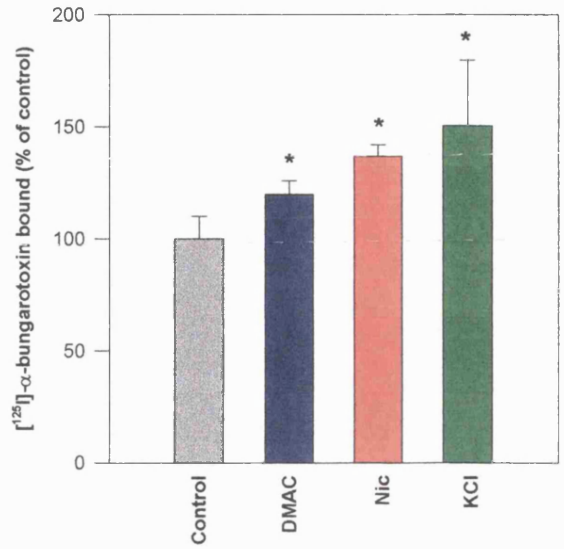

Figure 3.2. Upregulation of [^{125}I]-α-bgt binding sites in SH-SY5Y cultures. *SH-SY5Y cultures were exposed to chronic drug treatment with either nicotinic agonists DMAC (10 μM), nicotine (nic; 10 μM) or KCl depolarisation (20 mM) for 4 days before the binding assays were performed. Values are the mean ± S.E.M. from at least 4 independent cultures. * Significantly different from control at $p<0.05$; one way ANOVA.*

3.4.3. [^{3}H]-MLA binding to SH-SY5Y membranes:

3.4.3.1. Optimisation of [^{3}H]-MLA binding to SH-SY5Y membranes:

In order to minimise amounts of SH-SY5Y cells used it was decided to prepare SH-SY5Y cell membranes using aliquots of a known protein concentration in each assay tube. The binding of [^{3}H]-MLA to SH-SY5Y cell membranes increased in a linear manner as the quantity of SH-SY5Y membranes was increased. Based on these results, 200 μg protein of SH-SY5Y cell membranes was chosen to use for further

experimentation in saturation binding assays for [^{3}H]-MLA as this quantity of protein gave a satisfactory specific binding signal without using too many SH-SY5Y cells.

3.4.3.2. Saturation of [^{3}H]-MLA binding to SH-SY5Y membranes:

Saturation binding of [^{3}H]-MLA to 7 day confluent SH-SY5Y cell membranes treated with nicotine, KCl or no drugs for 4 days were compared. A range of concentrations of the novel α7-selective ligand [^{3}H]-MLA (2.5-20 nM) was used (Figure 3.3). Data reveal that [^{3}H]- MLA bound in a saturable manner to this cell line. These binding assays allowed for the determination of B_{max} (surface and intracellular [^{3}H]-MLA binding) and K_D values to be calculated from drug treated cells for comparison with values for membranes from control untreated SH-SY5Y cells. Scatchard analysis is consistent with one population of receptor binding site in the SH-SY5Y cell line, as previously suggested by Davies *et al.* (1999) for rat brain membranes. In control SH-SY5Y cells binding was saturable with observed B_{max} values of 28.02 fmoles [^{3}H]-MLA bound/mg protein with a K_D value of 3.02 nM (Table 3.2). Chronic treatment with either nicotine or KCl significantly increased B_{max} values but did not significantly alter K_D values after upregulation. These values suggest that nicotine and KCl depolarisation upregulate [^{3}H]-MLA binding sites in terms of fmoles [^{3}H]-MLA bound/mg of protein. Upregulation mediated by nicotine resulted from an increase in the amount of nAChR rather than from an increase in the affinity of α7* nAChR for nicotine, a similar result found after nicotine treatment and detection of α7* (Molinari *et al.*, 1998) and α4β2 nAChR (Schwartz and Kellar, 1983; Bencherif *et al.*, 1995). The large increases observed with B_{max} after nicotine and KCl treatment is

probably representative of [^{3}H]-MLA binding to intracellular populations of α7* nAChR.

Table 3.2. B_{max} and K_D values for [^{3}H]-MLA saturation binding to SH-SY5Y cells. * *Significantly different from control at $p<0.05$; one way ANOVA.*

Treatment	B_{max} (fmol /mg)	K_D (nM)
Control	28.0 ± 2.2	3.0 ± 0.56
Nicotine (10 μM)	92.2 ± 3.4*	2.1 ± 0.47
KCl (20 mM)	118.5 ± 8.6*	2.2 ± 0.62

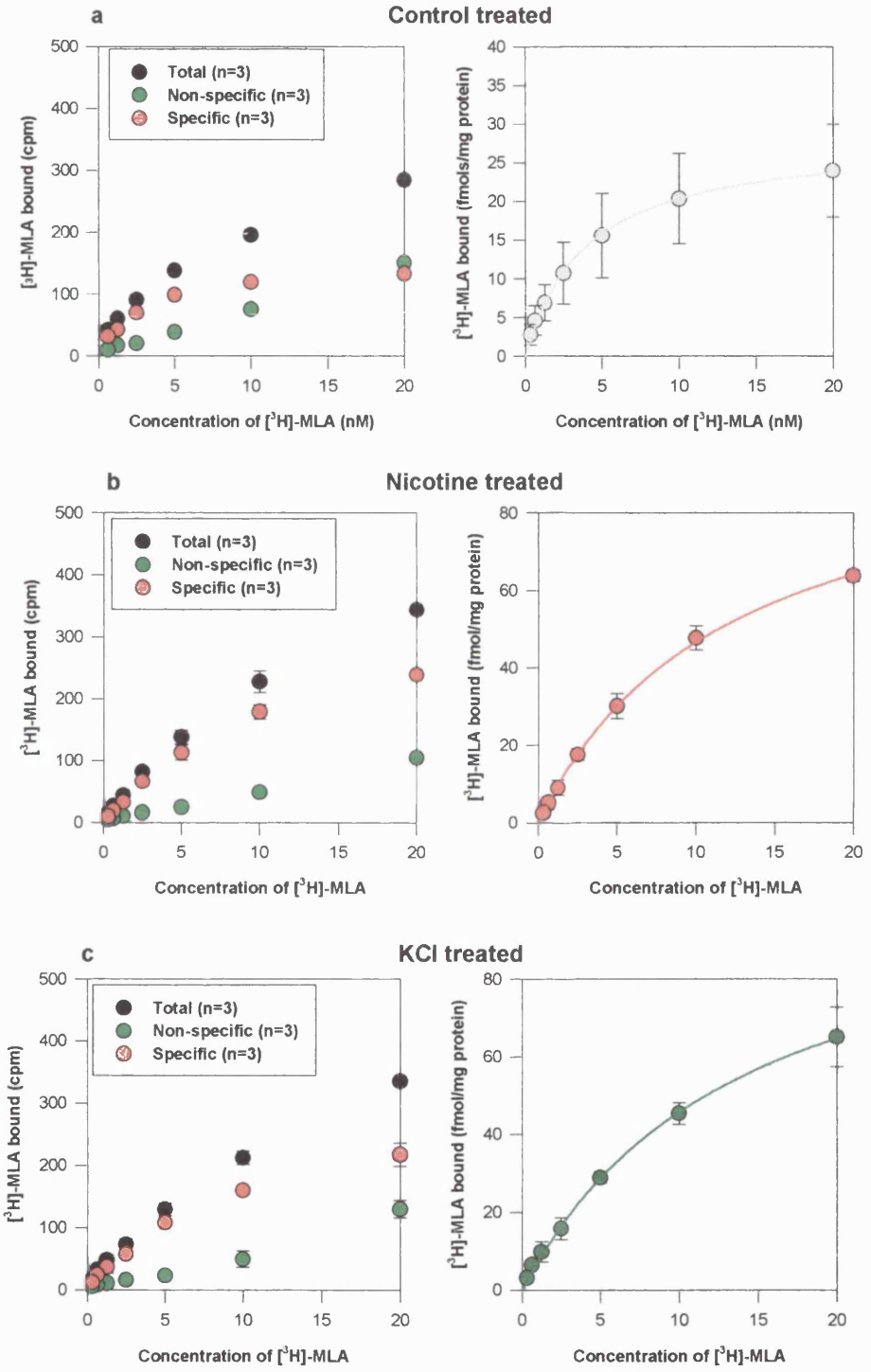

Figure 3.3. Saturation binding of [^{3}H]-MLA to SH-SY5Y cells in situ. *Saturation binding was performed on 7 day confluent SH-SY5Y membrane preparations treated for 4 days with (a) no drugs, control, (b) nicotine or (c) KCl. The panels on the left show total, non-specific and specific binding (cpm), with the panels on the right showing the concentration of [^{3}H]-MLA bound against specific binding expressed in fmol [^{3}H]-MLA bound/mg protein. Values are the mean ± S.E.M. from at least 3 independent cultures. Saturation data was fitted to a hyperbolic curve equation ($[B_{max}* [L]]/K_D + [L]$).*

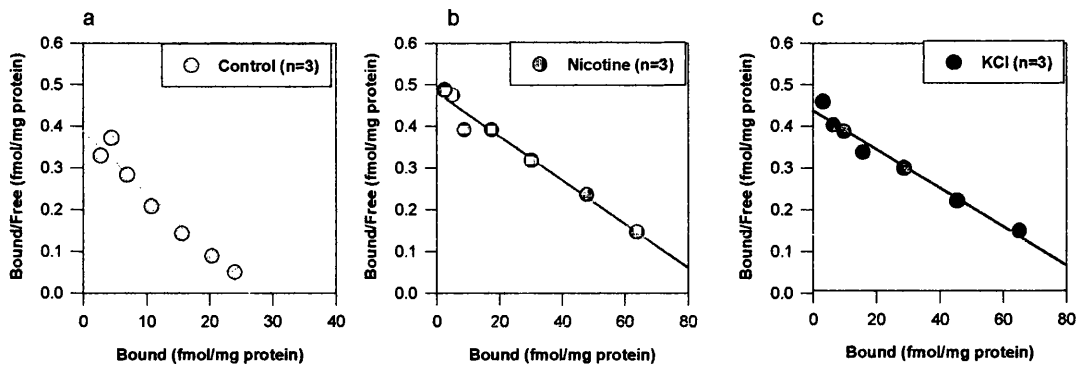

Figure 3.4. Scatchard analyses of [^{3}H]-MLA saturation binding. *Saturation binding data was transformed to linearity by using the Scatchard equation for (a) control, (b) nicotine or (c) KCl treated SH-SY5Y cells.*

3.4.4. Mechanisms of nicotine- and KCl-evoked upregulation of putative α7* nAChR in SH-SY5Y cultures:

Experiments were performed to investigate the cellular mechanisms underlying nicotinic agonist- and KCl-evoked upregulation of α7* nAChR in SH-SY5Y cells. To identify if the phenomenon of upregulation evoked by these compounds arise from different cellular pathways as indicated by the data in hippocampal cultures. Further experiments were performed on SH-SY5Y cultures in the presence of specific inhibitors. Exposure of cultures to the L-type Ca^{2+} channel blocker, verapamil (5 μM) or the CaM-kinase II inhibitor, KN-62 for 4 days had no significant effect on numbers of [^{125}I]-α-bgt binding sites when applied alone and did not abolish nicotine-evoked upregulation (Figure 3.5a, b) Upregulation mediated by nicotine was maintained at 44 ± 16% (n=4) and 40 ± 16% (n=4) in the presence of verapamil and KN-62 respectively. In contrast, verapamil and KN-62 were found to prevent the upregulation elicited by KCl depolarisation (Figure 3.5a). Results obtained with SH-SY5Y cell cultures are in close

accordance with and extend the [^{125}I]-α-bgt binding data generated from the primary hippocampal cultures described in section 2.7.2.2. These results suggest that the process of upregulation of [^{125}I]-α-bgt binding sites in hippocampal neurones and the SH-SY5Y human neuroblastoma cell line evoked by nicotine and KCl depolarisation arise through the mediation of different cellular mechanisms.

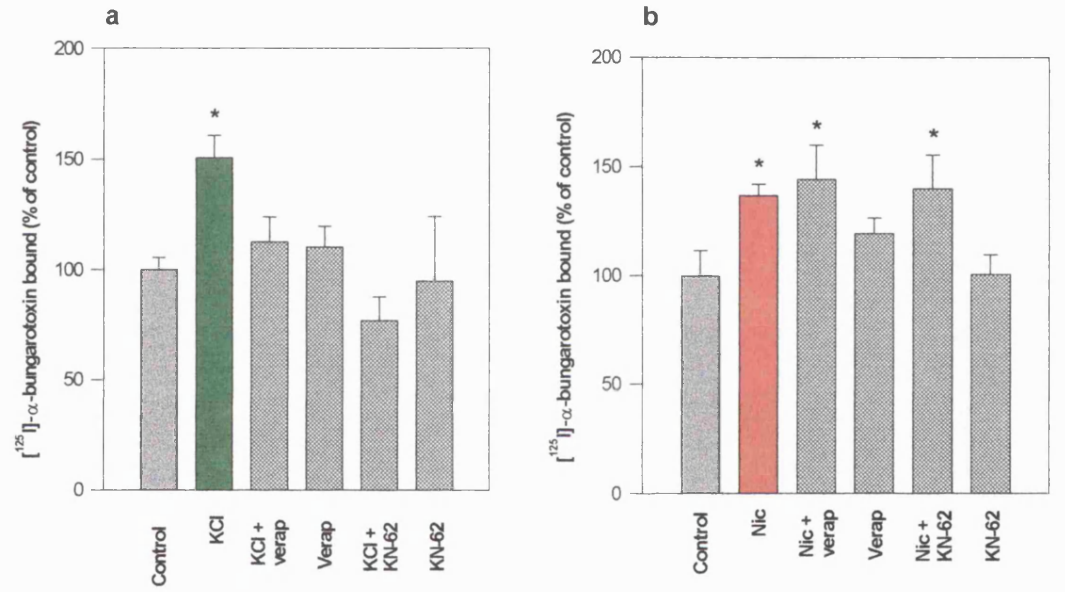

Figure 3.5. Inhibition of upregulation of [^{125}I]-α-bgt binding sites in SH-SY5Y cultures. *SH-SY5Y cultures were exposed to chronic drug treatments for 4 days to investigate the effects of verapamil (verap; 5 μM) and KN-62 (5 μM) on (a) KCl- (20 mM) and (b) nicotine- (nic; 10 μM)) evoked upregulation of [^{125}I]-α-bgt binding sites. Values are the mean ± S.E.M. from at least 4 independent cultures. * Significantly different from control at $p<0.05$; one way ANOVA.*

A preliminary investigation into the dependence on protein synthesis of the process of upregulation elicited by nicotine or by KCl depolarisation in SH-SY5Y cells was undertaken using cycloheximide (Figure 3.6). Cycloheximide is a general blocker of protein synthesis and therefore would prevent the synthesis of new nAChR (Peng *et al.*,

1994b). Cycloheximide (35 μM) treatment for 4 days significantly reduced the level of α7* nAChR detected by [^{125}I]-α-bgt binding by 75% and 64% (Figure 3.6a, c respectively) and decreased the fmol [^{125}I]-α-bgt bound/mg protein compared to control cells (Figure 3.6.b, d). There were also fewer cells observed in the wells after cycloheximide treatment, another sign reflecting the toxic nature of this effective inhibitor of protein synthesis over the time-course of this drug treatment regime. The treatment of cycloheximide alone was not significantly different from its corresponding combined treatment with either chronic KCl or nicotine. This indicates that KCl or nicotine treatment in the presence of cycloheximide does not result in upregulation of [^{125}I]-α-bgt binding sites due to the maintained reduction of protein levels. In the absence of cycloheximide, KCl and nicotine upregulated [^{125}I]-α-bgt binding sites to 60 ± 23% (n=4) and 43 ±6% (n=3) respectively above control. Treatment with a combination of KCl/cycloheximide or nicotine/cycloheximide produced no upregulation of [^{125}I]-α-bgt binding sites. Due to the general deleterious effect of cycloheximide on SH-SY5Y cells, and no upregulation produced by KCl or nicotine in the presence of cycloheximide, it may be interpreted that this effect is due to a cytotoxic action of cycloheximide on SH-SY5Y cells. The inhibition of protein synthesis by cycloheximide identifies that protein synthesis is a requirement for normal cell maintenance in SH-SY5Y cells.

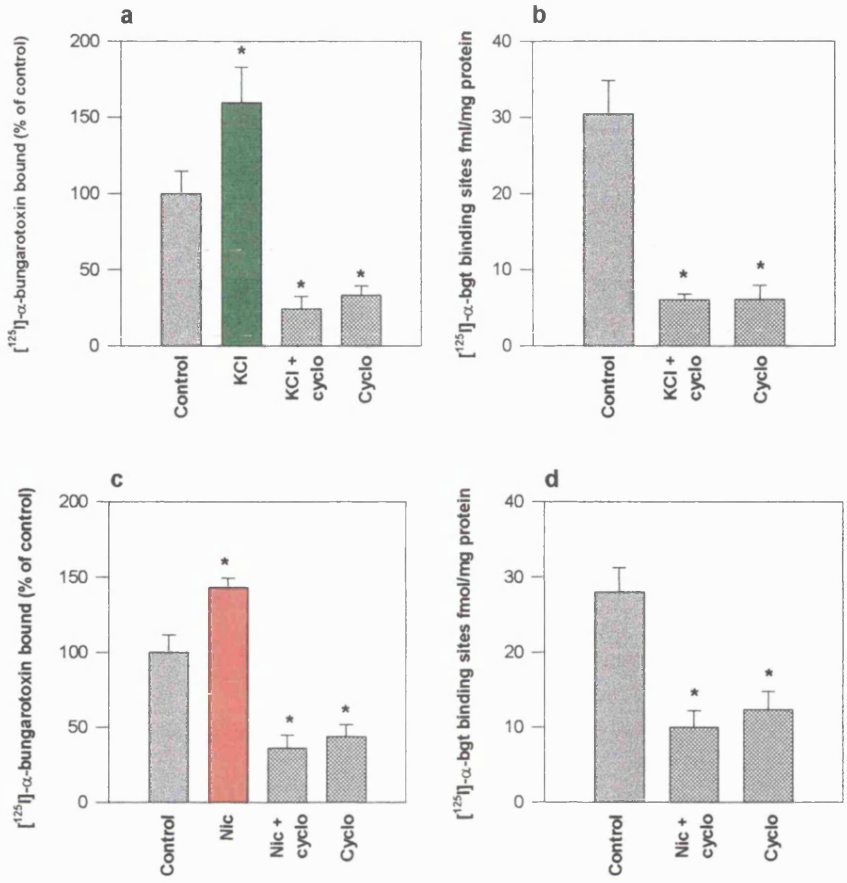

Figure 3.6. The effect of cycloheximide on [^{125}I]-α-bgt binding sites in SH-SY5Y cultures. *SH-SY5Y cultures were exposed to chronic drug treatments for 4 days to investigate the effects of cycloheximide (cyclo; 35 μM) on (a, b) KCl (20 mM) and (c, d) nicotine (nic; 10 μM) evoked upregulation of [^{125}I]-α-bgt binding sites expressed as a percentage of control (a, c) and fmol [^{125}I]-α-bgt bound/mg protein (b, d). Values are the mean ± S.E.M. from at least 3 independent cultures. * Significantly different from control at $p<0.05$; one way ANOVA.*

3.4.5. Upregulation of [^{3}H]-epibatidine binding sites in SH-SY5Y cultures:

In addition to [^{125}I]-α-bgt binding sites, SH-SY5Y cells also express α3* nAChR sites that can be identified with [^{3}H]-epibatidine binding (Peng *et al.*, 1997; Wang *et al.*, 1998). In the absence of drugs, cultures expressed 69 ± 4 fmoles [^{3}H]-epibatidine

binding sites/mg protein (Table 3.1). Chronic nicotine (10 μM) treatment of SH-SY5Y cultures for 4 days upregulated [^{3}H]-epibatidine binding to 36 ± 6% (n=13; Figure 3.7) above control binding. DMAC (10 μM) produced a comparable upregulation of [^{3}H]-epibatidine binding sites to 43 ± 8% (n=13; Figure 3.7). These responses are similar in magnitude to the changes evoked by nicotine and DMAC with [^{125}I]-α-bgt binding to SH-SY5Y cells (Table 3.1). In contrast to the response to nicotinic agonists, KCl depolarisation (20 mM) failed to significantly upregulate α3* nAChR (107 ± 5%, n=13; Figure 3.7, Table 3.1).

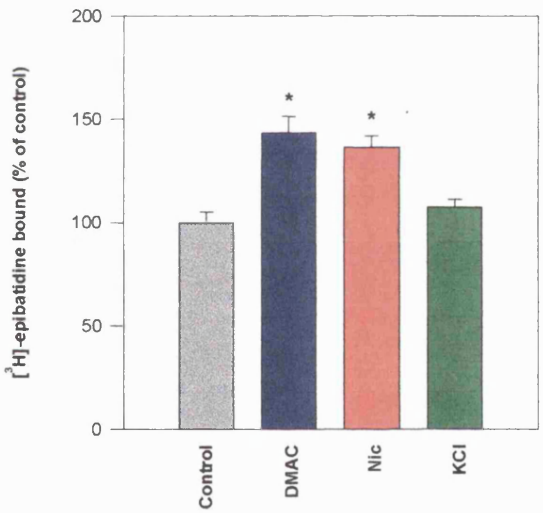

Figure 3.7. Upregulation of [^{3}H]-epibatidine binding sites in SH-SY5Y cultures. *SH-SY5Y cultures were exposed to chronic drug treatment with either nicotinic agonists DMAC (10 μM), nicotine (nic; 10 μM) or KCl depolarisation (20 mM) for 4 days before binding assays were performed. Values are the mean ± S.E.M. from at least 5 independent cultures. * Significantly different from control at $p<0.05$; one way ANOVA.*

3.4.6. Mechanisms of nicotinic agonist-evoked upregulation of [^{3}H]-epibatidine binding sites in SH-SY5Y cultures:

Verapamil and KN-62 (Figs. 3.8 and 3.9 respectively) in the presence of either nicotine or DMAC did not block the upregulation elicited by these compounds.

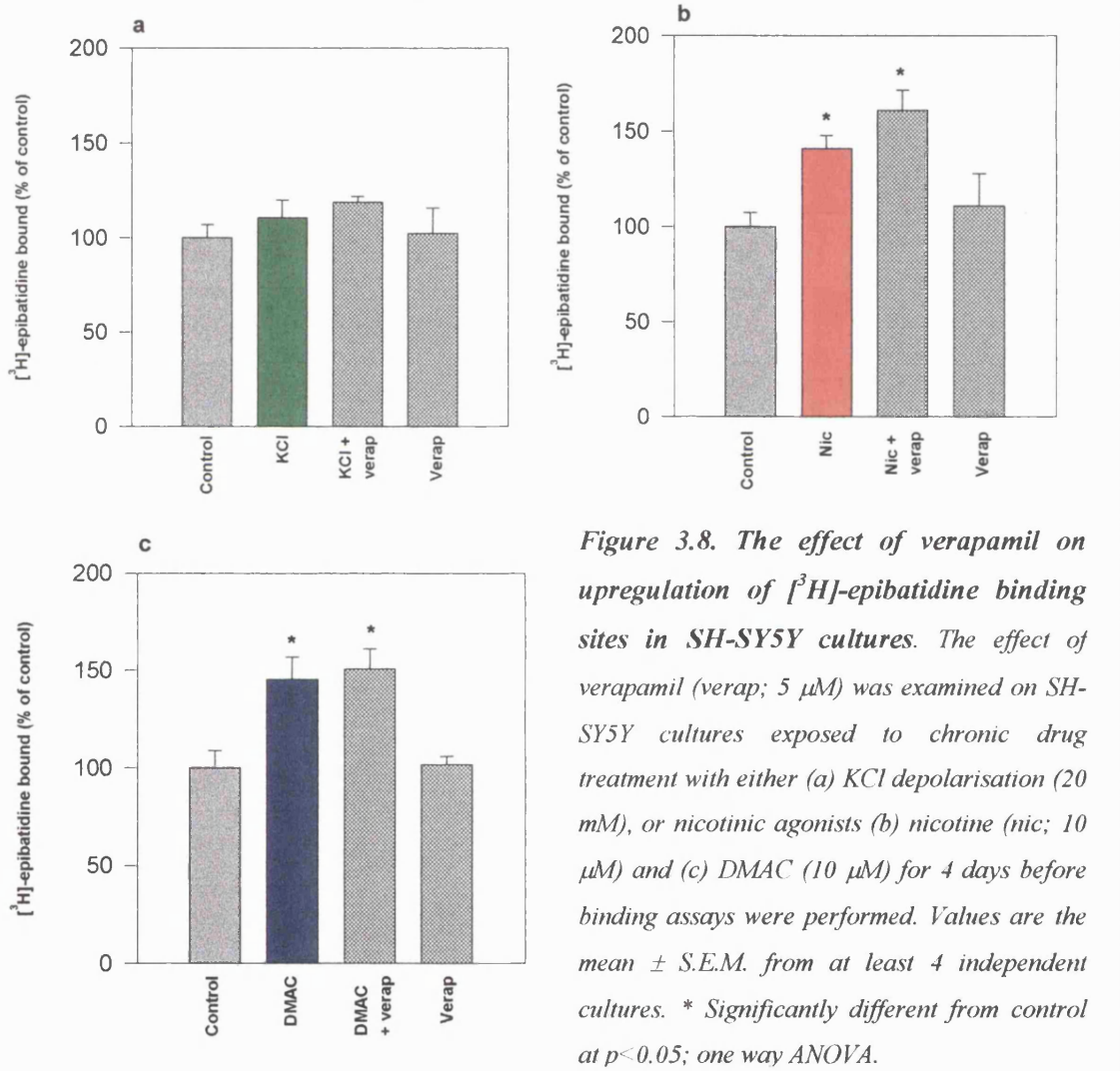

Figure 3.8. The effect of verapamil on upregulation of [^{3}H]-epibatidine binding sites in SH-SY5Y cultures. *The effect of verapamil (verap; 5 μM) was examined on SH-SY5Y cultures exposed to chronic drug treatment with either (a) KCl depolarisation (20 mM), or nicotinic agonists (b) nicotine (nic; 10 μM) and (c) DMAC (10 μM) for 4 days before binding assays were performed. Values are the mean ± S.E.M. from at least 4 independent cultures. * Significantly different from control at $p<0.05$; one way ANOVA.*

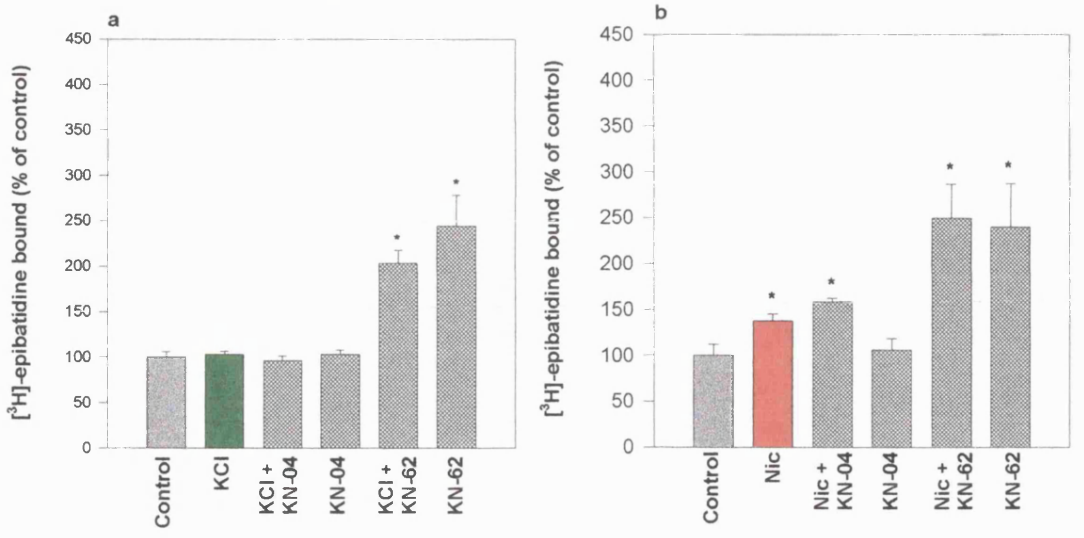

Figure 3.9. The effect of KN-62 and KN-04 on upregulation of [^{3}H]-epibatidine binding sites in SH-SY5Y cultures. *The effect of KN-62 (5 μM) and KN-04 (5 μM) were examined on SH-SY5Y cultures exposed to chronic drug treatment with either (a) KCl depolarisation (20 mM), or nicotinic agonists (b) nicotine (nic; 10 μM) and (c) DMAC (10 μM) for 4 days before binding assays were performed. Values are the mean ± S.E.M. from at least 4 independent cultures. * Significantly different from control at $p<0.05$; one way ANOVA.*

KN-62 applied alone to SH-SY5Y cultures for 4 days, in the absence of nicotinic agonist or KCl depolarisation, produced a marked upregulation of the [^{3}H]-epibatidine binding sites to 144 ± 34%, 140 ± 48% and 176 ± 35 above control shown in Figure 3.9a, b and c respectively. The effect of KN-04, an inactive analogue of KN-62 that does not inhibit CaM-kinase II, was also investigated. KN-04 alone had no effect on the number of [^{3}H]-epibatidine binding sites, when compared to the control condition

(Figure 3.9). This suggests that KN-62 elicits upregulation of α3* nAChR through the inhibition of CaM-kinase II.

The effect of a PKC inhibitor was also investigated to identify if this signalling protein was involved in the cellular mechanism underlying the upregulation of [^{3}H]-epibatidine binding sites by nicotinic agonists. The effect of Ro 31-8220, a PKC inhibitor, was investigated on nicotinic agonist mediated upregulation. Figure 3.10 shows that Ro 31-8220 (1 μM) had no effect on [^{3}H]-epibatidine binding when applied alone. When co-applied with either nicotine or DMAC, R0 31-8220 did not abolish the nicotinic agonist-evoked upregulation of [^{3}H]-epibatidine binding sites. Upregulation mediated by either nicotine or DMAC was maintained to 53 ± 3% (n=6) and 53 ± 2% (n=6) respectively above control binding in the presence of Ro 31-8220. This shows that a PKC signalling pathway is not involved in the upregulation of [^{3}H]-epibatidine binding sites mediated by these nicotinic agonists.

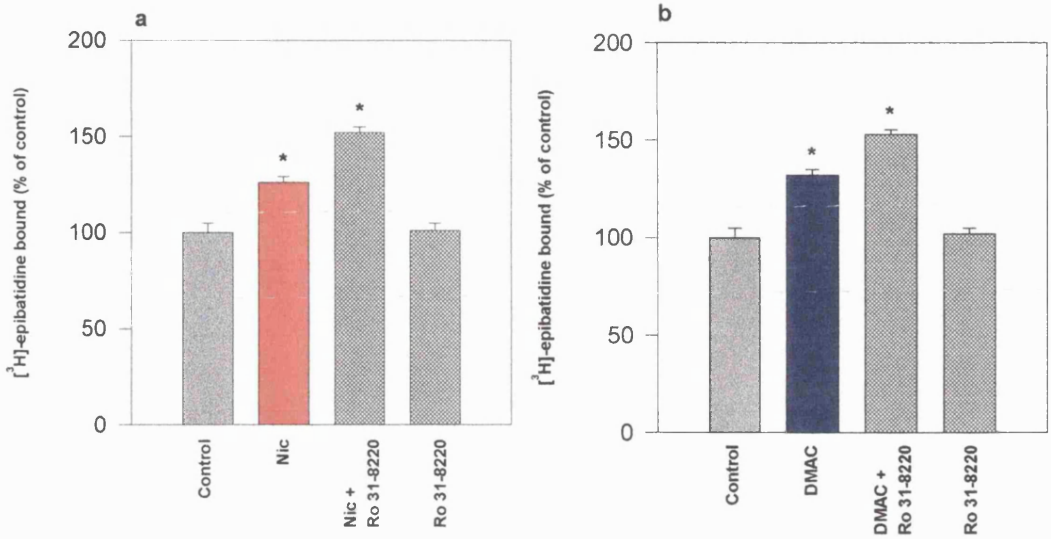

Figure 3.10. The effect of a PKC inhibitor on upregulation of [^{3}H]-epibatidine binding sites in SH-SY5Y cultures. *The effect of Ro 31-8220 (1 μM) was examined on SH-SY5Y cultures that were exposed to chronic drug treatment with nicotinic agonists (a) nicotine (nic; 10 μM) or (b) DMAC (10 μM) for 4 days before binding assays were performed. Values are the mean ± S.E.M. from at least 4 independent cultures. * Significantly different from control at $p<0.05$; one way ANOVA.*

Section 2: Detection and quantitation of nAChR subunit RNA in SH-SY5Y cells after chronic drug treatment.

3.5. Introduction.

Section 1 has established that chronic nicotine, DMAC and KCl depolarisation differentially upregulate α3* and α7* nAChR subtypes in the SH-SY5Y human neuroblastoma cell line. De Koninck and Cooper (1995) reported data on the regulation of nAChR genes in neonatal rat superior cervical ganglion (SCG) neurones developing in culture. Rat SCG neurones are known to contain α3, α5, α7, β2 and β4 nAChR subunits (Mandelzys *et al.*, 1994). It was shown that in untreated cells, α7 mRNA levels decreased over a period of 3 days when compared to initial control levels. Exposure of these neurones to high K^+ at the time of plating maintained the level of α7 mRNA at their initial plating value after 72 hours in the presence of KCl. If SCG neurones were exposed to membrane depolarisation with KCl (40 mM) for 48 hours, this treatment was shown to evoke a specific and significant increase in surface α-bgt binding when compared to untreated control cultures (De Koninck and Cooper, 1995). This increase in α-bgt binding after KCl treatment is correlated to a significant increase in the level of expression of α7 subunit mRNA in SCG neurones developing in culture, with little effect on the other nAChR transcripts expressed in SCG neurones.

De Koninck and Cooper (1995) also investigated the effect of protein kinase activity on nAChR subunit expression. When activators or inhibitors of PKA, PKC or tyrosine kinase were applied, no change in the level of expression of nAChR subunit transcripts was observed. The proposed mechanism of KCl-evoked upregulation of α7 subunit

mRNA expression through Ca^{2+} influx, was concluded to be via L-type VOCC and the result of a CaM-kinase II pathway, due to inhibition of upregulation in the presence of L-type VOCC blockers and CaM-kinase II inhibitors (De Koninck and Cooper, 1995). KCl depolarisation therefore elicits an increase in transcription resulting in an increase of the α7 subunit mRNA, evoking an eventual upregulation of surface α7* nAChR identified by [^{125}I]-α-bgt binding. In contrast to KCl treatment, chronic nicotine (1 mM) failed to upregulate transcription of either α3 or α7 subunit mRNAs in the SH-SY5Y cell line (Peng *et al*, 1997).

In this section, the level of nAChR subunit RNA expression was examined after chronic drug treatment to determine whether the results reported by De Koninck and Cooper (1995) were observed in the present study after KCl treatment applied to SH-SY5Y cells. This is in contrast to the expected lack of change of α7 RNA expression after chronic nicotine treatment. This investigation aimed to attempt whether increases in binding of [^{125}I]-α-bgt and [^{3}H]-epibatidine to nAChR after chronic drug treatment are accompanied by increases in the level of expression of corresponding nAChR subunit genes. The experiments described in this section involve chronically treating confluent SH-SY5Y cells for 4 days with nicotine (10 μM), DMAC (10 μM) or KCl (20 mM) before isolating either total or poly $(A)^+$ RNA for Northern blot and RT-PCR analysis.

3.5.1. Aims:

This section aims to investigate whether chronic exposure, for 4 days, with nicotine, DMAC or a depolarising concentration of KCl induce changes in the expression of α3 and α7 subunit RNA isolated from SH-SY5Y cell cultures.

3.6. Methods.

3.6.1. Drugs and reagents:

Molecular biological grade chemicals were purchased from BDH chemicals (Poole, Dorset, U.K.), Sigma Chemical Company Ltd. (Poole, Dorset, U.K.) or Fisons Scientific Equipment (Leicestershire, U.K.). Agarose was supplied by Biogene Ltd. (Kimbolton, Cambridgeshire, U.K.) and ethidium bromide and diethyl pyrocarbonate (DEPC) by Sigma. Restriction endonucleases were supplied by NEB (Hitchin, Hertfordshire, U.K.). T4 DNA ligase was from Gibco BRL (Renfrewshire, Scotland).

The reagents for RT-PCR and the preparation of total cellular RNA at Organon Laboratories were supplied by Promega. RNase treated solutions used in the Northern analysis protocols performed in Bath were from Helana Biosciences (Eppendorf) and the DIG-labelling and hybridisation biochemicals were from Roch Boehringer. The dynabeads used to isolate poly $(A)^+$ RNA were from Dynal. The human α3 and α7 nAChR cDNAs were cloned by Organon Laboratories. G_3PDH was purchased from Clontech.

3.6.2. Preparation of probes for RT-PCR and Northern Analysis (A):

3.6.2.1. Design and synthesis of primers for PCR:

The primer sequences for α3, α7 and cyclophilin amplification were replicas of those used in earlier reports (Burnet *et al.*, 1994; Gopalakrishnan *et al.*, 1995; Gorbounova *et al.*, 1998). The primer sequences (human versions), positions and the PCR product sizes are shown in Table 3.3.

Table 3.3. Primer sequences used for PCR amplification of the α3 and α7 nAChR subunits and cyclophilin used in the present study.

Subunit	Sequence	Position	Size (bp)
α3	5'-GTGAATTC-TTCAGCCGCGCAGAGTCCA-3'	(1,179-1,198)	286
	5'-ATAAGCTT-GGCAACATACTTCCAATCATC-3'	(1,429-1,449)	
α7	5'-CGCCACATTCCACACTAAC-3'	(300-318)	256
	5'-ACCTTTCACTCCTCTTGCC-3'	(538-556)	
cyclophilin	5'-GACAAGGTCCCAAAGACAGC-3'	(121-140)	235
	5'-GTCCAGCATTTGCCATGGAC-3'	(335-355)	

3.6.2.2. Calculation of annealing temperature for primers:

Predicted melting point temperatures (Tm) of primers were estimated using either the following equations (Lowe *et al.*, 1990):

$$Tm = 4(GC) + 2(AT) \quad \text{or} \quad Tm = 62.3 + 0.41(G+C\%)-500/\text{amplified length}$$

3.6.2.3. Amplification and purification of α3, α7 and cyclophilin PCR products:

The primers used for α3, α7 and cyclophilin detection were in a lyophilised form and were resuspended to 60 pmoles/μl for the PCR reaction (Table 3.4) performed in a Perkin-Elmer, Model PTC-100™ (from MJ Research, Inc) thermo-cycling machine with the conditions shown in Table 3.5.

Table 3.4. Reagents used in the PCR reaction.

Reagent	Volume
10 x buffer	5 µl
dNTP (10 mM of each dNTP)	1 µl
Primer 1	1 µl
Primer 2	1 µl
DNA (whole brain cDNA)	1 µl
Amplitaq gold (1 unit/µl)	0.5 µl
dH_20	40.5 µl

Table 3.5. The conditions used in the PCR reaction.

Conditions
Denature; 94°C 10 min
Denature; 94°C 30 s }
Anneal; 60/52°C 30 s }x 30 cycles
Extend; 68°C 1 min }
Extend; 68°C 10 min

PCR products were analysed by agarose gel electrophoresis: 10 µl DNA samples were loaded with 0.25 vol. loading dye (15% Ficol, 0.25% bromophenol-blue, 0.25% xylene cyanol) onto a 1.5% agarose DNA gel made with 1 x Tris acetate buffer (TAE; 0.04M Tris-acetate, 0.001 mM EDTA, pH 7.6) containing 0.5 µg/ml ethidium bromide. DNA products were viewed under UV transillumination before being photographed using Kodak film. The sizes of the PCR products were estimated from the migration of a DNA size marker run concurrently (100-bp DNA ladder; GibcoBRL Life

Technologies, U.K.). The α3, α7 and cyclophilin DNA products were visible as single bands at 286, 256 and 235 bp.

The Geneclean® kit (Bio 101) spin method was used for the purification of the DNA bands excised from the TAE agarose gel. In brief GC spin glassmilk (400 µl) was added to a spin filter before adding the α3, α7 or cyclophilin bands excised from the DNA gel. The contents were heated to 55°C for 5 min in order to melt the gel and inverted every minute to prevent the matrix from settling. After incubation, the supernatant was collected by microcentrifugation into a clean tube. The filter was washed twice with GC spin new wash (500 µl) and microcentrifuged for 30 s after each wash. A final centrifugation of 1 min was used to dry the pellet. The spin filter was transferred to a fresh tube and nuclease free water (20 µl) was added to resuspend the glassmilk by gently vortexing for 1-2 s.

3.6.2.4. Ligation of DNA:

The purified DNA PCR product (10 µl) was incubated at 68°C for 20 min with amplitaq gold (0.5 µl), 10 x PCR buffer (1µl) and dNTPs to ensure that the PCR product had 'A' overhangs to ensure that ligation would be successful. The fresh PCR product (6 µl; approximately 10 ng) was mixed with 10 x ligation buffer (1 µl), PCR 2.1 vector (2 µl; 25ng/µl; Invitrogen) and T4 DNase ligase (1 µl; consisting of 50 mM Tris-HCl (pH 7.5), 10 mM $MgCl_2$, 10 mM dithiothreitol, 1 mM ATP, 25 µg/ml BSA) and incubated at 14°C overnight.

3.6.2.5. Transformation of competent cells:

An appropriate number of vials of One shot™ bacteria (Invitrogen) were thawed on ice and β-mercaptoethanol (2 µl; 0.5 M) was added into each vial. The cells were mixed by stirring gently with a pipette tip and 2 µl of the prechilled ligated DNA reaction mixture was added into the cells and stirred with the pipette tip to mix before incubating on ice for 30 min. Cells were heat-shocked for exactly 30 s at 42°C and then chilled on ice for 2 min. Luria-Bertani (LB) medium (250 µl; 10 g bacto-tryptone, 5 g yeast extract, 5 g NaCl dissolved and made up to 1 litre in dd$H_2$0) was added to each vial and the cells incubated at 37°C in a shaker for 30 min. The cells were then plated onto a prewarmed LB agar plate (LB substituted with 15 g agar) containing 50 µg/ml ampicillin and X-Gal. After overnight incubation at 37°C, the plates were placed at 4°C for 2-3 h for colour development. Individual white colonies, indicating the presence of the inserted DNA, were transferred, using sterile techniques, to 1.5 ml of LB medium containing 50 µg/ml ampicillin and incubated in a shaking incubator at 37°C overnight.

3.6.2.6. Isolation of plasmid DNA using the Promega Wizard™ *Plus* miniprep method:

After overnight growth at 37°C, an aliquot of the culture (1.5 ml) was transferred to a fresh microcentrifuge tube and pelleted by centrifugation (10,000 x g; 1 min). The pellet was resuspended by vortexing in 250 µl of cell resuspension solution (50 mM Tris-HCl (pH 8.0), 10 mM EDTA, 100 µM RNase A) before lysing the cells by the addition of 250 µl cell lysis solution (0.2 M NaOH, 1% (w/v) SDS). The contents were mixed by inversion. After complete lysis, 350 µl neutralisation solution (3 M potassium acetate, 11.5% (v/v) glacial acetic acid, pH 4.6) was added. Following mixing by inversion, the

bacterial lysate was centrifuged at 14,000 x g for 10 min at room temperature. A Wizard™ *Plus* miniprep column (Promega) was prepared by attaching a vacuum adapter with Luer-Lok® extension fitting to one port of the manifold. Spin columns were attached to the vacuum adapter and the cleared bacterial lysate was transferred into the spin column by decanting the liquid. Vacuum pressure was applied to draw the liquid though the column. Wash solution (750µl; 1 M NaCl, 50 mM 3-[*N*-morpholino]propanesulfonic acid (MOPS; pH 7.0), 15% (v/v) ethanol) was added to the column and passed through by vacuum. The washing procedure was repeated using 250 µl wash solution. After removal of the wash solution by vacuum, the spin column was removed and placed into a clean microcentrifuge tube, before centrifugation at 14,000 x g for 1 min to remove any remaining wash solution. The column was transferred to a clean microcentrifuge tube and nuclease free water (100 µl) added to the spin column to elute the plasmid DNA by centrifugation (14,000 x g; 1 min).

3.6.2.7. Restriction endonuclease digestion of DNA

DNA samples (10 µl) were digested with the restriction enzyme EcoR1 (1 µl) in 10 x reaction buffer (2 µl; consisting of 50 mM NaCl, 100 mM Tris-HCl, 10 mM $MgCl_2$, 0.025% Triton X-100 (pH 7.5)). Sterile water was added to a volume of 20 µl and the reaction incubated at 37°C for 1 h. Samples (20 µl with 3 µl loading buffer) were run on a 1.5% agarose gel to check for the presence of the appropriate insert.

3.6.3. SH-SY5Y cell culture:

SH-SY5Y cells were grown and maintained in 75 cm^2 flasks containing 20 ml of supplemented medium and maintained at 37°C in 5% CO_2/humidified air (see section 3.3.2 for maintenance of SH-SY5Y cell cultures). Cultures for total RNA preparation were subcultured in 6 well plates at a seeding density of 10^5 cells/ml (adapted from Vaughan *et al.*, 1993). Once confluent, SH-SY5Y cultures were treated chronically for 4 days with either nicotinic agonists (nicotine; 10 μM and DMAC; 10 μM) or KCl (20 mM) as described in section 2.4.2. Human embryonic kidney (HEK) cells were also used at Organon as a comparison for the level of expression of the α7 or α7/5-HT_3 subunit RNAs compared to the expression of α7 subunit RNA isolated from SH-SY5Y cells. The HEK cells had been transfected and the total RNA isolated by Organon (prior to 1998).

3.6.4. Total RNA preparation at Organon Laboratories:

Total RNA was prepared using the SV-Total RNA kit from Promega. Total cellular RNA was isolated from confluent SH-SY5Y cells chronically treated with or without drugs for 4 days. SH-SY5Y cell cultures were washed with warm PBS before trypsinising the cells. The cell suspension was placed into a 50 ml tube containing SH-SY5Y medium and centrifuged (300 x g, 5 min). The pellet was resuspended in 25 ml of ice cold sterile PBS solution before re-centrifuging. The PBS was carefully removed before adding SV RNA lysis buffer (175 μl; 4 M GTC, 0.01 M Tris (pH 7.5), 0.97% β-mercaptoethanol). The samples were mixed well by vortexing before being transferred to a microcentrifuge tube. SV RNA dilution buffer (350 μl) was added to the samples, the tube capped and inverted several times to ensure that the solution was well mixed.

Samples were incubated at 70°C for 3 min before being centrifuged (14,000 x g; 10 min at room temperature). The resulting clear lysate was pipetted into a fresh centrifuge, ethanol (200 µl; 95%) added and mixed with a pipette 3-4 times.

Samples were transferred to separate spin column assemblies. After centrifugation (14,000 x g, 1 min), SV RNA wash solution (600 µl; 60 mM potassium acetate, 10 mM Tris-HCl and 60% ethanol (95%, RNase free)) was added to the spin column assembly before an identical centrifugation process. Freshly prepared DNase incubation mix (50 µl; 40 µl yellow core buffer (0.0225 M Tris (pH 7.5), 1.125 M NaCl, 0.0025% yellow dye (w/v)), 5 µl of 0.09 M $MgCl_2$ and 5 µl of DNase) was applied to each sample, ensuring that the whole of the filter was covered by the mixture. After a 15 min incubation at 20°C DNase stop solution (200 µl; 2 M guanidine isothiocyanate, 4 mM Tris-HCl (pH 7.5) and 57% ethanol (95%, RNase free)) was added evenly over the filters before centrifugation (14,000 x g, 1 min). Two washing steps followed, the first was with SV RNA wash solution in ethanol (600 µl), centrifuged at 14,000 x g for 1 min, followed by a second wash of SV RNA wash solution in ethanol (250 µl) and centrifuged at 14,000 x g for 2 min. The cap was removed from the spin basket by twisting and the spin basket was placed into an elution tube, each spin basket had its own elution tube. Nuclease free water (100 µl) was added to completely cover the surface of the membrane to elute the sample RNA. The spin basket assemblies were centrifuged (14,000 x g, 1 min) to spin the RNA down from the filter. At this point the spin basket was removed and discarded and the elution tubes capped and stored at -80°C until use.

3.6.4.1. Concentration of RNA by ethanol precipitation:

RNA samples were thawed on ice before concentrating the RNA by precipitation with 0.1 volumes of RNase free sodium acetate (3 M) and 2.5 volumes of absolute ethanol at -20°C overnight, centrifuged at high speed (14,000 x g) for 30 min. The pellet was washed with 70% ethanol, centrifuged (14,000 x g; 10 min), and allowed to air dry after removal of most of the ethanol, before resuspending in sterile RNase free water.

3.6.4.2. Estimation of concentration of RNA:

Total cellular RNA samples isolated from SH-SY5Y cells were diluted 1:100 in DEPC-treated sterile water. Spectrophotometer (Perkin Elmer UV/VIS Lambda 11) readings were obtained at absorbencies A_{260} and A_{280}. The concentration of RNA was calculated using the equation:

$$RNA = A_{260} \times 40 \times \text{dilution factor}$$

Standards = 1 O.D. unit for RNA corresponds to 40 μg/ml

The ratio (A_{260}/A_{280}) provides an estimation of the purity of the RNA preparation. A ratio of 2.0 indicates a high purity of RNA. A ratio greater than 2.0 indicates contamination with DNA, while a lower figure indicates protein contamination.

3.6.5. RT-PCR:

Total RNA was isolated and precipitated as described in sections 3.6.4 and 3.6.4.1 and resuspended to give the same concentration in each tube. The reagents used for RT-PCR are shown in Table 3.6. All RT-PCR reagents were supplied by Promega. RT-PCR reactions for each of the drug and untreated control RNA samples were performed using

specific primers for human α3, α7 nAChR subunits and cyclophilin (see section 3.6.2.1); controls were performed in parallel with nuclease free water substituting the sample RNA.

Table 3.6. Reagents and their volumes used in the RT-PCR reaction.

Reagent	Volume
Nuclease free water	32 µl
AMV/Tfl 5 x reaction buffer	10 µl
dNTP mixture (10 mM each of dATP, dCTP, dGTP and dTTP)	1 µl
Downstream primer	1 µl
Upstream primer	1 µl
$MgSO_4$, 25 mM	2 µl
AMV reverse transcriptase	1 µl
Tfl DNA polymerase	1 µl
RNA sample (or RNase free H_2O for control)	1 µl

Thermocycling conditions included an initial reverse transcription step of 45 min at 48°C followed by denaturation of cDNA for 2 min at 94°C. This was followed by 30 s at 94°C, primers hybridise to the template at previously calculated annealing temperatures (60°C for α3 and cyclophilin; 52°C for α7, see section 3.6.2.2) for 30 s and then the strands were elongated at 68°C for 1 min, these three steps were repeated for 40 cycles. Finally a 10 min step at 68°C was included to ensure the PCR fragments were fully elongated and that no single stranded products remained in the reaction tube. Following thermocycling, 10 µl of reaction product was run on a 1.5% agarose electrophoretic gel for analysis by UV illumination.

3.6.6. Gel electrophoresis:

Total cellular RNA (5 µl/10 µg) or poly $(A)^+$ RNA (5µl) samples were made up to 20 µl with loading dye (48% formamide, 10.7% 10 x 2-[*N*-morpholino]ethanesulphonic acid (MESA): 200 mM MOPS, 50 mM sodium acetate, 10 mM EDTA in DEPC water; pH 7, kept at 4°C in the dark, 17.3% formaldehyde (37% stock), 17.3% DEPC treated water, 6.7% glycerol (80%) and 0.01% bromophenol blue) and incubated at 65°C for 15 min to allow for denaturation of the RNA. After incubation, the samples were centrifuged in a microfuge before placing on ice for 2 min. Ethidium bromide (2 µl; 1 mg/ml) was added to each sample before loading onto a 1% agarose gel using RNAse-free filter pipette tips and running in 1 x MESA (diluted with DEPC treated water) as the running buffer. The samples were electrophoresed at 150 V until the bromophenol blue dye front migrated approximately 75% down the gel. At this point the gel was photographed using UV light on a transilluminator prior to sample transfer onto a nylon membrane.

3.6.7. Capillary transfer to the membrane blot:

RNA was transferred by a downward capillary transfer method from the gel to a Nytran membrane (modified from Chomczynski, 1992); the downward transfer apparatus was assembled as depicted in Figure 3.11. After transfer was complete (usually overnight), the membrane was exposed briefly to UV illumination to crosslink the RNA to the membrane.

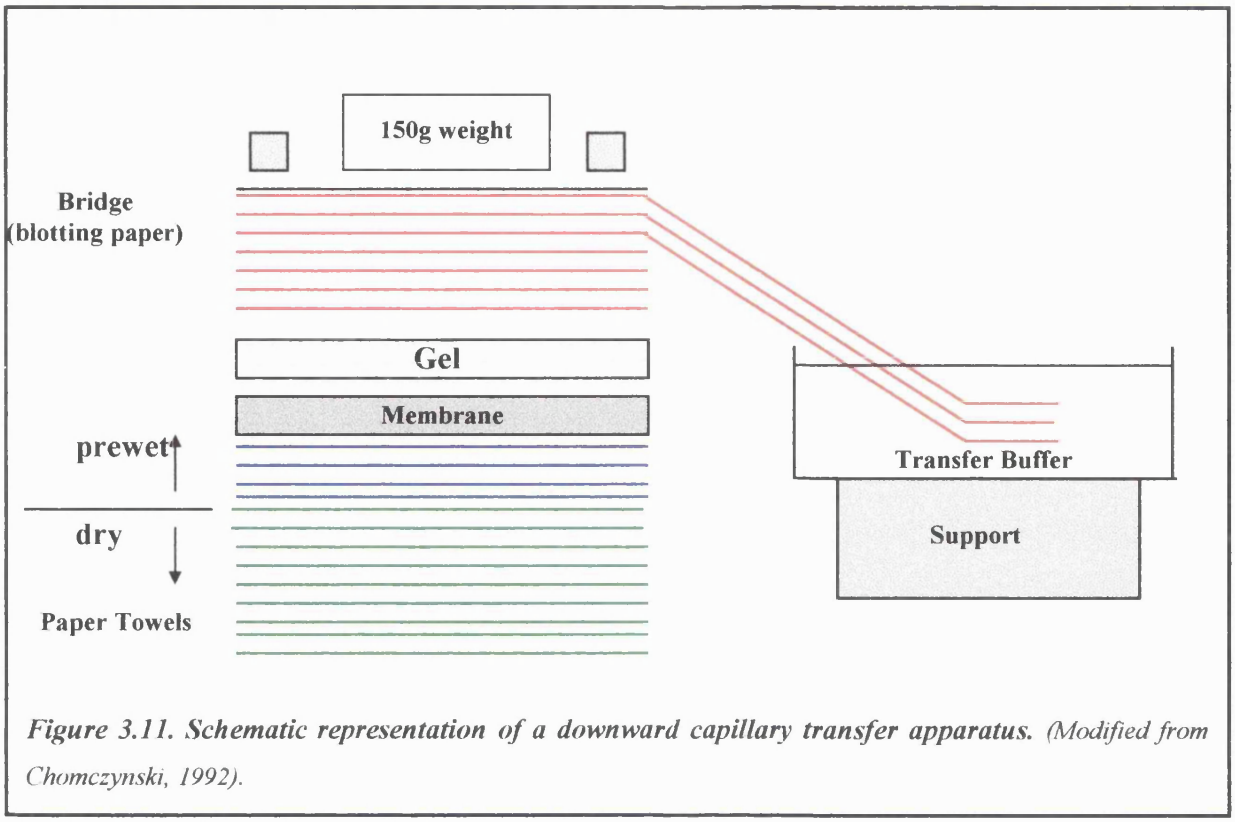

Figure 3.11. Schematic representation of a downward capillary transfer apparatus. *(Modified from Chomczynski, 1992).*

3.6.8. Labelling the probes, hybridisation and membrane washes:

Hybridisation (Northern Max™) was performed using ^{32}P-dCTP-labelled human α3 or α7 with cyclophilin purified DNA products (obtained as described in section 3.6.2). Human cyclophilin cDNA was used as a heterologous probe to determine the amount of human cyclophilin RNA expressed in the SH-SY5Y cell line, enabling normalization of the α3 and α7 subunit transcript signals within each lane. The following reagents were used to label the α3, α7 and cyclophilin DNAs: DNA (3 µl) and DEPC-treated water (10 µl) were initially boiled for 3 min, microfuged briefly before the addition of high prime (4 µl) and dCTP (^{32}P) (3 µl; 10 µCi/µl). Samples were then placed at 37°C for 15 min to ensure denaturation of the DNA. Either ^{32}P-dCTP-labelled α3, α7 and cyclophilin probes were used to probe the SH-SY5Y sample RNA transferred onto the

nylon membrane. This involves a prehybridisation step during which the membrane is incubated at 42°C for 2 h with the labelled DNA probes diluted in preheated ZIP-Hyb solution (10 ml/100 cm^2) in hybridisation tubes in a roller oven. Membranes were washed initially with low and then high stringency wash solutions at room temperature and 42°C respectively to remove any unbound ^{32}P-dCTP from the membrane. On removal of the high stringency wash solution the membranes were wrapped in plastic wrap to prevent drying out and exposed to Kodak film for autoradiography at -80°C for varying lengths of time.

3.6.9. Analysis of data:

Scanned images were quantified using an Arcus II scanner from AGFA and Zero-Dscan version 1 image software from Scanalytics, Inc to analyse band densities from the autoradiographs.

3.7. Preparation of probes for Northern analysis (B):

3.7.1. Subcloning DNA fragments:

Specific fragments (300-500 bp) of interest for α3 and α7 cDNAs (positions 1180 to 1449 and 505 to 728 respectively), were cloned into the vector PCR 2.1 (Invitrogen), sequenced and used as putative specific nAChR subunit fragments to be labelled with digoxigenin (DIG). Initially the vector was linearised upstream of the α3 and α7 sequences by restriction digest allowing the creation of run-off transcripts of uniform length. The DNA was purified by phenol/chloroform extraction and ethanol precipitation as follows. Phenol (Tris treated, pH 8), chloroform and isoamyl alcohol

were added to the resuspended DNA in the ratio 25:24:1 in a sterile microfuge tube. The contents were shaken to form a milky suspension and then centrifuged for 1 min. The top aqueous layer was transferred to a clean microfuge tube and an equal volume of chloroform added before re-centrifugation. The top aqueous layer was again transferred to a sterile microfuge tube before adding 0.1 volumes of sodium acetate (3 M; pH 5.3) and 2 volumes of ethanol. The contents of the tube were left at 4°C overnight to allow precipitation of the DNA. The solution was then spun at 13,000 rpm for 1 h at 4 °C before washing the pellet in 75% ethanol for 1 h at 13,000 rpm at 4°C. The DNA pellet was air dried before resuspending in DEPC-treated water.

3.7.2. Labelling partial α3, α7, and G_3PDH cDNA sequences with digoxigenin (DIG) labelled UTP mix:

The labelling reaction was set up as follows: 1 μg of the purified DNA template, 2 μl NTP labelling mix (10 x), 2 μl 10 x transcription buffer, 0.5 μl RNase inhibitor (40 units/μl), DEPC-treated water to 18 μl, 2 μl T7 polymerase (20 units/ μl) (all reagents Roche Boehringer Mannheim; see also Table 3.7). Following mixing and brief centrifugation, this reaction was allowed to proceed at 37°C for 2 h before the addition of 2 μl RNase free, DNase I (10 units/μl) for a further incubation of 15 min at 37°C to remove the DNA template. EDTA (2 μl, 200 mM; pH8) was added to terminate the reaction. The DIG-labelled RNA probes were stored at -20°C before quantitation with a DIG-labelled control.

Table 3.7. Reagents for DIG-labelling RNA.

Reagent	Components
NTP labelling mix	10 mM ATP, 10 mM CTP, 10 mM GTP, 6.5 mM UTP, 3.5 mM DIG UTP; in Tris-HCl, pH 7.5
10 x transcription buffer	400 mM Tris-HCl (pH 8), 60 mM $MgCl_2$, 100 mM dithioerythritol, 20 mM spermidine, 100 mM NaCl

3.7.3. Estimation of the yield of DIG-labelled DNA:

The yield of DIG-labelled α3, α7 and G_3PDH RNA was estimated by comparison with serial dilutions of an appropriate labelled standard control RNA (supplied by Roche Boehringer Mannheim) in a spot test on nylon membranes with a dilution series of the DIG-labelled sample RNA. The standard labelled control RNA (2 µl) was mixed with DEPC-treated water (38 µl; final concentration of 20 ng/µl) before performing serial dilutions to give concentrations from 1 ng/µl to 0.01 pg/µl. The α3, α7 and G_3PDH DIG-labelled probes were serially diluted in an identical manner as to the standard DIG-labelled control.

Highly diluted solutions of RNA in water are not very stable, therefore immediately after the dilutions were made in RNase free water, 1 µl aliquots of each control dilution were spotted onto a piece of dry positively charged nylon membrane (Roche Boehringer Mannheim). The experimental RNA dilutions were spotted on a second row below the corresponding dilutions of control diluted spots (Figure 3.12). The nucleic acids were fixed to the membrane by UV cross-linking for 5 min. The membrane was briefly washed in washing buffer (maleic acid buffer with 0.3% (v/v) Tween®20; see Table 3.9) before incubation in blocking buffer for 30 min at room temperature. Anti-DIG-alkaline phosphatase antibody was diluted 1:10,000 in blocking buffer and the membrane was

incubated for a further 30 min in this diluted antibody solution at room temperature. The membrane was subsequently washed twice, 15 min per wash, in washing buffer at room temperature before equilibration of membrane in detection buffer for 2 min.

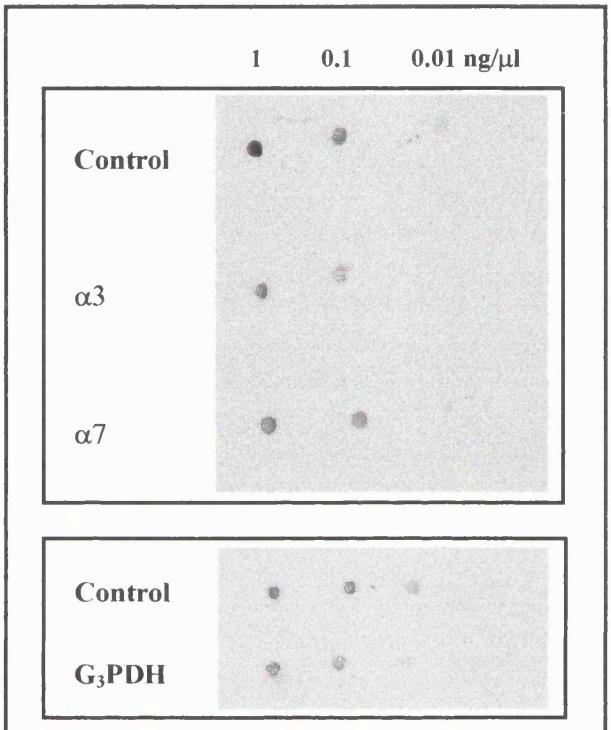

Figure 3.12. Estimation of the yield of DIG-labelled DNA. *Dilutions of the labelled control RNA with exact concentrations of 1, 0.1 and 0.01 ng/µl are shown with the newly labelled α3, α7 and G_3PDH DNA diluted in identical serial dilutions to the control were spotted on, fixed to, and directly detected on a nylon membrane, with chemiluminescent detection.*

A 1:100 dilution of disodium 3-(4-methoxyspiro {1,2-dioxetane-3,2'-(5'-chloro) tricyclo [3.3.1.1^{3,7}] decan}-4-yl) phenyl phosphate (CSPD®; 25 mM) in detection buffer was carried out before applying 0.5 ml of this chemiluminescent substrate dropwise on top of the membrane scattering the drops over the surface of the membrane. The

membrane at this stage has been placed between two sheets of acetate (plastic). The top sheet of acetate was wiped with a damp tissue to remove any air bubbles present between the sheet and to create a liquid seal. The filter was incubated at room temperature for 5 min before sealing all sides of the acetate using a heat sealer. To shorten exposure times the filter was incubated at 37°C for 15 min, after which the membrane was exposed to X-ray film for 2 h detection of the chemiluminescent signal. Figure 3.12 shows the estimation of yield of α3, α7 and G_3PDH DIG-labelled RNA probes.

3.8. Preparation of total RNA isolated from SH-SY5Y cells at Bath:

SH-SY5Y cells were cultured and chronically treated with nicotine, DMAC or KCl in 175 cm^2 flasks exactly as described for SH-SY5Y cells cultured in 75 cm^2 in section 3.3.3. After 4 days in the presence of drugs, cultures were washed and total RNA was isolated using a TRIZOL reagent method of extraction (Life Technologies). In brief, cells were directly lysed in a culture flask by the addition of TRIZOL reagent (1 ml per 10 cm^2) and passing the cell lysate through a pipette several times. The samples were incubated for 5 min at room temperature to permit the complete dissociation of nucleoprotein complexes. Chloroform (0.2 ml per 1 ml of TRIZOL reagent) was added and the tubes shaken vigorously for 15 s. The samples were incubated for a further 3 min at room temperature before centrifuging at 12,000 x g for 10 min at 4°C. The upper aqueous phase, containing the RNA, was transferred to a Corex tube and the RNA precipitated by the addition of isopropyl alcohol (5 ml per 10 ml TRIZOL used for the initial homogenisation). Samples were incubated at room temperature for 10 min and centrifuged at 12,000 x g for 10 min at 4°C. The RNA pellet was resuspended in ethanol

(75%: 10 ml per 10 ml TRIZOL initially used). Samples were centrifuged at 7,500 x g for 5 min at 4°C. The RNA pellet was vacuum dried for 5 min and dissolved in 0.5% (w/v) SDS by passing through a pipette and incubating for 10 min at 55-60°C. RNA was quantified as described in section 3.6.4.2.

3.9. Preparation of poly $(A)^+$ RNA:

Poly $(A)^+$ RNA was subsequently isolated from total RNA using Dynabeads® Oligo $(dT)_{25}$ magnetic beads (Dynal), 2.8 μm in diameter, with a 25 nucleotide long chain of deoxythymidylate attached covalently to the bead surface via a 5' linker group. Beads were stored in PBS containing 0.02% sodium azide. An aliquot of bead suspension (0.2 ml; 1 mg) was pipetted into a 1.5 ml microfuge tube and placed into a Dynal MPC®-E magnetic particle concentrator and the supernatant removed. The beads were washed by the addition of 100 μl 2 x binding buffer (20 mM Tris-HCl, pH 7.5, 1 M LiCl, 2 mM EDTA) followed by resuspension in 100 μl 2 x binding buffer. Total RNA (200 μg) samples were dissolved in 100 μl DEPC-treated water, incubated for 2 min at 65°C to disrupt the secondary structure before adding to the washed beads. The poly $(A)^+$ RNA was allowed to anneal for 5 min on a rotating platform at room temperature before placing on the magnetic stand to allow separation and removal of the supernatant. After washing the beads twice with 200 μl washing buffer (10 mM Tris-HCl, pH 7.5, 0.15 M LiCl, 1 mM EDTA), they were resuspended in 30 μl elution buffer (10 mM Tris, pH 7.5) before incubating at 65°C for 2 min. Eluted poly $(A)^+$ RNA was extracted immediately after separation from the beads and used directly for Northern blot analysis.

3.10. Denaturing formaldehyde gel electrophoresis:

Agarose (1 g) was added to 124 ml DEPC-treated water in a conical flask and heated in a microwave to melt the agarose. Once cooled to 55°C, 15 ml 10 x MESA and 11 ml 37% formaldehyde were added, swirled to mix and the gel poured immediately into a Perspex gel rig, and left to set for approximately 45 min. All apparatus was pre-treated with 1% hydrogen peroxide to denature RNases. The gel rig was placed in a horizontal electrophoresis tank and 1 x MESA was added until the gel was submerged. Samples were prepared by mixing poly $(A)^+$, or total RNA with 10 µl freshly prepared formaldehyde gel loading buffer and the DIG-labelled RNA molecular weight marker was prepared by the addition of 16 µl loading buffer to 4 µl marker. All samples were incubated at 65°C for 15min and chilled on ice after a brief centrifugation. Samples were loaded onto the gel and the gel was run at 80 V for 4 h. The cast and gel were transferred to a plastic box and washed with 20 x SSC to remove formaldehyde. The composition of solutions used for Northern blot analysis are shown in Table 3.8.

*Table 3.8. **Composition of Northern Blot solutions.** *RNase-free solutions were prepared with 0.1% DEPC treated water.*

Solution	Components
10 x MESA*	200 mM MOPS, 50 mM sodium acetate, 10 mM EDTA; pH 7
Electrophoresis buffer*	1 x MESA
Formaldehyde gel loading buffer*	7.2 ml Deionised formamide, 1.6 ml 10 x MESA, 2.6 ml deionised formaldehyde, 2.6 ml water, 1 ml 80% glycerol, 0.01% (v/v) bromophenol blue
Formaldehyde	Commercially available as a 37% solution (12.3 M) in water
20 x SSC*	3 M NaCl, 300 mM sodium citrate; pH 7

3.11. Northern transfer:

The RNA was blotted from the gel onto a piece of Boehringer positively charged nylon membrane by capillary transfer overnight at room temperature. RNA was then cross-linked to the membrane by UV illumination for 5 min.

3.12. Hybridisation and detection of Northern blot:

The composition of solutions used for hybridisation and detection are shown in Table 3.9.

*Table 3.9. **Composition of solutions used for hybridisation and detection.** *RNase-free solutions were prepared with 0.1% DEPC treated water.*

Solution	Components
Pre-hybridisation solution/DIG easy-hybridisation buffer*	Commercially available hybridisation buffer granules reconstituted in water (Boehringer Mannheim)
2 x Wash solution*	2 x SSC, containing 0.1% (w/v) SDS
0.5% x Wash solution*	0.5 x SSC, containing 0.1% (w/v) SDS
Maleic acid buffer*	100 mM maleic acid, 150 mM NaCl; pH 7.5
Washing buffer*	100 mM maleic acid, 150 mM NaCl; pH 7.5; 0.3% Tween 20
Blocking solution*	Commercially available solution diluted 1:10 in maleic acid buffer
Detection Buffer*	100 mM tris-HCl, 100 mM NaCl; pH 9.5
TE buffer	10 mM Tris, 1 mM EDTA; pH8

Following removal of the marker lane from the membrane, the blot was placed in a hybridisation bottle and incubated with 20 ml prehybridisation solution (DIG Easy Hyb, Roche Boehringer Mannheim) at 68°C for 1 h. The DIG-labelled probe was meanwhile

heat-denatured in a boiling water bath for 10 min and diluted in 5 ml prehybridisation solution at a concentration of 100 ng/ml (hybridisation buffer). Prehybridisation buffer was discarded and the blot was incubated at 68°C overnight with hybridisation buffer (DIG Easy Hyb) and the cDNA probe (final concentration of 100 ng/hybridisation buffer volume). Following hybridisation the blot was washed twice, 15 min per wash, in 2 x wash solution at room temperature followed by 2 washes in 0.5 x wash solution at 68°C. All further steps were carried out at room temperature unless stated otherwise. The marker lane was included in all further steps.

The membrane was equilibrated in washing buffer for 1 min (maleic acid buffer containing 0.3% (v/v) Tween 20). This was discarded and the membrane was blocked by gentle agitation in blocking solution for 1 h. The blot was incubated with gentle agitation for 30 min with anti-Digoxigenin antibody (diluted 1:10,000 in blocking solution). The antibody solution was discarded and the membrane gently washed twice in washing buffer. The membrane was equilibrated in detection buffer for 2 min. Meanwhile CSPD® was diluted 1:100 in detection buffer. The membrane was placed between 2 sheets of acetate and 0.5 ml chemiluminescent substrate was scattered dropwise on the surface. The top sheet was lowered and wiped with a damp tissue to remove air bubbles and the bag was sealed and incubated at room temperature for 5 min. To decrease time taken for the chemiluminescent reaction to reach equilibrium, the membrane was incubated at 37°C for 15 min before exposure to X-ray film (Roche Boehringer Mannheim) for approximately 20 min. Sometimes the film had to be left overnight for detection of a signal.

3.13. Results.

RT-PCR and Northern blot hybridisation analysis were used to determine whether the increased levels of nicotinic binding sites found after chronic nicotine, DMAC or KCl treatment described in Section 1 were due to increased transcription of nAChR subunit genes resulting in an increase in the level of expression of α3 and α7 subunit RNA.

The SH-SY5Y cell line was used to investigate the expression of the α3 and α7 nAChR subunits. Total RNA samples isolated from SH-SY5Y cells were used in an RT-PCR protocol to amplify both the α3 and α7 transcript signals and hence confirm their expression. RT-PCR analysis of α3, α7, and the internal standard housekeeping gene cyclophilin, expressed in total cellular RNA samples isolated from control and drug treated SH-SY5Y cells with nicotine (10 μM), DMAC (10 μM) or KCl depolarisation (20 mM) are shown in Figure 3.13. The α3, α7 and cyclophilin RT-PCR products were visible as single bands at 286, 256 and 235 bp as indicated in Figure 3.13.

One of the disadvantages of RT-PCR, although sensitive, it cannot be used as a direct quantitative method for analysing significant differences in the level of expression of different transcripts. This is a major drawback of exponential amplification, in that small sample-to-sample differences in amplification potentially translate to huge differences in the product yield. Therefore the α3 and α7 subunit RNA signals amplified from SH-SY5Y cells chronically treated with drugs could not be directly quantitated to their corresponding control untreated RNA samples, or normalised to the internal standard housekeeping gene due to the putative exponential amplification process that occurs in the process of RT-PCR.

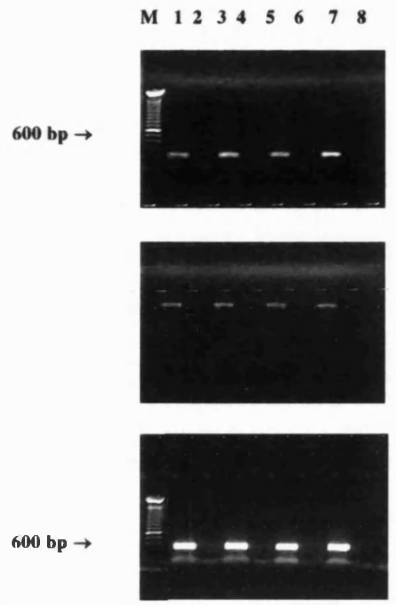

Figure 3.13. Reverse transcriptase PCR (RT-PCR) analysis of α3, α7 and cyclophilin expression. *Total RNA was extracted from confluent SH-SY5Y cells after chronic treatment with either DMAC (10 μM; lanes 3 and 4), nicotine (10 μM; lanes 5 and 6) or KCl (20 mM; lanes 7 and 8) for 4 days. All control untreated (lanes 1 and 2) and drug treated RNA used in the RT-PCR protocol also had RT-PCR performed without reverse transcriptase added to the reaction mix to test for contaminating genomic DNA template (lanes 2, 4, 6 and 8). Water controls, with no RNA added are also included. Samples were run on a 1.5% agarose gel and viewed by UV illumination.*

It was then decided to investigate by quantitative evaluation, the level of expression of the α3 and α7 nAChR subunit RNA levels expressed in control untreated and chronic drug treated SH-SY5Y cells. Northern blot hybridisation analysis was performed using total RNA isolated form control and drug treated SH-SY5Y cells. This technique remains the standard for detection and quantitation of RNA levels, and permits a direct relative comparison of message abundance between samples on a single nylon membrane. Initial experiments performed at Organon Laboratories using total RNA produced faint or no bands when probed for the α7 transcript (Figure 3.16c). Figure 3.14 shows samples of total RNA run on a 1% agarose gel (a) before and (b) after transfer to a membrane, clearly showing in (b) that the samples have been successfully transferred.

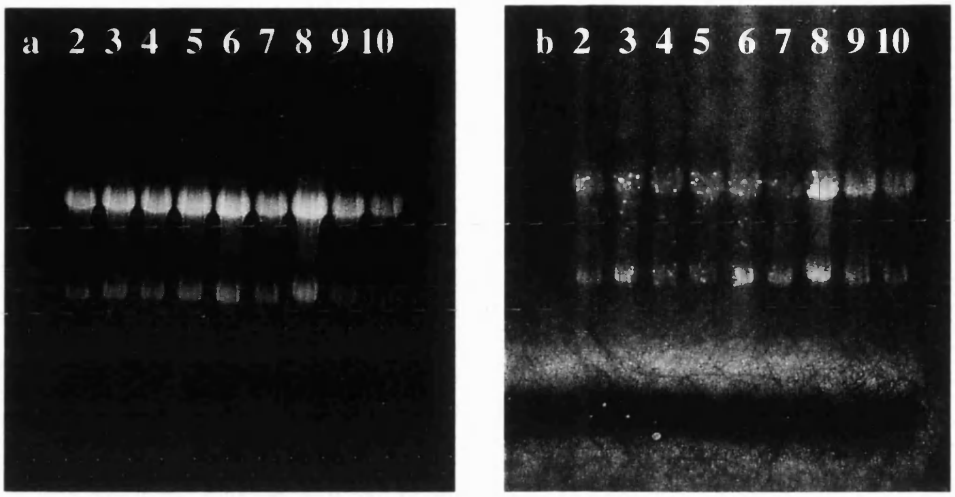

Figure 3.14. A representative RNA agarose gel. *Total RNA (10 μg) isolated from SH-SY5Y cells (lanes 2 and 4), HEK cells (lanes 5 and 9) or from HEK cells containing the α7/5-HT$_3$ chimera (lanes 3, 6-8 and 10) were run on 1% agarose gel and visualised by UV illumination. Panel (a) shows two distinct bands in each lane of the total RNA samples, this corresponds to rRNA. Panel (b) was viewed under UV illumination after transfer to a nylon membrane.*

Figure 3.15 shows the corresponding autoradiographs for Figure 3.14 after the membranes were probed with (a) α3 and cyclophilin or (b) α7 and cyclophilin with a 6 or 16 day exposure respectively. In panel (a) lanes 2 and 4 contain total RNA samples isolated from control SH-SY5Y cells and the α3 transcript can easily be observed (band at 3.6 kDa). The other lanes are total RNA prepared from either HEK cells (lanes 5, 9) or HEK cells containing either α7 (lanes 6-8) or the α7/5-HT$_3$ chimera (lanes 3 and 10) and do not express the α3 nAChR subunit.

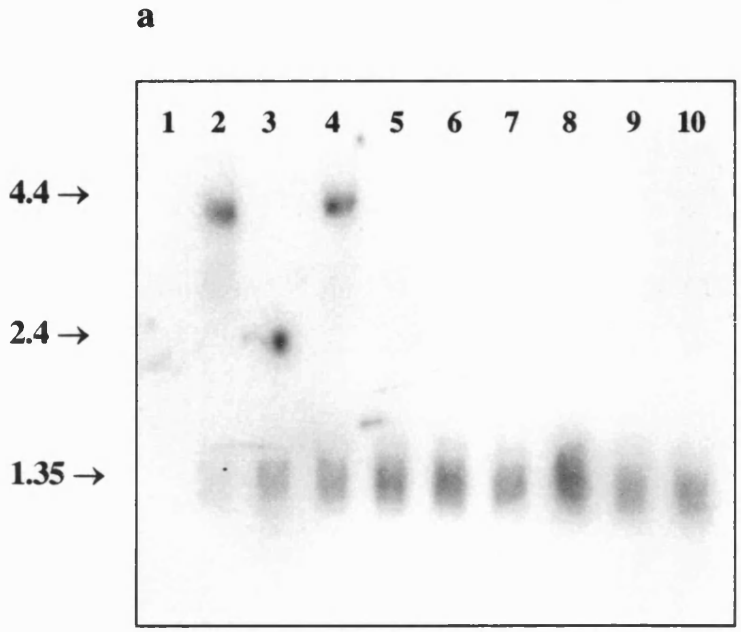

Lane

1). RNA Markers
2). SH-SY5Y (11.5.98) P30
3). HEK + α7/5-HT$_3$ chimera
4). SH-SY5Y (27.1.98)
5). HEK 27.1.98
6). HEK + α7 1.5
7). HEK + α7 2.25
8). HEK + α7 2.75
9). HEK (4.12 97)
10). HEK + α7/5-HT$_3$ chimera

Figure 3.15. Typical autoradiographs obtained after hybridisation. *Total RNA samples extracted from SH-SY5Y cells and HEK cells (expressing either α7 or the α7/5-HT$_3$ chimera) were transferred to a nylon membrane and crosslinked before performing hybridisation. Panel (a) was probed with α3 and cyclophilin for a 6 day exposure; panel (b) was probed with α7 and cyclophilin for a 16 day exposure using ^{32}P labelled DNA probes. Kodak film was placed over the membrane, sealed in a cartridge box and placed at -80°C being developed. (Total RNA had previously been isolated from HEK, HEK/α7 and HEK/ α7/5-HT$_3$ cells for a different project under investigation at Organon Laboratories and were used as a positive control for the detection of the α7 nAChR subunit).*

Figure 3.15b shows the absence of an α7 transcript in lanes 2 and 4 that contain total RNA isolated and prepared from SH-SY5Y cells whereas lanes 3, 6-8 and 10, samples of RNA isolated from HEK cells containing either the α7 subunit or the α7/5-HT_3 chimera, show distinct bands for the α7 or α7/5-HT_3 transcript respectively (at approximatley 2.4 kDa, serving as a positive control).

Figure 3.16a shows a representative 1% agarose gel run with total RNA samples isolated from control and drug treated SH-SY5Y cells with corresponding autoradiographs for the detection of α3 (Figure 3.16b) and α7 (Figure 3.16c) transcripts for 6 or 16 days exposure respectively. Cyclophilin was used as the internal standard gene. The scanned images shown in Figures 3.16b and c were quantified by analysing band optical densities obtained from the autoradiographs. Band density was normalised by correlating the α3 and α7 RNA bands to their corresponding cyclophilin bands for each sample. Quantitation of the level of α3 and α7 subunit RNA isolated from SH-SY5Y cells chronically treated with nicotine (10 μM), DMAC (10 μM) and KCl (20 mM) were then expressed as a percentage of the α3 and α7 bands obtained in the control untreated cells (expressed as 100%). The values obtained from this independent experiment are shown in Table 3.10. Values obtained reveal that expression of the α3 transcript are 99%, 97% and 102% of control values for nicotine (10 μM), DMAC (10μM) and KCl (20 mM) treated SH-SY5Y cells respectively. This preliminary independent result indicates that chronic drug treatment with nicotinic agonists, nicotine or DMAC, and a depolarising concentration of KCl do not upregulate α3 total cellular RNA levels in SH-SY5Y cells. The bands for the α7 transcript detected in SH-SY5Y cells were extremely faint and hard to analyse once scanned, thus producing no

conclusive results on the effect of these chronic drug treatments when compared to control.

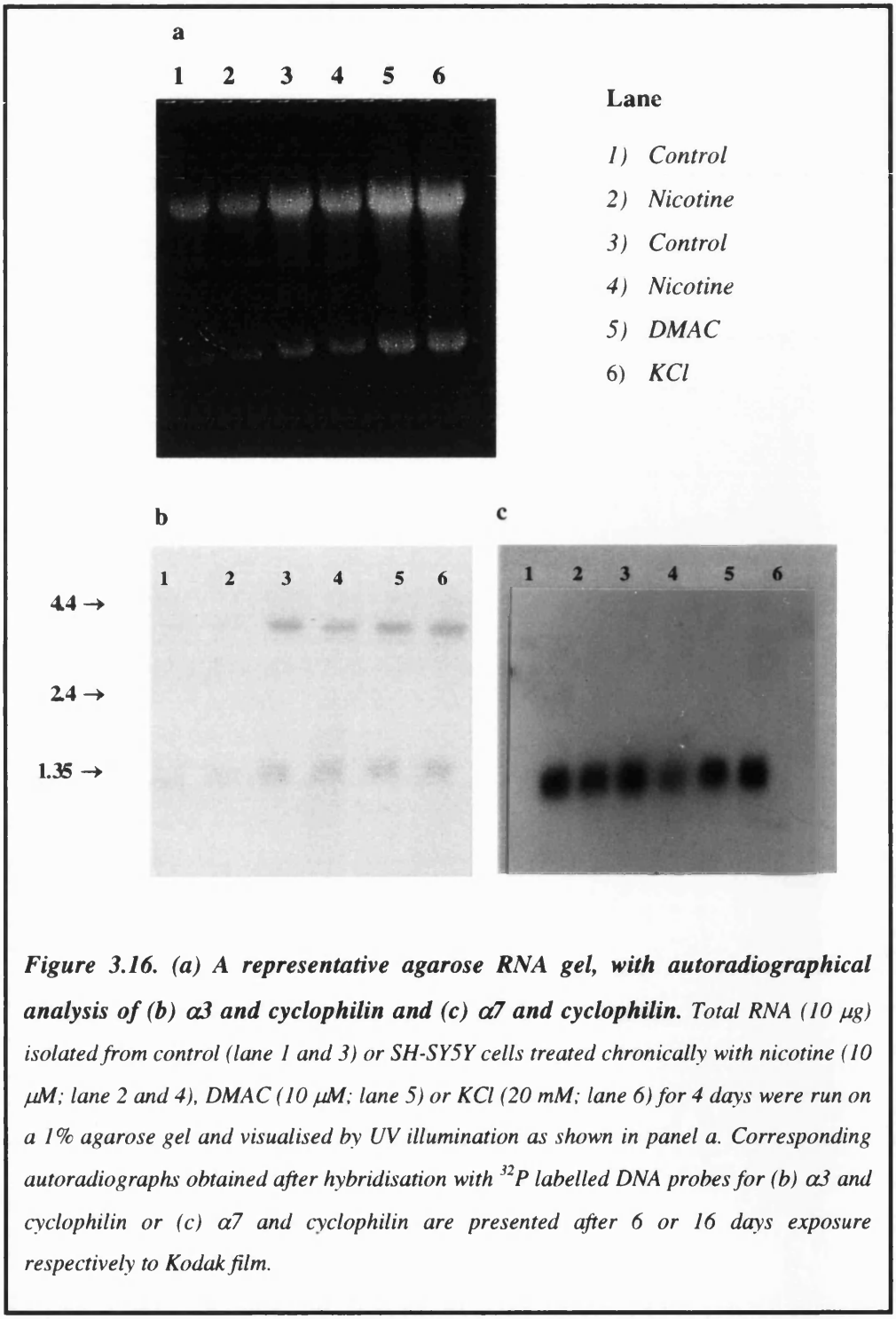

Figure 3.16. (a) A representative agarose RNA gel, with autoradiographical analysis of (b) α3 and cyclophilin and (c) α7 and cyclophilin. *Total RNA (10 μg) isolated from control (lane 1 and 3) or SH-SY5Y cells treated chronically with nicotine (10 μM; lane 2 and 4), DMAC (10 μM; lane 5) or KCl (20 mM; lane 6) for 4 days were run on a 1% agarose gel and visualised by UV illumination as shown in panel a. Corresponding autoradiographs obtained after hybridisation with ^{32}P labelled DNA probes for (b) α3 and cyclophilin or (c) α7 and cyclophilin are presented after 6 or 16 days exposure respectively to Kodak film.*

Table 3.10. The level of expression of α3 and α7 nAChR subunit RNA expressed as a percentage of these subunits present in untreated control cells. *Confluent SH-SY5Y cells were pretreated for 4 days with nicotine (10 μM), DMAC (10 μM) or KCl (20 mM) before isolating total RNA. RNA (10 μg) samples were run on a 1% agarose gel before being probed with ^{32}P labelled cDNA probes for α3, α7 and cyclophilin. The level of expression of α3 and α7 transcripts were normalised to the level of expression of their corresponding cyclophilin housekeeping gene before expressing these as a percentage of the α3 and α7 RNA obtained from control untreated cells. (n.d. Denotes not detectable).*

	nAChR subunit transcript (as % of control)	
Drug treatment	**α3**	**α7**
Nicotine	99	97
DMAC	97	n.d.
KCl	102	n.d.

The result obtained for α7 RNA levels after chronic nicotine treatment when compared as a percentage of control indicates that α7 RNA levels are putatively unaltered by this treatment for 4 days. Due to nicotine treatment upregulating [^{125}I]-α-bgt binding sites in SH-SY5Y cells, indicative of putative α7* nAChR, the unaltered α7 RNA levels after nicotine treatment suggests that nicotine-induced upregulation of α7* nAChR is possibly by a post-transcriptional mechanism.

Figure 3.17 shows a Northern blot of various human brain regions probed for the α7 subunit transcript and cyclophilin to demonstrate that the α7 nAChR subunit transcript can be detected by this protocol. After 24 h exposure, the cyclophilin bands are clearly visible, but a longer exposure of 16 days was required to identify the respective α7 transcript bands. These data indicate that the Northern analysis procedure used at

Organon Laboratories, for the detection of both α3 and α7 transcripts is effective. This procedure reliably detects α7 transcripts in HEK cells expressing α7 nAChR subunits or the α7/5-HT_3 chimera (Figure 3.15b) and in various regions of human brain tissue (Figure 3.17), in contrast to the extremely low level of α7 expression in SH-SY5Y cells that is difficult to detect (Figs. 3.15b, 3.16c). Low level α7 subunit expression in SH-SY5Y cells may result in comparative but harder to detect increases of [^{125}I]-α-bgt binding after chronic drug treatment compared to primary hippocampal cultures.

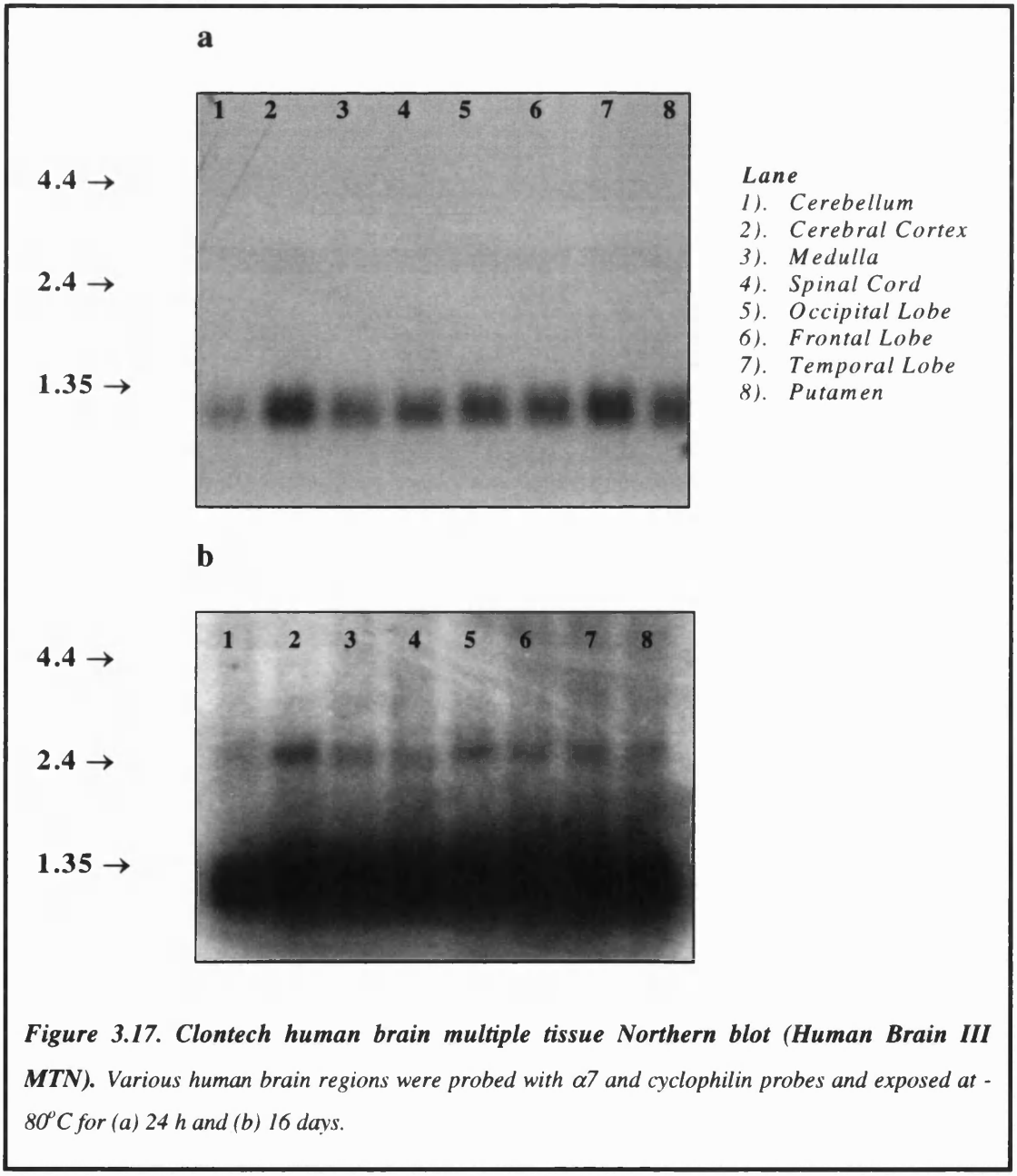

Figure 3.17. Clontech human brain multiple tissue Northern blot (Human Brain III MTN). *Various human brain regions were probed with α7 and cyclophilin probes and exposed at -80°C for (a) 24 h and (b) 16 days.*

On consideration of the preliminary data generated at Organon Laboratories, it was decided to repeat the Northern analysis at Bath, on control and drug treated SH-SY5Y cells, using DIG-labelled DNA probes to detect the α3 and α7 nAChR subunit RNA. Total RNA and also poly $(A)^+$ RNA was isolated from SH-SY5Y cells. Approximately 1-4% of total RNA in the cytoplasm of a typical eukaryotic cell is mature poly $(A)^+$ RNA. By using poly $(A)^+$ RNA in the Northern analysis procedure, the α3 and α7 signals should give cleaner results with reduced background and therefore produce a signal with greater sensitivity and intensity. Total cellular RNA was used in all subsequent Northerns as the poly $(A)^+$ RNA proved more susceptible to degradation. The data for each drug treatment was normalised to their internal standard G_3PDH before being expressed as a percentage of the control values and are summarised in Figure 3.18.

The results parallel the initial preliminary data (generated at Organon Laboratories) in that the nicotinic agonists, nicotine and DMAC, and KCl depolarisation do not alter the level of expression of α3 RNA expressed in SH-SY5Y cells after 4 days of chronic drug treatment (n=3). On analysis of the α7 data (n=1; bands observed were still faint), nicotine and DMAC do not significantly change the expression of the α7 transcript, relative to control, when normalised to their G_3PDH internal standard. This is in contrast to chronic KCl treatment that increases the expression of the α7 subunit RNA to 137% above control levels of expression. Nicotinic agonist and KCl treatment both upregulate [^{125}I]-α-bgt binding in SH-SY5Y cells; the increase in α7 RNA observed after KCl treatment but not after nicotinic agonist treatment suggests that KCl-evokes upregulation of putative α7* nAChR by increased transcription of α7 subunit RNA.

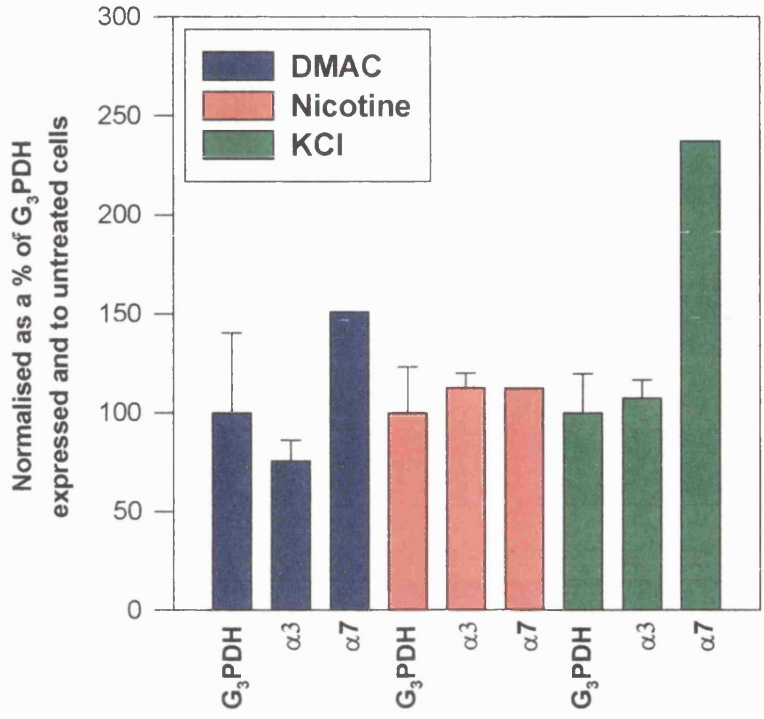

Figure 3.18. Level of expression of G_3PDH, α3 and α7 total RNA extracted from SH-SY5Y cells relative to control untreated cells. *Amounts of α3 and α7 subunit total RNA were measured from SH-SY5Y cells that had been treated with DMAC (10 μM), nicotine (10 μM), KCl (20 mM) or no drugs for control (not shown but are expressed as 100%), using Northern blot analysis. Each set of blots was used to quantify the level of nAChR subunit expression by scanning the autoradiographs and normalisation to the expression of G_3PDH as an internal standard control in each of the drug treated conditions relative to control (100%). Values for G_3PDH and α3 are the mean ± S.E.M. from at least 3 independent sets of total RNA and the α7 data are from 1 set of total RNA.*

Section 3: Visualisation of α3 and α7* nAChR subunits in SH-SY5Y cells.*

3.14. Introduction.

So far this Chapter has described data revealing that α3* and α7* nAChR are upregulated in SH-SY5Y cells by different chronic drug treatments and by different cellular mechanisms. This section will describe experiments that use specific antibodies and confocal microscopy to identify populations of α3 and α7 nAChR subunits in both control and drug treated SH-SY5Y cells. The aim was to elucidate whether the distribution of these α3 and α7 nAChR subunits is altered after chronic drug treatment compared with control untreated conditions. Confocal microscopy as a technique is briefly introduced in section 3.14.2.

3.14.1. nAChR subunit composition and monoclonal antibodies to nAChR subunits:

The α3 and α7 subunits are of interest to this project because they are definitive of α3* and α7* nAChR. nAChR containing the α3 subunit are capable of forming receptor complexes in various combinations with β2, β4 and α5 and are found in autonomic ganglia where they play a post-synaptic role (Vernallis *et al.*, 1993; Ullian *et al.*, 1997). The α3 nAChR subunit mRNA can be found in high abundance in the thalamus (e.g. dorsomedial and ventro-posterolateral regions), moderate to low abundance in most cortical regions (e.g. prefrontal, motor, entorhinal, cingular and temporal) and in low levels of expression in the hippocampus, dentate gyrus and

cerebellum in human brain (for review see Paterson and Nordberg, 2000). The α7 subunits usually have an extra- or peri-synaptic location and can be found within the same ganglionic neurones as α3* nAChR (Vernallis *et al.*, 1993; Horch and Sargent, 1995). In human brain, α7 nAChR subunit mRNA can be detected in high abundance in the motor cortex and hippocampus (α7* nAChR are also detected with [^{125}I]-α-bgt, with highest density of binding observed in the hippocampus), moderate abundance in the dentate gyrus, caudate putamen, prefrontal cortex and dorsomedial thalamus, with lower expression in the entorhinal cortex and cerebellum (for review see Paterson and Nordberg, 2000). The SH-SY5Y cell line endogenously expresses both α3 and α7 nAChR subunits and is therefore a useful model cell line to visualise these subunits that are upregulated after chronic drug treatment.

From the sequences of cDNAs encoding nAChR subunits it has been possible to design and synthesise peptides to generate subunit-selective antibodies. These antibodies can be used to identify and investigate various aspects of receptor structure, function, biosynthesis and their general pharmacological characterisation (Lindstrom, 1986; Whiting *et al.*, 1987). Other advantages of antibodies include their ability to identify novel ligand binding sites and the orientation of the subunits within the nAChR complex (Beroukhim and Unwin, 1995). Antibodies may not possess all of the desired properties even if they are binding at the correct subunit, for example they may not cross-react with nAChR from the desired species of interest. There is also a problem if the antibody only binds to the native receptor subunit or to the denatured receptor subunit. More problems can still arise when the correct antibody is used in the correct species, if the procedure for preparing and fixing of the tissue is too harsh and leads to either the destruction of the epitope or creates an environment that is inaccessible for histological localisation. Usually when the correct antibody has been produced, is used

in the correct species with an optimised fixation protocol, the immunoaffinity purification and quantitation of nAChR (Peng *et al.*, 1994b), or other receptors of interest, can be identified.

The binding sites for the endogenous nAChR ligand, ACh, are thought to be at the interfaces of specific subunits, one always being the α subunit (Karlin and Akabas, 1995; see section 1.2). Antibodies have been synthesised to distinguish between the two ACh binding sites located on the muscle nAChR (Mihovilovic and Richman, 1987). The different conformational transitions of α subunits can be detected by their ability to bind a conformation-dependent monoclonal antibody (mAb) directed at the main immunogenic region (MIR), e.g. mAb 35, or the ability to bind α-bgt with moderate affinity. Antibodies that bind to the extracellular surface of the α subunit usually do not interfere with the functional properties of the nAChR, however, function can be inhibited if antibodies bind to sites which are at or near to the ACh binding site (Lindstrom, 1986). An antibody capable of exhibiting high affinity and specificity to only one type of nAChR subunit is ideal as a biochemical probe as it will reliably detect the subunit under investigation without cross reacting with other nAChR subunits. To date there are still some nAChR subunits to which there are no specific antibodies available. However, the resulting subunit specific antibodies that have been generated are extremely powerful tools suitable as biochemical probes for the detection of nAChR located in the CNS and are able to reveal structural information about receptor stoichiometry, synthesis and assembly *in vitro*.

3.14.2. Fluorescent immunostaining and the scanning laser confocal microscope:

The confocal microscope can accommodate light sources of different wavelengths and is capable of exciting a vast range of fluorophores that can be used to probe various cell lines or larger whole tissue specimens. The confocal microscope used in this study (Zeiss LSM 510) uses a laser beam as the light illumination source used to scan the specimen under investigation. There is a variety of commonly used sources of excitation for the confocal laser scanning microscope (CLSM) system including, argon (Ar; 488 nm and 514 nm), krypton (Kr; 568 nm), argon-krypton (Ar-Kr; 488 nm, 514 nm and 568 nm) and helium-neon (He-Ne; 633 nm) (Dailey *et al.*, 1999).

This study uses the technique of fluorescent immunostaining using the specificity of antibodies (mAbs and polyclonal antibodies) in conjunction with the CLSM to visualise various nAChR subunits present in SH-SY5Y cells. Recent developments have led to the production of a plethora of specific probes that allow for specific nAChR subunits to be labelled. The fluorescent dye fluorescein isothiocyanate (FITC) (a standard green dye) is excited by argon laser radiation at a wavelength of 488 nm, emits green light and can be used as a secondary antibody in the detection process of particular nAChR subunits. The CLSM is a useful instrument to use for the visualisation of surface and cellular components in 3-D. By means of using CLSM and fluorescent probes to identify subcellular structures in living cells. However, prolonged exposure of the specimen to any form of laser radiation can result in the phenomenon of photobleaching of the fluorescent secondary antibody used.

The conventional light microscope is often used to visualise living cells dynamically *in situ* in culture. Problems arise with epi-fluorescence, as there is often background fluorescence glowing from structures present above and below the optical plane of interest and therefore obscures and visually impairs much relevant morphology of

biological structures, particularly in multicellular specimens due to out-of-focus signals. When using the light microscope vital areas of interest can be obscured, predominantly when examining thick specimens, and therefore lacks the ability to generate much of the ultrastructural and out-of-focus information, except when working with cells which have a flattened appearance (White *et al.*, 1987; Shotton, 1989). This is also a disadvantage when using transmission electron microscopy (EM) which is capable of producing 2-dimensional (2-D) images of cut sections that have been subjected to fixation. The preparation and fixation procedures during the production of serial sections can damage living cells as well as extremely laborious.

The confocal microscope is a powerful new imaging tool equipped with either a scanning laser or stage that has been developed to circumvate previous technical complications with out-of-focus blur (Shotton, 1989; Paddock, 1999). This technique offers several advantages and improvements over both the conventional light microscope and EM equivalents. It is a solution to their problems by providing high contrast and improved clarity when optically sectioning and viewing both living and fixed thick specimens (White *et al.*, 1987). This technique has new prospects to elucidate morphological and spatial characteristics of cell structure, physiological properties occurring within cell in culture, processes occurring within various intact biological tissue specimens in their native tissue environment in 3-D, details that have previously been difficult to detect.

The confocal microscope has an exceptionally shallow depth of field. This property enables detailed and direct optical sections of between 0.5-1.5 μm in thickness to be obtained rather than an overall image of the entire specimen under investigation as is obtained when viewed under a conventional equivalent light microscope (Wright and Schatten, 1991). The confocal instrument used in this series of experiments (Zeiss LSM

510 confocal microscope (Oberkochen, Germany) is comprised of a finely focused light source (a moving laser beam) capable of scanning the SH-SY5Y cells under investigation. The laser travels through a pin hole located in front of the photodetector which aids in the elimination out-of-focus blurred data with the help of a small aperture located to the front of the photodetector (Wright and Schattan, 1991) (Figure 3.19). The resulting images have greater resolution and produce improved epi-fluorescent images when compared to images with a high level of background non-specific staining produced by a conventional microscope (White *et al.*, 1987).

This imaging technique relies on its ability to reject out-of-focus light. This property leads to an increase in the signal-to-noise ratio and results in the production of sharp, high-contrast images of cells and their subcellular components (even within relatively thick samples) (Brakenhoff *et al.*, 1985; Shotton, 1989; Dailey *et al.*, 1999). Confocal images have a depth discriminated fluorescence image that has high spatial resolution compared to using a standard epi-fluorescence microscope. The depth is created from a series of captured 2-D optical images obtained by scanning the specimen point-by-point with a laser beam from successively different levels of depth of focus, also known as a Z-series.

Non-invasive optical sections obtained with the confocal approach are captured from scanning in a series of different optical sections obtained from different focal planes (the X-Y plane and also vertically in the X-Z plane; this enables depth (Z-axis) and lateral (X-axis) scanning to be obtained) (Wright and Schatten, 1991). These series of optical sections can be collected, combined and used to reconstruct orthogonal images that yield information on the final dynamic 3-D cryoarchitectural image of structures under investigation.

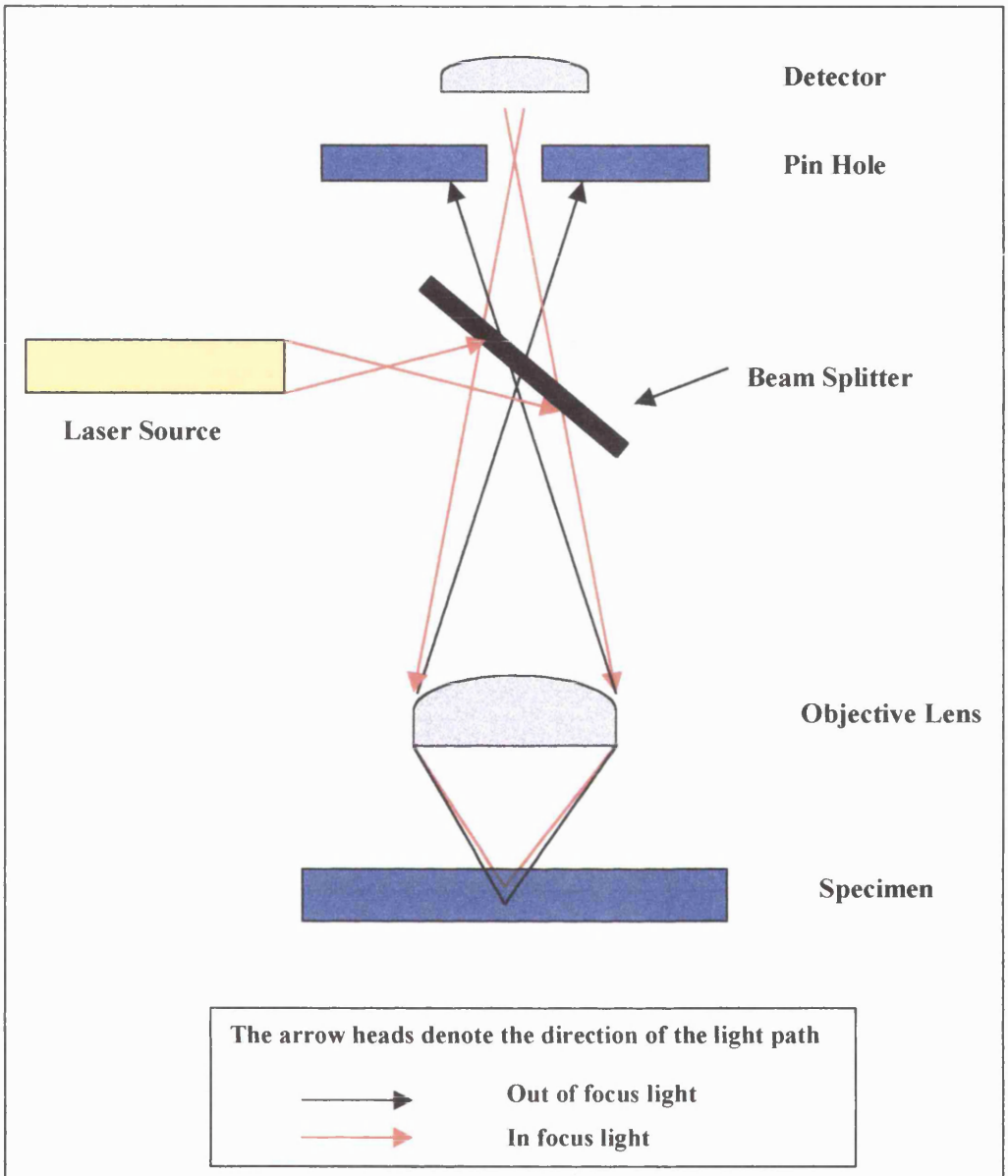

Figure 3.19. Diagram to illustrate the essential components of a confocal laser scanning microscope (modified from Shotton, 1989).

Recent technological advances in computer systems allow for rapid image acquisition times, processing, storage and manipulation of the scanned image data, which in the past has been difficult to obtain from biological specimens. The clarity of the images produced, provide an exciting and powerful insight into the topology of cellular

structure, tissue organisation and functional properties due to the reduction of 3-D point spread by the unique optical sectioning of the CLSM.

3.15. Aims:

The aim of this section is to undertake a preliminary investigation into the intracellular localisation of α3 and α7 nAChR subunits in control untreated SH-SY5Y cells and following nAChR upregulation by chronic treatment with either nicotinic agonists (nicotine and DMAC) or KCl depolarisation. This will show whether upregulation of nAChR evoked by these drug treatments results in an increase of intracellular receptor subunits and whether these subunits are in diffuse or punctate populations.

3.16. Methods.

3.16.1. Cell culture: maintenance of SH-SY5Y cells:

SH-SY5Y cells were routinely cultured and maintained as described in section 3.3.2. Cells for confocal microscopy were seeded at a density of 5 x 10^5 cells/cm^2 onto sterile 2 cm^2 glass coverslips in 200 µl volumes. After 90 min to ensure attachment of the cells to the coverslips, prewarmed medium was added to a volume of 3 ml to each of the coverslips in well areas of a 6 well cell culture plate.

3.16.1.1. Chronic drug treatment to SH-SY5Y cells:

After 24 h, maintenance medium was gently aspirated from the SH-SY5Y cells grown on coverslips and replaced by either 3 ml maintenance medium (control) or this medium containing either nicotine (10 μM), DMAC (10 μM) or KCl (20 mM) for drug treated conditions (see section 2.4.2). Cells were maintained at 37°C in 5% CO_2/humidified air for a further 4 days before preparation for confocal microscopy. After 4 days incubation, drugs were removed by washing four times with warm medium over a 30 min period. Medium was removed from the cells and replaced by 1 ml warm sterile PBS, before proceeding to the immunostaining method (see section 3.16.3). Control sister cultures of SH-SY5Y cells were cultured in parallel for 4 days prior to staining and visualisation.

3.16.2. Antibodies:

Primary antibodies were as follows: α3 nAChR subunit specific Sc-1771 goat polyclonal IgG, stored as a stock of 200 μg/ml at 4°C, from Santa Cruz Biotechnology, (Santa Cruz, CA.) and used in a 1/200 dilution; α7 nAChR subunit specific mAb 306 was a generous gift donated by Dr. Jon Lindstrom (Dept. of Neuroscience, University of Pennsylvania Med. Sch., Philadelphia, PE, USA), it was stored at -20°C and used in a dilution of 1/1000.

Secondary antibodies were as follows: for α3 nAChR subunit detection, either biotinylated rabbit anti-goat IgG (H+L) affinity purified (1:200 dilution from stock kept at 4°C) then FITC-labelled streptavidin as a tertiary label was used in a dilution of 1:500 or an anti-goat IgG FITC labelled antibody was used. The secondary antibodies used for

α3 detection were purchased from Vectorlabs., (Peterborough, U.K.) The secondary antibody used in the detection of α7 nAChR subunits was a horse anti-mouse IgG (H+L), FITC labelled, rat absorbed affinity purified antibody (1:50 dilution), also purchased from Vectorlabs., (Peterborough, U.K.)

3.16.3. Immunofluorescence labelling of α3 and α7 nAChR subunits in SH-SY5Y cells:

The immunostaining procedure was adapted from Maimone and Merlie (1993). In brief, glass coverslips with adherent SH-SY5Y cells were transferred to individual wells of a 6 well plate and washed with 1 ml of warm PBS before incubating with 1 ml of fixative solution (1% paraformaldehyde, L-lysine (100 mM), sodium metaperiodate (10 mM), and 0.1% saponin in PBS) for 20 min at room temperature. The cells were then rinsed with PBS and permeabilised for 10 min in 1 % Triton X-100 in PBS (La Rochelle *et al.*, 1989) before being washed x 3 in PBS and immediately immunostained as follows.

The cells were initially blocked in 10% FCS (diluted in PBS) for 30 min prior to immunostaining. For staining, the coverslips were inverted (so that the cells were on the under surface) onto 100 µl drops of the primary antibody solution (placed on a piece of parafilm) for either α3 or α7 subunits (1:200 and 1:1000 dilutions respectively in 10% FCS in PBS for 2 h in humid conditions at room temperature (see Figure 3.20). Any unbound primary antibody was rinsed from the cells by placing the coverslips in fresh 6 well culture plates and washing x 3 by 5 min washes in PBS.

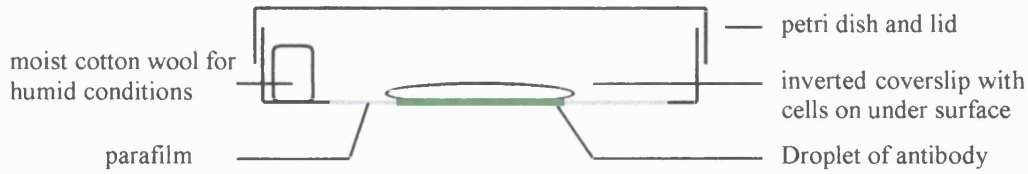

Figure 3.20. Schematic representation of single fluorescence labelling of SH-SY5Y cells. *SH-SY5Y cells were grown to confluency on glass coverslips in 6 well culture plates before chronically treating for 4 days with nicotine (10 μM), DMAC (10 μM) or KCl (20 mM). The cells were fixed and permeabilised before labelling for α3 or α7 nAChR subunits. Coverslips were inverted onto droplets of antibody before washing and mounting with vectashield on glass slides. Negative controls were incubated in parallel, on sister cultures of SH-SY5Y cells, they were incubated in blocking solution before proceeding to incubation with secondary antibody.*

The bound antibody was detected by incubation with a relevant fluorescently labelled secondary antibody by inverting the coverslip onto 100 μl drops of this secondary antibody solution. For α3 subunit detection, incubation was with a biotinylated goat anti-rabbit IgG (stock diluted 1:200 in 10% FCS in PBS; 1 h at room temperature). The coverslips were washed x 3 by 5 min washes in PBS before inverting coverslips for a further hour, at room temperature in the dark on 100 μl drops of FITC-labelled streptavidin as a tertiary label. After incubation with the primary α3 antibody, detection was also performed with a secondary anti-goat IgG FITC labelled antibody (stock diluted 1:200 in 10% FCS in PBS; 1 h at room temperature) to try to decrease background staining found with FITC-labelled strepavidin. For secondary α7 subunit detection, incubation was with an anti-mouse IgG FITC labelled antibody (stock diluted 1:50 in 10% FCS in PBS). The cells were incubated with the secondary antibody at room temperature, in dark (in the case of FITC), humid conditions. After 1 h the

coverslips were washed x 3 by 5 min washes in PBS to remove excess secondary fluorescence tag and then briefly in distilled water before being mounted in Vectashield on clean glass microscope slides, sealed with nail varnish and stored at 4°C in the dark until ready for visualisation under the CLSM. Negative controls were set up in parallel with cells treated chronically with drugs. On the day of labelling, the cells were incubated with 10% FCS (instead of primary antibody) and stained with a single secondary antibody. This was to make sure that the secondary antibody did not produce a fluorescence signal on its own.

3.16.3.1. Confocal protocol:

Prepared SH-SY5Y cells were visualised using a Zeiss LSM 510 confocal microscope (Oberkochen, Germany) equipped with an argon-krypton mixed gas laser (488 nm wavelength) for detection of FITC labelling and using a 63 x 1.4 differential interference contrast (DIC) oil objective lens. The images collected and recorded were processed using Adobe Photoshop 3.0 (Adobe Systems, Mountain View, CA, USA).

3.17. Results.

3.17.1. SH-SY5Y cell morphology:

The images obtained from confocal microscopy provide details of the SH-SY5Y cell line morphology: images illustrate the flattened, ovoid morphology of SH-SY5Y cells that have been in culture for approximately 5 days. It can be observed that the cells project processes that form contacts with neighbouring cells. There is considerable morphological homogeneity within the population of SH-SY5Y cells stained in each of

the panels shown in Figs. 3.21, 3.23 and 3.25. All of the cells used in this preliminary immunofluorescence investigation into the localisation of α3 and α7 nAChR subunits were fixed and permeabilised, because the primary antibodies used recognised intracellular epitopes. This enables an analysis of total intracellular located receptor subunits to be visualised.

3.17.2. Immunolabelling of nAChR α3 subunits in control and drug treated cells:

The α3 specific goat polyclonal antibody Sc-1771 was used to label the intracellular distribution of α3 nAChR subunits in permeabilised SH-SY5Y cells. These experiments were performed to visualise the location of the α3 nAChR subunits and also to identify whether there was a change in expression after the nicotinic agonist-evoked upregulation. The negative control immunolabelling confocal pictures obtained and presented in Figure 3.21a and b have a filamentous background staining. These cells were only labelled with a secondary antibody and tertiary FITC-labelled strepavidin. This staining may be representative of biotin binding to an intracellular structure detected with the FITC-labelled strepavidin. These results should be viewed with caution due to the filamentous background staining with biotin making detection of the α3 nAChR subunit difficult.

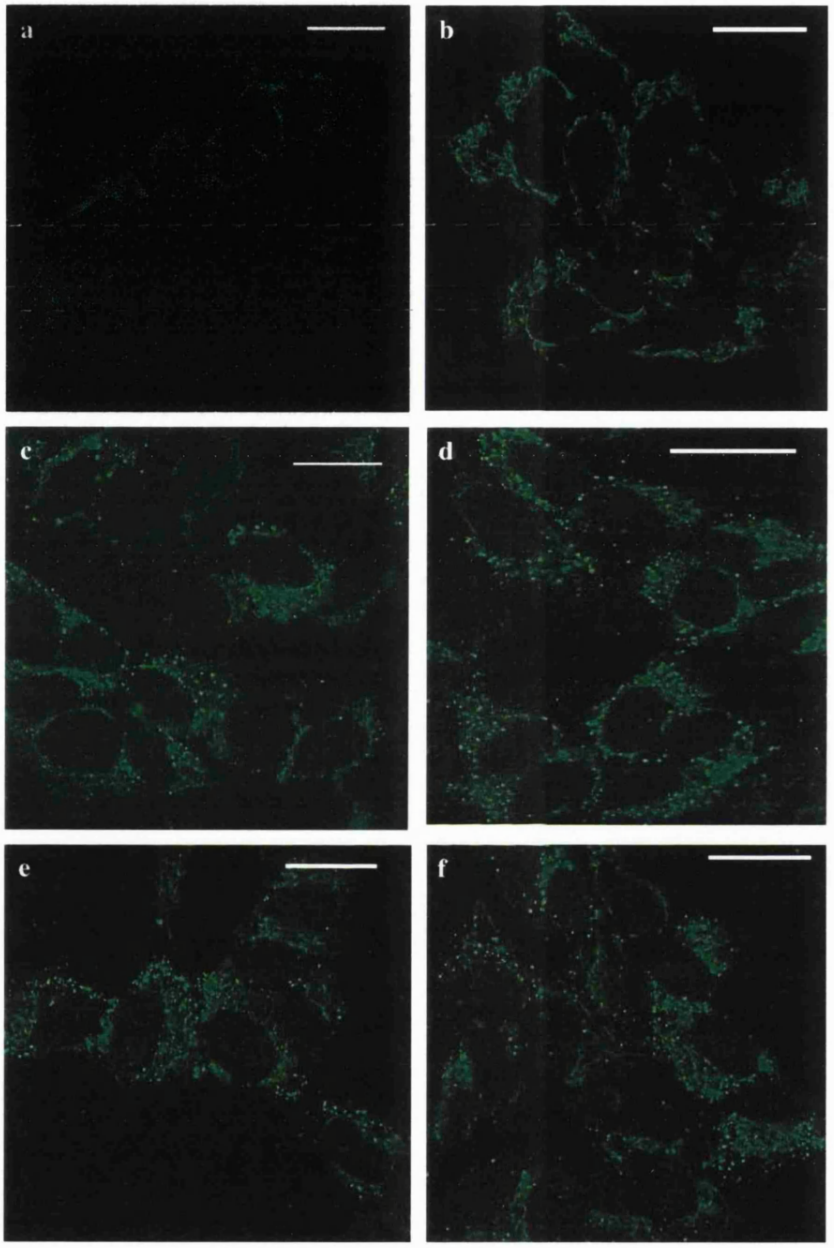

Figure 3.21. Detection of α3 nAChR subunits in the SH-SY5Y cell line. *α3 nAChR subunits were visualised in SH-SY5Y cells in either (c) control, (d) nicotine (10 μM), (e) DMAC (10 μM) or (f) KCl (20 mM) treated cells by immunofluorescent staining of fixed cells with Sc-1771 for 2 h at room temperature followed by a biotinylated antibody and FITC-labelled streptavidin. Panels (a) and (b) are negative controls labelled only with the secondary antibodies. All cells were permeabilised with 1% Triton X-100 for 10 min to visualise total α3 nAChR subunits before labelling with Sc-1771. All scale bars represent 20 μm and representative images are shown.*

Confocal images of SH-SY5Y cells grown under standard control, untreated conditions are shown in Figure 3.21c. The population of SH-SY5Y cells is heterogeneous with respect to their expression of the α3 nAChR subunit, intracellular fluorescence is relatively widespread throughout the cytoplasm with some cells clearly expressing more α3 subunits than others. In control conditions (Figure 3.21c) the FITC-labelled strepavidin binding to the α3 nAChR subunit primarily has an intracellular location with fluorescence surrounding the nucleus. The staining pattern of the α3 subunit is hard to recognise due to the background filamentous staining but appears punctate and heterogenous.

Section 1 described how nicotinic agonist treatment but not KCl depolarisation for 4 days upregulated α3* nAChR, detected by significant increases in [^{3}H]-epibatidine binding from control. Cultured cells were exposed to chronic nicotinic agonist treatment with either 10 μM nicotine (Figure 3.21d) or 10 μM DMAC (Figure 3.21e) for 4 days before fixation, permeabilisation and immunolabelling for the α3 subunit. In these agonist treated cultures there seems to be a slightly greater proportion of staining of the α3 nAChR subunit within the cytoplasm surrounding the nucleus and also extending into the cytoplasmic projections. Cultures chronically treated with a depolarising concentration of KCl (20 mM) appear to have α3 subunit labelling similar to control conditions with fluorescence staining not as intense as that found in nicotinic agonist treated cells. In all of the panels observed in Figure 3.21 the labelling of surface α3 nAChR subunits is difficult to distinguish, due to the α3 primary polyclonal Ab recognising an intracellular portion of the α3 nAChR subunit.

The non-specific filamentous background fluorescence obtained with the negative controls presented in Figure 3.21, led to further experiments performed with the primary

α3 polyclonal antibody but using an anti-goat IgG FITC labelled secondary antibody to try to reduce background staining. Representative negative controls for control, nicotine (10 μM), DMAC (10 μM) and KCl (20 mM) treated SH-SY5Y cells are shown in Figure 3.22a-d respectively.

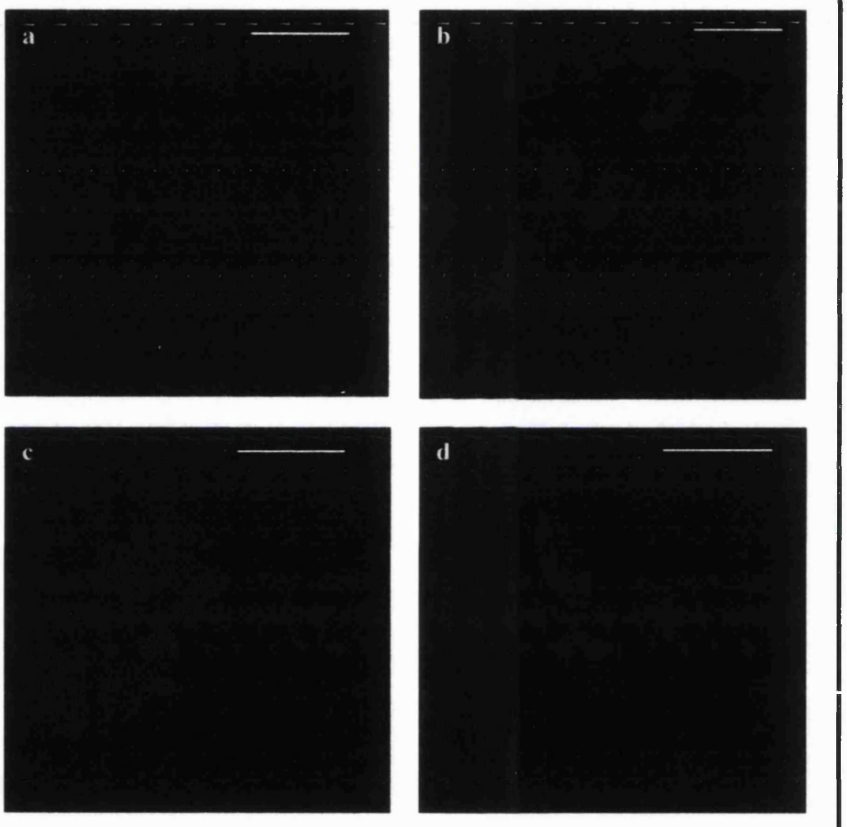

Figure 3.22. Representative negative control staining for α3 nAChR subunit localisation in the SH-SY5Y cell line. *(a) Control, (b) nicotine (10 μM), (c) DMAC (10 μM) or (d) KCl (20 mM) treated SH-SY5Y cells were visualised after immunofluorescent staining of fixed cells with blocking solution for 2 h at room temperature followed by an anti-goat IgG FITC labelled antibody. All cells were permeabilised with 1% Triton X-100 for 10 min before initial blocking stage. All scale bars represent 20 μm.*

The images produced for negative controls using the FITC labelled secondary antibody alone to control or drug treated SH-SY5Y cells showed low non-specific background

staining, facilitating the detection of the specific α3 nAChR subunit fluorescence signal (Figure 3.23a-d).

Figure 3.23 shows populations of SH-SY5Y cells expressing the α3 nAChR subunit at different levels with some cells expressing little α3 nAChR subunit. In control cultures (Figure 3.23a), the α3 subunit has a widespread intracellular location within the cytoplasm with some cells showing more intense fluorescence. The staining patterns of the α3 nAChR subunit appear to be punctate and the majority of α3 subunit staining is roughly spherical in shape. The effect of 4 day treatment with either 10 μM nicotine (Figure 3.23b) or 10 μM DMAC (Figure 3.23c) on α3 subunit distribution in cultured cells, produces a greater intensity of fluorescence. This is particularly evident in the nicotine treated cells where the staining of α3 nAChR subunits is punctate in small discrete spherical compartments scattered asymmetrically throughout the cell cytoplasm, in the cytoplasmic extensions as well as surrounding the nucleus of the cell and on the cell surface/or close to the cell surface. KCl treated cultures (Figure 3.23d), show fluorescence staining of the α3 nAChR at levels of expression similar to control untreated SH-SY5Y cell cultures.

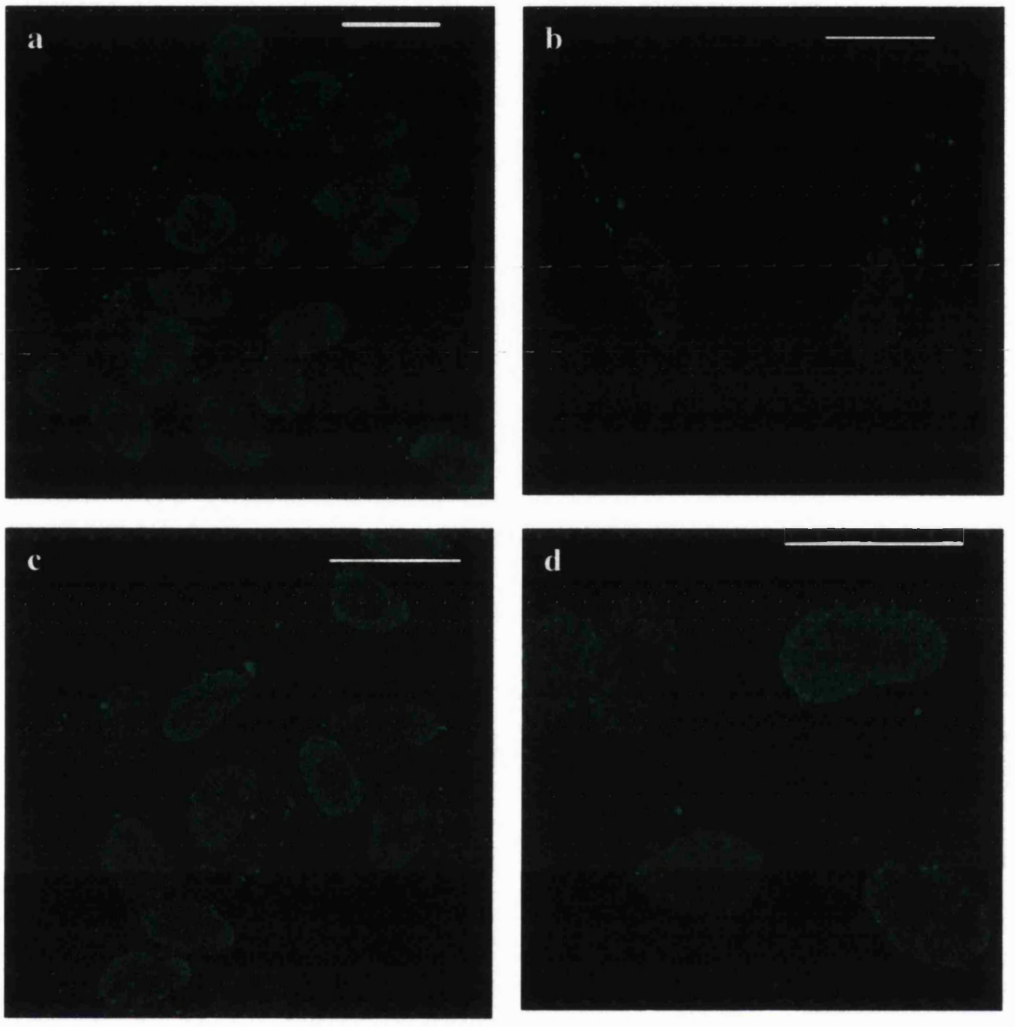

Figure 3.23. α3 nAChR subunit localisation in the SH-SY5Y cell line. *α3 nAChR subunits were visualised in SH-SY5Y cells in either (a) control, (b) nicotine (10 μM), (c) DMAC (10 μM) or (d) KCl (20 mM) treated cells by immunofluorescent staining of fixed cells with Sc-1771 for 2 h at room temperature followed by an anti-goat IgG FITC labelled antibody. All cells were permeabilised with 1% Triton X-100 for 10 min to visualise total α3 nAChR subunits before labelling with Sc-1771. All scale bars represent 20 μm.*

3.17.3. Distribution of α7 nAChR subunits in control and drug treated cells:

The cellular distribution of α7 nAChR subunits in cells under control, untreated and upregulated conditions was investigated by immunocytochemical detection with the α7 nAChR subunit specific primary mAb 306 and secondary labelling with a FITC-labelled antibody. Figure 3.24 and 3.25 represent negative controls and positive staining respectively. The cells visualised in Figure 3.24 were not incubated with the primary mAb 306, but instead were incubated with blocking solution and then with the secondary anti-goat IgG FITC-labelled antibody, identifying low non-specific fluorescence that subsequently did not interfere with specific α7 nAChR subunit detection (Figure 3.25).

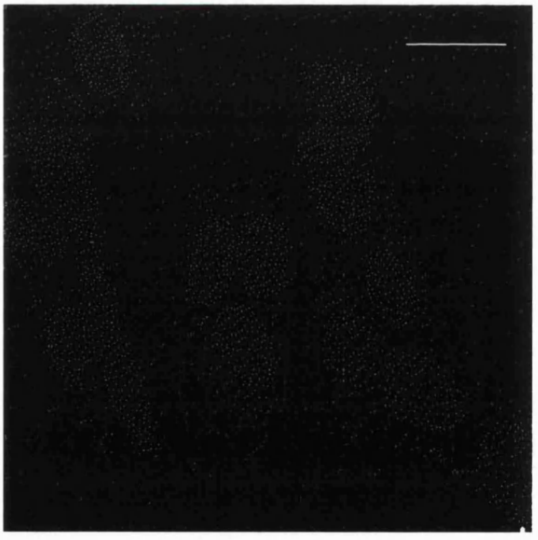

Figure 3.24. Representative negative control staining for α7 nAChR subunit localisation in the SH-SY5Y cell line. *SH-SY5Y cells were permeabilised with 1% Triton X-100 for 10 min before incubation with blocking solution for 2 h at room temperature followed by an anti-mouse IgG FITC labelled antibody before visualising. All scale bars represent 20 μm.*

Figure 3.25 shows α7 nAChR subunit staining in control, untreated cells or cells that had been treated chronically for 4 days with either 10 μM nicotine, 10 μM DMAC or (20 mM) KCl represented in Figure 3.25a-d respectively. The population of control,

untreated SH-SY5Y cells are homogeneous with respect to their expression of the α7 nAChR subunit (Figure 3.25a). The distribution of fluorescence for α7 nAChR subunits in control cells appears to be predominantly intracellular in the cytoplasm and cytoplasmic projections with little surface labelling. Staining is punctate in nature and uniform in the nuclear region/or over the nucleus in control SH-SY5Y cell populations.

SH-SY5Y cells treated with nicotine for 4 days have predominant intracellular α7 nAChR subunit staining, with fluorescence being uniform throughout the cytoplasm (Figure 3.25b). In DMAC treated cells (Figure 3.25c), there is a greater intensity of staining for the α7 nAChR subunit compared to control, untreated cultures. Staining is again predominantly intracellular with fluorescence observed in the cytoplasm and cytoplasmic extensions. Figure 3.25d shows cells treated with KCl for 4 days prior to immunolabelling with the specific α7 nAChR subunit mAb 306. Staining of α7 nAChR subunits was found to be intracellular and asymmetrically located around the cell nucleus. The staining of KCl treated cells appears to be less intense than that observed in control or nicotinic agonist treated SH-SY5Y cells. A reason for this could be attributed to photobleaching due to the longer time taken to locate a population of cells. KCl may predominantly upregulate surface α7 nAChR subunits which are not distinguished by mAb 306 binding in permeabilised cells.

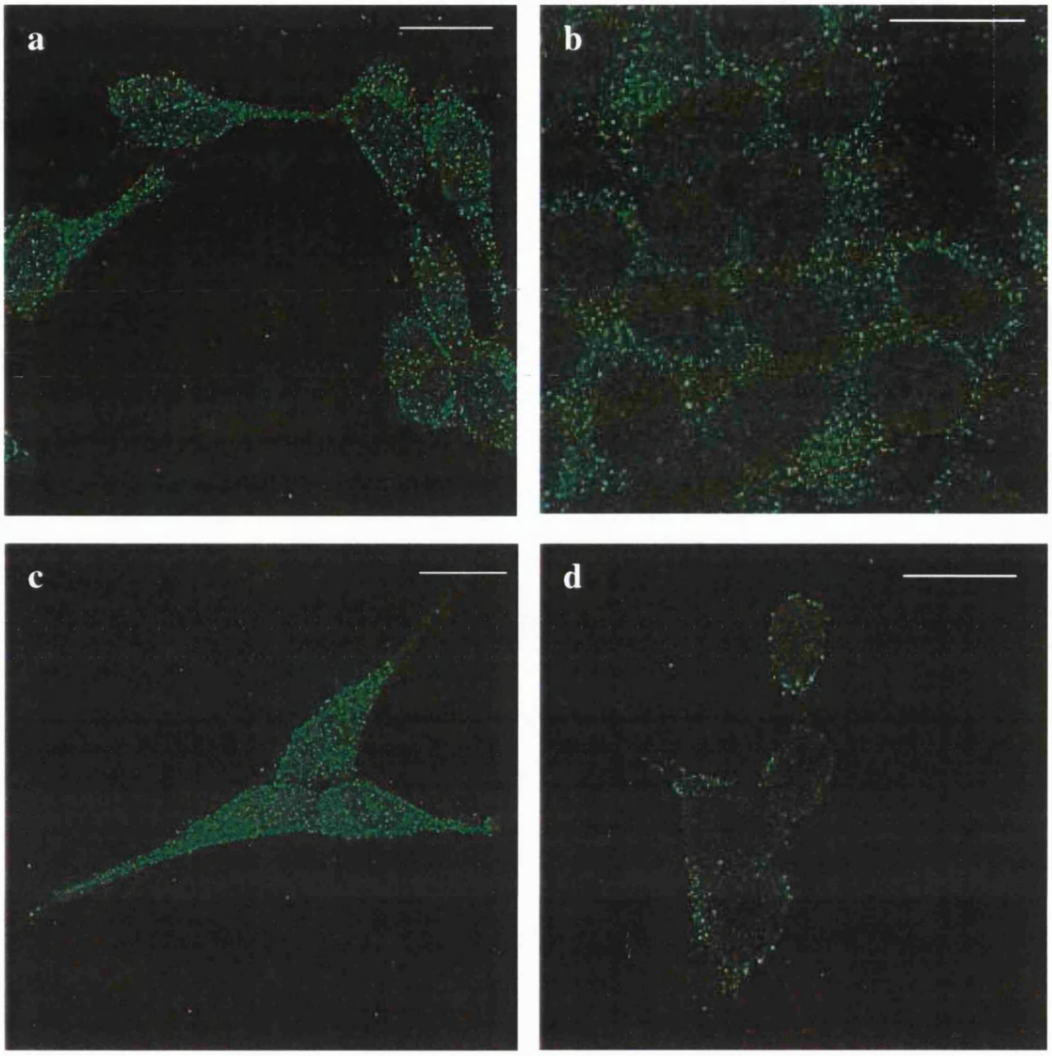

Figure 3.25. α7 nAChR subunit localisation in the SH-SY5Y cell line. *α7 nAChR subunits were visualised in SH-SY5Y cells in either (a) control, (b) nicotine (10 μM), (c)DMAC (10 μM) or (d) KCl (20 mM) treated cells by immunofluorescent staining of fixed cells with mAb 306 for 2 hr at room temperature followed by an anti-mouse IgG FITC labelled antibody. All cells were permeabilised with 1% Triton X-100 for 10 min to visualise total α7 nAChR subunits before labelling with mAb 306. Scale bars represent 20 μm.*

If time had permitted, this preliminary investigation into the visualisation of α3 and α7 nAChR subunits in SH-SY5Y cells would have been followed by optimising the conditions used in the labelling protocol. It would be desirable to also detect surface

labelling of α3 and α7 nAChR subunits, but this would require different antibodies that recognise extracellular epitopes or using non-permeabilised cells in the protocol. Surface versus intracellular staining could be compared in control and drug treated SH-SY5Y cells.

It must be emphasised that the findings from this confocal microscopy study are preliminary. This confocal study has implicated that there are changes in the cellular location and intensity of staining of α3 and α7 nAChR subunits after drug treatments that evoke upregulation of nAChR subunits. It must be emphasised that the results relate to the immunolabelling of α3 and α7 nAChR subunits detected in the form of both unassembled and assembled nAChR complexes.

Section IV: Discussion of results.

This Chapter has investigated drug treatments that influence the expression of α3* and α7* nAChR in SH-SY5Y cells grown in culture. Novel findings reveal that the nAChR subunits under investigation were differentially regulated by different chronic drug treatments and that these drug treatments produced upregulation of the nAChR subunits by different cellular mechanisms.

Upregulation of nAChR after prolonged agonist treatment appears to contradict the paradigm that chronic agonist exposure results in receptor down regulation while long term exposure to antagonists elicit receptor upregulation (for review, see Creese and Sibley, 1980). Previous studies have shown that the concentration of nicotine required to evoke upregulation of either α3* and α7* nAChR was higher than those required to elicit upregulation of the α4β2 nAChR complex (Peng *et al.*, 1997; Wang *et al.*, 1998). Concentration-response analyses have shown that nicotine concentrations from between 10 μM and 1 mM were required to promote significant upregulation of either [^{3}H]-epibatidine (Wang *et al.*, 1998) or [^{125}I]-α-bgt binding sites in SH-SY5Y cells (Peng *et al.*, 1997) or HEK-293 cells transfected with human α7 neuronal nAChR subunits (Molinari *et al.*, 1998). The requirement for these greater concentrations of nicotine to evoke upregulation of α3* and α7* nAChR, compared to the α4β2 nAChR, is probably due to their lower affinity for nicotine. In the present study by using [^{3}H]-epibatidine and [^{125}I]-α-bgt binding to SH-SY5Y cells to label and α3* and α7* nAChR respectively, a comparison could be made between 1) the ability of different drug treatments to alter the binding sites detected by these radiolabelled compounds and 2) between the [^{125}I]-α-bgt binding data obtained from primary hippocampal and SH-SY5Y cell cultures.

3.18. Upregulation of [^{125}I]-α-bgt binding sites in SH-SY5Y cells:

To demonstrate whether upregulation of [^{125}I]-α-bgt binding sites was evoked in SH-SY5Y cells, different chronic drug treatments previously shown to evoke upregulation of [^{125}I]-α-bgt binding sites in primary hippocampal cultures (see section 2.7.2) were applied to SH-SY5Y cells grown in culture. The extent of upregulation of [^{125}I]-α-bgt binding sites, above control levels, in SH-SY5Y cell cultures induced by 20 mM KCl (51 ± 10%) and the nicotinic agonists nicotine (10 μM; 37 ± 5%) and DMAC (10 μM; 20 ± 6%) are reminiscent of the increases observed in rat primary hippocampal neuronal cultures after chronic treatment with these drugs (see section 2.7.2.1). The magnitude of upregulation evoked by nicotine is in agreement with a recent report where the level of α7* nAChR expression in SH-SY5Y cells was increased by approximately 30% using a higher concentration of nicotine at 1 mM for 4 days (Peng *et al.*, 1997). These data indicate that the SH-SY5Y neuroblastoma cell line is a valid model for the study of upregulation of nAChR and the cellular mechanisms underlying this phenomenon.

Previous investigations examined the effect of other activator ligands such as DMPP (see section 2.8.1), GTS-21 and (±)-epibatidine, to determine whether the phenomenon of upregulation was unique to nicotine (Molinari *et al.*, 1998). These compounds were also found to produce a concentration-dependent upregulation of [^{125}I]-α-bgt binding sites above control levels in α7 transfected HEK-293 cells (Molinari *et al.*, 1998). The present study did not encompass the effect of antagonists, however previously antagonists have been reported to upregulate α7 nAChR in cultured cells. Molinari *et al.* (1998) observed that the α7 nAChR antagonist MLA promoted a concentration-dependent upregulation of [^{125}I]-α-bgt binding sites in HEK-293 cells transfected with human α7 subunits.

The novel α7 selective antagonist MLA, was made available to us in the tritiated form and it was decided to perform saturation analysis of [^{3}H]-MLA binding to SH-SY5Y membrane preparations. The data revealed that nicotine-induced and KCl-evoked increases in α7* nAChR result from an increase in the amount of α7 binding sites rather than from an increase in the affinity of α7* nAChR for nicotine (Table 3.2). This agrees with previous data reported for nicotine-evoked upregulation of the α7* nAChR in SH-SY5Y cells and HEK-293 cells (Peng *et al.*, 1997; Molinari *et al.*, 1998). In the present study there appears to be one class of [^{3}H]-MLA binding site in SH-SY5Y cells (K_D = 3 nM with a respective B_{max} value of 28.0 fmol [^{3}H]-MLA bound/mg protein) (Table 3.2). These values are in close accordance with respective B_{max} value of 25.6 fmol [^{125}I]-α-bgt bound/mg protein reported by Lukas *et al.* (1993) for [^{125}I]-α-bgt binding to SH-SY5Y cell membrane preparations. The site labelled both on the surface and intracellularly in the present study by [^{3}H]-MLA probably reflects the same site labelled with [^{125}I]-α-bgt on the cell surface (Lukas *et al.*, 1993) and identifies the putative homomeric α7* nAChR.

Preliminary confocal analysis was used in the present study to label the α7 nAChR subunits with the α7 nAChR subunit specific mAb, mAb 306 that specifically binds to the intracellular portion of the loop between TM3 and TM4 of the α7 nAChR subunit. The fluorescence observed in control and drug treated cells was predominantly of α7 subunits located within the cell cytoplasm where they would be non-functional and not detected by [^{125}I]-α-bgt binding assays *in situ*. Chronic treatment with DMAC for 4 days produced the greatest intensity of intracellular labelling of the α7 subunit, followed by nicotine and KCl depolarisation. This is the opposite order compared to their ability to upregulate surface α7* nAChR detected with [^{125}I]-α-bgt binding. It would be of

interest to compare intracellular to surface staining to identify if these chronic drug treatments upregulate surface α7 subunits to a similar extent as observed in binding studies. This could be achieved by using non-permeabilised cells and labelling them with rhodamine labelled α-bgt to identify surface α7 subunits. This would identify whether KCl upregulates surface α7 nAChR subunits in preference to intracellular α7 subunits and would also enable comparisons to be drawn with nicotinic agonist-evoked upregulation of surface versus intracellular subunit labelling.

The experiments reported in the present study so far have shown that α7* nAChR are upregulated by KCl and nicotinic agonists in SH-SY5Y cells and that these treatments produce an increase in surface [^{125}I]-α-bgt binding sites (B_{max}) with no change in K_D. It was then decided to investigate the mechanisms underlying the process of upregulation of [^{125}I]-α-bgt binding sites evoked by these chronic drug treatments and to elucidate whether Ca^{2+} influx and protein kinase pathways were involved.

3.18.1. Mechanisms of nicotine- and KCl-evoked upregulation of putative α7* nAChR in SH-SY5Y cultures:

De Koninck and Cooper (1995) previously demonstrated that an increase in surface [^{125}I]-α-bgt binding sites evoked by KCl depolarisation (40 mM) was paralleled by an increase in α7-gene expression in sympathetic neurones developing in culture. Further experiments identified an essential role for CaM-kinase II in the induction of the α7 gene (De Koninck and Cooper, 1995). There is a well-established role of sustained Ca^{2+} entry via L-type VOCC and activation of CaM-kinase II in gene activation, via phosphorylation of transcription factors and regulation of immediate early gene transcription (Greenberg *et al.*, 1992). CaM-kinase II is a ubiquitous multifunctional,

cytosolic enzyme activated by signal transduction pathways that result in the elevation of $[Ca^{2+}]_i$ (for review see, Schulman, 1993). This protein kinase is abundant in brain where it is enriched in neurones (Bennett *et al.*, 1983; Ouimet *et al.*, 1984) and has been implicated in diverse cellular functioning. CaM-kinase II has been suggested to have a pivotal role in the regulation of synaptic strength and growth of dendrites (Mayford *et al.*, 1995; Lisman *et al.*, 1997; Wu and Cline, 1998), in the maturation of synapses during development (Wu *et al.*, 1996) and to encode 'memory' in neurones (Lisman, 1985, 1994; Malinow *et al.*, 1988; Silva *et al.*, 1992).

To establish if Ca^{2+} influx and/or the activation of a CaM-kinase II pathway were essential mechanisms underlying nicotinic agonist- or KCl-evoked upregulation of $[^{125}I]$-α-bgt binding sites in SH-SY5Y cells, experiments were performed using the L-type Ca^{2+} channel blocker, verapamil (5 μM) and the potent CaM-kinase II inhibitor KN-62 (5 μM). KN-62 has previously been found to have a K_i value of 0.9 μM for inhibition of CaM-kinase II activity, with inhibition being competitive with respect to calmodulin and hence binding directly to the calmodulin binding site on the enzyme (Tokumisto *et al.*, 1990). Verapamil and KN-62 were found to inhibit KCl-evoked upregulation but had no effect on nicotine-induced upregulation of $[^{125}I]$-α-bgt binding sites. These binding data generated with the SH-SY5Y cell line closely parallel the differential sensitivity of primary hippocampal cultures to verapamil and KN-62. This suggests that the mechanism is common to different types of neurones. Upregulation evoked by nicotine was neither dependent on Ca^{2+} flux through L-type VOCC nor involved a CaM-kinase II pathway, as increases in $[^{125}I]$-α-bgt were maintained in the presence of either verapamil or KN-62. Figure 3.26 summarises these results. These data compliment the data produced by De Koninck and Cooper (1995) in SCG neurones

and provide further support that SH-SY5Y cells are a valid model system to investigate the mechanisms of nAChR upregulation operating in the CNS.

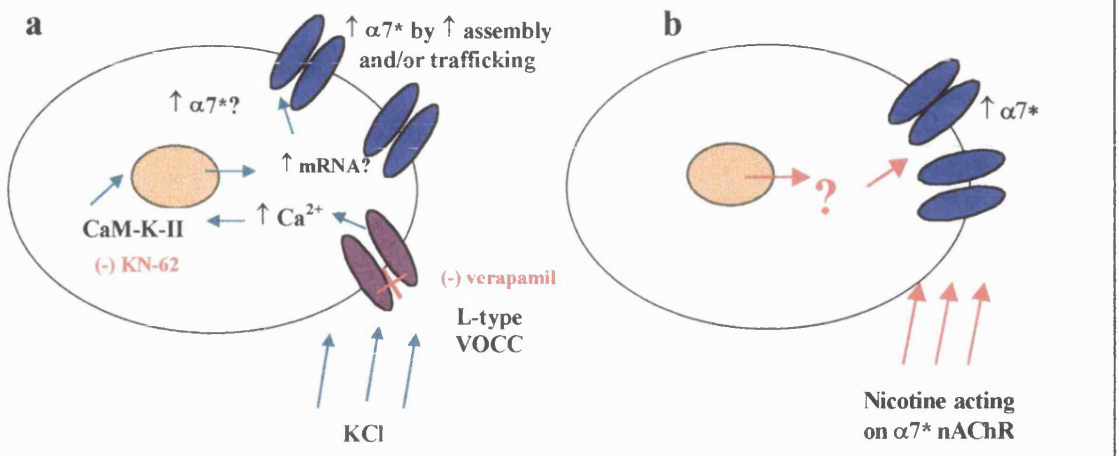

Figure 3.26. A representation of KCl- and nicotinic agonist-evoked upregulation of [^{125}I]-α-bgt binding sites in SH-SY5Y cells. *Chronic treatment of SH-SY5Y cells for 4 days upregulates [^{125}I]-α-bgt binding sites (indicated as receptors on the cell surface) after (a) KCl depolarisation by Ca^{2+} influx through L-type VOCC and by a CaM-kinase II-dependent pathway or (b) Nicotine by a pathway not involving L-type VOCC or CaM-kinase II.*

CaM-kinase II has recently been reported to act as a critical signalling element required to regulate changes in synaptic strength of the density of glutamatergic synapses within the ventral nerve cord synapses in *Caenorhabditis elegans* (*C. elegans*) (Rongo and Kaplan, 1999). It was found that a coupling of CaM-kinase II and VOCC was the mechanism for maintaining the level of AMPA-type glutamate receptors (GLR-1) at a constant density in *C. elegans* (Rongo and Kaplan, 1999). In wild-type worms Ca^{2+} influx via VOCC and CaM-kinase II activity promoted the transport of GLR-1 from the cell body to synapses. Wild-type *C. elegans* have a single CaM-kinase gene, unc-43; in worms lacking the unc-43 gene GLR-1 accumulates in the cell body. This could be analogous to and be a putative mechanism occurring with KCl-evoked

upregulation of the density of α7* nAChR in both SH-SY5Y cells and primary hippocampal neurones in culture. Under KCl depolarisation, VOCC channels are activated and increase $[Ca^{2+}]_i$ within the cell. CaM-kinase II is activated by Ca^{2+} and could regulate receptor trafficking perhaps by augmenting the transport of nascent receptors from the cell cytoplasm to increase [^{125}I]-α-bgt binding sites located on the cell surface. In the presence of the CaM-kinase II inhibitor KN-62, this process could be disrupted and would therefore result in the inhibition of upregulation of surface α7* nAChR. It would be reasonable to suggest that these α7* nAChR could be accumulated intracellularly within the cell cytoplasm, resulting in a level of expression of surface [^{125}I]-α-bgt binding sites similar to control untreated cells. The accumulated intracellular α7* nAChR would not be detected with [^{125}I]-α-bgt binding assays due to the large, protinaceous cell impermeant nature of this radiolabelled snake toxin and its inability to penetrate the cytoplasm and label intracellular α7* nAChR. A proposed scheme for this process is summarised in Figure 3.27. [^{3}H]-MLA, an α7 antagonist that is capable of crossing the cell membrane, would aid in the detection of any intracellular α7* nAChR accumulated in the presence of KN-62. This would help to distinguish a role for CaM-kinase II in receptor assembly and trafficking or gene transcription (or both).

The activity of CaM-kinase II has been previously reported as having dual regulation by membrane voltage (Xiao *et al.*, 1994; Williams *et al.*, 1996) and by Ca^{2+} influx via depolarisation of L-type VOCC (Jefferson *et al.*, 1991; Ocorr and Schulman, 1991; MacNicol and Schulman, 1992; Xiao *et al.*, 1994). ICK, a CaM-kinase II peptide inhibitor (CaM-kinase II fragment-(290-309)), abolished calcium currents elicited by Ca^{2+} influx or by membrane depolarisation in cardiac myocytes (Xiao *et al.*, 1994). This

modulatory effect of CaM-kinase II by depolarisation may be extrapolated to the increased KCl concentration applied to SH-SY5Y cells or primary hippocampal neurones and could establish a positive feedback loop evoked by KCl by placing the Ca^{2+} channel proteins into conformations more favourable for phosphorylation by CaM-kinase II (Xiao *et al.*, 1994).

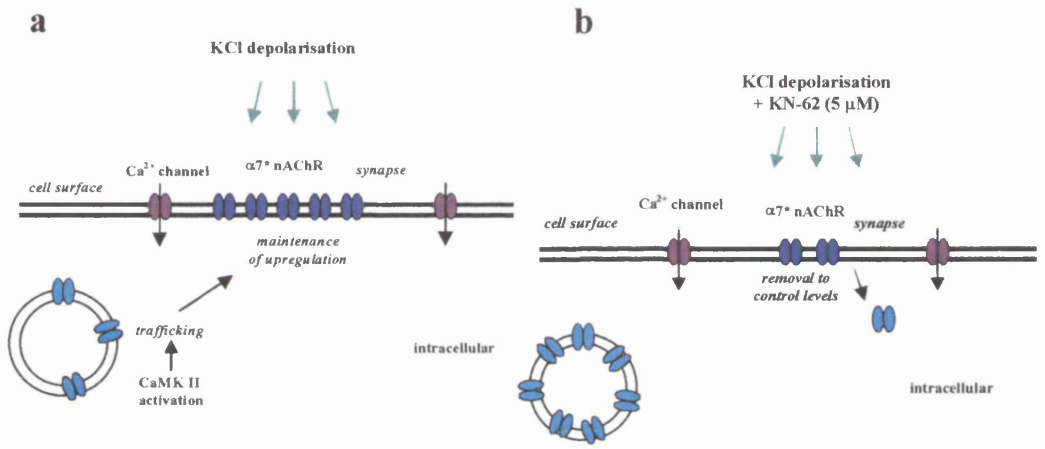

Figure 3.27. A model for CaM-kinase II (CaMK II) regulation of α7* nAChR evoked by KCl depolarisation in SH-SY5Y cells or primary hippocampal neurones. *(a) KCl depolarisation mediates Ca^{2+} influx through VOCC, CaM-kinase II is activated by Ca^{2+} to putatively promote transport of intracellular α7* nAChR from the 'stores' to synapses, and addition or stability at nicotinic synapses located on the cell surface, detected by [^{125}I]-α-bgt (indicated as receptors on the surface). (b) illustrates the inhibitory effect of KN-62 on KCl-evoked upregulation of surface [^{125}I]-α-bgt binding sites, leading to an accumulation of α7* nAChR within the cell cytoplasm due to inhibition of CaM-kinase II activity (indicated as receptors intracellularly, undetected by [^{125}I]-α-bgt). Adapted from Rongo and Kaplan, (1999).*

KN-62 has also been proposed to inhibit depolarisation-dependent Ca^{2+} influx via VOCC without affecting Ca^{2+} mobilisation from intracellular stores (Williams *et al.*, 1996) as well as inhibiting CaM-kinase II in small cell lung carcinoma (SCLC) SCC-9 cells (Williams *et al.*, 1995). VOCC in SCLC seem to be regulated in a similar manner to those found in neuronal cells. The ability of CaM-kinase II to phosphorylate L-type

(Chang *et al.*, 1991) and N-type (Hell *et al.*, 1994) VOCC provides a possible mechanism by which CaM-kinase II could regulate the activity of VOCC. Li *et al.* (1992) suggested that KN-62 mediated inhibition by direct blockade of VOCC in HIT-T15 cells, rather than a CaM-kinase dependent pathway. This was concluded after KN-62 was found to inhibit VOCC in previously depolarised cells that should have been fully activated by CaM-kinase II and hence insensitive to subsequent addition of this inhibitor. In contrast, Williams *et al.* (1995) demonstrated that KN-62 did not significantly inhibit VOCC activity in SCC-9 cells previously depolarised before the application of KN-62 and therefore these cells have fully activated CaM-kinase II. Pre-incubation with KN-62 was found to inhibit depolarisation-dependent autophosphorylation of CaM-kinase II (Williams *et al.*, 1996). These findings are consistent with the hypothesis that the inhibition of VOCC by KN-62 in SCC9 cells is due to inactivation of CaM-kinase II, rather than a direct block of VOCC.

In the experiments described in the present study, KN-62 may inhibit KCl-evoked upregulation of α7* nAChR by an inhibitory action on CaM-kinase II and/or by a direct blockade of VOCC after co-application of KCl with KN-62. The underlying mechanism by which CaM-kinase II promotes upregulation of α7* nAChR trafficking and localisation is as yet unknown. Upregulation of α7* nAChR by KCl depolarisation could be a form of neuronal plasticity utilised to maintain synapses and their growth in developing neurones.

3.19. Upregulation of [^{3}H]-epibatidine binding sites in SH-SY5Y cells:

After investigating the effect of chronic drug treatment on numbers of α7* nAChR, it was decided to examine the effect of these same chronic drug treatments on α3*

nAChR detected with [^{3}H]-epibatidine binding. In SH-SY5Y cells, [^{3}H]-epibatidine could label a variety of different subtypes of human α3* nAChR, namely α3β2, α3β2α5, α3β4, α3β4α5 and α3α5β2β4 combinations. All of these receptor complexes respond in a concentration dependent manner to ACh and are therefore capable of forming functional nicotinic receptor ion channels (Wang *et al.*, 1998). Wang *et al.* (1998) previously demonstrated that upregulation of α3* nAChR depended on the presence of the β2 subunit, and that approximately 56% of α3* receptors also contained the β2 subunit. Hence, α3β2 and α3β2α5 heterogeneous nAChR complexes were upregulated after chronic exposure to nicotine and carbamylcholine whereas their β4 counterparts were not significantly altered (Wang *et al.*, 1998). Intrinsic differences between the β2 and β4 subunits, including differences in their efficiency of synthesis, maturation or assembly of the different β subunits with α3 subunits, could determine the fate of α3 nAChR subunits with regard to upregulation. These differences may lead to alterations in the turnover of receptor numbers, with the α3β2 receptor complex being longer lived and more stable than the α3β4. It seems that an alteration in receptor synthesis, maturation or assembly is a logical explanation for nicotine-evoked upregulation because in the absence of protein synthesis, nicotine still upregulates the amount of α3β2 nAChR to 25% as compared to in the absence of cycloheximide (6-fold upregulation versus 24-fold upregulation) (Wang *et al.*, 1998). In the tsA201 cell line stably transfected with α3 and β2 subunits, nicotine-evoked upregulation was observed as soon as after 15 minutes exposure (Wang *et al.*, 1998). Due to this rapid increase in nAChR numbers, the upregulation is probably mediated by an enhanced assembly of α3 and β2 subunits from subunit reserves already present in the cells, rather than from an increase in *de novo* subunit synthesis (Wang *et al.*, 1998). This concept of enhanced

subunit maturation or assembly of upregulated α3* nAChR evoked by nicotine is also proposed by Peng *et al.* (1997).

The binding assays performed over the course of this project to detect α3* nAChR used a modest concentration of [^{3}H]-epibatidine at 500 pM. This concentration of radioligand will predominantly detect β2* nAChR (Wang *et al.*, 1998). In the present study [^{3}H]-epibatidine binding sites were differentially upregulated by chronic drug treatment. Nicotinic agonists, nicotine (10 μM) and DMAC (10 μM) were found to upregulate [^{3}H]-epibatidine binding sites to 36 ± 6% and 43 ± 8% respectively above control levels observed in untreated SH-SY5Y cells. The upregulation of [^{3}H]-epibatidine binding sites reported in this study is somewhat lower than previously reported for SH-SY5Y cells (Peng *et al.*, 1997). In the present study, lower concentrations of nicotine (10 μM) were used to evoke upregulation, compared to previous reports that have generally used 1 mM nicotine to elicit upregulation of the α3* and also α7* nAChR in SH-SY5Y cells: therefore a lower level of upregulation might be expected. The recent report by Peng *et al.* (1997) revealed a 575% increase in total α3* nAChR with only a 30-40% increase of surface α3* nAChR expressed in SH-SY5Y cells after chronic nicotine (1 mM) exposure. This concentration of nicotine is 400-fold higher than concentrations required for the upregulation of α4β2 nAChR expressed in fibroblast M10 cells (Peng *et al.*, 1997; Warpman *et al.*, 1998; Whiteaker *et al.*, 1998) and 100-fold higher than used in the present study.

There is evidence that upregulation of the α3* nAChR is mediated at the cell surface as the membrane impermeable quaternary nitrogen containing ligand carbamylcholine also induced a concentration-dependent upregulation of intracellular α3* nAChR in SH-SY5Y cells (Peng *et al.*, 1997). The channel blocker mecamylamine was found not to

upregulate α3* nAChR and did not inhibit upregulation evoked by nicotine. This implies that mecamylamine itself does not induce the conformation of α3* nAChR required for upregulation, and that ion flow through α3 nAChR is not a requisite signal to the intracellular compartment of SH-SY5Y cells to initiate the rapid upregulation of α3* nAChR (Peng *et al.*, 1997).

Previous studies have revealed that upregulated α3* nAChR are mainly located intracellularly in SH-SY5Y cells after chronic exposure to nicotine (Peng *et al.*, 1997; Wang *et al.*, 1998). Confocal analysis was employed in the present study to detect α3* nAChR subunits by using a polyclonal antibody that labels the intracellular portion of the loop between TM3 and TM4 of the α3 nAChR subunit. Most of the fluorescence observed was of α3 nAChR subunits located within the cell cytoplasm where they would be non-functional. Peng *et al.* (1997) demonstrated the inhibition of nicotine-evoked upregulation of α3* nAChR by using antigenic modulation, and that the receptors affected by nicotine had previously been located on the surface of SH-SY5Y cells. Perhaps chronic exposure to nicotinic agonists leads to receptor internalisation and accumulation rather than receptor degradation.

Specific antibodies that label extracellular portions of the α3 subunit were not available to us at the time of this study, but would be useful as a comparison for total versus surface α3 nAChR subunits in control and drug treated cells. Both nicotine and DMAC treated cells appeared to have greater intracellular staining of the α3 nAChR subunit than control conditions. Chronic KCl depolarisation resulted in the staining of α3 nAChR subunits similar to that in control untreated SH-SY5Y cells. This is consistent with the finding that KCl depolarisation does not upregulate α3* nAChR as

detected by [^{3}H]-epibatidine binding. This is in contrast to KCl-evoked upregulation of [^{125}I]-α-bgt binding sites in both SH-SY5Y cells and in primary hippocampal cultures.

By using the technique of confocal microscopy qualitatively this method allows for the assessment of the presence or absence of different nAChR subunits by using a variety of specific mAb for different nAChR subunits. Quantitative analysis of the fluorescence signal recorded from different samples and treatment conditions will vary due to different coverslips used and if the mAb was applied slightly longer than another. A numerical estimate of the mean fluorescence intensity can be made, however a large sample population would be required to generate a reliable quantitative statistical analysis.

3.19.1. Mechanisms of nicotinic agonist-evoked upregulation of [^{3}H]-epibatidine binding sites in SH-SY5Y cultures:

The interesting finding that KCl upregulated α7* but not α3* nAChR and that the nicotinic agonists nicotine and DMAC evoked upregulation of both α3* and α7* nAChR led to further analysis of the underlying mechanisms of nicotinic agonist-induced upregulation of [^{3}H]-epibatidine binding sites. Experiments were conducted to investigate the effect of Ca^{2+} influx using verapamil, the inhibition of CaM-kinase II with KN-62 and the effect of inhibiting PKC with Ro 31-8220. None of these compounds were able to prevent the nicotine or DMAC evoked upregulation of [^{3}H]-epibatidine binding sites. This demonstrated that nicotinic agonist-evoked upregulation of α3* nAChR was not mediated by Ca^{2+} influx through L-type VOCC, nor by CaM-kinase II or PKC pathways.

A surprising yet interesting result was obtained when KN-62 was applied to SH-SY5Y cultures alone for 4 days. A huge 2-3 fold upregulation of [^{3}H]-epibatidine binding was produced when compared to control untreated cells. To determine if this effect was a specific action due to the inhibition of CaM-kinase II, the effect of KN-04 was investigated. KN-04 is an inactive structural analogue of KN-62 and therefore does not inhibit CaM-kinase II (Ishikawa *et al.*, 1990). SH-SY5Y cultures in the presence of KN-04 for 4 days produced no change from control in the level of [^{3}H]-epibatidine binding, indicating that the upregulation obtained with KN-62 must reflect a direct inhibitory action of CaM-kinase II. The upregulatory effect of KN-62 was maintained in the presence of nicotinic agonists with a particular enhancement in the presence of DMAC. If the Rongo and Kaplan (1999) proposal for regulation of the density of glutamatergic synapses by a CaM-kinase II-dependent pathway is taken into consideration (as described in section 3.18.1), it may help to relate to and understand the maintenance of α3* nAChR in control cells and the enhanced [^{3}H]-epibatidine binding detected in the presence of KN-62. A proposed scheme is shown in Figure 3.28 for the regulation of [^{3}H]-epibatidine binding sites in control and KN-62 treated SH-SY5Y cells.

This scheme could account for the huge increase in α3* nAChR detected in the presence of KN-62 alone due to inhibition of CaM-kinase II and a potential alteration in the trafficking of α3 from the cell cytoplasm to expression on the cell surface. This would promote the accumulation of α3* nAChR subunits within the cytoplasm that are labelled together with surface α3 binding sites by [^{3}H]-epibatidine, due to its cell permeant nature (which is in contrast to the membrane impermeable [^{125}I]-α-bgt). Conformation of an increase in intracellular receptors detected with [^{3}H]-epibatidine

could be performed in the presence of ACh to block [^{3}H]-epibatidine binding to surface receptors.

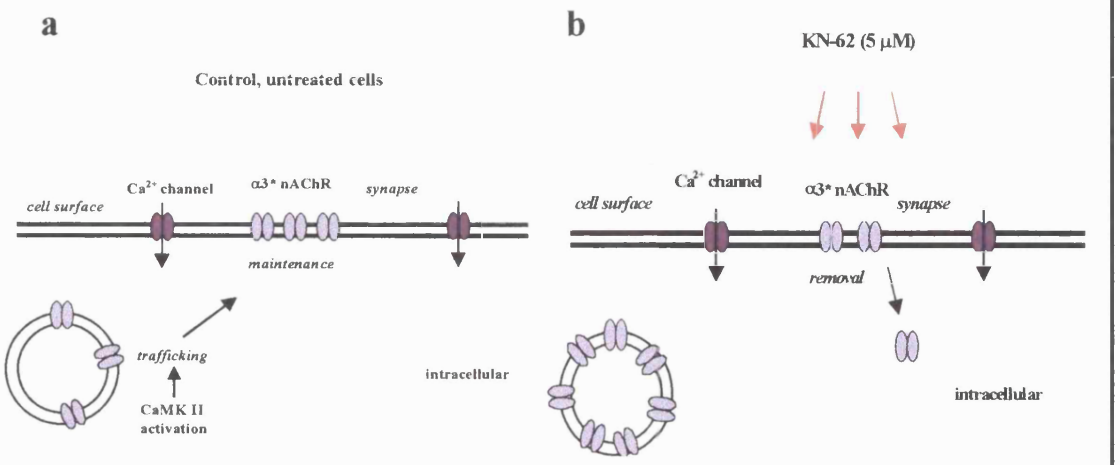

Figure 3.28. A model for CaM-kinase II (CaMK II) regulation of α3* nAChR in SH-SY5Y cells. *(a) In control conditions CaM-kinase II activity promotes the transport of α3* nAChR from the cell cytoplasm to the cell surface, and addition or stability at nicotinic synapses located on the cell surface to maintain basal levels of α3* nAChR (b) Illustrates the effect of KN-62 in control cells leading to an accumulation of α3* nAChR within the cell cytoplasm due to inhibition of CaM-kinase II activity (receptors detected by [^{3}H]-epibatidine are indicated as ∞, located on the surface and intracellularly in SH-SY5Y cells). Adapted from Rongo and Kaplan (1999).*

If a huge upregulation of [^{3}H]-epibatidine binding sites is maintained by KN-62 in the presence of ACh, it would confirm that KN-62 promotes upregulation of non-functional intracellular α3* nAChR perhaps by a process involving the disturbance of trafficking of α3* nAChR from the cell cytoplasm to cell surface (adapted from the hypothesis proposed by Rongo and Kaplan, 1999). Upregulation of [^{3}H]-epibatidine binding sites produced by KN-62 alone is perhaps not quite so surprising as first thought. The action of KN-62 is interesting with respect to a possible trafficking pathway of α3* nAChR in control cells involving a CaM-kinase II, analogous to the regulation of glutamatergic synapses in *C. elegans* (Rongo and Kaplan, 1999)

3.20. Is transcription involved in the upregulation of α3 and α7 nAChR subunits in SH-SY5Y cells?:

The mechanism by which nicotinic agonists increase α3* and α7* nAChR numbers remains unknown. One possible explanation is that the increase in these receptor subtypes is regulated by increases in transcription or stabilisation of the poly $(A)^+$ RNA, producing an elevation in the quantity of RNA encoding for the receptor subunits. Initial studies performed in Section 2 used the technique of reverse transcription, coupled with the polymerase chain reaction (RT-PCR) which is an extremely sensitive method for detecting the expression of specific RNA transcripts. The apparent low expression of the α7 subunit in SH-SY5Y cells was not a problem, as the detection of any gene using this technique is not limited by the paucity of initial starting material. In the process of PT-PCR the RNA template during the procedure of reverse transcriptase is copied into a complementary DNA (cDNA) transcript, this is followed by a series of polymerase chain reactions (PCR) that exponentially amplifies the cDNA by a thermostable DNA polymerase. Warpman *et al.* (1998) performed RNase protection assays with SH-SY5Y cells to identify the levels of different subunit transcripts and found it hard to quantitate the level of α7 expression in SH-SY5Y cells, due to the α7 mRNA content being below the level of detection compared to the other nAChR transcripts. RT-PCR analysis in the present study identified the presence of both α3 and α7 nAChR subunits in SH-SY5Y cells, but because of the amplification technique it was not possible to quantitate the level of expression of these subunits in drug treated conditions versus control untreated cells.

A recent study demonstrated that nicotine treatment (1 mM for 4 days) increased the density of α3* and α7* nAChR without upregulating the transcription of α3 and α7

subunit mRNA (Peng *et al.*, 1997). The present study also demonstrated the failure of nicotinic agonists to upregulate α3 and α7 nAChR RNA levels by Northern analysis. Northern blotting is a time-consuming method that requires RNase-free techniques and reagents, as this method of RNA detection is extremely vulnerable to RNA degradation. The result obtained with α7 is preliminary, as levels of the α7 RNA were difficult to detect when using either total cellular RNA or poly $(A)^+$ RNA in Northern analysis. Northern analysis allows for a direct relative comparison of message abundance between samples on a single membrane.

KCl depolarisation (20 mM) did not alter the level of expression of the α3 transcript, but it did upregulate the α7 transcript to 137% above control levels. This preliminary result is in agreement with the significant increase of 156 ± 15% (above control expression) detected for the α7 subunit transcript after 40 mM KCl applied to sympathetic SCG neurones for 48 hours (De Koninck and Cooper, 1995). The induction of expression of the α7 nAChR subunit by membrane depolarisation can therefore be postulated to be due to an influx of Ca^{2+} through L-type VOCC and by a CaM-kinase II dependent pathway identified by KN-62. The effects of KN-62 are perhaps due in part to inhibition of Ca^{2+} influx via a possible inhibition at VOCC, this has been discussed above in section 3.18.1 and also addressed by Li *et al.* (1992) and Wyllie and Nicoll (1994). L-type VOCC have previously been reported to have a role in the regulation of the expression of immediate early genes within neurones (Murphy *et al.*, 1991b; Bading *et al.*, 1993; Bessho *et al.*, 1994; Enslen and Soderling, 1994; Rosen *et al.*, 1994; Ghosh and Greenberg, 1995) and to target the nucleus (Srinivasan *et al.*, 1994).

Together, the binding data suggest that upregulation of $[^{125}I]$-α-bgt and $[^3H]$-epibatidine binding sites evoked by nicotinic agonists are not mediated by an increase in

α3 or α7 nAChR subunit RNA. These data are in agreement with Peng *et al.* (1997) who observed no change in α3 or α7 mRNA levels after chronic nicotine exposure. Figure 3.29 summarises the proposed action of KCl depolarisation and nicotinic agonists on α3* and α7* nAChR in the SH-SY5Y cell line.

Previous *in vivo* and *in vitro* studies investigating high affinity nicotinic binding sites, have shown that upregulation of the α4β2 nAChR complex by nicotinic agonists is by an increase in the B_{max} (fmoles/mg protein) with no apparent increase in affinity of the α4β2 nAChR for nicotine (Bencherif *et al.*, 1995). Peng *et al.* (1994b) reported that nicotine increases α4β2 AChR in transfected M10 cells with no change in the level of α4 or β2 subunit mRNA expression. A process involving increased transcription has therefore been ruled out as a possible pathway for the resulting upregulation of mRNAs coding the α4 or β2 subunits. This has been also been demonstrated *in vivo* (Flores *et al.*, 1992; Marks *et al.*, 1992) as well as *in vitro* (Peng *et al.*, 1994b, 1997; Zhang *et al.*, 1995; Warpman *et al.*, 1998). Peng *et al.* (1994b) reported that chronic nicotine induced upregulation of α4β2 nAChR may involve post-transcriptional mechanisms. A variety of hypotheses have arisen to suggest post-transcriptional mechanisms including, a decrease in receptor turnover (Peng *et al.*, 1994b), the recruitment of nAChR from a pre-existing pool of receptors (Bencherif *et al.*, 1995), an increased efficiency of assembly of subunits into receptor complexes (Rothhut *et al.*, 1996), or indeed altered rates of translation (Gopalakrishnan *et al.*, 1997). It should also be taken into consideration that these studies with high affinity nAChR are all from cell lines that have been transfected with the α4 and β2 subunits and not from a system where they are endogenously expressed. Using cell lines transfected with either α3 and β2 subunits or

α7 nAChR subunits would be useful to compare data generated in SH-SY5Y cells that endogenously express α3β2* and α7* nAChR.

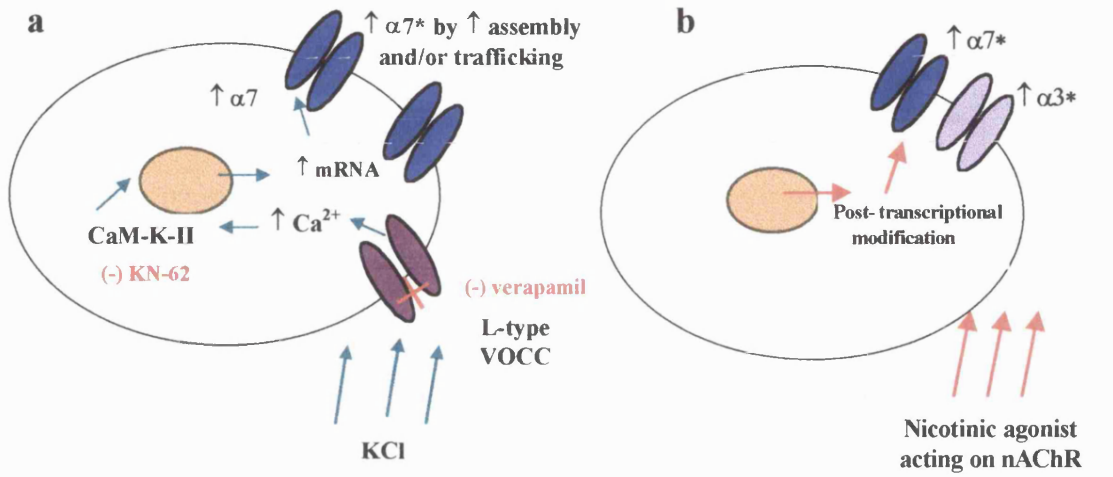

Figure 3.29. A representation of KCl- and nicotinic agonist-evoked upregulation of nAChR binding sites in SH-SY5Y cells. *Chronic treatment of SH-SY5Y cells for 4 days with either (a) KCl depolarisation upregulates [^{125}I]-α-bgt binding sites by Ca^{2+} influx through L-type VOCC and by a CaM-kinase II-dependent pathway that increases the transcription of α7* nAChR subunit RNA or (b) Nicotinic agonist-evoked upregulation of [^{3}H]-epibatidine and [^{125}I]-α-bgt binding sites by a post-transcriptional modification.*

The identification of a post-transcriptional mechanism of upregulation for α4β2 nAChR mediated by chronic nicotine may also be extrapolated to the SH-SY5Y cell line for both the α3* and α7* nAChR. The failure of chronic nicotinic agonist treatment to upregulate transcription of α3 or α7 subunit RNA in SH-SY5Y cells is consistent with previous observations with the effect of nicotine in brain tissue on α4 and β2 subunit expression (Marks *et al.*, 1992). This study therefore leads to the proposal that nicotinic agonists upregulate α3* and α7* nAChR by a post-transcriptional mechanism that may be similar to that upregulating the α4β2 high affinity nAChR. Studies with the tsA2013 cell line transfected with α3 and β2 nAChR subunits conclude that chronic nicotine treatment evoked upregulation by an assortment of processes, including an

increase in the rate of nAChR subunit synthesis, maturation and assembly (Wang *et al.*, 1998).

Bencherif *et al.* (1995) examined possible mechanisms underlying upregulation of the high affinity α4β2 nAChR using both primary cultures of fetal rat brain cortex and the M10 clonal cell line. The former naturally expresses high affinity [^{3}H]-nicotine binding sites whereas the latter are stably transfected with the α4 and β2 nAChR subunits which are under the control of a dexamethasone-inducible promoter. Removal of dexamethasone (1 μM; 2 days) from M10 cultures terminates the synthesis of new α4β2 nAChR and enables the study of degradation of α4β2 receptors, a 50% reduction in [^{3}H]-nicotine binding was observed after 24 hours (Bencherif *et al.*, 1995). If nicotine (1 μM) is applied to the cells at the time of removal of the dexamethasone an elevation from control values in the level of [^{3}H]-nicotine binding results. The effect of chronic nicotine was interpreted to be a result of degradation of pre-existing nAChR and recruitment of nAChR complexes from a finite pool of receptors previously undetected by high affinity agonist binding. In cells where nicotine is applied at the time of removal of dexamethasone, the prevention of new receptor synthesis is compensated for by the recruitment of receptors from the finite pool, giving the impression of a reduction in receptor turnover. In cells already exposed to nicotine treatment to upregulate nAChR before dexamethasone withdrawal, the pool containing receptor reserves is used and will hence not make up for subsequent receptor degradation.

Peng *et al.* (1997) argue against a decrease in the degradation rate of α3* nAChR after chronic nicotine treatment compared to control. Cells treated with or without nicotine before the addition of cycloheximide to block protein synthesis of new nAChR, did not alter the turnover rate of α3* nAChR (Peng *et al.*, 1997). This is in contrast to

observations found with the action of cycloheximide on α4β2 nAChR (Peng *et al.*, 1994b; Rothhut *et al.*, 1996), indicative that a decrease in nAChR turnover may be restricted to cell lines that have been stably transfected with subunits rather than endogenously expressing them. The action of cycloheximide was not investigated in the present study with [^{3}H]-epibatidine binding due to its observed cytotoxicity and general deleterious effect when previously applied to SH-SY5Y cells either alone or with chronic KCl and nicotine treatment to detect changes in [^{125}I]-α-bgt binding (see section 3.4.4).

To conclude, from this and previous studies the underlying mechanism of KCl-evoked upregulation of surface [^{125}I]-α-bgt binding sites involves L-type VOCC and a CaM-kinase II pathway which in turn leads to an increase in α7 subunit RNA. In contrast, the mechanism underlying nicotinic agonist-induced upregulation of α3, α7 and α4β2 nAChR subtypes remains unknown. From this study, upregulation of [^{125}I]-α-bgt and [^{3}H]-epibatidine binding sites evoked by nicotinic agonists is not clear but does not seem to involve Ca^{2+} flux through L-type VOCC, a CaM-kinase II or PKC pathway or by increasing the level of either α3 or α7 subunit RNA levels. Chronic nicotinic agonist treatment indicates that the upregulation of α3* and α7* nAChR must be via a post-transcriptional mechanism and perhaps this mechanism shares pharmacological and cellular properties with the mechanism of upregulation of the higher affinity α4β2 nAChR.

Chapter 4. Functional Studies in SH-SY5Y cells.

4.1. Introduction to the calcium signal and the cell:

Ca^{2+} has been proposed as a key common biological regulator and trigger that gives rise to many diverse cellular events. Ca^{2+} acts as an internal signal and can be considered as a universal ionic messenger important in cellular signal transduction and has a role in a variety of neuronal processes. Examples of events involving a minute Ca^{2+} flux across the cell membrane include the secretion of hormones, the release of neurotransmitters from the presynaptic nerve terminal into the synaptic cleft, neuronal excitation and plasticity that is responsible for the processes of learning and memory (Miller, 1988; Berridge *et al.*, 1998; Fossier *et al.*, 1999). The Ca^{2+} signal is required as a signal for cell life, fertilisation, development and proliferation of cells. Ca^{2+} has also been implicated in the disintegration of cells (necrosis) and in programmed cell death (apoptosis) (Miller, 1988; Berridge *et al.*, 1998; for review see, Toescu, 1998) after a rapid influx of Ca^{2+} passes into the cell and produces a prolonged Ca^{2+} rich environment, as associated with cerebral ischaemia, and other pathological disease states including AD, AIDS and cancer. AD and PD are of interest with respect to neuronal nAChR, due to these conditions having altered numbers of receptors in specific brain regions, as introduced in sections 1.9.2 and 1.9.3. The paradoxical action of Ca^{2+} (life and death signal) has a pivotal role in conveying different incoming signals received at the cell surface, to mediate an increase in $[Ca^{2+}]_i$ and activate Ca^{2+}-dependent intracellular signalling pathways within cells (Berridge, 1998; Berridge *et al.*, 1998).

The resting $[Ca^{2+}]_i$ within a cell is usually in the range 50 to 100 nM which is about ten thousand times lower than the extracellular $[Ca^{2+}]$ (Miller, 1988; Taylor and Broad, 1998). In the past there have been difficulties associated with the measurement of such intracellular free ion concentrations. Recent advances in this field have made it possible

to detect Ca^{2+} in many cellular scenarios. Developments include the founding of user-friendly fluorescent chelating agents, fura-2, fluo-3, quin-2 and indo-1, that have advanced the investigation of different intracellular ion concentrations within the cytosol of living cells (Tsien, 1988; Neher, 1995). *In vitro* cell biology has been transformed by the development of fluorescent agents that undergo a change in their fluorescent profile after ion binding. Fluorescent chelating agents allow the quantitative measurement of cytosolic free $[Ca^{2+}]$ and a comparison between control and drug stimulated conditionings. Using SH-SY5Y cells loaded with a fluorescent chelating agent, exact concentrations of an acute drug challenge can be applied to the cells in suspension and produce direct drug-concentration-response relationships.

The fluorescent probes used to identify changes in $[Ca^{2+}]_i$ have had an enormous impact due to their non-destructive nature to living cells once loaded into the cellular cytoplasmic compartment. These probes are useful for investigating the changes in $[Ca^{2+}]_i$ in living cells evoked by different external stimuli. Previously, SH-SY5Y cells have been used to investigate the effects of muscarinic (Lambert and Nahorski, 1990; Lambert *et al.*, 1990; Murphy *et al.*, 1991a; Forsythe *et al.*, 1992) and nicotinic responses (Forsythe *et al.*, 1992), and bovine chromaffin cells to examine increases in $[Ca^{2+}]_i$ evoked by nicotine (López *et al.*, 1993). The parent SK-N-SH human neuroblastoma cell line has been used to identify Ca^{2+} influxes mediated via nAChR and VOCC (Noronha-Blob *et al.*, 1989). Cell lines stably transfected with nAChR subunits have also been used to examine nAChR responses for example, GH_4C_1 rat pituitary cells (Quik *et al.*, 1997) and HEK cells stably transfected with $\alpha 7$ nAChR subunits (Molinari *et al.*, 1998).

4.1.2. Mechanisms that raise $[Ca^{2+}]_i$; Ca^{2+} entry pathways and release from internal stores:

At a cellular level, Ca^{2+} is capable of entering cells by several routes. Activation of either VOCC opened by voltage, or receptor-operated Ca^{2+} channels for example, glutamate receptors that respond to NMDA (Rogers and Dani, 1995), will mediate Ca^{2+} entry to the cell from extracellular sources (Figure 4.1). nAChR also represent a class of receptors permeable to Ca^{2+} as well as Na^{2+} (for review, see Sargent 1993). In particular, the α7* nAChR possess the greatest Ca^{2+}:Na^{2+} permeability when the α7 subunit gene is expressed as homomeric receptors in *Xenopus* oocytes, values are similar to those reported for the NMDA receptor (Séguéla *et al.*, 1993; Rogers and Dani, 1995).

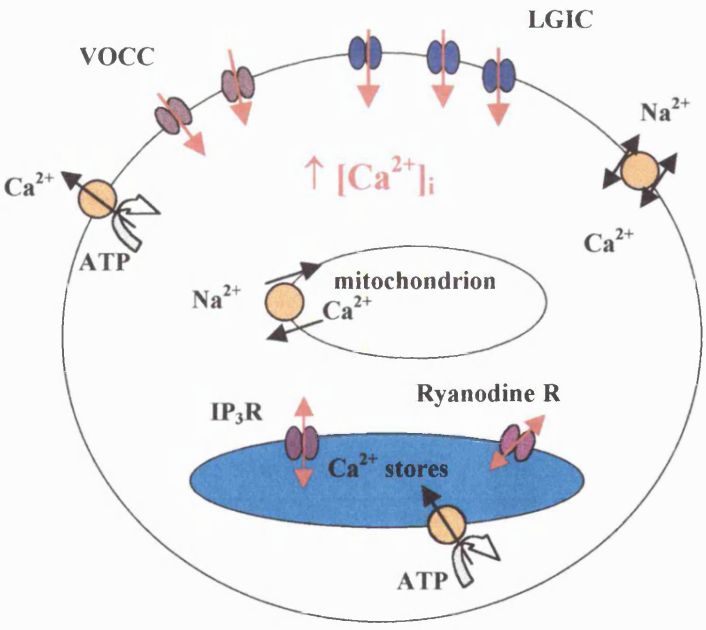

Figure 4.1. A schematic representation of the major cellular Ca^{2+} transport pathways showing both Ca^{2+} buffering and elevating pathways within the cell.

Ca^{2+} can also be released into the cell from internal stores, via store-operated Ca^{2+} channels located on the endoplasmic or sarcoplasmic reticulum (Berridge, 1993; Taylor and Broad, 1998). The endoplasmic reticulum is an important continuous membrane structural network within cells which maintains a large $[Ca^{2+}]$ gradient (Berridge, 1998). The presence of inositol 1,4,5-trisphosphate (IP_3) and ryanodine receptors on the surface of the endoplasmic reticulum allows for the release of accumulated stored Ca^{2+} into the cytosol of the cell if Ca^{2+} levels are raised within the cytosol (Ca^{2+}-induced Ca^{2+}-release). In essence, the involvement of both the plasma membrane and the endoplasmic reticulum regulate the flux of Ca^{2+} into and out of the cell cytosol from extracellular and accumulated Ca^{2+} stores depending on the $[Ca^{2+}]_i$ and can be considered as a binary system working synergistically to control a vast array of Ca^{2+}-dependent processes.

4.1.3. Considerations when measuring changes in $[Ca^{2+}]_i$ with fluorescent ion dyes:

Indicator dyes used for ion measurements are chelating agents commonly modelled on EGTA, a Ca^{2+}-selective chelating agent that is non-fluorescent and is well suited to buffer Ca^{2+} in physiological ranges (for review, see Cobbold and Rink, 1987). EGTA has selectivity for Ca^{2+} over the smaller divalent cation Mg^{2+} by an affinity of approximately five to six orders of magnitude. Chelating agents, by definition, are highly charged molecules and are therefore unable to penetrate the apolar cell membrane. This means that the active form of the chelating agent can not be used to initially load the cell. Cell loading is usually accomplished using uncharged membrane permeable acetoxymethyl (AM) esters that will not bind the ion under investigation. After cell entry the AM ester is acted upon by non-specific esterases leading to the conversion of the AM-dye into the impermeable active free-acid form of the dye which

is capable of ion binding and is trapped within the cell cytoplasm. The binding of Ca^{2+} to the active free-acid form of the chelating dye changes the fluorescence signal properties in the presence of Ca^{2+} compared to the unbound form. Ca^{2+} fluorescent indicators are widely available, easy to use in experimental protocols and are therefore useful tools used to measure changes in fluorescence (which can be converted to changes in $[Ca^{2+}]_i$). These fluorescent agents have transformed and helped to further elucidate the mechanisms involved in mediating changes in cytosolic Ca^{2+}. A suitable ion dye should incorporate the following:

1). To determine fluorescence changes and for quantitative analysis of $[Ca^{2+}]_i$ evoked by different compounds, an indicator dye that exhibits a shift in its excitation spectrum upon Ca^{2+} binding is useful. This will establish a ratio of the dye in the Ca^{2+}-free and Ca^{2+}-bound form, from which the $[Ca^{2+}]_i$ can be calculated by a simple equation (see section 4:2.3.1).

2). Of central importance is the dissociation constant (K_D), this is a measure of the ability of a chelating agent to bind the target ion, which in the present study is Ca^{2+}, and can be considered as its binding strength. By definition the K_D of a chelation indicator dye is the half-saturation point for that dye. The K_D should be compatible with the $[Ca^{2+}]$ range of interest and is usually expressed in units of concentration. The smaller the value of the K_D the more powerful and selective a chelating agent is, therefore a K_D of in the nanomolar range will be a better target ion binder than an agent with a greater K_D value, for example fura-2 has a K_D value of 224 nM.

3). As mentioned above, the form of the chealting agent is important for cell loading. The uncharged, hydrophobic dextran or AM esters are favoured for their ease of loading and membrane permeable nature. Within the cell after loading, these agents are cleaved by cellular esterases to generate the dye in a membrane impermeant nature.

4.1.4. Ratiometric calcium dyes:

4.1.4.1. Fura-2:

When ratiometric dyes are used in fluorescence studies, they allow for the generation of quantitative information on changes in $[Ca^{2+}]_i$. Fura-2 is typically the Ca^{2+} indicator dye of choice used for many functional fluorescence studies (Murphy *et al.*, 1991a; Forsythe *et al.*, 1992; Barrantes *et al.*, 1995b; Sharples *et al.*, 2000) and has been widely used in imaging microscopy techniques performed on single cells grown on coverslips and also following photometric changes in cell suspensions. This indicator dye is excited by ultraviolet (UV) radiation at 340 nm in the Ca^{2+}-bound form and at 380 nm in the Ca^{2+}-free form with an emission at 510 nm. The ratio of the fluorescence produced at 340 nm/380 nm is directly correlated to $[Ca^{2+}]_i$ by the Grynkiewicz equation (Grynkiewicz *et al.*, 1985) (see section 4.2.3.1). Fura-2 is approximately 30 fold brighter that quin-2 (the first practical non-ratiometric dye) due to it possessing a greater extinction coefficient, increased quantum efficiency and being more resistant to photobleaching. Complete de-esterification of the AM-ester dye is necessary after loading for accurate $[Ca^{2+}]_i$ estimates. Sometimes these AM-esters are incompletely de-esterified, perhaps due to low levels of cytosolic esterase activity, and result in compartmentalisation into organelles (Tsien, 1988).

4.1.4.2. Indo-1

Indo-1 is another ratiometric dye that possesses brighter fluorescence and a higher K_D at 250 nM than compared to fura-2. In contrast to fura-2, this fluorescence Ca^{2+} chelator produces a shift in its emission maximum rather than an excitation shift after Ca^{2+} binding with the Ca^{2+}-bound and Ca^{2+}-free forms emitting at 400 and 475 nm respectively (Grynkiewicz *et al.*, 1985). Indo-1 is more susceptible to photobleaching than fura-2, but is less problematic in terms of incomplete hydrolysis and organelle compartmentalisation.

4.1.5. Non-ratiometric dyes:

Non-ratiometric dyes are excited at one wavelength: UV (quin-2) or visible (fluo-3, fluo-4) and have a higher emission wavelength, thus resulting in a change in fluorescence intensity without a shift in the ratio of wavelength. Quin-2 provided the first useful measurements of resting and activated $[Ca^{2+}]_i$, and binds Ca^{2+} with a 1:1 stochiometry and a K_D of 114 nm, which increases with increased ionic strength and increases approximately two fold when the temperature is increased from room temperature to 37°C (Cobbold and Rink, 1987). This dye also suffers from poor fluorescence brightness (Rink and Pozzan, 1986).

A newer dye, fluo-3 is excited by light in the visible wavelength range, providing advantages of reduced autofluoresence from tissue/cells loaded with this agent. Fluo-3 does not undergo a wavelength shift after binding Ca^{2+}, has a 40 fold fluorescence intensity increase and a weaker affinity for Ca^{2+} (K_D = 400 nM) when compared to quin-2 so concentrations of up to 5-10 μM are permitted. This dye has the advantages of causing less photodamage and possesses higher absorbency, thus allowing a lower

concentration of dye on loading. Fluo-4 is another dye based on fluo-3 that possesses further improvements for fluorescence procedures and is capable if generating stronger fluorescence signals.

4.1.6. Aims:

The main aim of this Chapter is to establish an assay for nicotine- and KCl-evoked functional responses by monitoring fluorescence changes in fura-2 loaded SH-SY5Y cell suspensions. Changes in $[Ca^{2+}]_i$ provide information on the source of Ca^{2+} entry to the cell after receptor activation. Chronic drug treatments that have been shown to upregulate nAChR in this cell line will also be applied to establish the functional status of upregulated nAChR in response to acute challenges with either nicotine or KCl. These experiments will provide an insight into the functional properties of responses to both acute and chronic application of nicotinic agonists and KCl depolarisation.

4.2. Methods.

4.2.1. Drugs and reagents:

Nicotine, KCl and verapamil were made up daily in distilled water before addition to the cuvette of SH-SY5Y cell suspensions. (±)-Anatoxin-a and mecamylamine were stored as stocks of 1 mM in distilled water, at -20°C. α-CTX-ImI and α-CTX-MII were kept as stocks of 100 μM and 11.2 μM, respectively, in distilled water at -20°C. MLA was kept at -20°C in absolute ethanol, as stocks of 1 μM and 100 μM. Nicotine, DMAC, KCl, verapamil, KN-62, KN-04 used for chronic treatment of SH-SY5Y cells

were made up as described in sections 2.4.2 and 3.3.3 and applied to cells on day 1 of drug treatment.

Cadmium chloride and mecamylamine were purchased from Sigma; (±)-anatoxin-a fumarate was purchased from Tocris, (Cookson, U. K.); α-CTX-MII was synthesised as previously described (Cartier *et al.*, 1996; Kaiser *et al.*, 1998); fura-2, AM solution in dry DMSO was purchased from Molecular Probes, (Eugene, Oregon USA). MLA was provided by Dr. I. S. Blaghbrough, (Dept. Pharmacy and Pharmacology, University of Bath, U.K.).

4.2.2. Maintenance of SH-SY5Y cells:

SH-SY5Y cells were sub-cultured and grown to confluency in 175 cm^2 flasks containing 25 ml of supplemented medium as described in section 3.3.2. For chronic treatments, drugs were added 3-5 days after the cells reached confluency in the 175 cm^2 flasks. Four days later, the confluent 7-9 day old cultures were harvested for measurement of $[Ca^{2+}]_i$.

4.2.3. Measurement of $[Ca^{2+}]_i$:

Measurements of $[Ca^{2+}]_i$ from SH-SY5Y cells in suspension were made as previously described (Murphy *et al.*, 1991a; Forsythe *et al.*, 1992; Sharples *et al.*, 2000). In brief, cultures were washed twice with warm Ca^{2+}-free PBS (150 mM NaCl, 8 mM K_2HPO_4, 2 mM KH_2PO_4, pH 7.4, 37°C) before removing the cells by incubating for 3 min at 37°C in Ca^{2+}-free PBS. The cell suspension was centrifuged (500 x g, 3 min) and the cell pellet resuspended in 5 ml of Ca^{2+}-free HEPES buffer (10 mM HEPES, 145 mM

NaCl, 5 mM KCl, 1 mM $MgCl_2$-6-hydrate, 0.5 mM Na_2HPO_4 and 5.5 mM glucose dissolved in millipore water, pH 7.4) and recentrifuged (500 x g, 3 min). The cells were loaded with 5 μM fura-2 AM (similar to Lambert and Nahorski, 1990) by resuspending the pellet in 3 ml Ca^{2+}-free HEPES buffer containing 0.25% (w/v) BSA, to improve the solubilisation of the dye. Cells were incubated for 45 min in darkness at room temperature; this enables the fura-2 AM to be internalised within the cytoplasm of the SH-SY5Y cells where it becomes hydrolysed by non-specific esterases into the cell impermeant Ca^{2+}-sensitive fura-2 free acid (see Figure 4.2).

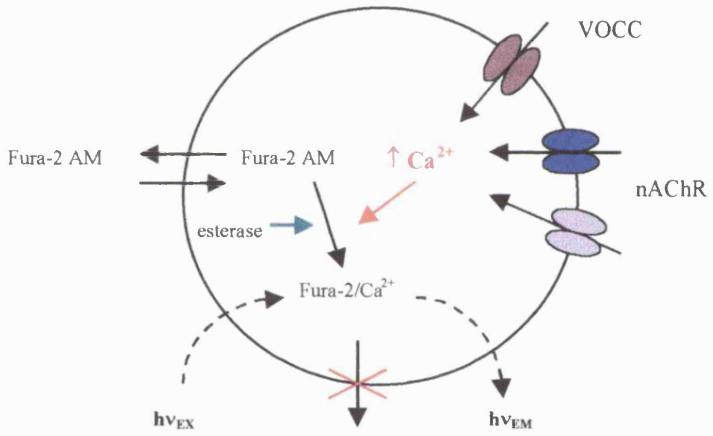

Figure 4.2. Determination of $[Ca^{2+}]_i$ in SH-SY5Y cells using fura-2 AM. *SH-SY5Y cells loaded with fura-2 AM incorporate the dye into their cytoplasm where it undergoes hydrolysis by non-specific esterases to produce the cell-impermeant Ca^{2+}-sensitive fura-2 free acid. Membrane depolarisation opens VOCC and nAChR activation increases the $[Ca^{2+}]_i$. Ca^{2+} binds to fura-2 causing a shift in its excitation wavelength ($h\nu_{EX}$) from λ=380 nm to λ=340 nm. Fluorescence emission ($h\nu_{EM}$) is monitored at λ=510 nm. After each experiment calibration was performed by the sequential addition of 0.5% Triton X-100 followed by 20 mM EGTA to obtain R_{max} and R_{min} values respectively, which are used to calculate $[Ca^{2+}]$ using the Grynkiewicz equation.*

Excess free dye was removed by x 4 washes by centrifugation (500 x g, 3 min) with 5 ml of Ca^{2+}-free HEPES buffer. When investigating the effect of the α7-selective antagonist α-bgt on nicotinic mediated responses, α-bgt (final concentration 50 nM) was co-incubated with fura-2 AM for 45 min at room temperature.

The cell density was adjusted to 1-2 x 10^6 cells/ml and $[Ca^{2+}]_i$ was measured in 2 ml aliquots of cells kept in suspension using a magnetic cell stirred cuvette, maintained at 37°C by a thermostatically controlled heat exchanger, in a PTI dual-excitation photofluorimeter. The excitation wavelengths were 340 nm and 380 nm, with an emission wavelength of 510 nm, 4 nm slit width, equipped with Pti software version 2.060 (Photon Technology International Inc., Deerpark Drive, South Brunswick, NJ08852 USA). Before the addition of nicotinic agonist or KCl, 2 mM $CaCl_2$ was introduced into the cuvette and the fura-2 fluorescence was monitored for 80 s (see Figure 4.3). Where used, antagonists (mecamylamine (10 μM), MLA (10 nM, 100 nM, 1 μM), α-CTX-IMI (1 μM) or α-CTX-MII (112 nM)), or inhibitors KN-62 (5 μM), its inactive analogue, KN-04 (5 μM) or the L-type VOCC blocker verapamil (5 μM)) were added 5 min before the addition of acute nicotine or KCl.

4.2.3.1. Calibration of $[Ca^{2+}]_i$ measured in SH-SY5Y cells suspensions:

At the end of the experiment with each cuvette of SH-SY5Y cells in suspension, calibration was performed. This was achieved by sequentially adding 0.5% Triton X-100 to lyse the cells in order to obtain R_{max} (the fluorescence of Ca^{2+}-saturated dye), followed by 20 mM EGTA to determine R_{min}, the fluorescence signal quenching the dye (Figure 4.3).

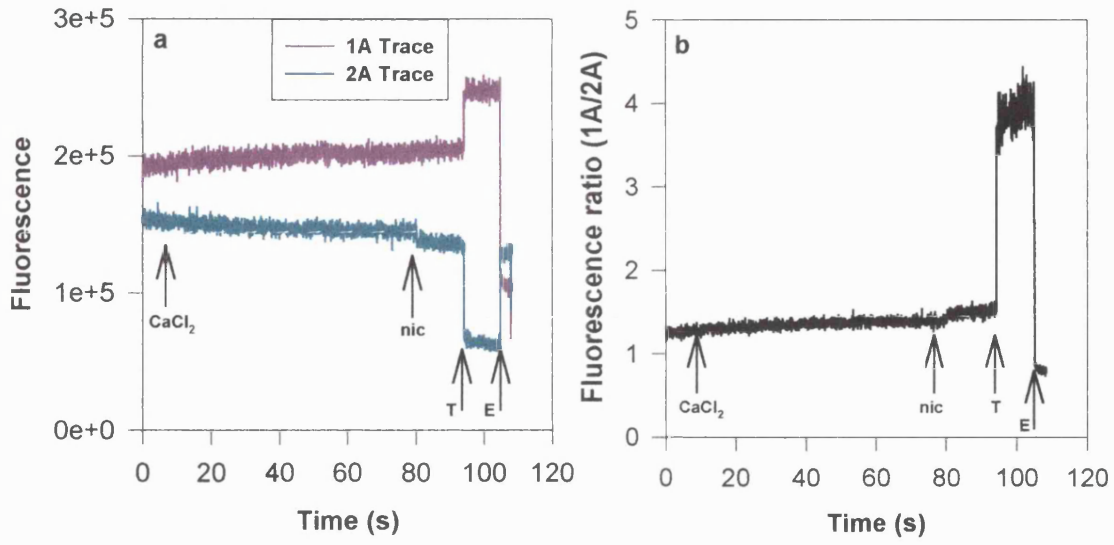

Figure 4.3. Respective fluorescence traces for (a) Fura-2 at 340 nm and 380 nm as traces 1A and 2A and as (b) the fluorescence ratio of 340 nm/380 nm. *SH-SY5Y cell suspensions were loaded with 5 μM fura-2 before measuring the changes in fluorescence after the application of $CaCl_2$ for 80 s until a stable baseline has been recorded before the application of nicotine (nic; 10 μM (small response observed on this scale)). Calibration was determined by the addition of 0.5% Triton X-100 (T) followed by 20 mM EGTA (E).*

$[Ca^{2+}]_i$ was determined from the fluorescence ratio of fura-2 at 340 nm/380 nm excitation (A_{340}/A_{380}; given as R below) (Figure 4.3b) as described by the Grynkiewicz Equation (Grynkiewicz *et al.*, 1985):

$$[Ca^{2+}]_i = K_D*[(R-R_{min})/(R_{max}-R)]*(S_{f2}/S_{b2})$$

where K_D is the dissociation constant of fura-2 for Ca^{2+} binding, 224 nM (Tsien *et al.*, 1982), R_{min} is the fluorescence ratio under "zero" Ca^{2+} conditions, R_{max} is the fluorescence ratio under saturating Ca^{2+} conditions and S_{f2}/S_{b2} is the ratio for fluorescence values of Ca^{2+}-free and Ca^{2+}-saturated fura-2, measured at the excitation wavelengths 380 nm and 340 nm respectively and emission at 510 nm. The ratio of

fluorescence at the two wavelengths, 380 nm and 340nm, is directly related to the ratio of the two forms of the dye and can be used to calculate $[Ca^{2+}]_i$.

4.2.4. Data Analysis:

Changes in $[Ca^{2+}]_i$ were expressed as mean ± S.E.M. and, where appropriate, as a percentage of the increase in $[Ca^{2+}]_i$ recorded from control cells. For concentration-response curves, agonist responses were calculated as a percentage of the change in $[Ca^{2+}]_i$ produced by a maximum stimulating concentration of agonist or KCl depolarisation, assayed in parallel SH-SY5Y cell suspensions on the same day. Data were expressed as means ± S.E.M. of at least five determinations and the EC_{50} value for concentration-response curves was calculated by fitting the data to the Hill equation, using the non-linear least squares curve fitting facility of Sigma Plot V2.0 for windows:

$$\% \text{ maximal stimulation} = 100\%/(1+[L]/EC_{50})^{nH}$$

where n_H is the Hill number, [L] is the concentration of the nicotinic agonist or KCl depolarisation, and EC_{50} is the concentration of ligand that produces 50% maximum stimulation. All data were analysed statistically using an analysis of variance (ANOVA) for repeated measures using SPSS (Statistics Package for Social Scientists, PC version).

4.3. Results.

4.3.1. Acute nicotine and KCl depolarisation increase $[Ca^{2+}]_i$ in SH-SY5Y cells:

The resting $[Ca^{2+}]_i$ in fura-2-loaded SH-SY5Y cells was 140 ± 4 nM (n=160). An acute challenge of nicotine produced an increase in fluorescence, which relates to an elevation of $[Ca^{2+}]_i$ (Figure 4.4b). Acute nicotine stimulation resulted in a rapid increase in fluorescence reaching a maximum within 1-2 s that was sustained as a plateau (Figure 4.4b inset). This plateau level was taken to be the value of the nicotine-evoked response and used to derive the $[Ca^{2+}]_i$. Nicotine-evoked increases in $[Ca^{2+}]_i$ in a concentration-dependent manner, with a maximum increase observed in response to 100 μM nicotine, which elevated $[Ca^{2+}]_i$ by 102 ± 9 nM from its resting level (n=29; Figure 4.4a). Taking this increase in $[Ca^{2+}]_i$ in response to 100 μM nicotine as 100%, responses to a range of nicotine concentrations were analysed in parallel, and used to construct a concentration response curve (Figure 4.4b). The half-maximum response (EC_{50}) for nicotine-evoked increases in $[Ca^{2+}]_i$ was 7.5 ± 4 μM.

Acute stimulation with KCl depolarisation also produced a concentration-dependent response to $[Ca^{2+}]_i$ (Figure 4.4c) with a rapid increase in $[Ca^{2+}]_i$ and produced a maximum value after 1-2 s of application. This level of $[Ca^{2+}]_i$ was maintained as a steady plateau similar to the responses evoked by nicotine (see inset Figure 4.4c). The maximum increase in $[Ca^{2+}]_i$ was achieved with 80 mM KCl, which increased the $[Ca^{2+}]_i$ by 100 ± 12 nM (n=12). Taking the response to 80 mM KCl as 100% a concentration-response curve was constructed for KCl (Figure 4.4c). The EC_{50} corresponded to 26 ± 8 mM KCl.

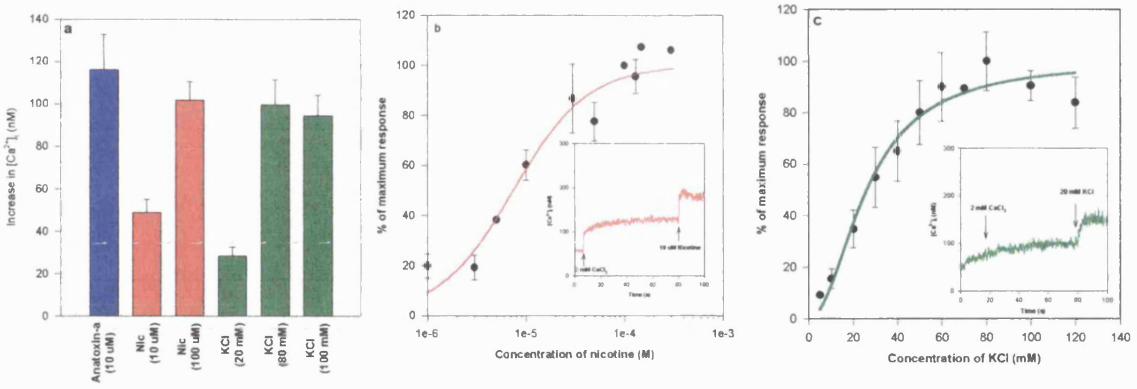

Figure 4.4. The effect of nicotinic agonists and KCl depolarisation on $[Ca^{2+}]_i$ in SH-SY5Y cell suspensions. *(a) Increases in $[Ca^{2+}]_i$ evoked by (±)-anatoxin-a (10 μM), nicotine (nic; 10 μM, 100 μM) and KCl depolarisation (20 mM, 80 mM, 100 mM). (b) A concentration response curve was constructed with a range of nicotine concentrations. The response to 100 μM nicotine was taken as 100% and all other values were expressed as a percentage of this. (Inset) A representative time course trace of $[Ca^{2+}]_i$ evoked by nicotine (10 μM). (c) A concentration response curve was constructed with a range of KCl concentrations. The response to 80 mM KCl was taken as 100% and all other values were expressed as a percentage of this. (Inset) A representative time course trace of $[Ca^{2+}]_i$ evoked by of KCl. Data points for both dose response curves were fitted to the Hill equation. All values are the mean ± S.E.M. from at least 5 independent cultures.*

The increase in $[Ca^{2+}]_i$ evoked by (±)-anatoxin-a (10 μM) was measured in parallel with nicotine and KCl, and was found to elicit a response comparable to that of 100 μM nicotine (Figure 4.4a). We have previously shown that this concentration of (±)-anatoxin-a produces a maximum effect (Sharples *et al.*, 2000) and the present results indicate that nicotine (100 μM) and (±)-anatoxin-a (10 μM) are equally efficacious in evoking increases in $[Ca^{2+}]_i$. This observation is compatible with the fact that (±)-anatoxin-a is approximately 10 fold more potent than nicotine. The increases in $[Ca^{2+}]_i$ induced by 100 μM nicotine and by 10 μM (±)-anatoxin-a are also similar to that evoked by a maximum effective concentration of KCl (Figure 4.4a).

4.3.2. The effect of nicotinic antagonists on nAChR evoked increases in $[Ca^{2+}]_i$:

Nicotinic antagonists were examined for their effect on nicotine-evoked increases of $[Ca^{2+}]_i$ in fura-2 loaded SH-SY5Y cell suspensions. The increase in $[Ca^{2+}]_i$ after acute nicotine was completely blocked when SH-SY5Y cells were exposed to 10 μM mecamylamine for 5 min before the nicotine challenge (Figs 4.5 and 4.6a). Mecamylamine itself had no effect on basal levels of $[Ca^{2+}]_i$ (Figure 4.5). This result confirms that the response to nicotine is mediated by nAChR.

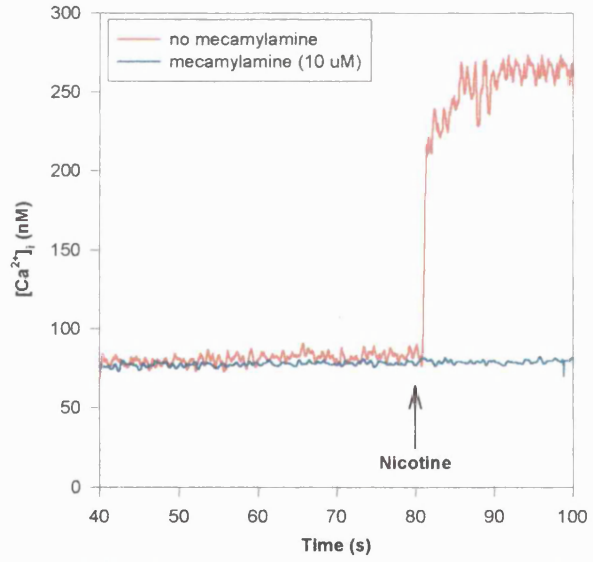

Figure 4.5. The effect of mecamylamine on nicotine-evoked increases in $[Ca^{2+}]_i$ in SH-SY5Y cells. *The effect of nicotine (100 μM) was observed in the presence and absence of mecamylamine (10 μM). The antagonist was applied 5 min prior to exposure to nicotine and was found to completely abolish the nicotine-evoked increase in $[Ca^{2+}]_i$ without significantly affecting the basal intracellular $[Ca^{2+}]_i$.*

To characterise pharmacologically which nAChR subtypes might be involved in mediating the elevation in $[Ca^{2+}]_i$ in SH-SY5Y cells, a selection of chemically distinct, subtype-selective antagonists were used to address the relative contributions of different nAChR subtypes to the plateau of Ca^{2+} entry evoked by nicotine. This was achieved either by incubating the antagonist with the SH-SY5Y cells at the time of fura-2 loading

(when using α-bgt), or for a 5 min incubation of antagonist following the initial Ca^{2+} transient and before the subsequent application of an acute nicotine challenge.

The SH-SY5Y cell line has previously been shown to possess functional α3β2* nAChR, that are upregulated after chronic nicotine treatment (Wang *et al.*, 1998). α3* nAChR in SH-SY5Y cells are possible candidates for the functional response mediated by nicotine. The α3β2-selective antagonist α-CTX-MII (112 nM; Cartier *et al.*, 1996) was found to block 50 ± 5% of the increase in $[Ca^{2+}]_i$ evoked by 10 μM nicotine (Figure 4.6a).

In addition to α3* nAChR, nAChR containing the α7 subunit are also present in SH-SY5Y cells. To explore if α7* nAChR contribute to the functional response mediated by nicotine, MLA was examined. Because MLA is selective for α7* nAChR when used at low nM concentrations, rather than having absolute specificity, it was decided to examine the concentration-dependency of MLA inhibition of nicotinic-evoked (10 and 100 μM) increases in $[Ca^{2+}]_i$ (Figure 4.6b). The increase in the $[Ca^{2+}]_i$ in response to 10 μM nicotine was inhibited by 38 ± 10% (n = 6), 44 ± 4% (n = 3) and 53 ± 11% (n = 3) by 10 nM, 100 nM and 1 μM MLA respectively, compared to control responses. These concentrations of MLA blocked the elevation in $[Ca^{2+}]_i$ mediated by 100 μM nicotine by 30 ± 9% (n =3), 31 ± 13% (n = 4) and 49 ± 6% (n = 5) respectively (Figure 4.6b). The lower concentration of MLA (10 nM) significantly inhibited responses to both 10 and 100 μM nicotine by similar amounts, and this degree of inhibition was not increased by a great deal after raising the concentration of MLA to 100 nM. These data suggest an inhibition of the $[Ca^{2+}]_i$ evoked by nicotine is mediated in part by α7* nAChR. This was further verified using two other α7-selective antagonists. α-CTX-IMI (1 μM; Pereira *et al.* (1996)) and α-bgt (50 nM) were found to block 10 μM nicotine-evoked increases in

$[Ca^{2+}]_i$ by 39 ± 5% (n = 4) and 41 ± 8% (n = 5) respectively; these results are comparable to the 40 ± 6% (n = 4) inhibition mediated by MLA (10 nM) (Figure 4.6a). These data show an α7 component of the $[Ca^{2+}]_i$ mediated response by 10 μM nicotine.

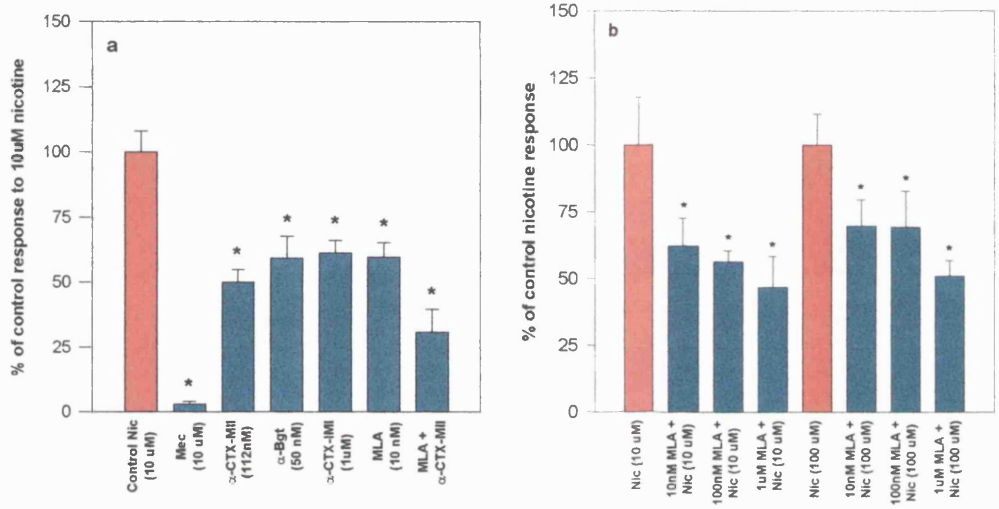

Figure 4.6. The effect of nicotinic antagonists on increases in $[Ca^{2+}]_i$ evoked by nicotine in fura-2 loaded SH-SY5Y cells. *SH-SY5Y cell suspensions were incubated with either (a) mecamylamine (mec; 10 μM), α-conotoxin-MII (α-CTX-MII; 112 nM), α-bungarotoxin (α-bgt; 50 nM), α-conotoxin-IMI (α-CTX-IMI; 1 μM), MLA (10 nM), or co-application of MLA (10 nM) and α-CTX-MII (112 nM) prior to an acute nicotine challenge. (b) The effect of various concentrations of MLA were investigated on the response to acute nicotine (10 μM and 100 μM). The control response to nicotine (nic; 10 μM or 100 μM) was measured in parallel and expressed as 100%. All other responses were calculated as a percentage of this acute nicotinic response in untreated control cells. Each bar represents the mean ± S.E.M. of at least 4 independent experiments. * Indicates significantly different from control at $p<0.05$; one way ANOVA.*

When MLA (10 nM) and α-CTX-MII (112 nM) were applied together for 5 min to SH-SY5Y cells in suspension, a partially additive inhibition of the nicotine-evoked increase in $[Ca^{2+}]_i$ of 69 ± 9% was produced that was significantly different from the inhibition evoked by MLA (10 nM) or α-CTX-MII when applied alone. The α7- and α3β2-insensitive portion of the functional nicotinic response could be due to α3β4*

nAChR, but selective antagonists for this receptor subtype are not commercially available. These data indicate that functional responses evoked by nicotine are mediated by at least two receptor subtypes, α3β2* and α7* nAChR.

4.3.3. Acute nicotine and KCl increase $[Ca^{2+}]_i$ in SH-SY5Y cells via L-type VOCC:

Analysis of functional responses is perhaps made more complicated due to Ca^{2+} entry into the cell by other mechanisms for example via Ca^{2+} channels. Nicotine- and KCl-evoked increases in $[Ca^{2+}]_i$ were dependent on the presence of extracellular Ca^{2+} (data not shown). Section 3.4.4 has reported that KCl-evoked upregulation in contrast to nicotine-evoked upregulation of surface [^{125}I]-α-bgt binding sites involves Ca^{2+} entry via L-type VOCC and a CaM-kinase II-dependent pathway, in contrast to upregulation of these sites evoked by nicotinic agonists. It was therefore decided to explore the effect of the phenylalkylamine L-type VOCC blocker, verapamil. A 5 min exposure to verapamil (5 μM) resulted in the inhibition of both nicotine (10 μM, 100 μM) and KCl (80 mM) evoked increases in $[Ca^{2+}]_i$ when compared to control (Table 4.1). The responses to 10 μM and 100 μM nicotine were inhibited by 53 ± 7% (n = 4) and 82 ± 4% (n = 3) respectively, and responses to KCl (80 mM) appeared to be slightly less sensitive to verapamil showing 31 ± 1% (n = 3) inhibition compared to control.

Chronic treatment of SH-SY5Y cells with verapamil (5 μM) for 1 or 4 days prior to harvesting was also investigated. These treatments produced similar levels of inhibition of the nicotinic-induced increase in $[Ca^{2+}]_i$ by 53 ± 12% (n = 3; 1 day) and 48 ± 4% (n = 4; 4 days), compared with responses to nicotine (10 μM) from untreated, control cells assayed in parallel (Table 4.1). Thus the effect of prior chronic treatment with verapamil

is comparable to the inhibition of the $[Ca^{2+}]_i$ evoked by nicotine observed after an acute 5 min application of verapamil to the cuvette of cells. However, responses to 20 mM KCl were inhibited to 42 ± 5% (n = 3) and 50 ± 4 % (n = 4) after 1 or 4 days prior exposure to verapamil respectively. This contrasts with the lack of effect of an acute application of verapamil on $[Ca^{2+}]_i$ evoked by 20 mM KCl (inhibition of 8 ± 2%; n = 14). Thus chronic application of verapamil has a similar effect on responses to 10 μM nicotine and 20 mM KCl, whereas the acute (5 min) application of this drug has a greater effect on the nicotine-evoked response.

Table 4.1. The effect of acute and chronic treatment with verapamil on increases in $[Ca^{2+}]_i$ in SH-SY5Y cells stimulated by acute nicotine and KCl depolarisation. *Significantly different from control, *p<0.05, (One way ANOVA); n.d. not determined.*

		Verapamil (5μM) $[Ca^{2+}]_i$ % of control			**$CdCl_2$ (200 μM) $[Ca^{2+}]_i$ (% of control)**
Acute drug challenge		**5 min**	**1 Day pretreatment**	**4 Days pretreatment**	**5 min**
Nic	10 μM	47 ± 7% (n=4)*	47 ± 12% (n=3)*	52 ± 4% (n=4)*	24 ± 3% (n=2)*
	100 μM	18 ± 4% (n=3)*	n.d.	n.d.	n.d.
KCl	20 mM	91 ± 2% (n=14)	58 ± 5% (n=3)*	50 ± 4% (n=4)*	n.d.
	80 mM	69 ± 1% (n=3)*	n.d.	n.d.	n.d.

Due to the possibility of verapamil having a non-specific action on nicotinic receptors, the effect of $CdCl_2$, a general blocker of VOCC which does not block nicotinic currents at the concentration used (200 μM) (Quik *et al.*, 1997), was examined on nicotine-evoked increases in $[Ca^{2+}]_i$ accumulation. No significant change in the basal

$[Ca^{2+}]_i$ was observed after a 5 min incubation with $CdCl_2$ (200 μM) compared to untreated, control cells prior to the application of nicotine. The elevation in $[Ca^{2+}]_i$ evoked by acute nicotine (10 μM) was inhibited by 76 ± 3% (n = 2) in cells pretreated with $CdCl_2$. This indicates that a major proportion of the nicotine-evoked response arises from activation of VOCC. Taken together these results confirm that nicotine and KCl depolarisation increase $[Ca^{2+}]_i$ in part through Ca^{2+} influx via VOCC, possibly of the L-type subclass.

4.3.4. The effect of chronic drug treatments on nicotine- or KCl-evoked responses:

Chronic exposure (4 days) to nicotine (10 μM), DMAC (10 μM) and KCl (20 mM) was investigated. These concentrations of drugs have previously been demonstrated to differentially evoke upregulation of nAChR subtypes after this chronic drug exposure regime (see sections 3.4.2 and 3.4.5). Cells subjected to these chronic drug treatments were challenged with 10 μM and 100 μM nicotine and 20 mM KCl and increases in $[Ca^{2+}]_i$ examined (Figure 4.7). Nicotine and KCl at concentrations of 10 μM and 20 mM respectively, were chosen to elicit submaximum responses whereas nicotine at the higher concentration of 100 μM was chosen to evoke a maximum increase in $[Ca^{2+}]_i$.

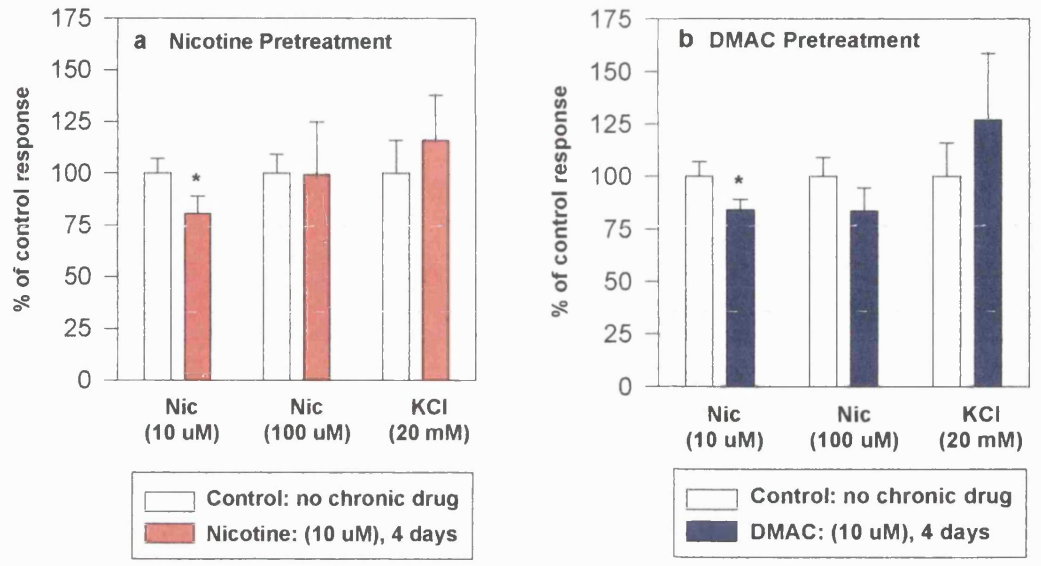

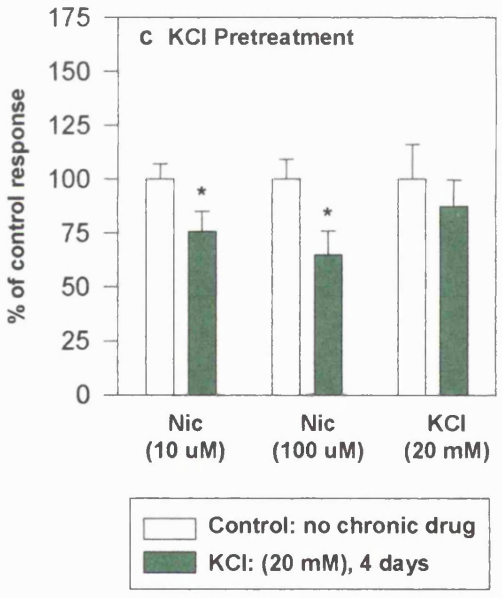

Figure 4.7. The effect of chronic drug treatment on $[Ca^{2+}]_i$ in SH-SY5Y cells. *SH-SY5Y cells were treated with (a) chronic nicotine (nic; 10 μM), (b) chronic DMAC (10 μM) and (c) chronic KCl (20 mM) for 4 days. On the day of assay the cells were washed rigorously before measuring $[Ca^{2+}]_i$. The effect of acute nicotine (nic; 10 μM, 100 μM) and KCl (20 mM) applied to untreated control cells was taken as 100% and the response to acute drug challenges were calculated as a percentage of this control. Each bar represents the mean ± S.E.M. of at least 4 independent experiments. * Indicates significantly different from control at $p<0.05$; one way ANOVA.*

Chronic treatment with both nicotine (10 μM) and DMAC (10 μM) produced significant decreases in the $[Ca^{2+}]_i$ measured after an acute submaximum-stimulating concentration of nicotine (10 μM) but no significant differences after acute maximum stimulating nicotine (100 μM) or KCl challenges (Figure 4.7a and b). Chronic

pretreatment with KCl (20 mM) elicited significant decreases in function after acute submaximum or maximum nicotine concentrations. Although not significant, there was a trend towards a decrease in functional responses after an acute KCl challenge in chronic KCl pretreated cells when compared to untreated, control cells (Figure 4.7c). Responses to acute DMAC were not investigated due to its intense colour, even when diluted, which was found to interfere with the fluorescence recording.

4.3.5. The effect of acute MLA on nicotine-evoked responses produced by SH-SY5Y cells after chronic drug treatment:

SH-SY5Y cells chronically treated with nicotine or KCl caused a significant decrease in the $[Ca^{2+}]_i$, evoked by an acute nicotine challenge, by 27 ± 13% (n = 3) and 26 ± 7% (n = 4) respectively, compared to the nicotine response elicited in untreated control cells. The effect of acute MLA (10 nM) on nicotine-evoked responses was examined in cells chronically treated with either nicotine or KCl, to identify if there were any changes in the proportion of $[Ca^{2+}]_i$ mediated via α7* nAChR. Acute MLA incubation inhibited the increase in $[Ca^{2+}]_i$ evoked by a challenge with nicotine applied to control cells by 40 ± 8% (n = 5; Figure 4.8) in agreement with our previous experiments (Figure 4.6). Chronic nicotine pretreated cells (4 days), significantly increased the $[Ca^{2+}]_i$ when challenged with acute nicotine (52 ± 22%; n = 6) after a 5 min incubation with MLA (compared to chronic nicotine treated cells not exposed to MLA) (Figure 4.8). This increase in $[Ca^{2+}]_i$ evoked by a nicotine challenge in chronic nicotine treated cells after a preincubation with MLA, results in a similar increase in $[Ca^{2+}]_i$ as observed with a nicotine challenge in untreated cells. However, chronic KCl pretreated cells exposed to MLA for 5 min prior to an acute nicotinic challenge, inhibited the nicotine-evoked

increase in $[Ca^{2+}]_i$ by 9 ± 9% (n = 7) when compared to the response evoked in the absence of MLA. MLA therefore had no significant effect on the nicotine-evoked $[Ca^{2+}]_i$ response in KCl pretreated cells (Figure 4.8).

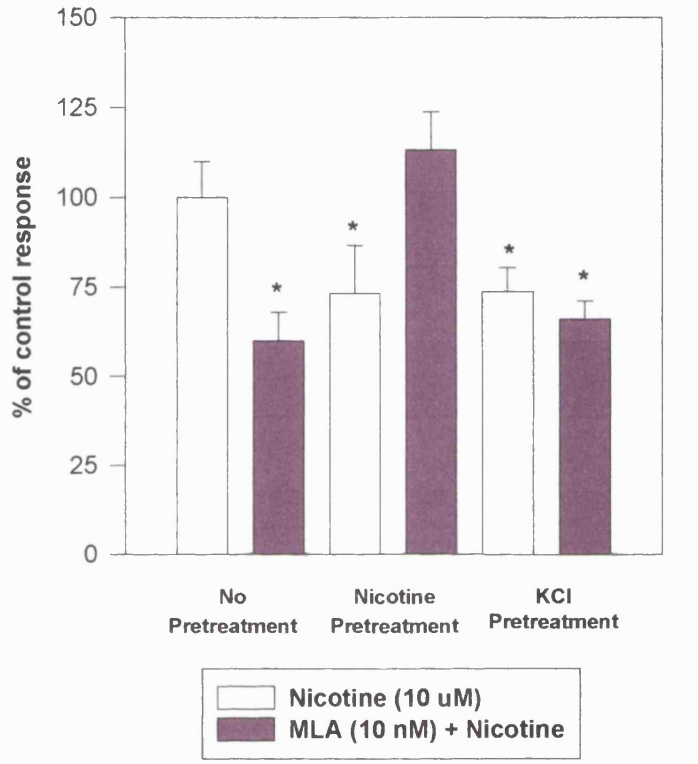

Figure 4.8. The effect of acute MLA on $[Ca^{2+}]_i$ evoked by nicotine in chronically treated cells. *Fura-2 loaded SH-SY5Y cell suspensions were incubated for 5 min with MLA (10 nM) prior to an acute drug challenge with nicotine (10 μM). Increases in $[Ca^{2+}]_i$ (nM) were recorded from control, nicotine (10 μM) or KCl (20 mM) pretreated cells. The data are expressed as a percentage of the acute nicotine (10 μM)-evoked increase in $[Ca^{2+}]_i$ measured in untreated control cells. Each bar represents the mean ± S.E.M. of at least 4 independent experiments. * Indicates significantly different from the nicotine-evoked response in control untreated cells at $p<0.05$; one way ANOVA.*

4.3.6. The effect of chronic treatment with KN-62 or KN-04 on acute nicotine- and KCl-evoked responses in SH-SY5Y cells:

This study has previously shown that chronic treatment with KN-62 alone (5 μM; 4 days) dramatically upregulates [^{3}H]-epibatidine binding sites in SH-SY5Y cells (see section 3.4.6). It was therefore decided to investigate whether chronic exposure of SH-SY5Y cells to either KN-62 (5 μM) or its inactive analogue, KN-04 (5 μM) altered the subsequent response to acute nicotine (10 μM) or KCl (20 mM). KN-04 treatment had no significant effect on basal levels of Ca^{2+} in SH-SY5Y cells prior to stimulation with nicotine or KCl (basal $[Ca^{2+}]_i$ were 112 ± 10 nM (control, n = 3) and 125 ± 4 nM (KN-04, n = 14). However in KN-62-treated cells, basal $[Ca^{2+}]_i$ was 97 ± 5nM (n = 14) which was significantly lower when compared to control levels ($p<0.05$) in untreated cells. Acute nicotine (10 μM) or KCl (20 mM) produced similar increases in $[Ca^{2+}]_i$ in KN-04 pretreated cells and untreated cultures grown and assayed in parallel (Table 4.2). In contrast, KN-62 pretreatment significantly reduced responses of $[Ca^{2+}]_i$ evoked by both acute nicotine and KCl, when compared to either control or KN-04 pretreated cells (Table 4.2). If the nicotine- and KCl-evoked increases in $[Ca^{2+}]_i$ are taken into consideration and compared to the baseline $[Ca^{2+}]_i$ in each condition, the comparative increases in $[Ca^{2+}]_i$ are not significantly different from each other (Table 4.3). Therefore, although chronic KN-62 treatment decreases the basal $[Ca^{2+}]_i$ compared to control, acute drug challenges evoke similar increases in $[Ca^{2+}]_i$ when expressed as a percentage of the basal $[Ca^{2+}]_i$ for each chronic condition, compared to those observed in control cells (Table 4.3).

Table 4.2. Comparison of increases in $[Ca^{2+}]_i$ evoked by nicotine (10 μM) or KCl (20 mM) in untreated control cells and cells that were chronically treated with KN-04 (5 μM) or KN-62 (5 μM) for 4 days. *Subsequent changes elicited by nicotine or KCl are expressed as a percentage of the increase in $[Ca^{2+}]_i$ evoked by nicotine or KCl in untreated control cells. Significantly different from control, *p<0.05, (One way ANOVA).*

	Pretreatment		
	Control	**KN-04 (5 μM)**	**KN-62 (5 μM)**
Nicotine (10 μM) (% of control)	100 ± 5 (n=3)	106 ± 6 (n=5)	82 ± 1 (n=5)*
KCl (20 mM) (% of control)	100 ± 14 (n=3)	95 ± 7 (n=3)	75 ± 6 (n=3)*

Table 4.3. Comparison of the $[Ca^{2+}]_i$ evoked by nicotine (10 μM) or KCl (20 mM) as a percentage of the basal $[Ca^{2+}]$ in each condition. *Significantly different from control, *p<0.05, (One way ANOVA).*

	Pretreatment		
	Control	**KN-04 (5 μM)**	**KN-62 (5 μM)**
Basal $[Ca^{2+}]$ (nM) (for nicotine-evoked responses)	112 ± 10 (n=3)	125 ± 4 (n=14)	97 ± 5 (n=14)*
Nicotine evoked ↑ $[Ca^{2+}]_i$ as a % of the basal $[Ca^{2+}]$	19 ± 3 (n=3)	18 ± 2 (n=3)	20 ± 3 (n=3)
Basal $[Ca^{2+}]$ (nM) (for KCl-evoked responses)	100 ± 6 (n=3)	123 ± 12 (n=3)	92 ± 12 (n=3)
KCl evoked ↑ $[Ca^{2+}]_i$ as a % of the basal $[Ca^{2+}]$	14 ± 1% (n=3)	18 ± 10 (n=3)	19 ± 3 (n=3)

4.4. Discussion.

The purpose of this Chapter was to evaluate the responses evoked by nicotine and KCl depolarisation in control and chronic drug treated SH-SY5Y cells loaded with fura-2, and to evaluate the proportion of Ca^{2+} influx through various nAChR subtypes and their functional status after chronic drug treatment. nAChR are highly permeable to Ca^{2+}, therefore the influx of this ion through the activated receptor can be utilised as a measure of nAChR function. nAChR possess a Ca^{2+} permeability, which in the case of α7* nAChR, is comparable to NMDA glutamate receptors (Rogers and Dani, 1995) and upon activation a substantial Ca^{2+} influx into the cell is generated. The SH-SY5Y cell line and its parent human neuroblstoma cells, SK-N-SH have previously been shown to be useful cell lines in which to study reproducible fura-2/quin-2 fluorescence changes in response to depolarisation by KCl or activation of nicotinic and muscarinic receptors by nicotine and muscarine respectively (Noronha-Blob *et al.*, 1989; Lambert and Nahorski, 1990; Lambert *et al.*, 1990; Murphy *et al.*, 1991a).

Cell suspensions of fura-2 loaded SH-SY5Y cells and quin-2/fura-2 loaded SK-N-SH cells have previously shown the basal $[Ca^{2+}]_i$ to range from 70 ± 8 mM (Lambert and Nahorski, 1990; 1.3 mM $CaCl_2$), 98 ± 4 nM (Martin *et al.*, 1999), 129 ± 8 mM (Noronha-Blob *et al.*, 1989; 1 mM $CaCl_2$) to 199 ± 14 nM (Murphy *et al.*, 1991a; 1 mM $CaCl_2$) at rest. Ca^{2+} responses in neurons upon nicotinic agonist stimulation have also been observed in rat CNS primary hippocampal neuronal cultures (Barrantes *et al.*, 1995b) and in SH-SY5Y cells (Sharples *et al.*, 2000) with basal $[Ca^{2+}]_i$ in the range of 200-400 nM. In this study the basal $[Ca^{2+}]_i$ was approximately 140 nM after 80 s in the presence of 2 mM $CaCl_2$ before the addition of agonist, which is in the range of values reported in the literature. In the presence of 2 mM $CaCl_2$ both KCl and nicotine evoked

concentration-dependent increases in $[Ca^{2+}]_i$ with maximum stimulation occurring at 80 mM and 100 μM and half maximum stimulation occurring at 26 ± 8 mM and 7.5 ± 4 μM, respectively. These values are similar to responses evoked by nicotine and KCl in the parent SK-N-SH cell line (Noronha-Blob *et al.*, 1989) and in SH-SY5Y cells (Lambert *et al.*, 1990).

In the present study the accumulation of $[Ca^{2+}]_i$ induced by the maximum effective concentration of nicotine is comparable to the $[Ca^{2+}]_i$ evoked by the maximum effective concentration of KCl in this cell line. (±)-Anatoxin-a is a product of the freshwater alga *Anabena flos-aquae* and a potent nicotinic agonist; for comparison, the effect of (±)-anatoxin-a was examined as this compound was previously shown to produce maximum stimulation of $[Ca^{2+}]_i$ at concentrations of 10 μM, being 10 fold more potent than nicotine (Sharples *et al.*, 2000). (±)-Anatoxin-a (10 μM) was found to be equally efficacious in stimulating increases in $[Ca^{2+}]_i$ as compared to 100 μM nicotine and 80 mM KCl depolarisation consistent with (±)-anatoxin-a being at least 10 fold more potent than nicotine, in this system. The increases in $[Ca^{2+}]_i$ evoked by nicotine are small in comparison to the dramatic fluorescence increases induced by muscarinic agonists in the SH-SY5Y cells line (Murphy *et al.*, 1991a; Forsythe *et al.*, 1992; Martin *et al.*, 1999).

In the absence of extracellular Ca^{2+}, both nicotine and KCl challenges were completely ineffective in augmenting $[Ca^{2+}]_i$. A previous study examining the effect of fluo-3 loaded chick ciliary ganglion neurones, when challenged with nicotine (0.5 – 1 μM) or KCl depolarisation (50 mM), were found to produce detectable fluorescence responses that were prevented in the presence of the Ca^{2+} chelator, EGTA, reminiscent of the Ca^{2+}-dependence observed in this study. This cell line is therefore a suitable

model system for studying the functional responses evoked by KCl depolarisation and nAChR activation after acute drug challenges and hence for examining the effect of chronic drug treatments on nicotine- and KCl-evoked responses.

4.4.1. Acute nicotinic antagonist treatment and $[Ca^{2+}]_i$ measured in response to nicotine:

4.4.1.1. Mecamylamine-sensitivity of the nicotinic response:

The nicotinic evoked increases in $[Ca^{2+}]_i$ are mediated in a mecamylamine-sensitive manner. In the presence of mecamylamine there is a 100% inhibition of the increase in $[Ca^{2+}]_i$ induced by an acute nicotinic challenge. This result demonstrates that nicotine activates nAChR, resulting in the stimulation of a Ca^{2+}-dependent accumulation of $[Ca^{2+}]_i$ in SH-SY5Y cells. In addition to this non-selective nicotinic antagonist, further experiments were performed with nAChR subtype selective antagonists to explore the nAChR subtypes that may be involved in mediating the nicotinic-evoked increase in $[Ca^{2+}]_i$.

4.4.1.2. nAChR subtypes involved in mediating the nicotine-evoked stimulation of $[Ca^{2+}]_i$ in SH-SY5Y cells:

Two major classes of nAChR are abundantly expressed in SH-SY5Y cells. One class of nAChR contain the α3 subunit resulting in receptor combinations of α3 or α3 and α5 with either the β2 or β4 subunits. The α3β2* nAChR have previously been shown to be upregulated after chronic nicotine treatment *in vitro* (Wang *et al.*, 1998). These α3* nAChR desensitise relatively slowly and are insensitive to α-bgt blockade (Zhang *et al.*, 1994). The second class of nAChR located within SH-SY5Y cells can be recognised by

their sensitivity to α-bgt blockade and contain the α7 gene product (Couturier *et al.*, 1990; Vernallis *et al.*, 1993; Blumenthal *et al.*, 1999).

Previous studies have demonstrated that activation of both α3* and α7* nAChR cause depolarisation and increase the $[Ca^{2+}]_i$ directly by means of their permeability to Ca^{2+} and indirectly via VOCC (Vijayaraghavan *et al.*, 1992; Rathouz *et al.*, 1995). Specific inhibitors of these classes of nAChR were used to elucidate the nAChR subtypes mediating this response. The results demonstrate that α-CTX-MII, a selective antagonist that binds to the interface between α3 and β2 subunits in α3β2* nAChR (Cartier *et al.*, 1996), blocked 50% of the evoked increase in $[Ca^{2+}]_i$ elicited by 10 μM nicotine. This identifies α3β2* nAChR being involved in the functional nicotinic-evoked response in $[Ca^{2+}]_i$ in SH-SY5Y cells.

It was also decided to investigate the action of α7-selective antagonists and their effect on nicotinic-induced elevations of $[Ca^{2+}]_i$ in SH-SY5Y cells. Vijayaraghavan *et al.* (1992) established that preincubating chick ciliary ganglion neurones with α-bgt (20-50 nM) for 40 min prior to the nicotine challenge, abolished the effect of nicotine elevating $[Ca^{2+}]_i$ above resting levels. MLA also abolished the nicotinic response of ciliary ganglion neurones with an IC_{50} of 1-2 nM (Vijayaraghavan *et al.*, 1992). This is consistent with the study by Séguéla *et al.* (1993) who showed that at least a portion of the increase in $[Ca^{2+}]_i$ is the result of Ca^{2+} flux through α7* nAChR when this receptor subtype is expressed as homomeric nAChR in *Xenopus* oocytes. Whole-cell patch-clamp recording from chick ciliary ganglion neurones *in situ* demonstrates that approximately 49% of the charge entering these cells was mediated by an α-bgt-sensitive synaptic current, further demonstrating that α7* nAChR evoke increases in $[Ca^{2+}]_i$ in neurones.

MLA is selective for α7* nAChR at low nanomolar concentrations; therefore the effect of a range of concentrations of MLA on nicotine-evoked fluorescence responses in SH-SY5Y cells was investigated. In the present study, the partial inhibition of nicotine-evoked responses by MLA (10 nM – 1 μM) is similar to the level of inhibition (56 ± 7%) of nicotine-induced fluorescence responses observed after incubating ciliary ganglion neurones with MLA (10 nM) (Vijayaraghavan *et al.*, 1992). The increase in $[Ca^{2+}]_i$ accumulation evoked by a maximum effective concentration of nicotine (100 μM) was also inhibited by MLA in a concentration-dependent manner; 10 nM and 100 nM MLA diminished the 100 μM nicotine-evoked elevation in $[Ca^{2+}]_i$ by approximately 30%, with 1 μM MLA increasing this inhibition to 49 ± 6%.

The present study used a prior incubation with a variety of α7-selective nicotinic antagonists: MLA (10 nM), α-bgt, α-CTX-IMI, to investigate the Ca^{2+} release evoked by an acute challenge with nicotine. All of these antagonists partially blocked the nicotinic mediated increase in $[Ca^{2+}]_i$ by approximately 40%. Taken together, the results are consistent with the specific blockade of α7* nAChR. The coincubation of an α3β2- and an α7-selective antagonist did not produce a complete block of the nicotinic mediated response, the block was only partially additive, producing an inhibition of approximately 70%, indicating that the nicotine-evoked accumulation of $[Ca^{2+}]_i$ is mediated by at least two populations of nAChR; one class containing α3β2 interfaces and the other subtype containing α7 nAChR subunits. The remaining portion of fluorescence maintained in the presence of MLA and α-CTX-MII could be due to Ca^{2+} influx through α3β4* nAChR. At the time of this study selective antagonists for α3β4* nAChR were not available to us. The α-CTX, α-CTX-AU1B has been demonstrated to be selective for α3β4* nAChR and will be a useful pharmacological ligand to

characterise the proportion of Ca^{2+} flux mediated through these nAChR in SH-SY5Y cells if it becomes available generally (Luo *et al.*, 1998).

4.4.2. The role of VOCC in nicotine- and KCl-evoked responses:

Both α3* and α7* nAChR function have been shown to increase $[Ca^{2+}]_i$ indirectly, by producing sufficient current to depolarise the membrane and subsequently activate VOCC (Vijayaraghavan *et al.*, 1992; Rathouz *et al.*, 1995). Vijayaraghavan *et al.* (1992) demonstrated that the rise in $[Ca^{2+}]_i$ evoked by nicotine and KCl depolarisation was abolished by Ca^{2+} channel blockers when applied to chick ciliary ganglion neurones.

Verapamil, a phenylalkylamine that inhibits L-type VOCC, was used to examine its effect on the fluorescence signal evoked by an acute nicotine challenge and KCl depolarisation. Prior incubation with verapamil indicated that approximately 50% of the nicotine-evoked response appeared to be dependent on activation of L-type Ca^{2+} channels. To confirm that verapamil was exerting its effect on L-type VOCC and not indirectly on nAChR (as is the case for the dihydropyridines, another class of L-type Ca^{2+}-channel blockers (López *et al.*, 1993)), Cd^{2+}, an ion that generally blocks several classes of VOCC with no affinity for nAChR was examined. Cd^{2+} abolished most of the nicotine-induced fluorescence response, inferring that much of the increase in $[Ca^{2+}]_i$ resulting from nAChR activation depended on VOCC. Previous studies have also shown that pretreatment with the VOCC blocker Cd^{2+} substantially abolished nicotine-induced increases in $[Ca^{2+}]_i$ in rat hippocampal neurones (Barrantes *et al.*, 1995b) and nicotine- and KCl-evoked increases in $[Ca^{2+}]_i$ in chick ciliary ganglion neurones (Vijayaraghavan *et al.*, 1992). This implies that Ca^{2+} influx through activated nAChR causes membrane depolarisation, enough to open VOCC and to evoke an approximate

75% influx of Ca^{2+}, via L- and probably N-type VOCC in SH-SY5Y cells. The opening of VOCC by nAChR evoked membrane depolarisation has been implicated as a mechanism for the modulation of neurotransmitter release by presynaptic nAChR (Soliakov and Wonnacott, 1996).

Verapamil was found to partially block the KCl depolarisation response at both maximum and submaximum concentrations. This is in agreement with the effect of nifedipine, a dihydropyridine that acts preferentially on high threshold Ca^{2+} channels, which was found to block the nicotine-evoked signal while only partially blocking the KCl-induced response (Vijayaraghavan *et al.*, 1992). Nifedipine was applied 3 min before the challenge with either nicotine or KCl, an incubation period analogous to that used for verapamil in the present study (Vijayaraghavan *et al.*, 1992). KCl (25 mM) evoked a response that was 90 ± 8% compared to control in the presence of nifedipine, which parallels closely to the 91 ± 2% KCl-evoked response observed in the present study after verapamil. This identifies a difference in blockade evoked by L-type VOCC blockers on nicotine- and KCl-induced fluorescence responses in SH-SY5Y cells. This implies that different VOCC predominate in evoking the nicotine and KCl responses or that the KCl-induced response (20 mM) is not, in general, significantly inhibited by individual channel classes for example the L-type VOCC subtype after a short duration of exposure to verapamil.

The functional data generated in the present study was derived from cell suspensions of SH-SY5Y cells. This allows for an average fluorescence response from the whole population of cells in suspension to be recorded. The fluorescence response is therefore expressed as a percentage of basal fluorescence before the application of acute drug challenges rather than resolving local changes of $[Ca^{2+}]_i$ that may be higher under the plasma membrane after nAChR and VOCC activation. Studies that measure single cell

Ca^{2+} fluorescence may be useful to identify the influx of Ca^{2+} into SH-SY5Y cells after nicotine and KCl drug challenges and to dissect and quantitate the proportion of Ca^{2+} entering the cell by specific subtypes of VOCC and nAChR rather than observing global changes in $[Ca^{2+}]_i$.

4.4.3. The effect of chronic drug treatments on nicotine- and KCl-evoked responses:

4.4.3.1. Chronic treatment with nicotinic agonists and KCl:

Chronic treatment with either nicotine, DMAC or KCl upregulates the number of [^{125}I]-α-bgt binding sites on the surface of SH-SY5Y cells. In cells that have been chronically treated with nicotine or DMAC at the same concentrations that elicit upregulation, there is a decrease in the functional response evoked by a sub-maximum concentration of nicotine. There are no significant differences in the responses evoked by a maximum stimulating concentration of nicotine or KCl (20 mM) recorded from cells chronically treated with nicotine or DMAC. This result indicates that upregulated α7* nAChR display decreased functional responses, as fluorescence responses evoked by cells treated with nicotinic agonists are not significantly different from responses evoked by control cells even though there is an increase in [^{125}I]-α-bgt binding in terms of B_{max}. This decrease in receptor function could be viewed as a consequence of upregulation and a compensatory mechanism to aid in the reduction of $[Ca^{2+}]_i$ mediated by activation of upregulated α7* nAChR and would serve as an essential neuroprotective mechanism, given the reported high Ca^{2+} permeability of this LGIC and allow for optimal neuronal responsiveness *in vivo*. Chronic KCl treatment significantly diminishes the response evoked by nicotine at both half-maximum and maximum

concentrations with a trend to decrease the response evoked by an acute challenge with KCl. This indicates that chronic treatment with KCl, upregulates α7* nAChR as detected with [^{125}I]-α-bgt binding to the surface of SH-SY5Y cells, and these receptors also have a decrease in their functional activity compared to untreated control cells.

In terms of [^{3}H]-epibatidine binding, the responses are complicated as the experiments reported here have measured total cellular [^{3}H]-epibatidine binding sites in SH-SY5Y cells located both on the cell surface and also intracellularly, hence detecting both potentially functional and non-functional nAChR respectively. If the majority of sites upregulated by nicotinic agonist treatment are located intracellularly as proposed by Peng *et al.* (1997), Wang *et al.* (1998) and Whiteaker *et al.* (1998), this could explain the observed decrease in nicotinic agonist evoked response. Surface receptors are perhaps transported from the cell surface and/or accumulated intracellularly (Peng *et al.*, 1997; Wang *et al.*, 1998) hence accounting for the decreased functional responses mediated by the existing surface nAChR. Chronic KCl treatment does not significantly alter [^{3}H]-epibatidine binding sites, therefore the significant decreased fluorescence responses evoked by acute nicotine and the trend towards decreased responses evoked by a KCl challenge could be due to decreased function of the surface [^{3}H]-epibatidine binding sites. However, if KCl-evokes a change in α3* nAChR distribution by transporting receptors from the cell surface to cytoplasm of SH-SY5Y cells this could also explain differences in functional activity of α3* nAChR. KCl treatment does not alter the total number of [^{3}H]-epibatidine binding sites compared to control cells. However, if after KCl treatment a greater proportion of non-functional intracellular versus functional surface [^{3}H]-epibatidine binding sites are expressed, an overall reduction in nAChR function will result due to the lower expression of functional nAChR located on the cell surface.

In the case of chronic KCl treatment, reduced functional responses may be the result of a prolonged effect of KCl on VOCC in SH-SY5Y cells. De Lorme and McGee (1986) investigated the regulation of VOCC mediated by changes in membrane potential. It was shown that depolarisation of PC12 cells, by elevating the extracellular K^+ concentration (15 - 70 mM for up to 6 days), evoked a concentration-dependent loss of [^{3}H]-nitrendipine binding (De Lorme and McGee, 1986). The decrease of [^{3}H]-nitrendipine binding was due to a decrease in the maximum number of binding sites (B_{max}) without a change in the K_D, suggesting that the changes in [^{3}H]-nitrendipine binding evoked by chronic depolarisation reflect changes in the number of functional VOCC on the cell membrane. The present study shows that there is a trend for $[Ca^{2+}]_i$ evoked by acute drug challenges to be decreased after chronic KCl treatment compared to control, this could also be due to decreased numbers of VOCC in SH-SY5Y cells after KCl treatment. This could be verified by examining the verapamil-sensitive component of nicotine- and KCl-evoked responses in both nicotine and KCl chronically treated cells, to show if the L-type VOCC mediated component is decreased.

Wang *et al.* (1998) demonstrated that chronic nicotine treatment of tsA201 cells transfected with α3 and β2 nAChR subunits did not alter the functional response compared to control cells, as demonstrated by nicotinic application (100 μM) and whole cell patch clamp analysis. This higher nicotine concentration corresponds to the maximum stimulating concentration of nicotine used as a drug challenge in this present study; this concentration of nicotine had no significant effect on the function of nicotine and DMAC treated cells compared to control. The decreased responses evoked after chronic drug treatment are not due to residual ligand present due to the rigorous washout procedure before fura-2 loading of the SH-SY5Y cells. Lukas (1991) investigated functional activation of nAChR in TE671/RD (containing muscle type

nAChR) human clonal cell line and in PC12 cells after chronic nicotinic ligand exposure. After 3-72 hours exposure of either nicotine or carbamylcholine, treatments that previously induced upregulation of nAChR ligand binding sites, resulted in complete loss of function of nAChR in the TE671 cells and near complete loss of nAChR function in PC12 cells (Lukas, 1991). Hsu *et al.* (1996) investigated the effect of sustained nicotine exposure on α3β2* nAChR expressed in oocytes. Peak responses to 7 μM nicotine were observed before and after 48 hour exposure to nicotine (1 μM). Responses were decreased by 50-60% after exposure to nicotine for 24-48 hours with half-life of recovery of 7.5 hours (Hsu *et al.*, 1996). Functional inactivation may be another process occurring in the present study with SH-SY5Y cells after acute challenges with sub-maximum stimulating concentrations of nicotine. There is also the possibility that chronic nAChR activation and KCl depolarisation influence other aspects of the cells ability to enhance $[Ca^{2+}]_i$ by modulating cellular pathways downstream of nAChR activation. Such aspects relating to altered $[Ca^{2+}]_i$ signalling and chronic drug treatment have yet to be addressed in this field.

4.4.3.2. The effect of MLA on functional responses evoked by cells after chronic nicotinic agonist and KCl treatment:

To identify if the α7-sensitive component of nicotine-evoked responses in SH-SY5Y cells is altered after chronic treatment with either nicotine or KCl, the effect of MLA was investigated in both control and drug treated cells. The application of MLA to control cells results in the inhibition of the nicotine-evoked elevation of $[Ca^{2+}]_i$; in nicotine pretreated cells there is a significant reduction in the response evoked by nicotine that is significantly increased after a 5 min incubation with MLA. In KCl treated cells there is a significant decrease in the fluorescence response elicited by

nicotine with no significant difference in the presence of MLA. Additional approaches are needed to disentangle the nature and interplay between the effect of MLA when applied to chronic nicotine treated cells compared to untreated cells. Further experiments will help to elucidate the source of the increase in $[Ca^{2+}]_i$, whether it is from extracellular sources or from Ca^{2+} mobilisation from intracellular stores. MLA alone has no effect on basal levels of $[Ca^{2+}]_i$ but after chronic nicotine treatment when nAChR are less responsive to the same dose of nicotine, the presence of MLA in this condition acts to enhance the nicotine-evoked $[Ca^{2+}]_i$. Perhaps chronic nicotine treatment reduces the number of functionally available nAChR due to functional inactivation where nicotine would act like an "antagonist", then when the cells are exposed to MLA for a brief incubation this could increase the $[Ca^{2+}]_i$ evoked by nicotine. This intriguing effect of MLA on nicotine treated SH-SY5Y cells will be investigated in the near future in Dr Wonnacott's laboratory.

4.4.3.3. Chronic treatment with a CaM-kinase II inhibitor:

Previous data presented in this study identified that KCl-evoked upregulation of $[^{125}I]$-α-bgt binding sites in both primary hippocampal cultures (see section 2.7.2) and in SH-SY5Y cells (see section 3.4.4) was mediated by a CaM-kinase II dependent pathway and by Ca^{2+} influx through L-type VOCC. In the present study when KN-62 was applied alone for 4 days there was no change in $[^{125}I]$-α-bgt binding sites but a huge upregulation of $[^{3}H]$-epibatidine binding sites resulted and was not observed after chronic KN-04 treatment. This suggested that upregulation of $[^{3}H]$-epibatidine binding sites evoked by KN-62 was by a CaM-kinase II dependent pathway. It was therefore decided to further investigate the effect of KN-62 and elucidate if chronic KN-62 treatment altered $[Ca^{2+}]_i$ within SH-SY5Y cells due to inhibition of CaM-kinase II.

Chronic KN-62 treatment decreased the basal $[Ca^{2+}]_i$ compared to control and KN-04 treated SH-SY5Y cells. This effect could be due to the ability of KN-62 to block VOCC or its inhibition of a CaM-kinase II dependent mechanism, hence lowering the $[Ca^{2+}]_i$. The nicotine- and KCl-evoked responses in SH-SY5Y cells chronically treated with KN-62 was significantly lower compared to the increase evoked by nicotine in control untreated cells and in KN-04 treated cells. However, if the drug-evoked increases of $[Ca^{2+}]_i$ are compared to the initial basal $[Ca^{2+}]_i$, the fluorescence increases in each of the conditions (either control, KN-04 or KN-62 treated) are of the same proportion of the basal level of $[Ca^{2+}]_i$ for each condition. As mentioned above, this lower basal $[Ca^{2+}]_i$ could be due to inhibition of CaM-kinase II, VOCC or perhaps an effect on Ca^{2+} mobilisation within the cytoplasm to produce a decrease in $[Ca^{2+}]_i$ after chronic KN-62 treatment for 4 days. This indicates that KN-62 pretreatment does not reduce the proportion of nicotine-evoked response compared to control cells, but has a decreased response due to a lower initial basal $[Ca^{2+}]_i$ level.

Together the data in this Chapter demonstrate that nicotine and KCl evoke $[Ca^{2+}]_i$ accumulation in a concentration- and Ca^{2+}-dependent manner. The nicotine-evoked response has been shown to be mediated by both $\alpha7^*$ and $\alpha3\beta2^*$ nAChR subtypes. Chronic drug treatments that differentially upregulate [^{125}I]-α-bgt and [^{3}H]-epibatidine binding sites in SH-SY5Y cells have also generated changes in the $[Ca^{2+}]_i$ evoked by nicotine and KCl challenges. This maybe related to changes in receptor numbers and their location in SH-SY5Y cells, although other targets (for example, VOCC) have also been discussed.

Chapter 5. Conclusions.

From the present study I conclude that:

- Increasing the KCl concentration form 5 to 20 mM upregulated [^{125}I]-α-bgt binding sites in primary hippocampal neurones, and in the SH-SY5Y human neuroblastoma cell line. KCl upregulates α7* nAChR by Ca^{2+} influx through L-type VOCC, a CaM-kinase II dependent pathway and by increasing the expression of α7 subunit RNA. In contrast, neither the level of [^{3}H]-epibatidine binding sites nor α3 subunit RNA levels were affected by chronic KCl treatment in SH-SY5Y cells. The finding in this study that chronic KCl depolarisation uniquely regulates the expression of α7 nAChR through L-type VOCC and a CaM-kinase II pathway, may reflect a mechanism underlying some form of neuronal plasticity and a possible role for α7 nAChR in neuronal development, synaptic plasticity and axonal regeneration after neuronal injury.
- The nicotinic agonists, nicotine and DMAC, upregulated [^{125}I]-α-bgt (by increasing B_{max} with no change in K_D) and [^{3}H]-epibatidine binding sites in SH-SY5Y cells; these sites were not upregulated by a mechanism involving Ca^{2+} influx through L-type VOCC, CaM-kinase II- or PKC-dependent pathways or increased transcription of the α3 and α7 subunit RNA levels. These data suggest that upregulation of [^{3}H]-epibatidine and [^{125}I]-α-bgt binding sites evoked by nicotinic agonists were mediated by post-transcriptional mechanisms that may be similar to those mechanisms proposed for the upregulation of the high affinity α4β2 nAChR subtype.
- An interesting result was obtained with KN-62 when chronically applied to SH-SY5Y cells for 4 days; KN-62 did not alter [^{125}I]-α-bgt binding, in contrast to evoking a huge upregulation of [^{3}H]-epibatidine binding sites. This is attributed to

KN-62 inhibiting CaM-kinase II as KN-04, an inactive analogue of KN-62 had no significant effect on the level of [^{3}H]-epibatidine binding sites compared to control. This result has led to the hypothesis that KN-62 treatment could cause an intracellular accumulation of nAChR labelled by [^{3}H]-epibatidine.

- Both nicotine and KCl produced concentration- and Ca^{2+}-dependent increases in $[Ca^{2+}]_i$ in fura-2 loaded SH-SY5Y cells. Nicotinic responses were partially inhibited by L-type VOCC blockers, identified by blockade with verapamil, and completely abolished after prior exposure to mecamylamine. It was shown that α3β2* and α7* nAChR contribute to the nicotinic response, as indicated by the nAChR subtype selective antagonists α-CTX-MII and a variety of α7-selective compounds, α-bgt, α-CTX-IMI and MLA (10 nM). MLA was found to block nicotine-evoked fluorescence responses in a concentration-dependent manner.

- Chronic nicotinic agonist treatment significantly decreased the fluorescence response evoked by a sub-maximum concentration of nicotine indicating that, although these chronic drug treatments elicit upregulation of [^{125}I]-α-bgt and [^{3}H]-epibatidine binding sites, the upregulated receptors located on the surface are less functional than nAChR located in control untreated cells.

- Chronic KCl treatment significantly decreased responses to nicotine and there was also a trend to decrease the fluorescence response evoked by an acute challenge with KCl compared to responses evoked in control untreated cells. These diminished functional responses could also be explained by KCl affecting the numbers of surface versus intracellular nAChR or by a reduction in numbers of VOCC, hence reducing functional responses.

- The effect of a 5 min incubation of MLA on cells chronically treated with nicotine resulted in enhanced functional responses evoked by nicotine. This unexpected result must be due to a synergistic effect of acute MLA and chronic nicotine treatment as there was no significant difference between the nicotine-evoked increase in $[Ca^{2+}]_i$ observed in chronic KCl treated cells in either the presence or absence of MLA. Subsequent experiments will need to be performed to address the role of extracellular Ca^{2+} and intracellular Ca^{2+} stores in mediating or amplifying the increase in the fluorescence response evoked by nicotine applied to (pre-MLA exposed) chronic nicotine treated SH-SY5Y cells. The source of this enhanced increase in $[Ca^{2+}]_i$ evoked by an acute nicotine challenge in nicotine treated cells after 5 min incubation with MLA will be investigated in Dr Wonnacott's laboratory in the near future.

- Chronic treatment for 4 days with KN-62 elicited significant decreases in the $[Ca^{2+}]_i$ evoked by both KCl and nicotine when compared to either control cells or cells pretreated for 4 days with KN-04, the inactive analogue of KN-62. There were no significant differences observed between control and KN-04 pretreated cells. Comparatively the increase in $[Ca^{2+}]_i$ evoked by acute nicotine or KCl expressed as a percentage of the basal $[Ca^{2+}]_i$ in each condition was not significantly different from each other. The lower basal level of $[Ca^{2+}]_i$ recorded in KN-62 treated SH-SY5Y cells suggests that intracellular Ca^{2+} may be mobilised by a CaM-kinase II pathway.

- Together these data demonstrate that chronic drug treatment regimes differentially upregulate the number of nicotinic binding sites by different cellular mechanisms producing changes in nAChR function as measured by changes in $[Ca^{2+}]_i$ using fura-2 fluorescence.

Previous studies investigating α3* and α7* nAChR have been less extensive than those performed with the high affinity α4β2 nAChR subtype. The experiments presented here produce a story consistent with previous reports with regard to upregulation of nAChR subunits after chronic nicotine treatment (Barrantes *et al.*, 1995a; Peng *et al.*, 1997; Molinari *et al.*, 1998) and that these receptors are located intracellularly. It was interesting to observe that KCl-evoked upregulation of [^{125}I]-α-bgt binding sites in both primary hippocampal cultures and SH-SY5Y cells was dependent on Ca^{2+} flux through L-type VOCC and the activation of CaM-kinase II. The increased expression of α7 subunit RNA in SH-SY5Y cells after chronic KCl treatment was in agreement with data generated in rat SCG neurones after chronic KCl depolarisation (De Koninck and Cooper, 1995). The signalling events downstream of CaM-kinase II leading to the increase in expression of the α7 nAChR subunit transcript have not been determined in this study.

The high Ca^{2+} permeability of α7* nAChR and their ability to raise $[Ca^{2+}]_i$ along with α3* nAChR, perhaps offers a physiological role for these nAChR subtypes to influence subsequent intracellular Ca^{2+}-dependent cellular events using Ca^{2+} as a second messenger within neurones. This implicates the activation of nAChR coupled with the activation of L-type VOCC to increase $[Ca^{2+}]_i$ with a resulting endorsement of neuronal survival. Previous studies have shown that nicotine and KCl treatment are implicated in the mediation of Ca^{2+}-dependent processes including neurite retraction (Pugh and Berg, 1994) and neurite growth (Chan and Quik, 1993; Solem *et al.*, 1995). Nicotine, carbachol and KCl depolarisation all promote survival of avian ciliary ganglion neurones and it was demonstrated that nicotinic agonist treatment enhanced survival by activation of α-bgt-sensitive nAChR (Hory-Lee and Frank, 1995) as well as α3* nAChR in these neurones (Pugh and Margiotta, 2000). Neuronal survival has also been

demonstrated in rat brain sections (Shimohama *et al.*, 1998), hippocampal (Semba *et al.*, 1996) and cerebellar neurones (Miñana *et al.*, 1998) and in PC12 cells (Egea *et al.*, 1999; Li *et al.*, 1999) resulting either from activation of α-bgt nAChR or membrane depolarisation.

Messi *et al.* (1997) reported that spinal cord motoneurones undergo cell death during embryonic development. Survival of these motoneurones is essential to prevent disorders such as amyotrophic lateral sclerosis. Activation of nAChR have been implicated in promoting cell survival of spinal cord motoneurones by significantly increasing the $[Ca^{2+}]_i$ to result in the rescue of a significant number of cultured spinal cord motoneurones (Messi *et al.*, 1997) and PC12 cells (Yamashita and Nakamura, 1996) from programmed cell death. Activation of both α3* and α7* nAChR may be necessary to ensure total neuronal survival. This could be a reason why after chronic drug treatment α3* and α7* nAChR are upregulated, but have differential functional responses when exposed to acute drug challenges. It is possible that both nAChR activation and KCl depolarisation elicit independent microdomains of high $[Ca^{2+}]_i$ and this may be physiologically relevant as a neuroprotective mechanism in developing neurones, in neurite retraction and in the mediation of Ca^{2+}-regulated events in neurones.

CaM-kinase II is a ubiquitous cytosolic enzyme involved in a number of cellular processes making it an attractive candidate in terms of regulating α7 subunit gene expression. CaM-kinase II has been implicated in long-term modifications of synaptic transmission via post-translational modifications of receptors, ion channels and altering neurotransmitter release (reviewed by Hanson and Schulman, 1992; Lisman, 1994) and in pathways involved with the storage of memory and the modulation of synaptic transmission. Some of these functional roles for CaM-kinase II have been suggested as

roles for the α7* nAChR. A Ca^{2+}-calmodulin mechanism has also been implicated in the promotion of survival of PC12 cells (Egea *et al.*, 1999) and chick spinal cord motoneurones (Soler *et al.*, 1998) evoked by membrane depolarisation. Depolarisation-induced neurite outgrowth with 45 mM KCl applied to PC12 cells, required CaM-kinase II and IV activation and was also reduced in the presence of L-type VOCC blockers (Solem *et al.*, 1995). Neuronal survival was prevented in the presence of VOCC blockers (Chan and Quik, 1993; Pugh and Berg, 1994; McGehee *et al.*, 1995, Role and Berg, 1996; Pugh and Margiotta, 2000). CaM-kinase II has also been implicated in the regulation of neurite outgrowth and growth cone motility in neuronal Neuro 2a and NG 108-15 neuroblastoma cell lines (Goshima *et al.*, 1993). These data are consistent with earlier reports of the developmental regulation of the α7* nAChR by depolarisation at the transcriptional level (Courtier *et al.*, 1990) and being dependent on a CaM-kinase II pathway and Ca^{2+} influx through VOCC (De Koninck and Cooper, 1995) and consistent with the transcriptional control of α7 subunit RNA in this study by KCl depolarisation.

Mandelzys *et al.* (1994) observed that there was greater than a three-fold increase in the level of expression for both the α3 and α7 nAChR subunit mRNA during the first two postnatal weeks in rat sympathetic neurones. This change in nAChR gene expression occurs during a period when most synapses are forming on these sympathetic neurones, providing yet further support that nAChR containing the α3 and α7 subunits are important during neuronal development. α3* and α7* nAChR may increase $[Ca^{2+}]_i$ during synapse formation to regulate second messenger systems that allow for the modulation of other proteins needed to establish synapses (see Changeux, 1991). Neurite retraction and synaptic remodelling are known to occur and be important during development. Presynaptic α-bgt-sensitive nAChR could provide a mechanism to terminate axonal growth during development and may also be extrapolated to

pathological sprouting of neural processes and synaptic reorganisation in the brain after seizures or neuronal injury. Perhaps there is synergy between nAChR activation, KCl depolarisation on neurones and the involvement of CaM-kinase II in the upregulation of [^{125}I]-α-bgt binding sites evoked by KCl implicating these processes in mechanisms underlying forms of synaptic plasticity.

Low level activation of α3* and α7* nAChR may also have important effects on intracellular Ca^{2+}-mediated events by creating high local concentrations of Ca^{2+} immediately beneath the plasma membrane after direct Ca^{2+} influx through these LGIC. This suggests a role for these nAChR subtypes in events related to synaptogenesis (De Koninck and Cooper, 1995). These effects may be neuroprotective due to the mode of entry of Ca^{2+} via nAChR and also by the activation of VOCC. Specific local changes in Ca^{2+} could be the trigger to activate other Ca^{2+}-dependent pathways or enzymes to regulate cell signalling and other cellular processes in neuronal cells. Collins *et al.* (1991) demonstrated that a sustained increase in $[Ca^{2+}]_i$ induced by raising KCl from 5 to 40 mM promoted neuronal survival in ciliary ganglion neurones. This effect was abolished in the presence of PN 200-110, a dihydropyridine VOCC blocker, thereby preventing KCl to induce survival of neurones.

The decrease in nAChR function observed after some chronic drug treatments may be a compensatory process so that during enhanced KCl or nAChR activated conditions there is not Ca^{2+} overload to the neurone that would induce apoptosis. One such function of nAChR activation would be to regulate the amount of Ca^{2+} entering the cell from extracellular sources and promote neuronal survival. By monitoring the levels of endogenous agonist ACh or membrane depolarisation this information could be relayed to trigger necessary Ca^{2+}-dependent cascades within neurones to regulate neuronal survival and ensure the prevention of or reduced apoptosis.

Continued study of α3* and α7* nAChR will help to elucidate physiological functional roles for these receptors. Upregulation of α3* and α7* nAChR have previously been shown to require higher concentrations of nicotine to evoke upregulation (Peng *et al.*, 1997; Wang *et al.*, 1998) compared to concentrations necessary to elicit upregulation of the high affinity α4β2 nAChR sites. These higher concentrations of nicotine may be relevant in some neurological conditions especially in schizophrenia where patients smoke excessively and have high plasma nicotine levels that could be capable of upregulating these specific nAChR subtypes, and neuroprotective in other neurological disorders such as AD and PD. The development of commercially available nAChR subtype-selective nicotinic ligands allow for further analyses and a better understanding of nicotinic-evoked modulation of nAChR, their modulation of signal transduction and involvement of Ca^{2+}-dependent cascades to mediate cellular functions including neuronal development, neuronal survival and their roles in neuromodulation and cytoprotection in pathological conditions and also as therapeutic applications in smoking cessation strategies.

References.

Adem A., Mattsson M. E., Norberg A. and Pahlman S. (1987). Muscarinic receptors in human SH-SY5Y neuroblastoma cell line: Regulation by phorbol ester and retinoic acid-induced differentiation. *Brain Res.*, **430**: 235-242.

Akabas M.H., Kaufmann C., Archdeacon P. and Karlin A. (1994). Identification of acetylcholine receptor channel-lining residues in the entire M2 segment of the α-subunit. *Neuron*, **13**: 919-927.

Alkondon M. and Albuquerque E. X. (1991). Initial characterisation of the nicotinic acetylcholine receptor in rat hippocampal neurons. *J. Recept. Res.*, **11**: 1001-1021.

Alkondon M. and Albuquerque E. X. (1993). Diversity of nicotinic acetylcholine receptors in rat hippocampal neurons I. Pharmacological and functional evidence for distinct structural subtypes. *J. Pharmacol. Exp. Ther.*, **265**: 1455-1473.

Alkondon M., Pereira E. F. R. and Albuquerque E. X. (1998). α-Bungarotoxin and methyllycaconitine-sensitive nicotinic receptors mediate fast synaptic transmission in interneurones of rat hippocampal slices. *Brain Res.*, **810**: 257-263.

Alkondon M., Pereira E. F. R., Wonnacott S. Albuquerque E. X. (1992). Blockade of nicotinic currents in hippocampal neurones defines methyllycaconitine as a potent and specific receptor antagonist. *Mol. Pharmacol.*, **41**: 802-808.

Amar M., Thomas P., Johnson C., Lunt G. G. and Wonnacott S. (1993). Agonist pharmacology of the neuronal α7 nicotinic receptor expressed in *Xenopus* oocytes. *F. E. B. S. Letts.*, **327**: 284-288.

Anand R., Conroy W. G., Schoepfer R., Whiting P. and Lindstrom J. (1991). Neuronal nicotinic acetylcholine receptors expressed in Xenopus oocytes have a pentameric quaternary structure. *J. Biol. Chem.*, **266**: 11192-11198.

Anand R., Peng X., and Lindstrom J. (1993a). Homomeric and native α7 acetylcholine receptors exhibit remarkably similar but non-identical pharmacological properties, suggesting that the native receptor is a heteromeric protein complex. *F. E. B. S. Letts.*, **327**: 241-246.

Anand R., Peng X., Ballesta J. J. and Lindstrom J. (1993b). Pharmacological characterisation of α-bungarotoxin-sensitive acetylcholine receptors immunoisolated from chick retina: contrasting properties of α7 and α8 subunit-containing subtypes. *Mol. Pharmacol.*, **44**: 1046-1050.

Anderson D. J. and Arneric S. P. (1994). Nicotinic receptor binding of [^{3}H]-cytisine, [^{3}H]-nicotine, and [^{3}H]-*N*-methylcarbamylcholine in rat brain. *Eur. J. Pharmacol.*, **253**, 261-267.

Arendash G. W., Sengstock G. J., Sanberg P. and Kem W. R. (1995). Improved learning and memory in aged rats with chronic administration of the nicotinic receptor agonist GTS-21. *Brain Res.*, **674**: 583-590.

Arias H. R. (2000). Localisation of agonist and competitive binding sites on nicotinic acetylcholine receptors. *Neurochem. Int.*, **36**: 595-645.

Ashton H. and Stepney R. (1982). Smoking psychology and pharmacology. Tavistock publications. London and New York.

Aubert I., Araujo D. M., Cécyre D., Robitaille Y., Gauthier S. and Quirion R. (1992). Comparative alterations of nicotinic and muscarinic binding sites in Alzheimer's and Parkinson's diseases. *J. Neurochem.*, **58**: 529-541.

Bading H., Ginty D. D. and Greenberg M. E. (1993). Regulation of gene expression in hippocampal neurones by distinct calcium signalling pathways. *Science*, **260**: 181-186.

Badio B. and Daly J. W. (1994). Epibatidine, a potent analgesic and nicotinic agonist. *Mol. Pharmacol.*, **45**: 563-569.

Badio B., Shi D., Garraffo H. M. and Daly J. W. (1995). Antinociceptive effects of the alkaloid epibatidine. Further studies on involvement of nicotinic receptors. *Drug Dev. Res.*, **36**: 46-59.

Balfour D. J. K. (1982). The effects of nicotine on brain neurotransmitter systems. *Pharmacol. Ther.*, **16**: 269-282.

Balfour D. J. K. (1989). Influence of nicotine on the release of monoamines in the brain. In: *Progress in brain research*. Norberg A., Fuxe K., Holmstedt B. and Sundwall A. (Eds.), **79**: 165-172.

Balfour D. J. K. (1990). Nicotine as the basis of the smoking habit. In *Psychotropic Drugs of Abuse*-Section 130 of the International Encyclopaedia of Pharmacology and Therapeutics. pp 453-481. Pergamon Press.

Balfour D. J. K. (1991). The neurochemical mechanisms underlying nicotine tolerance and dependence. In: The biology of drug tolerance and dependence (Ed: Pratt J. A.), Academic Press, pp 121-151.

Balfour D. J. K. (1994). Neural mechanisms underlying nicotine dependence. *Addiction*, **89**: 1419-1423.

Ballivet M., Nef P., Couturier S., Rungger D., Bader C. R., Bertrand D. and Cooper E. (1988). Electrophysiology of a chick neuronal nicotinic acetylcholine receptor expressed in *Xenopus* oocytes after cDNA injection. *Neuron*, **1**: 847-852.

Banker G. and Goslin K. (1991). Culturing nerve cells. Edited by Banker G. and Goslin K., MIT Press, Cambridge, Massachusetts and London, England.

Banker G. A. and Waxman A. B. (1988). Hippocampal neurones generate natural shapes in cell culture. In: *Intrinsic determinants of neuronal form and function*, pp 61-82. Edited by Lasek R. J. and Black M. M., New York, Alan R. Liss, Inc.. Edited by Lasek R. J. and Black M. M., New York, Alan R. Liss, Inc.

Barlow R. B. and Hamilton J. T. (1962). Effects of pH on the activity of nicotine and nicotine monomethiodide on the rat diaphragm preparation. *Br. J. Pharmacol.*, **18**: 543-549.

Barnard E. A. (1992). Receptor classes and the transmitter-gated ion channels *T. I. B. S.*, **17**: 368-374.

Barrantes G.E., Rogers A.T., Lindstrom J., and Wonnacott S. (1995a). α-Bungarotoxin binding sites in rat hippocampal and cortical cultures: initial characterisation, colocalisation with α7 subunits and up-regulation by chronic nicotine treatment. *Brain Res.*, **672**: 228-236.

Barrantes G. E., Murphy C. T., Westwick J. and Wonnacott S. (1995b). Nicotine increases intracellular calcium in rat hippocampal neurons via voltage gated calcium channels. *Neurosci. Letts.*, **196**: 101-104.

Batistatou A. and Greene L. A. (1991). Aurintricarboxylic acid rescues PC12 cells and sympathetic neurones from cell death cause by nerve growth factor deprivation: correlation with suppression of endonuclease activity. *J. Cell Biol.*, **115**: 461-471.

Bear M. F. (1996). A synaptic basis for memory storage in the cerebral cortex. *Proc. Natl. Acad. Sci.* USA., **93**: 13453-13459.

Bencherif M., Fowler K., Lukas R. J. and Lippiello P. M. (1995). Mechanisms of up-regulation of neuronal nicotinic acetylcholine receptors in clonal cell lines and primary cultures of fetal rat brain. *J. Pharmacol. Exp. Ther.*, **275**: 987-994.

Bennett J. A. and Dingledine R. (1995). Topology profile for a glutamate receptor: three transmembrane domains and a channel-lining reentrant membrane loop. *Neuron*, **14**: 373-384.

Bennett M. K., Erondu N. E. and Kennedy M. B. (1983). Purification and characterisation of a calmodulin-dependent protein kinase that is highly concentrated in brain. *J. Biol. Chem.*, **258**: 12735-12744.

Benowitz N.L. (1986). Clinical pharmacology of nicotine. *Ann. Rev. Med.*, **37**, 21-32.

Benowitz N. L. (1991). Nicotine and coronary heart disease. *T. C. M.*, **1**: 315-321.

Benowitz N. L. (1996). Pharmacology of nicotine: Addiction and Therapeutics. *Annl. Rev. Pharmacol. Toxicol.*,**36**: 597-613.

Benowitz N. L. and Jacob P. (1998). Pharmacokinetics and metabolism of nicotine and related alkaloids. In: *Neuronal nicotinic receptors: Pharmacology and therapeutic opportunities*, pp 213-234. Edited by Arneric S. P. and Brioni J. D. Wiley-Liss, New York, NY.

Benwell M. E. M. and Balfour D. J. K. (1984). Nicotine binding to brain tissue from drug-naïve and nicotine-treated rats. . *J. Pharm. Pharmacol.*, **37**: 405-409.

Benwell M. E. M., Balfour D. J. K. and Anderson J. M. (1988). Evidence that tobacco smoking increases the density of (-)-[^{3}H]-nicotine binding sites in human brain. *J. Neurochem.*, **50**: 1243-1247.

Beroukhim R. and Unwin N. (1995). Three-dimensional location of the main immunogenic region of the acetylcholine receptor. *Neuron*, **15**:323-331.

Berridge M. J. (1993). Inositol triphosphate and calcium signalling. *Nature*, **361**: 315-325.

Berridge M. J. (1998). Neuronal calcium signalling. *Neuron*, **21**: 13-26.

Berridge M. J., Bootman M. D. and Lipp P. (1998). Calcium - a life and death signal. *Nature*, **395**: 645-648.

Bertrand D., Bertrand S. and Ballivet M. (1992). Pharmacological properties of the homomeric α7-receptor. *Neurosci. Letts.*, **146**: 87-90.

Bessho Y., Nawa H. and Nakanishi S. (1994). Selective up-regulation of an NMDA receptor subunit mRNA in cultured cerebellar granule cells by K^+-induced depolarisation and NMDA treatment. *Neuron*, **12**: 87-95.

Betz H. (1990). Ligand-gated ion channels in the brain: the amino acid receptor superfamily. *Neuron*, **5**: 383-392.

Bhat R. V., Marks M. J. and Collins A. C. (1994). Effects of chronic nicotine infusion on kinetics of high-affinity nicotine binding. *J. Neurochem.*, **62**: 574-581.

Bjugstad K. B., Mahnir V. M., Kem W. R., Socci D. J. and Arendash G. W. (1996). Long-term treatment with GTS-21 or nicotine enhances water maze performance in aged rats without affecting the density of nicotinic receptor subtypes in neocortex. *Drug Dev. Res.*, **39**: 19-28.

Blumenthal E. M., Shoop R. D., and Berg D. K. (1999). Developmental changes in the nicotinic responses of ciliary ganglion neurones. *J. Neurophysiol.*, **81**: 111-120.

Bonhaus D. W., Bley K. R., Broka C. A., Fontana D. J., Leung E., Lewis R., Shieh A. and Wong E. H. F. (1995). Characterisation of the electrophysiological, biochemical and behavioural actions of epibatidine. *J. Pharmacol. Exp. Ther.*, **272**: 1199-1203.

Bottenstein J. E. and Sato G. H. (1979). Growth of a rat neuroblastoma cell line in a serum-free supplemented medium. *Proc. Natl. Acad. Sci. USA.*, **76**: 514-517.

Boulter J., Connolly J., Deneris E., Goldman D., Heinemann S. and Patrick J. (1987). Functional expression of two neuronal nicotinic acetylcholine receptors from cDNA clones identifies a gene family. *Proc. Natl. Acad. Sci. USA.*, **84**: 7763-7767.

Boulter J., O'Shea-Greenfield A., Duvoisin R. M., Connolly J., Wada E., Jensen A., Gardner P. D., Ballivet M., Deneris E. S., McKinnon D., Heinemann S. and Patrick J. (1990). α3, α5, and β4: Three members of the rat neuronal nicotinic acetylcholine receptor-related gene family from a gene cluster. *J. Biol. Chem.*, **265**: 4472-4482.

Bradford M. M. (1976). A rapid and sensitive method for the quantitation of microgram quantities of protein utilising the principle of protein dye binding. *Anal. Biochem.*, **72**: 248-254.

Brakenhoff G. J., van der Voort H. T. M., van Spronsen E. A., Linnemans W. A. M. and Nanninga N. (1985). Three-dimensional chromatin distribution in neuroblastoma nuclei shown by confocal scanning laser microscopy. *Nature*, **317**: 748-749.

Breese C. R., Marks M. J., Logel J., Adams C. E., Sullivan B., Collins A. C. and Leonard S. (1997). Effect of smoking history on [^{3}H]-nicotine binding in human post-mortem brain. *J. Pharmacol. Exp. Ther.*, **282**: 7-13.

Briggs C. A., Anderson D. J., Brioni J. D., Buccafusco J. J., Buckley M. J., Campbell J. E., Decker M. W., Donnelly-Roberts D., Elliott R. L., Gopalakrishnan M., Holladay M. W., Hui Y-H., Jackson W. J., Kim D. J. B., Marsh K. C., O'Neill A., Prendergast M. A., Ryther K. B., Sullivan J. P. and Arneric S. P. (1997). Functional characterisation of the novel neuronal nicotinic acetylcholine receptor ligand GTS-21 *in vitro* and *in vivo*. *Pharmacol. Biochem. Behav.*, **57**: 231-241.

Britto L. R. G., Keyser K. T., Lindstrom J. M., Karten H. J. (1992). Immunohistochemical localisation of nicotinic acetylcholine receptor subunits in the mesencephalon and diencephalon of the chick (*Gallus gallus*). *J. Comp. Neurol.*, **317**: 325-342.

Broide R. S., Robertson R. T. and Leslie F. M. (1996). Regulation of α7 nicotinic acetylcholine receptors in the developing rat somatosensory cortex by thalamocortical afferents. *J. Neurosci.*, **16**: 2956-2971.

Burnet P. W. J., Eastwood S. L. and Harrison P. J. (1994). Detection and quantitation of 5-HT1A and 5-HT2A receptor mRNA in human hippocampus using a reverse transcriptase-polymerase chain reaction (RT-PCR) technique and their correlation with binding site densities and age. *Neurosci. Letts.*, **178**: 85-89.

Cachelin A. B. and Jaggi R. (1991). β-subunits determine the time course of desensitisation in rat α3 neuronal nicotinic acetylcholine receptors. *Eur. J. Physiol. (Lond.)*, **419**: 579-582.

Cartaud J., Benedetti E. L., Cohen J. B., Meunier J. C. and Changeux J. P. (1973). Presence of a lattice structure in membrane fragments rich in nicotinic receptor protein from the electric organ of *Torpedo marmorata*. *F. E. B. S. Letts.*, **33**: 109-113.

Cartier G. E., Yoshikami D., Gray W. R., Luo S., Olivera B. M. and McIntosh J. M. (1996). A new α-conotoxin which targets α3β2 nicotinic acetylcholine receptors. *J. Biol. Chem.*, **271**: 7522-7528.

Castro N. G. and Albuquerque E. X. (1995). α-Bungarotoxin-sensitive hippocampal nicotinic receptor channel has a high calcium permeability. *Biophys. J.*, **68**: 516-524.

Chan J. and Quik M. (1993) A role for the neuronal nicotinic α-bungarotoxin receptor in neurite outgrowth in PC12 cells. *Neuroscience.*, **56**: 441-451.

Chang C. F., Gutierrez L. M., Mundina-Weilenmann C. and Hosey M. M. (1991). Dihydropyridine-sensitive calcium channels from skeletal muscle. *J. Biol. Chem.*, **266**: 16395-16400.

Changeux J. P. (1981). The acetylcholine receptor: an "allosteric" membrane protein. In *Harvey lectures*. Academic Press, **75**: 85-254.

Changeux, J. P., (1990). Functional architecture and dynamics of the nicotinic acetylcholine receptor: an allosteric ligand-gated ion channel. *Fidia Res. Found. Neurosci. Found. Lect.*, **4**: 21-168.

Changeux J. P. (1991). Compartmentalised transcription of acetylcholine genes during motor endplate epigenesis. *New Biol.*, **3**: 413-429.

Changeux J. P. and Edelstein S. J. (1998). Allosteric receptors after 30 years. *Neuron*, **21**: 959-980.

Chen D. and Patrick J. W. (1997). The α-bungarotoxin nicotinic acetylcholine receptor from rat brain contains only the α7 subunit. *J. Biol. Chem.*, **272**: 24024-24029.

Cheng Y-C. and Prusoff W. H. (1973). Relationship between the inhibition constant (K_i) and the concentration of inhibitor which causes 50 per cent inhibition (IC_{50}) of an enzymatic reaction. *Biochem. Pharm.*, **22**: 3099-3108.

Chiappinelli V. A. (1983). Kappa-bungarotoxin: A probe for the neuronal nicotinic receptor in the avian ciliary ganglion. *Brain Res.*, **277**: 9-21.

Chiara D. C. and Cohen J. B. (1997). Identification of amino acids contributing to high and low affinity *d*-tubocurarine sites in the *Torpedo* nicotinic acetylcholine receptor. *J. Biol. Chem.*, **272**: 32940-32950.

Chomczynski P. (1992). One-hour downward alkaline capillary transfer for blotting of DNA and RNA. *Anal. Biochem.*, **201**: 134-139.

Clarke P. B. S. (1992). The fall and rise of neuronal α-bungarotoxin binding proteins. *T. I. P. S.*, **13**: 407-413.

Clarke P. B. S., Schwartz R. D., Paul S. M., Pert C. B. and Pert A. (1985). Nicotinic binding in rat brain: autoradiographic representation of [^{3}H]-acetylcholine, [^{3}H]-nicotine and [^{125}I]-α-bungarotoxin. *J. Neurosci.*, **5**: 1307-1315.

Claudio T., Ballivet M., Patrick J and Heinemann S. (1983). Nucleotide and deduced amino acid sequence of *Torpedo californica* acetylcholine receptor γ subunit. *Proc. Natl. Acad. Sci.* USA., **80**: 1111-1115.

Cobbold P. H. and Rink T. J. (1987). Fluorescence and bioluminescence measurement of cytoplasmic free calcium. *Biochem. J.*, **248**: 313-328.

Collins A. C., Bhat R. V., Pauly J. R. and Marks M. J. (1990). Modulation of nicotinic receptors by chronic exposure to nicotinic agonists and antagonists. In Bock G., Marsh J. (eds): The biology of nicotine dependence. Ciba Foundation Symposia. West Sussex: John Wiley and Sons, pp 68-86.

Collins F., Schmidt M. F., Guthrie P. D. and Kater S. B. (1991). Sustained increase in intracellular calcium promotes neuronal survival. *J. Neurosci.*, **11**: 2582-2587.

Colquhoun L. M. and Patrick J. W. (1997). α3, β2, and β4 form heterotrimeric neuronal nicotinic acetylcholine receptors in *Xenopus* oocytes. *J. Neurochem.*, **69**: 2355-2362.

Conroy W. G. and Berg D. K. (1995). Neurons can maintain multiple classes of nicotinic acetylcholine receptors distinguished by different subunit compositions. *J. Biol. Chem.*, **270**: 4424-4431.

Conroy W. G., Vernallis A. and Berg D. K. (1992). The α5 gene product assembles with multiple acetylcholine receptor subunits to form distinctive receptor subtypes in brain. *Neuron*, **9**: 1-20.

Conti-Tronconi B. M., Dunn S. M. J., Barnard E. A., Dolly J. O., Lai F. A., Ray N. and Raftery M. A. (1985). Brain and muscle nicotinic acetylcholine receptors are different but homologous proteins. *Proc. Natl. Acad. Sci. USA.*, **82**: 5208-5212.

Cooper E., Couturier S. and Ballivet M. (1991). Pentameric structure and subunit stoichiometry of a neuronal nicotinic acetylcholine receptor. *Nature*, **350**: 235-238.

Costa L. G. and Murphy S. D. (1983). [^{3}H]-nicotine binding in rat brain: alteration after chronic acetylcholinesterase inhibition. *J. Pharmacol. Exp. Ther.*, **226**: 392-397.

Couturier S., Bertrand D., Matter J-M., Hernandez M-C., Bertrand S., Millar N., Valera S., Barkas T. and Ballivet M. (1990). A neuronal nicotinic acetylcholine receptor subunit (α7) is developmentally regulated and forms a homo-oligomeric channel blocked by αBTX. *Neuron*, **5**: 847-856.

Creese I. and Sibley D. R. (1980). Receptor adaptations to centrally acting drugs. *Ann. Rev. Pharmacol. Toxicol.*, **21**: 357-391.

Cully D. F., Vassilatis D. K., Liu K. K., Paress P. S., Van der Pleog L. H. T., Schaeffer J. M. and Arena J. P. (1994). Cloning of an avermectin-sensitive glutamate-gated chloride channel from *Caenorhabditis elegans*. *Nature*, **371**: 707-711.

Dailey M., Marrs G., Satz J. and Wait M. (1999). Concepts in imaging and microscopy: exploring biological structure and function with confocal microscopy. *Biol. Bull.*, **197**: 115-122.

Damaj M. I., Creasy K. R., Grove A. D., Rosecrans J. A. and Martin B. R. (1994). Pharmacological effects of epibatidine optical isomers. *Brain Res.*, **664**: 34-40.

Dani J. A. and Eisenman G. (1987). Monovalent and divalent cation permeation in acetylcholine receptor channels. *J. Gen. Physiol.*, **89**: 959-983.

Davies A. R. L., Hardick D. J., Blagbrough I. S., Potter B. V.L., Wolstenholme A. J. and Wonnacott S. (1999). Characterisation of the binding of [^{3}H]methylycaconitine: a new radioligand for labelling α7-type neuronal nicotinic acetylcholine receptors. *Neuropharmacol.*, **38**: 679-690.

Dávila-García M. I., Houghtling R. A., Qasba S. S. and Kellar K. J. (1999). Nicotinic receptor binding sites in rat primary neuronal cells in culture: characterisation and their regulation by chronic nicotine. *Mol. Brain Res.*, **66**: 14-23.

De Blas A. and Mahler H. R. (1978). Studies on nicotinic acetylcholine receptors in mammalian brain. Characterisation of a microsomal subfraction enriched in receptor function for different neurotransmitters. *J. Neurochem.*, **30**: 563-577.

Decker M. W. and Arneric S. P. (1998). Nicotinic acetylcholine receptor-targeted compounds: A summary of the development pipeline and therapeutic potential. In: *Neuronal nicotinic receptors: Pharmacology and therapeutic opportunities*, pp 395-411. Edited by Arneric S. P. and Brioni J. D., Wiley-Liss, New York, NY.

Decker M. W., Brioni J. D., Bannon A. W. and Arneric S. P. (1995). Diversity of neuronal nicotinic acetylcholine receptors: Lessons from behaviour and implications for CNS therapeutics. *Life Sci.*, **56**: 545-570.

De Fiebre C. M., Meyer E. M., Henry J. C., Muraskin S. I., Kem W. R. and Papke R. L. (1995). Characterisation of a series of anabaseine-derived compounds reveals that the 3-(4)-dimethylaminocinnamylidine derivative is a selective agonist at neuronal $\alpha7/^{125}$I-α-bungarotoxin receptor subtypes. *Mol. Pharm.*, **47**: 164-171.

De Koninck P. and Cooper E. (1995). Differential regulation of neuronal nicotinic ACh receptor subunit genes in cultured neonatal rat sympathetic neurones: specific induction of $\alpha7$ by membrane depolarisation through a calcium/calmodulin-dependent kinase pathway. *J. Neurosci.*, **15**: 7966-7978.

Delbono O., Gopalakrishnan M., Renganathan M., Monteggia L. M., Messi M. L. and Sullivan J. P. (1997). Activation of the recombinant human $\alpha7$ nicotinic acetylcholine receptor significantly raises intracellular free calcium. *J. Pharmacol. Exp. Ther.*, **280**: 428-438.

De Lorme E. M. and McGee R. Jr. (1986). Regulation of voltage-dependent Ca^{2+} channels of neuronal cells by chronic changes in membrane potential. *Brain Res.*, **397**: 189-192.

De Lorme E. M. and McGee R. Jr. (1988). Effects of prolonged depolarisation on nicotinic acetylcholine receptors on PC12 cells. *J. Neurochem.*, **50**: 1248-1252.

Deneris E. S., Boulter J., Swanson L.W., Patrick J. and Heinemann S. (1989). $\beta3$: A new member of nicotinic acetylcholine receptor gene family is expressed in brain. *J. Biol. Chem.*, **264**: 6268-6272.

Deneris E. S., Connolly J., Rogers S. W. and Duvoisin R. (1991). Pharmacological and functional diversity of neuronal nicotinic acetylcholine receptors. *T. I. P. S.*, **12**: 34-40.

Devillers-Thiéry A., Galzi J. L, Changeux J-P., Bertrand S. and Bertrand D. (1993). Functional architecture of the nicotinic acetylcholine receptor: a prototype of ligand-gated ion channels. *J. Memb. Biol.*, **136**: 97-112.

Devillers-Thiéry A., Giraudat J., Bentaboulet M. and Changeux J-P. (1979). The amino-terminal sequence of the 40,000 molecular weight subunit of the acetylcholine receptor protein from *Torpedo marmorata*. *F. E. B. S. Letts.*, **104**: 99-105.

Di Chiara G. (1992). Reinforcing drug seeking. *T. I. P. S.*, **13**: 428-429.

Dunnett S. B. and Björklund A. (1999). Prospects for new restorative and neuroprotective treatments in Parkinson's disease. *Nature*, **399**: suppl. A32-A39.

Egea J., Espinet C. and Comella J. X. (1999). Calcium influx activates extracellular-regulated kinase/mitogen-activated protein kinase pathway through a calmodulin-sensitive mechanism in PC12 cells. *J. Biol. Chem.*, **274**: 75-85.

Eichenbaum H., Schoenbaum G., Young B. and Bunsey M. (1996). Functional organisation of the hippocampal memory system. *Proc. Natl. Acad. Sci.* USA., **93**: 13500-13507.

Elgoyhen A. B., Johnson D. S., Boulter J., Vetter D. E. and Heinemann S. (1994). Alpha 9: an acetylcholine receptor with novel pharmacological properties expressed in rat hair cells. *Cell*, **79**: 705-715.

Enslen H. and Soderling T. R. (1994). Roles of calmodulin-dependent protein kinases and phosphatase in calcium-dependent transcription of immediate early genes. *J. Biol. Chem.*, **269**: 20872-20877.

Fagerström K. O., Pomerleau O., Giordani B. and Stelson F. (1994). Nicotine may relieve symptoms of Parkinson's disease. *Psychopharmacol.*, **116**: 117-119.

Fenster C. P., Rains M. F., Noerager B., Quick M. W. Lester R. A. (1997). Influence of subunit composition on desensitisation of neuronal acetylcholine receptors at low concentrations of nicotine. *J. Neurosci.*, **17**: 5747-5759.

Fenster C. P., Whitworth T. L., Sheffield E. B., Quick M. W. and Lester R. A. J. (1999). Upregulation of surface $\alpha4\beta2$ nicotinic receptors is initiated by receptor desensitisation after chronic exposure to nicotine. *J. Neurosci.*, **19**: 4804-4814.

Fiedler E. P., Marks M. J. and Collins A. C. (1987). Postnatal development of cholinergic enzymes and receptors in mouse brain. *J. Neurochem.*, **49**: 983-900.

Filatov G. N. and White M. M. (1995). The role of conserved leucines in the M2 domain of the acetylcholine receptor in the channel gating. *Mol. Pharmacol.*, **48**: 379-384.

Flores C. M., Rogers S. W., Pabreza L. A., Wolfe B. B. and Kellar K. J. (1992). A subtype of nicotinic cholinergic receptor in rat brain is composed of $\alpha4$ and $\beta2$ subunits and is upregulated by chronic nicotine treatment. *Mol. Pharmacol.*, **41**: 31-37.

Forsayeth J. R and Kobrin E. (1997). Formation of oligomers containing the β3 and β4 subunits of the rat nicotinic receptor. *J. Neurosci.*, **17**: 1531-1538.

Forsythe I. D., Lambert D. G., Hahorski S. R. and Linsdell P. (1992). Elevation of cytosolic calcium by cholinergic agonists in SH-SY5Y human neuroblastoma cells: estimation of the contribution of voltage dependent currents. *Br. J. Pharmacol.*, **107**: 207-214.

Fossier P., Tauc L. and Baux G. (1999). Calcium transients and neurotransmitter release at an identified synapse. *T. I. N. S.*, **22**: 161-166.

Freedman R., Coon H., Mylesworsley M., Orr-Utreger A., Oliney A., Davis A., Polymeropoulos M., Holik J., Hopkins J., Hoff M., Rosenthal J., Waldo M. C., Reimherr F., Wender P., Yaw J., Young D. A., Breese C. R., Adams C., Patterson D., Adler L. E., Kruglyak L., Leonard S. and Byerley W. (1997). Linkage of a neurophysiological deficit in schizophrenia to a chromosome 15 locus. *Proc. Natl. Acad. Sci. USA.*, **94**: 587-592.

Fucile S., Barabino B., Palma E., Grassi F., Limatola C., Mileo A. M., Alemà S., Ballivet M. and Eusebi F. (1997). α5 Subunit forms functional α3β4α5 nAChRs in transfected human cells. *NeuroReport*, **8**: 2433-2436.

Galzi J. L. and Changeux J. P. (1995). Neuronal nicotinic receptors: Molecular organisation and regulations. *Neuropharmacol.*, **34**: 563-582.

Galzi J-L., Revah F., Bessis A. and Changeux J. P. (1991). Functional architecture of the nicotinic acetylcholine receptor: from electric organ to brain. *Annu. Rev. Pharmacol. Toxicol.*, **31**: 37-72.

Geertsen S., Afar R., Trifaró J-M. and Quik M. (1998). Regulation of α-bungarotoxin sites in chromaffin cells in culture by nicotinic receptor ligands, K^+, and cAMP. *Mol. Pharm.*, **34**: 549-556.

Gerzanich V., Anand R. and Lindstrom J. (1994). Homomers of α8 and α7 subunits of nicotinic receptors exhibit similar channel but contrasting binding site properties. *Mol. Pharmacol.*, **45**: 212-220.

Gerzanich V., Kuryatov A., Anand R. and Lindstrom J. (1997). "Orphan" α6 Nicotinic AChR subunit can form a functional heteromeric acetylcholine receptor. *Mol. Pharmacol.*, **51**: 320-327.

Gerzanich V., Peng X., Wang F., Wells G., Anand R., Fletcher S. and Lindstrom J. (1995). Comparative pharmacology of epibatidine: a potent agonist for neuronal nicotinic acetylcholine receptors. *Mol. Pharmacol.*, **48**: 774-782.

Ghosh A. and Greenberg M. E. (1995). Calcium signalling in neurons: molecular mechanisms and cellular consequences. *Science*, **268**: 239-247.

Gopalakrishnan M., Buisson B., Touma E., Giordano T., Campbell J. E., Hu I. C., Donnelly-Roberts D., Arneric S. P., Bertrand D. and Sullivan J. P. (1995). Stable expression and pharmacological properties of the human α7 nicotinic acetylcholine receptor. *Eur. J. Pharmacol.*, 290: 237-246.

Gopalakrishnan M., Molinari E. J. and Sullivan J. P. (1997). Regulation of human α4β2 neuronal nicotinic acetylcholine receptors by cholinergic channel ligands and second messenger pathways. *Mol. Pharmacol.*, **52**: 524-534.

Gopalakrishnan M., Monteggia L. M., Anderson D. J., Molinari E. J., Piatonni-Kaplan M., Donelly-Roberts D., Arneric S. P. and Sullivan J. P. (1996). Stable expression, pharmacological properties and regulation of the human neuronal nicotinic acetylcholine α4β2 receptor. *J. Pharmacol. Exp. Ther.*, **276**: 289-297.

Gorbounova O., Svensson A-L., Jönsson P., Mousavi M., Miao H., Hellström-Lindahl E. and Norberg A. (1998). Chronic ethanol treatment decreases [^{3}H]-epibatidine and [^{3}H]-nicotine binding and differentially regulates mRNA levels of nicotinic acetylcholine receptor subunits expressed in M10 and SH-SY5Y neuroblastoma cells. *J. Neurochem.*, **70**: 1134-1142.

Goshima Y., Ohsako S. and Yamauchi T. (1993). Overexpression of Ca^{2+}/calmodulin-dependent protein kinase II in Neuro 2a and NG 108-15 neuroblastoma cell lines promotes neurite outgrowth and growth cone motility. *J. Neurosci.*, **13**: 559-567.

Goslin K. and Banker G. (1991). Rat hippocampal neurones in low-density culture. In: *Culturing nerve cells*, pp 251-281. Edited by Banker G. and Goslin K., Cambridge, Massachusetts, MIT Press.

Gotti C., Fornasari D. and Clementi F. (1997) Human neuronal nicotinic receptors. *Prog. Neurobiol.*, **53**: 199-237.

Gotti C., Hanke W., Maury K., Moretti M., Ballivet M., Clementi F. and Bertrand D. (1994). Pharmacology and biophysical properties of α7 and α7-α8 α-bungarotoxin receptor subtypes immunopurified from the chick optic lobe. *Eur. J. Neurosci.*, **6**: 1281-1291.

Gray W. R., Luque F. A., Galyean R., Atherton E., Sheppard R. C., Stone B. L., Reyes A., Alford J., McIntosh M., Olivera B. M., Cruz L. J. and Rivier J. (1984). Conotoxin GI: disulfide bridges, synthesis, and preparation of iodinated derivatives. *Biochemistry*, **23**: 2796-2802.

Gray W. R., Luque A. and Olivera B. M. (1981). Peptide toxins from *Conus geographus* venom. *J. Biol. Chem.*, **256**: 4734-4740.

Gray W. R., Olivera B. M. and Cruz L. J. (1988). Peptide toxins from venomous *Conus* snails. *Ann. Rev. Biochem.*, **57**: 665-700.

Gray R., Rajan A. S., Radcliffe K. A., Yakehiro M. and Dani J. A. (1996). Hippocampal synaptic transmission enhanced by low concentrations of nicotine. *Nature*, **383**: 713-716.

Greenberg M. E., Thompson M. A. and Sheng M. (1992). Calcium regulation of immediate early gene transcription. *J. Physiol. (Paris)*, **86**: 99-108.

Greene L. A. (1978). Nerve growth factor prevents the death and stimulates the neuronal differentiation of clonal PC12 pheochromocytoma cells in serum-free medium. *J. Cell Biol.*, **78**: 747-755.

Greene L. A., Sobeih M. M. and Teng K. K. (1991). Methodologies for the culture and experimental use of the PC12 rat pheochromocytoma cell line. In: *Culturing nerve cells*, pp 207-226. Edited by Banker G. and Goslin K., Cambridge, Massachusetts, MIT Press.

Greene L. A. and Tischler A. S. (1976). Establishment of a noradrenergic clonal line of rat adrenal pheochromocytoma cells which respond to nerve growth factor. *Proc. Natl. Acad. Sci.* USA., **73**: 2424-2428.

Grenningloh G., Gunderfinger E., Schmitt B., Betz H., Darlison M. G., Barnard E. A., Schofield P. R. and Seeburg P. H. (1987a). Glycine vs GABA receptors. *Nature*, **330**: 25-26.

Grenningloh G., Reinitz A., Schmitt B., Methfessel C., Zensen M., Beyreuther K., Gunderfinger E. D., and Betz H. (1987b). The strychnine-binding subunit of the glycine receptor shows homology with nicotinic acetylcholine receptors. *Nature*, **328**: 215-220.

Groot-Kormelink P. J., Luyten W. H. M. L., Colquhoun D. and Sivilotti L. G. (1998). A reporter mutation approach shows incorporation of the "orphan" subunit β3 into a functional nicotinic receptor. *J. Biol. Chem.*, **273**: 15317-15320.

Gross A., Ballivet M., Rungger D. and Bertrand D. (1991). Neuronal nicotinic acetylcholine receptors expressed in Xenopus oocytes: role of the α subunit in agonist sensitivity and desensitisation. *Eur. J. Physiol.*, **419**: 545-551.

Grynkiewicz G., Poenie M. and Tsien R. Y. (1985). A new generation of Ca^{2+} indicators with greatly improved fluorescence properties. *J. Biol. Chem.*, **260**: 3440-3450.

Hanson P. I. and Schulman H. (1992). Neuronal Ca^{2+}/calmodulin-dependent protein kinases. *Annu. Rev. Biochem.*, **61**: 559-601.

Harvey S. C. and Luetje C. W. (1996). Determinants of competitive antagonist sensitivity on neuronal nicotinic receptor beta subunits. *J. Neurosci.*, *16*: 3798-3806.

Harvey S. C., Maddox F. N. Luetje C. W. (1996). Multiple determinants of dihydro-β-erythroidine on rat neuronal nicotinic receptor α subunits. *J. Neurochem.*, **67**: 1953-1959.

Hell J. R., Appleyard S. M., Yokoyama C. T., Warner C. and Catterall W. A. (1994). Differential phosphorylation of two size forms of the N-type calcium channel α1 subunit which have different COOH termini. *J. Biol. Chem.*, **269**: 7390-7396.

Henderson L. P., Gdovin M. J., Liu C., Gardner P. D. and Maue R. A. (1994). Nerve growth factor increases nicotinic ACh receptor gene expression and current density in wild-type and protein kinase A-deficient PC12 cells. *J. Neurosci.*, **14**: 1153-1163.

Herz J. M., Johnson D. A. and Taylor P. (1989). Distance between the agonist and non-competitive inhibitor sites on the nicotinic acetylcholine receptor. *J. Biol. Chem.*, **264**: 12439-12448.

Holladay M. W., Cosfoed N. D. P. and McDonald I. A. (1998). Natural products as a source of nicotinic acetylcholine receptor modulators and leads for drug discovery. In: *Neuronal nicotinic receptors: Pharmacology and therapeutic opportunities*, pp253-270. Edited by Arneric S. P. and Brioni J. D., Wiley-Liss, New York, NY.

Holladay M. W., Lebold S. A. and Lin N-H. (1995). Structure-activity relationships of nicotinic acetylcholine receptor agonists as potential treatments for dementia. *Drug Dev. Res.*, **35**: 191-213.

Hopkins C., Grilley M., Miller C., Shon K-J., Cruz L. J., Gray W. R., Dykert J., Rivier J., Yoshikami D. and Olivera B. M. (1995). A new family of Conus peptides targeted to the nicotinic acetylcholine receptor. *J. Biol. Chem.*, **270**: 22361-22367.

Horch H. L. W. and Sargent P. B. (1995). Presynaptic surface distribution of multiple classes of nicotinic acetylcholine receptors on neurones in chicken ciliary ganglion. *J. Neurosci.*, **15**: 7778-7795.

Hory-Lee F. and Frank E. (1995). The nicotinic blocking agents d-tubocurare and α-bungarotoxin save motoneurones from naturally occurring death in the absence of neuromuscular blockade. *J. Neurosci.*, **15**: 6453-6460.

Houghtling R. A., Davila-Garcia M. I. and Kellar K. J. (1995). Characterisation of (±)-[^{3}H]epibatidine binding to nicotinic cholinergic receptors in rat and human brain. *Mol. Pharmacol.*, **48**: 280-287.

Hsu Y-N., Amin J., Weiss D. S. and Wecker L. (1996). Sustained nicotine exposure differentially affects α3β2 and α4β2 neuronal nicotinic receptors expressed in *Xenopus oocytes*. *J. Neurochem.*, **66**: 667-675.

Hu M., Whiting Theobald N. L. and Gardner P. D. (1994). Nerve growth factor increases the transcriptional activity of the rat neuronal nicotinic acetylcholine receptor β4 subunit promoter in transfected PC12 cells. *J. Neurochem.*, **62**: 392-395.

Hughes J. R., Hatsukami D. K., Mitchell J. E. and Dahlgren L. A. (1986). Prevalence of smoking among psychiatric outpatients. *Am. J. Psychiatry*, **143**: 993-997.

Hulihan-Giblin B. A., Lumpkin M. A. and Kellar K. J. (1990). Effects of chronic administration of nicotine on prolactin release in the rat: Inactivation of prolactin response by repeated injections of nicotine. *J. Pharmacol. Exp. Ther.*, **252**: 21-25.

Hunter B. E., De Fiebre C. M., Papke R. L., Kem W. R. and Meyer E. M. (1994). A novel nicotinic agonist facilitates induction of long term potentiation in the rat hippocampus. *Neurosci. Letts.*, **168**: 130-134.

Inoue K. and Kenimer J. G. (1988). Muscarinic stimulation of calcium influx and norepinephrine release in PC12 cells. *J. Biol. Chem.*, **263**: 8157-8161.

Ishiguro H., Ichino N., Yamada K. and Nagatsu T. (1997). Nicotine regulates mRNA level of tyrosine hydroxylase gene but not that of nicotinic acetylcholine receptor genes in PC12 cells. *Neurosci. Letts.*, **228**: 37-40.

James J. R. and Norberg A. (1995). Genetic and environmental aspects of the role of nicotinic receptors in neurodegenerative disorders: emphasis on Alzheimer's disease and Parkinson's disease. *Behav. Genet.*, **25**: 149-159.

Jarvik M. E. (1991). Beneficial effects of nicotine. *Br. J. Addiction*, **86**: 571-575.

Jefferson A. B., Travis S. and Schulman H. (1991). Activation of a multi-functional Ca^{2+}/calmodulin-dependent protein kinase in GH_3 cells. *J. Biol. Chem.*, **266**: 1484-1490.

Johnson D. S., Martinez J., Elgoyhen A. B., Heinemann S. F. and McIntosh J. M. (1995). α-Conotoxin ImI exhibits subtype-specific nicotinic acetylcholine receptor blockade: preferential inhibition of homomeric α7 and α9 receptors. *Mol. Pharm.*, **48**: 194-199.

Johnston L.M. (1942). Tobacco smoking and nicotine. *Lancet*, **2**, 742.

Kaiser S. A., Soliakov L., Harvey S. C., Leutje C. W. and Wonnacott S. (1998). Differential inhibition by α-conotoxin-MII of the nicotinic stimulation of [^{3}H]-dopamine release from rat striatal synaptosomes and slices. *J. Neurochem.*, **70**: 1069-1076.

Kao P. N., Dwork A. J., Kaldany R. R., Silver M. L., Wideman J., Stein S. and Karlin A. (1984). Identification of the alpha-subunit cysteines specifically labelled by an affinity reagent for the acetylcholine receptor binding site. *J. Biol. Chem.*, **259**: 11662-11665.

Kao P. and Karlin A. (1986). Acetylcholine receptor binding site contains a disulfide crosslink between adjacent half-cystinyl residues. *J. Biol. Chem.*, **261**: 8085-8088.

Karlin A. (1991). Explorations of the nicotinic acetylcholine receptor. *Harvey Lect. Ser.*, **85**: 71-107.

Karlin A. (1993). Structure of nicotinic acetylcholine receptors. *Curr. Opin. Neurobiol.*, **3**: 299-309.

Karlin A. and Akabas M. H. (1995). Toward a structural basis for the function of nicotinic acetylcholine receptors and their cousins. *Neuron*, **15**: 1231-1244.

Kazmi S. M. and Mishra R. K. (1987). Comparative pharmacological properties and functional coupling of mu and delta opioid receptor sites in human neuroblastoma SH-SY5Y cells. *Mol. Pharmacol.*, **32**: 109-118.

Kem W. R. (1985). Structure and action of nemertine toxins. *Amer. Zool.*, **25**: 99-1111.

Kem W. R., Abott B. C. and Coates R. M. (1971). Isolation and structure of a hoplonemertine toxin. *Toxicon*, **9**: 15-22.

Kem W. R., Mahnir V. M., Papke R. L. and Lingle C. J. (1997). Anabaseine is a potent agonist on muscle and neuronal alpha-bungarotoxin-sensitive nicotinic receptors. *J. Pharmacol. Exp. Ther.*, **283**: 979-992.

Kemp G., Bentley L., McNamee M. G. and Morley B. J. (1985). Purification and characterisation of the α-bungarotoxin binding protein from rat brain. *Brain Res.*, **347**: 274-283.

Keyser K. T., Britto L. R. G., Schoepfer R., Whiting P., Cooper J., Conroy W., Brozozowska-Prechtl A., Karten H. J and Lindstrom J. (1993). Three subtypes of α-bungarotoxin-sensitive nicotinic acetylcholine receptors are expressed in chick retina. *J. Neurosci.*, **13**: 442-454.

Kihara T., Shimohama S., Sawada H., Kimura J., Kume T., Kochiyama H., Maeda T. and Akaike A. (1997). Nicotinic receptor stimulation protects neurones against β-amyloid toxicity. *Ann. Nerurol.*, **42**: 159-163.

Ksir C., Hakan R., Hall D. P. Jr and Kellar K. J. (1985). Exposure to nicotine enhances the behavioural stimulant effects of nicotine and increases binding of [^{3}H]-acetylcholine to nicotinic receptors. *Neuropharmacol.*, **24**: 527-531.

Kubalek E., Ralston S., Lindstrom J. and Unwin N. (1987). Location of subunits within the acetylcholine receptor by electron image analysis of tubular crystals from *Torpedo marmorata*. *J. Cell. Biol.*, **105**: 9-18.

Kulak J. M., Hguyen T. A., Olivera B. M. and McIntosh J. M. (1997). α-Conotoxin MII blocks nicotine-stimulated dopamine release in rat striatal synaptosomes. *J. Neurosci.*, **17**: 5263-5270.

Labarca C., Nowak M. W. , Zhang H., Tang L., Deshpande P. and Lester H. A. (1995). Channel gating governed by conserved leucine residues in the M2 domain of nicotinic receptors. *Nature*, **376**: 514-516.

Lambert D. G. and Nahorski S. R. (1990). Muscarinic-receptor-mediated changes in intracellular Ca^{2+} and inositol 1, 4, 5-triphosphate mass in a human neuroblastoma cell line, SH-SY5Y. *Biochem. J.*, 265: 555-562.

Lambert D. G., Whitham E. M., Baird J. G. and Nahorski S. R. (1990). Different mechanisms of Ca^{2+} entry induced by depolarisation and muscarinic receptor stimulation in SH-SY5Y human neuroblastoma cells. *Brain Res.*, **8**: 263-266.

Langosch D., Thomas L. and Betz H. (1988). Conserved quaternary structure of ligand-gated ion channels: the postsynaptic glycine receptor is a pentamer. *Proc. Natl. Acad. Sci.* USA., **85**: 7394-7398.

Lapchak P. A., Araujo D. M., Quirion R. and Collier B. (1989). Effect of chronic nicotine treatment on nicotinic autoreceptor function and *N*-[^{3}H]-methylcarbamylcholine binding sites in the rat brain. *J. Neurochem.*, **52**: 483-491.

La Rochelle W. J., Ralston E., Forsayeth J. R., Froehner S. C. and Hall Z. (1989). Clusters of 43-kDa protein are absent from genetic variants of C2 muscle cells with reduced acetylcholine receptor expression. *Dev. Biol.*, **132**: 130-138.

Leischow S. J. and Cook G. (1998). Nicotine and non-nicotine formulations for smoking cessation. In: *Neuronal nicotinic receptors: Pharmacology and therapeutic opportunities*, pp 323-336. Edited by Arneric S. P. and Brioni J. D., Wiley-Liss, New York, NY.

Léna C. and Changeux J-P. (1993). Allosteric modulations of the nicotinic acetylcholine receptor. *T. I. N. S.*, **16**: 181-186.

Leonard S., Adler L. E., Olincy A., Breese C. R., Gault J., Ross R. G., Lee M., Cawthra E., Nagamoto H. T. and Freedman R. (1998). The role of nicotine and nicotinic receptors in psychopathology. In: *Neuronal nicotinic receptors: Pharmacology and therapeutic opportunities*, pp 307-321. Edited by Arneric S. P. and Brioni J. D., Wiley-Liss, New York, NY.

Leonard S., Breese C. R., Adams C., Benhammou K., Gault J., Stevens K., Lee M., Adler L., Olincy A., Ross R. and Freedman R. (2000). Smoking and schizophrenia: abnormal nicotinic receptor expression. *Eur. J. Pharmacol.*, **393**: 237-242.

Li G., Hidaka H. and Wollheim C. B. (1992). Inhibition of voltage-gated Ca^{2+} channels and insulin secretion in HIT cells by the Ca^{2+}/calmodulin-dependent protein kinase II inhibitor KN-62: comparison with antagonists of calmodulin and L-type Ca^{2+} channels. *Mol. Pharm.*, **42**: 489-498.

Li Y., Papke R. L., He Y. J., Millard W. J. and Meyer E. M. (1999). Characterisation of the neuroprotective and toxic effects of α7 nicotinic receptor activation in PC12 cells. *Brain Res.*, **830**: 218-225.

Lindstrom J. (1986). Probing nicotinic acetylcholine receptors with monoclonal antibodies. *T.I.N.S.*, **Sept**: 401-407.

Lindstrom J. (1996). Monoclonal antibodies to nicotinic acetylcholine receptors. *Neurotransmissions XII*, **2**: 1-10.

Lindstrom J., Schoepfer R., Conroy W. G. and Whiting P. (1990). Structural and functional heterogeneity of nicotinic receptors, pp 23-52. In, The biology of nicotine dependence. Ciba Foundation Symposium 152. A Wiley-interscience Production.

Lippiello P. M., Sears S. B. and Fernandes K. G. (1987). Kinetics and mechanism of L-[^{3}H]-nicotine binding to putative high affinity receptor sites in rat brain. *Mol. Pharmacol.*, **31**: 392-400.

Lisman J. E. (1985). A mechanism for memory storage insensitive to molecular turnover: a bistable autophosphorylating kinase. *Proc. Natl. Acad. Sci.* USA, **82**: 3055-3057.

Lisman J. (1994). The CaM kinase II hypothesis for the storage of synaptic memory. *T. I. N. S.*, **17**: 406-412.

Lisman J., Malenka R. C., Nicoll R. A. and Malinow R. (1997). Learning mechanisms: the case for CaM-kinase II. *Science*, **276**: 2001-2002.

London E. D., Scheffel U., Kimes A. S. and Kellar K. J. (1995). In vivo labelling of nicotinic acetylcholine receptors in brain with [^{3}H]-epibatidine. *Eur. J. Pharmacol.*, **278**: R1-R2.

López M. G., Fonteríz R. I., Gandía L., de la Fuente M., Villarroya M., García-Sancho J. and García A. G. (1993). The nicotinic acetylcholine receptor of the bovine chromaffin cell, a new target for dihydropyridines. *Eur. J. Pharmacol.*, **247**: 199-207.

Loring R. H. and Zigmond R. E. (1988). Characterisation of neuronal nicotinic receptors by snake venom neurotoxins. *T. I. N. S.*, **11**: 73-77.

Lowe T., Sharefkin J., Yang s. Q. and Dieffenbach C. W. (1990). A computer program for selection of oligonucleotide primers for PCRs. *Nucleicacids Res.*, **18**: 1757-1761.

Luetje C. W. and Patrick J. (1991). Both α- and β-subunits contribute to the agonist sensitivity of neuronal nicotinic acetylcholine receptors. *J. Neurosci.*, **11**: 837-845.

Luetje C. W., Piattoni M. and Patrick J. (1993). Mapping of ligand binding sites of neuronal nicotinic acetylcholine receptors using chimeric alpha subunits. *Mol. Pharmacol.*, **44**: 657-666.

Luetje C. W., Wada K., Rogers S., Abramson S. N., Tsuji K., Heinemann K. and Patrick J. (1990). Neurotoxins distinguish between different neuronal nicotinic acetylcholine receptor subunit compositions. *J. Neurochem.*, **55**: 632-640.

Lukas R. J. (1991). Effects of chronic nicotine ligand exposure on functional activity of nicotinic acetylcholine receptors expressed by cells of the PC12 rat pheochromocytoma or the TE671/RD human clonal cell line. *J. Neurochem.*, **56**: 1134-1145.

Lukas R. J. (1998). Cell lines as models for studies of nicotinic acetylcholine receptors. In: *Neuronal nicotinic receptors: Pharmacology and therapeutic opportunities*, pp 81-97. Edited by Arneric S. P. and Brioni J. D., Wiley-Liss, New York, NY.

Lukas R. J., Changeux J. P., Le Novere N., Albuquerque E. X., Balfour D. J. K., Berg D. K., Bertrand D., Chiappinelli V. A., Clarke P. B. S., Collins A. C., Dani J. A., Grady S. R., Kellar K. J., Lindstrom J. M., Marks M. J., Quik M., Taylor P. M. and Wonnacott S. (1999). International Union of Pharmacology. XX. Current status of the nomenclature for nicotinic acetylcholine receptors and their subunits. *Pharmacol Rev.*, **51**: 397-401.

Lukas R. J., Norman S. A. and Lucero L. (1993). Characterisation of nicotinic acetylcholine receptors expressed by cells of the SH-SY5Y human neuroblastoma clonal line. *Mol. Cell. Neurosci.*, **4**: 1-12.

Luo S., Kulak J. M., Cartier E., Jacobsen R. B., Yoshikami D., Olivera B. M. and McIntosh J. M. (1998). α-conotoxin AUIB selectively blocks α3β4 nicotinic acetylcholine receptors and nicotine-evoked norepinephrine release. *J. Neurosci.*, **18**: 8571-8579.

MacAllan D. R. E., Lunt G. C., Wonnacott S., Swanson K. L., Rapoport H. and Albuquerque E. X. (1988). Methyllycaconitine and (+)-anatoxin-a differentiate between nicotinic receptors in vertebrate and invertebrate nervous systems. *F. E. B. S. Letts.*, **226**: 357-363.

MacNicol N. and Schulman H. (1992). Cross-talk between protein kinase C and multifunctional Ca^{2+}/calmodulin-dependent protein kinase. *J. Biol. Chem.*, **267**: 12197-12201.

Madhok T. C., Beyer H. S. and Sharp B. M. (1994). Protein kinase A regulates nicotinic cholinergic receptors and subunit messenger ribonucleic acids in PC12 cells. *Endocrinology*, **134**: 91-96.

Madhok T. C., Matta S. G. and Sharp B. M. (1995). Nicotine regulates nicotinic cholinergic receptors and subunit mRNAs in PC12 cells through protein kinase A. *Mol. Brain Res.*, **32**: 143-150.

Maimone M. M. and Merlie J. P. (1993). Interaction of the 43 kd postsynaptic protein with all subunits of the muscle nicotinic acetylcholine receptor. *Neuron*, **11**: 53-66.

Malinow R., Madison D. V. and Tsien R. W. (1988). Persistent protein kinase activity underlying long-term potentiation. *Nature*, **335**: 820-824.

Mandelzys a., De Koninck P and Cooper E. (1994). The developmental increase in ACh current densities on rat sympathetic neurones correlates with changes in nicotinic ACh receptor α-subunit gene expression and occurs independently of innervation. *J. Neurosci.*, **14**: 2357-2364.

Maricq A. V., Peterson A. S., Brake A. J., Myers R. M. and Julius D. (1991). Primary structure and functional expression of the 5-HT_3 receptor, a serotonin-gated ion channel. *Science*, **254**: 432-437.

Marin P., Manus M., Desagher S., Glowinski J. and Prémont J. (1994). Nicotine protects cultured striatal neurones against *N*-methyl-$_D$-aspartate receptor-mediated neurotoxicity. *NeuroReport*, **5**: 1977-1980.

Marks M. J. (1998). Desensitisation and the regulation of neuronal nicotinic receptors. In: *Neuronal nicotinic receptors: Pharmacology and therapeutic opportunities*, pp 65-80. Edited by Arneric S. P. and Brioni J. D., Wiley-Liss, New York, NY.

Marks M. J., Burch J. B. and Collins A. C. (1983). Effects of chronic nicotine infusion on tolerance development and nicotinic receptors. *J. Pharmacol. Exp. Ther.*, **226**: 817-825.

Marks M. J. and Collins A. C. (1982). Characterisation of nicotine binding in mouse brain and comparison with the binding of α-bungarotoxin and quinuclidinyl benzilate. *Mol. Pharmacol.*, **22**:554-564.

Marks M. J., Farnham D. A., Grady S. R. and Collins A. C. (1993a). Nicotinic receptor function determined by stimulation of rubidium efflux from mouse brain synaptosomes. *J. Pharmacol. Exp. Ther.*, **264**: 542-552.

Marks M. J., Grady S. R. and Collins A. C. (1993b). Downregulation of nicotinic receptor function after chronic nicotine infusion. *J. Pharmacol. Exp. Ther.*, **266**: 1268-1276.

Marks M. J., Pauly J. R., Gross S. D., Deneris E. S., Heinemann S. F. and Collins A. C. (1992). Nicotine binding and nicotinic receptor subunit RNA after chronic nicotine treatment. *J. Neurosci.*, **12**: 2765-2784.

Marks M. J., Stitzel J. A. and Collins A. C. (1985). Time course of the effects of chronic nicotine infusion on drug responses and brain regions. *J. Pharmacol. Exp. Ther.*, **235**: 619-628.

Marks M. J., Smith K. W. and Collins A. C. (1998). Differential agonist inhibition identifies multiple epibatidine binding sites in mouse brain. *J. Pharmacol. Exp. Ther.*, **285**: 377-386.

Marks M. J., Stitzel J. A., Romm E., Wehner J. M. and Collins A. C. (1986). Nicotinic binding sites in rat and mouse brain: comparison of acetylcholine, nicotine, and α-bungarotoxin. *Mol. Pharmacol.*, **30**: 427-436.

Markwell M. A. K., Haas S. M., Bieber L. L. and Tolbert N. E. (1978). A modification of the Lowry procedure to simplify protein determination in membrane and lipoprotein samples. *Anal. Biochem.*, **87**: 206-210.

Martin A. K., Nahorski S. R. and Willars G. B. (1999). Complex relationship between Ins(1,4,5)P_3 accumulation and Ca^{2+} signalling in a human neuroblastoma revealed by cellular differentiation. *Br. J. Pharmacol.*, **126**: 1559-1566.

Martino-Barrows A. M. and Kellar K. J. (1987). [^{3}H]-Acetylcholine and [^{3}H]-(-)-nicotine label the same recognition site in rat brain. *Mol. Pharmacol.*, **31**: 169-174.

Mayford M., Wang J., Kandel E. R. and O'Dell T. J. (1995). CaMKII regulates the frequency-response function of hippocampal synapses for the production of both LTD and LTP. *Cell*, **81**: 891-904.

McGhee D. S., Heath M. J. S., Gelbar S., Devay P. and Role L. W. (1995). Nicotine enhancement of fast excitatory synaptic transmission in CNS by presynaptic receptors. Science, 269: 1692-1696.

McGehee D. S. and Role L. W. (1995). Physiological diversity of nicotinic acetylcholine receptors expressed by vertebrate neurons. *Ann. Rev. Physiol.*, **57**: 521-546.

McIntosh M., Cruz L. J., Hunkapiller M. W., Gray W. R. and Olivera B. M. (1982). Isolation and structure of a peptide toxin from the marine snail *Conus magnus*. *Ach. Biochem. Biophys.*, **218**: 329-334.

McIntosh J. M., Santos A. D. and Olivera B. M. (1999). *Conus* peptides targeted to specific nicotinic acetylcholine receptor subtypes. *Annu. Rev. Biochem.*, **68**: 59-88.

McIntosh J. M., Gardner S., Luo S., Garrett J. E. and Yoshikami D. (2000). Conus peptide: novel probes for nicotinic acetylcholine receptor structure and function. *Eur. J. Pharmacol.*, **393**: 205-208.

McIntosh M., Yoshikami D., Mahe E., Nielsen D. B., Rivier J. E., Gray W. R. and Olivera B. M. (1994). A nicotinic acetylcholine receptor ligand of unique specificity, α-conotoxin ImI. *J. Biol. Chem.*, **269**: 16733-16739.

Messi M. L., Renganathan M., Grigorenko E., and Delbono O. (1997). Activation of α7 nicotinic acetylcholine receptors promotes survival of spinal cord motoneurones. *F. E. B. S. Letts.*, **411**: 32-38.

Meyer E. M., De Fiebre C. M., Hunter B. E., Simpkins C. E., Frauworth N. and De Fiebre N. E. C. (1994). Effects of anabaseine-related analogs on rat brain nicotinic receptor binding and on avoidance behaviours. *Drug Dev. Res.*, **31**: 127-134.

Meyer E. M., Tay E. T., Papke R. L., Meyers C., Huang G-L and De Fiebre C. M. (1997). 3-[2, 4-dimethoxybenzylidene] anabaseine (DMXB) selectively activates rat α7 receptors and improves memory-related behaviours in a mecamylamine-sensitive manner. *Brain Res.*, **768**: 49-56.

Mihovilovic M and Richman D. P. (1987). Monoclonal antibodies as probes of the α-bungarotoxin binding regions of the acetylcholine receptor. *J. Biol. Chem.*, **262**: 4978-4986.

Miller R. J. (1988). Calcium signalling in neurones. *T. I. N. S.*, **11**: 415-419.

Miñana M-D., Montoliu C., Llansola M., Grisolía S. and Felipo V. (1998). Nicotine prevents glutamate-induced proteolysis of the microtubule-associated protein MAP-2 and glutamate neurotoxicity in primary cultures of cerebellar neurones. *Neuropharmacol.*, **37**: 847-857.

Mishina M., Takai T., Imoto K., Noda M., Takahashi T., Numa S., Methfessel C. and Sakmann B. (1986). Molecular distinction between fetal and adult forms of muscle acetylcholine receptor. *Nature*, **321**: 406-411.

Miyazawa A., Fujiyoshi Y., Stowell M., Unwin N. (1999). Nicotinic acetylcholine receptor at 4..6 Å resolution: transverse tunnels in the channel wall. *J. Mol. Biol.*, **288**: 765-786.

Molinari E. J., Delbono O., Messi M. L., Renganathan M., Arneric S. P., Sullivan J. P. and Gopalakrisnan M. (1998). Up-regulation of human α7 nicotinic receptors by chronic treatment with activator and antagonist ligands. *Eur. J. Pharmacol.*, **347**: 131-139.

Morens D. M., Grandinetti A., Davis J. W., Ross G. W., White L. R. and Reed D. (1996). Epidemiological observations on Parkinson's disease: incidence and mortality in a prospective study of middle aged men. *Am. J. Epidemiol.*, **144**: 400-404.

Murphy N. P., Vaughan P. F. T., Ball S. G. and McCormack J. G. (1991a). The cholinergic regulation of intracellular calcium in the human neuroblastoma, SH-SY5Y. *J. Neurochem.*, **57**: 2116-2123.

Murphy T. H., Worley P. F. and Baraban J. M. (1991b). L-type voltage-sensitive calcium channels mediate synaptic activation of immediate early genes. *Neuron*, **7**: 625-635.

Myers R. A., Zafaralla G. C., Gray W. R., Abott J., Cruz L. J. and Olivera B. M. (1991). α-Conotoxins, small peptide probes of nicotinic acetylcholine receptors. *Biochemistry*, **30**: 9370-9377.

Nakaniski S. (1992). Molecular diversity of glutamate receptors and implications for brain function. *Science*, **258**: 597-603.

Nanri M., Kasahara N., Yamamoto J., Miyake H. and Watanabe H. (1997). GTS-21, a nicotinic agonist, protects against neocortical neuronal cell loss induced by the nucleus basalis magnocellularis lesion in rats. *Jpn. J. Pharmacol.*, **74**: 285-289.

Nef P., Oneyser C., Alliod C., Couturier S. and Ballivet M. (1988). Genes expressed in the brain define three distinct neuronal nicotinic acetylcholine receptors. *EMBO J.*, **7**: 595-601.

Neher E. (1995). The use of fura-2 for estimating Ca buffers and Ca fluxes. *Neuropharmacol.*, **34**: 1423-1442.

Noda M., Takahashi H., Tanabe T., Toyosato M., Furutani Y., Hirose T., Assai M., Inayama S., Miyata T. and Numa S. (1982). Primary structure of α-subunit precursor of *Torpedo californica* acetylcholine receptor deduced from cDNA sequences *Nature*, **299**: 793-797.

Noda M., Takahashi H., Tanabe T., Toyosato M., Kikyotani S., Furutani Y., Hirose T., Assai M., Takashima H., Inayama S., Miyata T. and Numa S. (1983a). Primary structures of β- and δ-subunit precursors of *Torpedo californica* acetylcholine receptor deduced from cDNA sequences. *Nature*, **301**: 251-255.

Noda M., Takahashi H., Tanabe T., Yoyosato M., Kikyotani S., Furutani Y., Hirose T., Takashima H., Inayama S., Miyata T. and Numa S. (1983b). Structural homology of *Torpedo californica* acetylcholine receptor subunits. *Nature*, **302**: 528-532.

Nordberg A., Lundqvist H., Hartvig P., Lilja A. and Langstrom B. (1995). Kinetic analysis of regional (S) (-) 11C-nicotine binding in normal and Alzheimer's brains. *In vivo* assessment using positron emission tomography. *Alzheimer's Dis. Assoc. Disord.*, **9**: 21-27.

Noronha-Blob L., Gover R. and Baumgold J. (1989). Calcium influx mediated by nicotinic receptors and voltage sensitive calcium channels in SK-N-SH human neuroblastoma cells. *Biochem. Biophys. Res. Comm.*, **162**: 1230-1235.

Ocorr K. A. and Schulman H. (1991). Activation of a multifunctional Ca^{2+}/calmodulin-dependent kinase in intact hippocampal slices. *Neuron*, **6**: 907-914.

Olivera B. M., McIntosh J. M., Cruz L. J., Luque F. A. and Gray W. R. (1984). Purification and sequence of a presynaptic peptide toxin from *Conus geographus* venom. *Biochemistry*, **23**: 5087-5090.

Olivera B. M., Rivier J., Clark C., Ramilo C. A., Corpuz D. R., Abogadie F. C., Mena E. E., Woodward S. R., Hillyard D. R. and Cruz L. J. (1990). Diversity of Conus neuropeptides. *Science*, **249**: 257-263.

Orr-Utreger A., Goldner F. M., Saeki M., Lorenzo I., Golberg L., De Baisi M., Dani J. A., Patrick J. W. and Beaudet A. L. (1997). Mice deficient in the α7 neuronal nicotinic acetylcholine receptor lack α-bungarotoxin binding sites and hippocampal fast nicotinic currents. *J. Neurosci.*, **17**: 9165-9171.

Ortells M. O. and Lunt G. (1995). Evolutionary history of the ligand-gated ion-channel superfamily of receptors. *T. I. N. S.*, **18**: 121-127.

Ospina J. A., Broide R. S., Acevedo D., Robertson R. T. and Leslie F. M. (1998). Calcium regulation of agonist binding to α7-type nicotinic acetylcholine receptors in adult and fetal rat hippocampus. *J. Neurochem.*, **70**: 1061-1068.

Ouimet C. C., McGuinness T. L. and Greengard P. (1984). Immunocytochemical localisation of calcium/calmodulin-dependent protein kinase II in rat brain. *Proc. Natl. Acad. Sci.* USA, **81**: 5604-5608.

Pabreza L. A., Dhawan S. and Kellar K. J. (1990). [^{3}H]-Cytisine binding to nicotinic cholinergic receptors in brain. *Mol. Pharmacol.* **39**: 9-12.

Paddock S. W. (1999). Confocal laser scanning microscope. *BioTechniques*, **27**: 992-1004.

Palma E., Maggi L., Barabino B., Eusebi F. and Ballivet M. (1999). Nicotinic acetylcholine receptors assembled from the α7 and β3 subunits. *J. Biol. Chem.*, **274**: 18335-18340.

Papke R. L., Duvoisin R. M. and Heinemann S. F. (1993). The amino terminal half of the nicotinic beta-subunit extracellular domain regulates the kinetics of inhibition by neuronal bungarotoxin. *Proc. R. Soc. Lond. B. Biol. Sci.*, **252**: 141-148.

Papke R. L. and Heinemann S. F. (1991). The role of the beta 4-subunit in determining the kinetic properties of rat neuronal nicotinic acetylcholine alpha3-receptors. *J. Physiol. (Lond.)*, **440**: 95-112.

Paterson D. and Nordberg A. (2000). Neuronal nicotinic receptors in the human brain. *Prog. Neurobiol.*, **61**: 75-111.

Pauly J. R., Grun E. U. and Collins A. C. (1992). Tolerance to nicotine following chronic treatment by injections: a potential role for corticosterone. *Psychopharmacol.*, **108**: 33-39.

Pauly J. R., Marks M. J., Gross S. D. and Collins A. C. (1991). An autoradiographic analysis of cholinergic receptors in mouse brain after chronic nicotine treatment. *J. Pharmacol. Exp. Ther.*, **258**: 1127-1136.

Pedersen S. E. and Cohen J. B. (1990). *d*-Tubocurarine binding sites are located at α-γ and α-δ subunit interfaces of the nicotinic acetylcholine receptor. *Proc. Natl. Acad. Sci.* USA, **87**: 2785-2789.

Peng X., Katz M., Gerzanich V., Anand R. and Lindstrom J. (1994a). Human α7 acetylcholine receptor: Cloning of the α7 subunit from the SH-SY5Y cell line and determination of pharmacological properties of native receptors and functional α7 homomers expressed in *Xenopus* oocytes. *Mol. Pharmacol.*, **45**: 546-554

Peng X., Gerzanich V., Anand R., Whiting P.J. and Lindstrom J. (1994b). Nicotine-induced increase in neuronal nicotinic receptors results from a decrease in the rate of receptor turnover. *Mol. Pharmacol.*, **46**: 523-530.

Peng X., Gerzanich V., Anand R., Wang F. and Lindstrom J. (1997). Chronic nicotine up-regulates α3 and α7 acetylcholine receptor subtypes expressed by the human neuroblastoma cell line SH-SY5Y. *Mol. Pharmacol.*, **51**: 776-784.

Pereira E. F. R., Alkondon M., McIntosh J. M. and Albuquerque E. X. (1996). α-Conotoxin-ImI: A competitive antagonist at α-bungarotoxin-sensitive neuronal nicotinic receptors in hippocampal neurones. *J. Pharmacol. Exp. Ther.*, **278**: 1472-1483.

Perkins K. A., Grobe J. E., Epstein L. H., Caggiula., Stiller R. L. and Jacob R. G. (1993). Chronic and acute tolerance to subjective effects of nicotine. *Pharmacol. Biochem. Behav.*, **45**: 375-381.

Perry D. C., Dávila-García M. I., Stockmeier C. A. and Kellar K. J. (1999). Increased nicotinic receptors in brains from smokers: membrane binding and autoradiography studies. *J. Pharmacol. Exp. Ther.*, **289**: 1545-1552.

Perry D. C. and Kellar K. J. (1995). [^{3}H]-Epibatidine labels nicotinic receptors in rat brain. An autoradiographic study. *J. Pharmacol. Exp. Ther.*, **275**: 1030-1034.

Perry E., Martin-Ruiz C., Lee M., Griffiths M., Johnson M., Piggott M., Haroutunian V., Buxbaum J. D., Nãsland J., Davis K., Gotti C., Clementi F., Tzartos S., Cohen O., Soreq H., Jaros E., Perry R., Ballard C., McKeith I. and Court J. (2000). Nicotinic receptor subtypes in human brain ageing, Alzheimer and Lewy body diseases. *Eur. J. Pharmacol.*, **393**: 215-222.

Perry E. K., Morris C. M., Court J. A., Cheng A., Fairbairn A. F., McKeith I. G., Irving D., Brown A. and Perry R. H. (1995). Alteration in nicotine binding sites in Parkinson's disease,

Lewy body dementia and Alzheimer's disease: Possible index of early neuropathology. *Neuroscience*, **64**: 385-395.

Perry R. H., Candy J., Perry E. K., Irving D., Blessed G., Fairbairn A. F. and Tomlinson B. E. (1982). Extensive loss of choline acetyltransferase activity is not reflected by neuronal loss in the nucleus of Meynert in Alzheimer's disease. *Neurosci. Letts.*, **33**: 311-315.

Popot J. L. and Changeux J. L. (1984). Nicotinic receptor of acetylcholine: structure of an oligomeric integral membrane protein. *Physiol. Rev.*, **64**: 1162-1239.

Pugh P. C. and Berg D. K. (1994). Neuronal acetylcholine receptors that bind α-bungarotoxin mediate neurite retraction in a calcium-dependent manner. *J. Neurosci.*, **14**: 889-896.

Pugh P. C. and Margiotta J. F. (2000). Nicotinic acetylcholine receptor agonists promote survival and reduce apoptosis of chick ciliary ganglion neurons. *Mol. Cell. Neurosci.*, **15**: 113-122.

Qian C., Li T., Shen T. Y., Libertine-Garahan L., Eckman J., Biftu T. and Ip S. (1993). Epibatidine is a nicotinic analgesic. *Eur. J. Pharmacol.*, **250**: R13-R14.

Quik M., Chomeris J., Komourian J., Lukas R. J. and Puchacz E. (1996). Similarity between rat brain nicotinic α-bungarotoxin receptors and stably expressed α-bungarotoxin binding sites. *J. Neurochem.*, **67**: 145-154.

Quik M., Philie J. and Choremis J. (1997). Modulation of α7 nicotinic receptor-mediated calcium influx by nicotinic agonists. *Mol. Pharm.*, **51**: 499-506.

Raftery M. A., Hunkapiller M., Strader C. D. and Hood L. E. (1980). Acetylcholine receptor: complex of homologous subunits. *Science*, **208**: 1454-1457.

Ramirez-Latorre J., Yu C. R., Qu P. F., Karlin A. and Role L. W. (1996). Functional contributions of α5 subunit to neuronal acetylcholine receptor channels. *Nature*, **380**: 347-351.

Rathouz M. M., Vijayaraghavan S. and Berg D. K. (1995). Acetylcholine differentially affects intracellular calcium via nicotinic and muscarinic receptors on the same population of neurones. *J. Biol. Chem.*, **270**: 14366-14375.

Rink TJ and Pozzan T (1986). Using quin2 in cell suspensions. *Cell Calcium*, **6**: 133-144.

Robinson D. and McGee R. Jr. (1985). Agonist-induced regulation of the neuronal nicotinic acetylcholine receptor of PC12 cells. *Mol. Pharm.*, **27**: 409-417.

Rogers A. and Wonnacott S. (1997). Differential upregulation of α7 and α3 subunit-containing nicotinic acetylcholine receptors in rat hippocampal and PC12 cell cultures. *Biochem. Soc. Trans.*, **25** (3), 544s.

Rogers M. and Dani J. A. (1995). Comparison of quantitative calcium flux through NMDA, ATP and ACh receptor channels. *Biophys. J.* **68**: 501-506.

Rogers S. W., Mandelzys A., Deneris E. S., Cooper E. and Heinemann S. (1992). The expression of nicotinic acetylcholine receptors by PC12 cells treated with NGF. *J. Neurosci.*, **12**: 4611-4623.

Role L. W. and Berg D. K. (1996) Nicotinic receptors in the development and modulation of CNS synapses. *Neuron*, **16**: 1077-1085.

Romano C. and Goldstein A. (1980). Stereospecific nicotine receptors on rat brain membranes. *Science*, **210**: 647-649.

Rongo C. and Kaplan J. M. (1999). CaMKII regulates the density of central glutamatergic synapses in vivo. *Nature*, **402**: 195-199.

Rose J. E., Behm F. M. and Levin E. D. (1993). Role of nicotine dose and sensory cues in the regulation of smoke intake. *Pharmacol. Biochem. Behav.*, **44**: 891-900.

Rose J. E., Herskovic J. E., Trilling Y. and Jarvik M. E. (1985). Transdermal nicotine reduces cigarette craving and nicotine preference. *Clinical Pharmacol. Ther.*, **38**: 450-456.

Rosen L. B., Ginty D. D., Weber M. J. and Greenberg M. E. (1994). Membrane depolarisation and calcium influx stimulate MEK and MAP kinase via activation of Ras. *Neuron*, **12**: 1207-1221.

Rothhut B., Romano S. J, Vijayaraghavan S. and Berg D. K. (1996). Post-translational regulation of neuronal acetylcholine receptors stably expressed in a mouse fibroblast cell line. *J. Neurobiol.*, **29**: 115-125.

Rowell R. P. and Li M. (1997). Dose-response relationship for nicotine-induced up-regulation of rat brain nicotinic receptors. *J. Neurochem.*, **68**: 1982-1989.

Rowell P. P. and Wonnacott S. (1990). Evidence for functional activity of up-regulated nicotine binding sites in rat striatal synaptosomes. *J. Neurochem.*, **55**: 2105-2110.

Rubboli F., Court J. A., Sala C., Morris C., Perry E. and Clementi F. (1994). Distribution of neuronal nicotinic receptor subunits in human brain. *Neurochem. Int.*, **25**: 69-71.

Rupniak N. M. J., Patel S., Webb J., Traynor J. R., Elliott J., Freedman S. B., Fletcher S. R. and Hill R. G. (1994). Antinociceptive and toxic effects of (+)-epibatidine oxalate attributable to nicotinic agonist activity. *Br. J. Pharmacol.*, **113**: 1487-1493.

Russell M. A. H. (1990). Nicotine intake and its control over smoking. In: Nicotine Psychopharmacology: molecular, cellular and behavioural aspects: (Eds: Wonnacott S., Russell M. A. H., Stolerman I. P.). Oxford University Press, pp 374-418.

Russell M. A. H. (1991). The future of nicotine replacement. *Br. J. Addict.*, **86**: 653-658.

Samuel N., Wonnacott S., Lindstrom J. and Futerman A. H. (1997). Parallel increases in [^{125}I]-α-bungarotoxin binding and α7 nicotinic subunit immunoreactivity during the development of rat hippocampal neurons in culture. *Neurosci. Letts.*, **222**: 179-182.

Sanderson E. M., Drasdo A. L., McCrea K. and Wonnacott S. (1993). Upregulation of nicotinic receptors following continuous infusion of nicotine is brain-region-specific. *Brain Res.*, **617**: 349-352.

Sargent P. B. (1993). The diversity of neuronal nicotinic acetylcholine receptors. *Annu. Rev. Neurosci.*, **16**: 403-443.

Schliefer L. S. and Eldefrawi M. E. (1974). Identification of the nicotinic and muscarinic acetylcholine receptors in subcellular fractions of mouse brains. *Neuropharmacol.*, **13**: 53-63.

Schmidt J. and Raftery M. A. (1973). A simple assay for the study of solubilised acetylcholine receptors. *Anal. Biochem.*, **52**: 349-352.

Schoepfer R., Conroy W. G., Whiting P., Gore M. and Lindstrom J. (1990). Brain α-bungarotoxin binding protein cDNAs and mAbs reveal subtypes of this branch of the ligand-gated ion channel gene superfamily. *Neuron*, **5**: 35-48.

Schulman H. (1993). The multifunctional Ca^{2+}/calmodulin-dependent protein kinase. *Curr. Opin. Cell Biol.*, **5**: 247-253.

Schwartz R. D. and Kellar K. J. (1983). Nicotinic cholinergic receptor binding sites in the brain: regulation *in vivo*. *Science*, **220**: 214-216.

Schwartz R. D. and Kellar K. J. (1985). *In vivo* regulation of [^{3}H]-acetylcholine recognition sites in brain by nicotinic cholinergic drugs. *J. Neurochem.*, **45**: 427-433.

Schwartz R. D., McGee R., Jr. and Kellar K. J. (1982). Nicotinic cholinergic receptors labelled by [^{3}H]-acetylcholine in rat brain. *Mol. Pharmacol.* **22**:56-62.

Séguéla P., Wadiche J., Dineley-Miller K., Dani J. A. and Patrick J. W. (1993). Molecular cloning, functional properties and distribution of rat brain α7: a nicotinic cation channel highly permeable to calcium. *J. Neurosci.*, **13**: 596-604.

Selkoe D. J. (1999). Translating cell biology into therapeutic advances in Alzheimer's disease. *Nature*, **399**: suppl. A23-A31.

Semba J., Miyoshi R. and Kito S. (1996). Nicotine protects against dexamethasone potentiation of kainic acid-induced neurotoxicity in cultured hippocampal neurones. *Brain Res.*, **735**: 335-338.

Sharples C. G. V., Kaiser S., Soliakov L., Marks M. J., Collins A. C., Washburn M., Wright E., Spencer J. A., Gallagher T., Whiteaker P. and Wonnacott S. (2000). UB-165: A novel nicotinic agonist with subtype selectivity implicates the α4β2* subtype in the modulation of dopamine release from rat striatal synaptosomes. *J. Neurosci.*, **20**: 2783-2791.

Shimohama S. (1996). Nicotinic agonists prevent neuronal cell death by glutamate and amyloid beta protein. *Neurobiol. Ageing.*, **17**: S40.

Shimohama S., Greenwald D. L., Shafron D. H., Akaika A., Maeda T., Kaneko S., Kimura J., Simpkins C. E., Day A. L. and Meyer E. M. (1998). Nicotinic α7 receptors protect against glutamate neurotoxicity and neuronal ischaemic damage. *Brain Res.*, **779**: 359-363.

Shotton D. M. (1989). Confocal scanning optical microscopy and its applications for biological specimens. *J. Cell. Sci.*, **94**: 175-206.

Sihver W., Gillberg P. G., Svensson A. L. and Norberg A. (1999). Autoradiographic comparison of the [^{3}H](-)nicotine, [^{3}H]cytisine and [^{3}H]epibatidine binding in relation to vesicular acetylcholine transport sites in the temporal cortex in Alzheimer's disease. *Neuroscience*, **94**: 685-696.

Silva A. J., Paylor R., Wehner J. M. and Tonegawa S. (1992). Impaired spatial learning in α-calcium-calmodulin kinase II mutant mice. *Science*, **257**: 206-211.

Sine S. M. and Claudio T. (1991). γ- and δ-subunits regulate the affinity and the cooperativity of ligand binding to the acetylcholine receptor. *J. Biol. Chem.*, **266**: 19369-19377.

Sine S. M., Kreinkamp H-J., Bren N., Maeda R. and Taylor P. (1995). Molecular dissection of subunit interfaces in the acetylcholine receptor: identification of determinants of α-conotoxin M1 selectivity. *Neuron*, **15**: 205-211.

Sivilotti L. G., McNeil D. K., Lewis T. M., Nassa M., Schoepfer R. and Colquhoun L. M. (1997). Recombinant nicotinic receptors, expressed in Xenopus oocytes, do not resemble native rat sympathetic ganglion receptors in single-channel behaviour. *J. Physiol. (Lond.)*, **500**: 123-138.

Smith M. A., Margiotta J. F., Franco A., Lindstrom J. M. and Berg D. K. (1983). Differential regulation of acetylcholine sensitivity and α-bungarotoxin-binding sites on ciliary ganglion neurones in cell culture. *J. Neurosci.*, **3**: 2395-2402.

Solem M., McMahon T. and Messing R. O. (1995). Depolarisation-induced neurite outgrowth in PC12 cells requires permissive, low level NGF receptor stimulation and activation of calcium/calmodulin-dependent protein kinase. *J. Neurosci.*, **15**: 5966-5975.

Soler R. M., Egea J., Mintenig G. M., Sanz-Rodriguez C., Iglesias M. and Comella J. X. (1998). Calmodulin is involved in membrane depolarisation-mediated survival of motoneurones by phosphatidylinositol-3-kinase- and MAPK-independent pathways. *J. Neurosci.*, **18**: 1230-1239.

Soliakov L. and Wonnacott S. (1996). Voltage-sensitive Ca^{2+} channels involved in nicotinic receptor-mediated [^{3}H]dopamine release from rat striatal synaptosomes. *J. Neurochem.*, **67**: 163-170.

Spande T. F., Garraffo H. M. , Edwards M. W., Yeh H. J. C., Pannell L. and Daly J. W. (1992). Epibatidine: a novel (chloropyridyl)azabicycloheptane with potent analgesic activity from an Ecuadorian poison frog. *J. Am. Chem. Soc.,* **114**: 3475-3478.

Spurden D. P., Court J. A., Lloyd S., Oakley A., Perry R., Pearson C., Pullen R. G. and Perry E. K. (1997). Nicotinic receptor distribution in the human thalamus: autoradiographical localisation of [^{3}H]-nicotine and [^{125}I]-α-bungarotoxin binding. *J. Chem. Neuroanat.*, **13**: 105-113.

Squire L. R. and Zola-Morgan S. (1988). Memory: brain systems and behaviour. *T.I.N.S.*, **11**: 170-175.

Srinivasan M., Edman C. F. and Schulman H. (1994). Alternative splicing introduces a nuclear localisation signal that targets multifunctional CaM kinase to the nucleus. *J. Cell Biol.*, **126**: 839-852.

Stolerman I. P. and Jarvis M. J. (1995). The scientific case that nicotine is addictive. *Psychopharmacol.*, **117**: 2-10.

Stroud R. M., McCarthy M. P. and Shuster M. (1990). Nicotinic acetylcholine receptor superfamily of ligand-gated channels. *Biochemistry*, **29**: 11009-11023.

Sullivan J. P., Decker M. W., Brioni J. D., Donnelly-Roberts D., Anderson D. J., Bannon A. W., Kang C-H., Adams P., Piatonni-Kaplan M., Buckley M. J., Gopalakrishnan M., Williams M. and Arneric S. P. (1994). (±)-Epibatidine elicits a diversity of *in vitro* and *in vivo* effects mediated by nicotinic acetylcholine receptors. *J. Pharmacol. Exp. Ther.*, **271**: 624-631.

Summers K. L., Kem W. R. and Giacobini E. (1997). Nicotinic agonist modulation of neurotransmitter levels in the rat frontoparietal cortex. *Jpn. J. Pharmacol.*, **74**: 139-146.

Sutherland G., Stapleton J. A., Russell M. A. H., Jarvis M. J., Hajek P., Belcher M. and Feyerabend C. (1992). Randomised controlled trial of nasal nicotine spray in smoking cessation, *The Lancet*, **340**: 324-329.

Takai T., Noda M., Mishina M., Shimizu S., Furutani Y., Kayano T., Ikeda T., Kubo T., Takahashi H., Takahashi T., Kuno M. and Numa S. (1985). Cloning, sequencing and expression of cDNA for a novel subunit of acetylcholine receptor from calf muscle. *Nature*, **315**: 761-764.

Taylor C. W. and Broad L. M. (1998). Pharmacological analysis of intracellular Ca^{2+} signalling: problems and pitfalls. *T. I. P. S.*, **19**: 370-375.

Toescu E. C. (1998). Apoptosis and cell death in neuronal cells: where does Ca^{2+} fit in ? *Cell Calcium*, **24**: 387-403.

Tokumisto H., Chijiwa T., Hagiwara M., Mizutani A., Terasawa M. and Hidaka H. (1990). KN-62, 1 - [*N, O* – Bis (5 – isoquinoline sulfonyl) – *N* – methyl – $_L$ - tyrosyl] – 4 - phenylpiperazine, a specific inhibitor of calcium/calmodulin-dependent protein kinase II. *J. Biol. Chem.*, **265**: 4315-4320.

Toyoshima C. and Unwin N. (1988). Ion channel of acetylcholine receptor reconstructed from images of postsynaptic membranes. *Nature, 336*: 247-250.

Tsien R. Y. (1988). Fluorescence measurement and photochemical manipulation of cytosolic free calcium. *T. I. N. S.*, **11**: 419-424.

Tsien R. Y., Pozzan T. and Rink T. J. (1982). Calcium homeostasis in intact lymphocytes: Cytoplasmic free calcium monitored with a new, intracellularly trapped fluorescent indicator. *J. Cell Biol.*, **94**: 325-334.

Ullian E. K., McIntosh J. M. and Sargent P. B. (1997). Rapid synaptic transmission in the avian ciliary ganglion is mediated by two distinct classes of nicotinic receptors. *J. Neurosci.*, **17**: 7210-7219.

Unwin N. (1993a). Nicotinic acetylcholine receptor at 9Å resolution. *J. Mol. Biol.*, **239**: 1101-1124.

Unwin N. (1993b). Neurotransmitter action: opening of ligand-gated ion channels. *Cell*, **72/** *Neuron*, **10** (Suppl.), 31-41.

Unwin N. (1995). Acetylcholine receptor channel imaged in the open state. *Nature*, **373**: 37-43.

Unwin N., Toyoshima C. and Kubalek E. (1988). Arrangement of the acetylcholine receptor subunits in the resting and desensitised states, determined by cryoelectron microscopy of crystallised *Torpedo* postsynaptic membranes. *J. Cell Biol.*, **107**: 1123-1138.

Vaughan P. F. T., Kaye D. F., Reeve H. L., Ball S. G. and Peers C. (1993). Nicotinic receptor-mediated release of noradrenaline in the human neuroblastoma SH-SY5Y. *J. Neurochem.*, **60**: 2159-2166.

Vernallis A. B., Conroy W. G. and Berg D. K. (1993). Neurones assemble acetylcholine receptors with as many as three kinds of subunits while maintaining subunit segregation among receptor subtypes. *Neuron*, **10**: 451-464.

Vijayaraghavan S., Pugh P. C., Zhang Z., Rathouz M. M and Berg D. K. (1992). Nicotinic receptors that bind α-bungarotoxin on neurones raise intracellular free Ca^{2+}. *Neuron*, **8**: 353-362.

Wang F., Gerzanich V., Wells G., Anand R., Peng X., Keyser K. and Lindstrom J. (1996). Assembly of human neuronal nicotinic receptor α5 subunits with α3, β2 and β4 subunits. *J. Biol. Chem.*, **271**: 17656-17685.

Wang F., Nelson M. E., Kuryatov A., Olale F., Cooper J., Keyser K. and Lindstrom J. (1998). Chronic nicotine treatment up-regulates human α3β2 but not α3β4 acetylcholine receptors stably transfected in human embryonic kidney cells. *J. Biol. Chem.*, **273**: 28721-28732.

Ward J. M., Cockcroft V. B., Lunt G. C., Smillie F. S. and Wonnacott S. (1990). Methyllycaconitine: a selective probe for neuronal α-bungarotoxin binding sites. *F. E. B. S. Letts.*, **270**: 45-48.

Warpman U., Friberg L., Gillespie A., Hellström-Lindahl E., Zhang X. and Nordberg A. (1998). Regulation of nicotinic receptor subtypes following chronic nicotinic agonist exposure in M10 and SH-SY5Y neuroblastoma cells. *J. Neurochem.*, **70**: 2028-2037.

West R. and Schneider N. (1987). Craving for cigarettes. *Br. J. Addict.*, **82**: 407-415.

Wheeler J. W., Olubajo O., Storm C. B. and Duffield R. M. (1981). Anabaseine: venom alkaloid of *Aphaenogaster* ants. *Science*, **211**: 1051-1052.

White J. G., Amos W. B. and Fordham M. (1987). An evaluation of confocal versus conventional imaging of biological structures by fluorescence light microscopy. *J. Cell. Biol.*, **105**: 41-48.

Whiteaker P., Davies A. R. L., Marks M. J., Blagbrough I. S., Potter B. V. L., Wolstenholme A. J., Collins A. C. and Wonnacott S. (1999). An autoradiographic study of the distribution of binding sites for the novel α7-selective nicotinic radioligand [^{3}H]-methyllycaconitine in the mouse brain. *Eur. J. Neurosci.*, **11**: 2689-2696.

Whiteaker P., McIntosh J. M., Luo S., Collins A. C. and Marks M. J. (2000). [^{125}I]-α-Conotoxin MII identifies a novel nicotinic acetylcholine receptor population in mouse brain. *Mol. Pharmacol.*, **57**: 913-925.

Whiteaker P., Sharples C. G. V. and Wonnacott S. (1998). Agonist induced up-regulation of α4β2 nicotinic acetylcholine receptors in M10 cells: pharmacological and spatial definition. *Mol. Pharmacol.*, **53**: 950-962.

Whitehouse P. J., Price D. L., Struble R. G., Clark A. W., Coyle J. T. and De Long J. T. (1982). Alzheimer's disease and senile dementia: loss of neurones in the basal forebrain. *Science*, **215**: 1237-1239.

Whiting P. J. and Lindstrom J. M. (1986). Purification and characterisation of a nicotinic acetylcholine receptor from chick brain. *Biochemistry*, **25**: 2082-2093.

Whiting P. and Lindstrom J. (1987a). Purification and characterisation of nicotinic acetylcholine receptor from rat brain. *Proc. Natl. Acad. Sci. USA*, **84**: 595-599.

Whiting P. and Lindstrom J. (1987b). Affinity labelling of neuronal acetylcholine receptors localises the neurotransmitter binding site to their β-subunit. *F. E. B. S. Letts.*, **213**: 55-60.

Whiting P. J. and Lindstrom J. M. (1988). Characterisation of bovine and human neuronal nicotinic acetylcholine receptors using monoclonal antibodies. *J. Neuroscience*, **8**: 3395-3404.

Whiting P., Liu R., Morley B. J. and Lindstrom J. M. (1987). Structurally different neuronal nicotinic acetylcholine receptor subtypes purified and characterised using monoclonal antibodies. *J. Neurosci.*, **7**: 4005-40016.

Whiting P. J., Schoepfer R., Conroy W. G., Gore M. J. and Keyser K. T. (1991a). Expression of nicotinic acetylcholine receptor subtypes in brain and retina. *Mol. Brain Res.*, **10**: 61-70.

Whiting P. J., Schoepfer R., Lindstrom J. and Priestley T. (1991b). Structural and pharmacological characterisation of the major brain nicotinic acetylcholine receptor subtype stably expressed in mouse fibroblasts. *Mol. Pharmacol.*, **40**: 463-472.

Williams C. L., Phelps S. H. and Porter R. A. (1996). Expression of Ca^{2+}/calmodulin-dependent protein kinase types II and IV, and reduced DNA synthesis due to the Ca^{2+}/calmodulin-dependent protein kinase inhibitor KN-62 (1-[*N*, *O*-bis(5-isoquinolinesulfonyl)-*N*-methyl-L-tyrosyl]-4-phenylpiperazine) in small cell lung carcinoma. *Biochem. Pharmacol.*, **51**: 707-715.

Williams C. L., Porter R. A. and Phelps S. H. (1995). Inhibition of voltage-gated Ca^{2+} channel activity in small cell lung carcinoma by the Ca^{2+}/calmodulin-dependent protein kinase inhibitor KN-62 (1-[*N*, *O*-bis(5-isoquinolinesulfonyl)-*N*-methyl-L-tyrosyl]-4-phenylpiperazine). *Biochem. Pharmacol.*, **50**: 1979-1985.

Wilner P. and Jones C. (1996). Effects of mood manipulation on subjective and behavioural measures of cigarette craving. *Behav. Pharmacol.*, **7**: 355-363.

Wisden W. and Seeburg P. H. (1992). $GABA_A$ receptor channels: from subunits to functional entities. *Curr. Opin. Neurobiol.*, **2**: 263-269.

Wonnacott S. (1987). Brain nicotine binding sites. *Human Toxicol.*, **6**: 343-353.

Wonnacott S. (1990). Characterisation of nicotinic receptor sites in the brain. In: Psychopharmacology: Molecular, cellular and behavioural aspects. (Eds: Wonnacott S., Russell M. A. H., Stolerman I. P.), Oxford University Press, pp 226-277.

Wright S. J. and Schatten G. (1991). Confocal fluorescence microscopy and three-dimensional reconstruction. *J. Electron Microsc. Tech.*, **18**: 2-10.

Wu G. and Cline H. T. (1998). Stabilisation of dendritic arbour structure *in vivo* by CaMKII. *Science*, **279**: 222-226.

Wu G., Malinow R. and Cline H. T. (1996). Maturation of a central glutamatergic synapse. *Science*, **274**: 972-976.

Wyllie D. J. A. and Nicoll R. A. (1994). A role fore protein kinases and phosphatases in the Ca^{2+}-induced enhancement of hippocampal AMPA receptor-mediated synaptic responses. *Neuron*, **13**: 635-643.

Xiao R-P., Cheng H., Lederer W. J., Suzuki T. and Lakatta E. G. (1994). Dual regulation of Ca^{2+}/calmodulin-dependent kinase II activity by membrane voltage and by calcium influx. *Proc. Natl. Acad. Sci.* USA, **91**: 9659-9663.

Yamashita H. and Nakamura S. (1996). Nicotine rescues PC12 cells from death induced by nerve growth factor deprivation. *Neurosci. Letts.*, **213**: 145-147.

Yates S. L., Bencherif M., Fluhler E. N. and Lippiello P. M. (1995). Up-regulation of nicotinic acetylcholine receptors following chronic exposure of rats to mainstream cigarette smoke or $\alpha4\beta2$ receptors to nicotine. *Biochem. Pharmacol.*, **50**: 2001-2008.

Yu C. R. and Role L. W. (1998a). Functional contribution of the $\alpha7$ subunit to multiple subtypes of nicotinic receptors in embryonic chick sympathetic neurones. *J. Physiol. (Lond.)*, **509**: 651-665.

Yu C. R. and Role L. W. (1998b). Functional contribution of the $\alpha5$ subunit to neuronal nicotinic channels expressed by chick sympathetic ganglion neurones. *J. Physiol. (Lond.)*, **509**: 667-681.

Zafaralla G. C., Ramilo C., Gray W. R., Karlstrom R., Olivera B. M. and Cruz L. J. (1988). Phylogenetic specificity of cholinergic ligands: α-conotoxin SI. *Biochemistry*, **27**: 7102-7105.

Zhang X., Gong Z-H., Hellström-Lindahl E. and Nordberg A. (1995).Regulation of α4β2 nicotinic acetylcholine receptors in M10 cells following treatment with nicotinic agonists. *NeuroReport*, **6**: 313-317.

Zhang Z. W., Vijayaraghavan S. Berg D. K. (1994). Neuronal acetylcholine receptors that bind α-bungarotoxin with high affinity function as ligand-gated ion channels. *Neuron*, **12**:167-177.

Zoli M., Léna C. Picciotto M. R. and Changeux J. P. (1998). Identification of four classes of brain nicotinic receptors using β2 mutant mice. *J. Neurosci.*, **18**: 4461-4472.

Zoltewicz J. A., Prokai-Tatrai K. and Bloom L. B. (1993). Long range transmission of polar effects in cholinergic 3-arylideneanabaseines. Conformations calculated by molecular modelling. *Heterocycles*, **35**: 171-179.